

solutions manual for

classical

electromagnetic

radiation

3 edition

Heald

Marion

solutions manual for

**classical
electromagnetic
radiation**

3 edition

MARK A. HEALD
Swarthmore College

JERRY B. MARION
Late, University of Maryland

Please check the Website for errata and other updated material:

www.swarthmore.edu/NatSci/mheald1/



Australia • Brazil • Japan • Korea • Mexico • Singapore • Spain • United Kingdom • United States

© 1995 Brooks/Cole, Cengage Learning

ALL RIGHTS RESERVED. No part of this work covered by the copyright herein may be reproduced, transmitted, stored, or used in any form or by any means graphic, electronic, or mechanical, including but not limited to photocopying, recording, scanning, digitizing, taping, Web distribution, information networks, or information storage and retrieval systems, except as permitted under Section 107 or 108 of the 1976 United States Copyright Act, without the prior written permission of the publisher.

For product information and technology assistance, contact us at
Cengage Learning Academic Resource Center,
1-800-423-0563

For permission to use material from this text or product,
submit all requests online at **www.cengage.com/permissions**
Further permissions questions can be emailed to
permissionrequest@cengage.com

ISBN-13: 978-0-030-97278-2

ISBN-10: 0-03-097278-7

Brooks/Cole
10 Davis Drive
Belmont, CA 94002-3098
USA

Cengage Learning products are represented in Canada by Nelson Education, Ltd.

For your course and learning solutions, visit **academic.cengage.com**

Purchase any of our products at your local college store or at our preferred
online store **www.ichapters.com**

TABLE OF CONTENTS

Chapter 1	Fundamentals of Static Electromagnetism	1
Chapter 2	Multipole Fields	19
Chapter 3	The Equations of Laplace and Poisson	32
Chapter 4	Dynamic Electromagnetism	54
Chapter 5	Electromagnetic Waves	67
Chapter 6	Reflection and Refraction	75
Chapter 7	Waveguides	81
Chapter 8	Retarded Potentials and Fields and Radiation by Charged Particles	
Chapter 9	Antennas	97
Chapter 10	Classical Electron Theory	106
Chapter 11	Interference and Coherence	118
Chapter 12	Scalar Diffraction Theory and the Fraunhofer Limit	124
Chapter 13	Fresnel Diffraction and the Transition to Geometrical Optics	132
Chapter 14	Relativistic Electrodynamics	136

Chapter 1

1-1. The Gaussian unit of charge (the "esu" or "statcoulomb") is defined by Coulomb's force law, Eq. (1.1). Therefore, $\text{dyne} \equiv (\text{esu})^2/\text{cm}^2$, and $\text{esu} \equiv \sqrt{(\text{dyne}\cdot\text{cm}^2)}$. But from $F = ma$, $\text{dyne} \equiv \text{g}\cdot\text{cm}/\text{s}^2$. Hence, in the basis units, $\text{esu} \equiv \text{cm}^{3/2}\cdot\text{g}^{1/2}\cdot\text{s}^{-1}$.

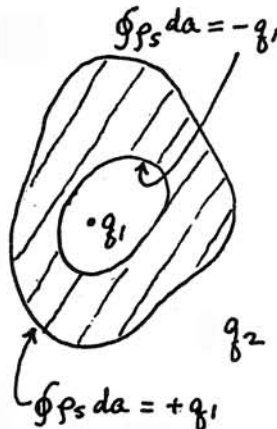
Capacitance is defined as the ratio of charge to potential difference (see Prob. 1-7). The Gaussian unit of potential ("statvolt") is equivalent to $\text{erg}/\text{esu} \equiv \text{dyne}\cdot\text{cm}/\text{esu}$. Hence, the capacitance unit ("statfarad") is $(\text{esu})^2/(\text{dyne}\cdot\text{cm}) \equiv (\text{cm}^3\cdot\text{g}\cdot\text{s}^{-2})/(\text{g}\cdot\text{cm}^2\cdot\text{s}^{-2}) \equiv \text{cm}$.

Conductivity is the ratio of current density to electric field. Hence, the Gaussian unit is $(\text{esu}\cdot\text{s}^{-1}\cdot\text{cm}^{-2})/(\text{dyne}\cdot\text{esu}^{-1}) \equiv (\text{esu})^2/(\text{dyne}\cdot\text{cm}^2\cdot\text{s}) \equiv \text{s}^{-1}$.

In SI units, the Coulomb force law contains the dimensional coefficient $1/4\pi\epsilon_0$. Therefore, the units of ϵ_0 are $\text{coulomb}^2/(\text{newton}\cdot\text{meter}^2)$. But $\text{C} \equiv \text{A}\cdot\text{s}$, and $\text{N} \equiv \text{kg}\cdot\text{m}/\text{s}^2$. Hence, $[\epsilon_0] = \text{A}^2\cdot\text{s}^4/(\text{kg}\cdot\text{m}^3)$. The unit of capacitance is the farad $\equiv \text{coulomb}/\text{volt}$, which works out to $\text{m}^{-2}\cdot\text{kg}^{-1}\cdot\text{s}^4\cdot\text{A}^2$; thus it is conventional to express the units of ϵ_0 as farad/meter.

Note: Although SI treats the ampere as an independent basis unit, the ampere is in fact defined implicitly in terms of the three mechanical units through the magnetic force law [combining the SI versions of Eqs. (1.36) and (1.54)], with the SI permeability coefficient defined as $\mu_0 \equiv 4\pi \times 10^{-7}$ henry/meter.

1-2. A conductor cannot support a static electric field in its interior: if there were a field, charge would flow contradicting the assumption of electrostatic equilibrium. There can be net charge on a conductor's surfaces. Imagine a Gaussian surface that lies entirely *within* the conductor (where \mathbf{E} vanishes), enclosing the cavity. Gauss' law demands that a charge totaling $-q_1$ is induced on the conductor's *inner* surface, distributed over the surface in such a way that it cancels q_1 's field within the conductor. Since the conductor has no net charge, a charge totaling $+q_1$ remains on the *outer* surface, distributed in such a way that it produces no field within the conductor.



A Gaussian surface drawn *outside* the conductor encloses net charge, and therefore the electric field does not vanish. Although this field is ultimately caused by q_1 , its spatial

distribution and the magnitude of force on q_2 depend upon the geometry of the *outer* surface of the conductor (and not upon the location of q_1 within the cavity, nor upon the shape of the *inner* surface).

The presence of q_2 induces an *additional* charge density on the outer surface of the conductor, distributed so that it cancels q_2 's field within the conductor. The integral of this additional surface charge is zero. There is a net force on the total outer-surface charge due to q_2 . Thus the action-reaction pair of Newton's third law is between q_2 and this total charge distribution on the outer surface of the conductor.

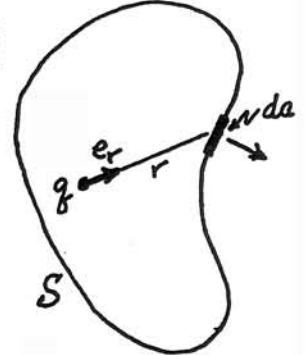
Similarly, there is an action-reaction pair of forces between q_1 and the induced charge distribution on the inner surface of the conductor, the magnitude of which depends upon the location of q_1 and the geometry of the inner surface. The conducting shell surrounding q_1 shields it from any influence by q_2 .

1-3. Consider a point charge q enclosed by an arbitrary Gaussian surface S . The flux of electric field through the element of area da is

$$\mathbf{E} \cdot \mathbf{n} da = \frac{q}{r^2} \mathbf{e}_r \cdot \mathbf{n} da$$

where \mathbf{n} is the outward unit normal to da . Meanwhile, the solid angle subtended by da at q is

$$d\Omega = \frac{da}{r^2} \mathbf{e}_r \cdot \mathbf{n}$$



Thus, the total flux through the Gaussian surface can be expressed as

$$\oint_S \mathbf{E} \cdot \mathbf{n} da = q \oint d\Omega$$

If the charge q is *inside* the surface S , the integral over all solid angle is 4π , independent of the precise location of q . If the charge is *outside* the surface, the integral is zero.

Since the total field \mathbf{E} is the linear (vector) sum of the fields of any number of point charges, we can write, in general,

$$\oint_S \mathbf{E} \cdot \mathbf{n} da = 4\pi q_{\text{encl}}$$

where q_{encl} represents the (scalar) sum of all charges enclosed by the surface. This is Eq. (1.6).

1-4. A spherically symmetric charge distribution is represented by a charge density $\rho(r)$, which does not depend on the angles θ and ϕ of spherical coordinates. If we choose as Gaussian surface a concentric sphere of radius R , then we can infer from the symmetry:

(1) The *direction* of the electric field \mathbf{E} at the surface is purely radial, hence everywhere *normal* to the Gaussian surface.

(2) The *magnitude* of the electric field is *constant* over the surface.

Therefore, the general flux integral in Gauss' law specializes to

$$\oint_S \mathbf{E} \cdot \mathbf{n} \, da \rightarrow \oint_S E_r \, da \rightarrow E_r \oint_S da = E_r 4\pi R^2$$

Equating this to the charge enclosed gives

$$\mathbf{E}(R) = E_r(R) \mathbf{n} = \frac{1}{R^2} \int_0^R \rho(r) 4\pi r^2 \, dr \, \mathbf{e}_r$$

But this is identical to Eq. (1.3) for the field of a point charge whose magnitude equals the total of the distributed charge up to radius R .

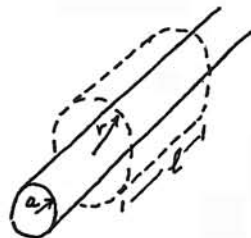
If the charge distribution extends beyond radius R , the value of the function $\rho(r)$ for $r > R$ has no effect on the field at R , *unless* the distribution ceases to be spherically symmetric!

1-5. Construct a Gaussian surface in the form of a coaxial cylinder of radius r and length b . We make two inferences from the axial symmetry: (1) The *direction* of the field produced by this charge must be purely radial (in cylindrical coordinates), normal to the chosen Gaussian surface. (2) The *magnitude* of the field can depend only on r (not upon ϕ or z). Thus the left side of Gauss' law, Eq. (1.6), can be evaluated as

$$\oint_S \mathbf{E} \cdot \mathbf{n} \, da \rightarrow E_r(r) 2\pi r b$$

(There is no contribution from the ends of the Gaussian surface because of the dot product.) The right-hand side of Gauss' law, proportional to the enclosed charge, depends upon whether r is less or greater than a . For $r < a$, the enclosed charge is zero, and the field within the hollow cylinder vanishes:

$$\mathbf{E}(r) = 0 \quad (r < a)$$



(It also vanishes inside the wall of the conductor, no matter how thick.)

For $r > a$, the enclosed charge is ρb , and the field is

$$\mathbf{E}(r) = \frac{1}{2\pi r b} 4\pi(\rho b) \mathbf{e}_r = \frac{2\rho \ell}{r} \mathbf{e}_r \quad (r > a)$$

For the potential Φ , we can use Eq. (1.13). It is most convenient to choose the reference point r_0 (where $\Phi = 0$) at the surface of the cylinder; then the potential outside the cylinder is

$$\Phi = - \int_{r_0}^r \mathbf{E} \cdot d\mathbf{l} \rightarrow - \int_a^r \frac{2\rho \ell}{r} \, dr = -2\rho \ell \ln\left(\frac{r}{a}\right) \quad (r > a)$$

The field-free hollow interior and the conductor wall are an equipotential region, where $\Phi = 0$. The potential blows up (negatively) at large cylindrical radii, but remains zero at large distances along the axis. Thus, in this case, the potential at "infinity" is different in different directions, and so "infinity" is not a suitable reference point. This anisotropy is an artifact of the idealization of an "infinitely" long cylinder.

1-6. The spherical symmetry is the same as Prob. 1-4. For a Gaussian surface of radius R , Gauss' law gives

$$E_r(R) 4\pi R^2 = 4\pi \int_0^R \rho(r) 4\pi r^2 \, dr$$

If E_r is to be a constant, then the integral must be proportional to R^2 , which implies that $\rho(r)$ is proportional to $1/r$. Let $\rho(r) = \alpha/r$, and evaluate the integral to obtain $2\pi\alpha R^2$. Therefore the constant field magnitude is $E_0 = 2\pi\alpha$, so that

$$\rho(r) = \frac{E_0}{2\pi r}$$

An alternative approach is to use the potential and Poisson's equation, Eq. (1.15). From Eq. (1.13), the constant radial field E_0 gives the potential function $\Phi(r) = -E_0 r$. The Laplacian operator for spherical symmetry, from Eq. (A.52), gives

$$\nabla^2 \Phi \rightarrow \frac{1}{r^2} \frac{\partial}{\partial r} \left(r^2 \frac{\partial \Phi}{\partial r} \right) = -\frac{2E_0}{r} = -4\pi\rho(r)$$

With spherical symmetry, the field right at the origin must be *zero* (if it weren't, the field's direction would violate the symmetry). The mathematics shows the charge density blowing up at the origin, a nonphysical idealization. If we cap ρ at a constant finite value close to the origin, then the field magnitude falls linearly to zero as $r \rightarrow 0$.

1-7. (a) For parallel plates, the uniform charge density $\rho_s = \pm q/S$ lies on the inner surfaces. Construct a Gaussian pillbox (Fig. 1-11) enclosing one of these surfaces. One face lies inside the conductor (where $\mathbf{E} = 0$); the other lies in the space between the plates (where the field is of constant magnitude and normal to the face). The flux through the cylindrical surface of the pillbox vanishes because the field has no normal component. If the face area is Δa , Gauss' law relates the field E to the charge q by

$$E \Delta a = 4\pi \frac{q}{S} \Delta a \quad \rightarrow \quad q = \frac{E S}{4\pi}$$

The difference of potential between the plates is simply $\Delta\Phi = Ed$. Therefore the capacitance is

$$C = \frac{q}{\Delta\Phi} = \frac{ES/4\pi}{Ed} = \frac{S}{4\pi d}$$

(In SI units, this appears as $C = \epsilon_0 S/d$.)

(b) By Prob. 1-4, the field in the space between the spheres is the same as a point charge q at the center of symmetry. The difference of potential between the spheres is therefore

$$|\Delta\Phi| = \int_a^b \frac{q}{r^2} dr = q \left(\frac{1}{a} - \frac{1}{b} \right)$$

So the capacitance is

$$C = \frac{q}{|\Delta\Phi|} = \frac{ab}{b-a}$$

[In SI, $C = 4\pi\epsilon_0 ab/(b-a)$. Note that this case reduces to the parallel-plate formula in the limit where the separation $a-b \rightarrow d$ is much less than a or b , and $4\pi a^2 \approx 4\pi b^2 \rightarrow S$.]

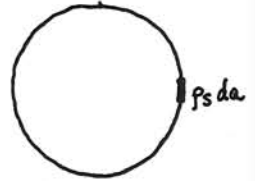
(c) From Prob. 1-5, the field between the cylinders is $E_r = 2\rho_\ell/r$, and therefore the potential difference is

$$|\Delta\Phi| = \int_a^b \frac{2\rho_\ell}{r} dr = 2\rho_\ell \ln\left(\frac{b}{a}\right)$$

The capacitance per unit length is

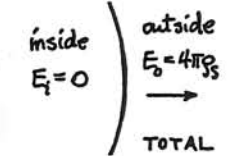
$$C_\ell = \frac{\rho_\ell}{|\Delta\Phi|} = \frac{1}{2 \ln(b/a)}$$

1-8. In order to find the force on an element of charge (the *test charge*), we must find the field at the position of this charge due to all charges of the system *excluding* the test charge. This removal of the test charge from the array of *source* charges spoils the spherical symmetry needed for a direct application of Gauss' law.

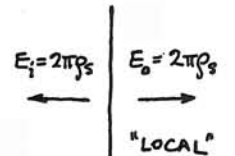


Rather than performing a brute-force integration of Coulomb's law, however, we can find the required net field by subtracting the field contributed by the test charge from the field of *all* the charges.

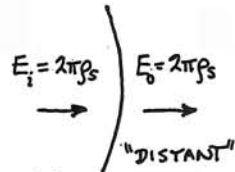
For the complete spherical bubble, the field inside is zero and the field just outside is $4\pi\rho_s$, radially outward.



But, locally, the element of test charge $\rho_s da$ appears to be part of an infinite plane of charge. By Gauss' law, the field of a charged plane is $2\pi\rho_s$, directed away from the plane on both sides.



By subtracting the "local" field from the "total" field, we find the required "distant" field at the test point. Note that this "distant" field is continuous across the location of the test charge element, which is to be expected since the test charge does not contribute to it.



Thus the force on the test charge is

$$dF = E dq = 2\pi \rho_s^2 da \quad (\text{outwards})$$

and the pressure is

$$p = \frac{dF}{da} = 2\pi \rho_s^2$$

What is the analogous force or pressure for a charged infinite cylinder?

1-9. A central force (or field) has the form $\mathbf{F}(r, \theta, \varphi) \rightarrow f(r) \mathbf{e}_r$. We wish to carry out the line integral of this force along an arbitrary path from the three-dimensional point $\mathbf{r}_A = (r_A, \theta_A, \varphi_A)$ to the point $\mathbf{r}_B = (r_B, \theta_B, \varphi_B)$:

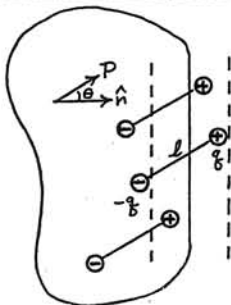
$$\int_{\mathbf{r}_A}^{\mathbf{r}_B} \mathbf{F} \cdot d\mathbf{r} = \int_{\mathbf{r}_A}^{\mathbf{r}_B} f(r) \mathbf{e}_r \cdot (\mathbf{e}_r dr + \mathbf{e}_\theta r d\theta + \mathbf{e}_\varphi r \sin\theta d\varphi)$$

$$= \int_{r_A}^{r_B} f(r) dr = \int_{r_A}^{r_B} f(r) dr$$

In the first line, we have written out the arbitrary integration step dr in full detail in spherical coordinates. The orthogonality of the unit vectors produces a purely one-dimensional integral—the integral of an exact differential. All sensitivity to the path's displacements in θ or ϕ is lost. Consequently the value of the integral is not only independent of the path, but also independent of the θ and ϕ coordinates of the end points.

A less formal approach is to consider a typical incremental contribution $\mathbf{F} \cdot d\mathbf{r}$. The dot product can be thought of as involving *either* the projection of \mathbf{F} onto $d\mathbf{r}$, or the projection of $d\mathbf{r}$ onto \mathbf{F} . Since, for central forces, \mathbf{F} is purely radial, the latter choice of projection shows that it is only increments in the path's radius (dr , not $d\theta$ or $d\phi$) that contribute to the integral.

1-10. (a) If the dipoles are "dumbbells" of length ℓ and they are aligned at the angle θ with the normal to the mathematical surface, any dipole will be cut apart if its center lies within $\pm (\ell/2)\cos\theta$ of the surface. For a surface element of area da , the dipoles in the volume $(\ell\cos\theta)(da)$ are cut. If there are N dipoles per unit volume, the number cut per unit area of this arbitrary surface is $N\ell\cos\theta$. This represents the magnitude of charge $qN\ell\cos\theta = P\cos\theta$.



(b) The polarization vector \mathbf{P} is in the sense of the positive ends of the dipoles. The convention is that the vector area element, $d\mathbf{a} = \mathbf{n} da$, is *outward* with respect to the (closed) Gaussian surface. Therefore, where \mathbf{P} is pointing outward with respect to the surface, the negative ends of the dipoles are *inside* the surface; and vice versa. We can use the dot product to express both the cosine of Part (a) and the sign of the "trapped" charge: the total bound charge enclosed by the Gaussian surface is $-\oint \mathbf{P} \cdot d\mathbf{a}$.

(c) Substituting in Gauss' law, Eq. (1.6), we have

$$\oint \mathbf{E} \cdot d\mathbf{a} = 4\pi \left(q_{\text{free}} - \oint \mathbf{P} \cdot d\mathbf{a} \right)$$

Transposing the bound-source term and conflating it with the field term produces Gauss' law for the \mathbf{D} field. The \mathbf{D} field is a hybrid, which is interesting because its flux depends on only the enclosed *free* charges.

(d) The molecules are now modeled as current loops of area S , with their normals making the angle θ with respect to the arbitrary line drawn through the region. Consider an element of the line $d\ell$, and a cross-sectional area Δa perpendicular to $d\ell$. This volume contains $N d\ell \Delta a$ loops, and their projected area perpendicular to $d\ell$ is $S\cos\theta$. The probable number of loops that the line threads in the distance $d\ell$ is therefore

$$\frac{(N d\ell \Delta a)(S\cos\theta)}{\Delta a} = NS d\ell \cos\theta$$



The current threaded is then

$$NIS d\ell \cos\theta = cM d\ell \cos\theta$$

A check of hand rules shows that for a closed line (contour) the linked current is positive in the right-handed sense when $\mathbf{M} \cdot d\mathbf{\ell}$ is positive. Substituting in Ampère's law, Eq. (1.37),

$$\oint \mathbf{B} \cdot d\mathbf{\ell} = \frac{4\pi}{c} \left(I_{\text{free}} + c \oint \mathbf{M} \cdot d\mathbf{\ell} \right)$$

Transposing the bound-current term and conflating it with the field term produces Ampère's law for the \mathbf{H} field. Again, the \mathbf{H} field is a hybrid, interesting because its circulation depends on only the linked *free* currents.

The significance of these arguments is that, because they can be applied to arbitrary Gaussian surfaces and Amperian loops within a molecular medium, the fields \mathbf{E} and \mathbf{B} are proper macroscopic averages of the microscopic internal fields. Likewise, the medium properties \mathbf{P} and \mathbf{M} , and the hybrid fields \mathbf{D} and \mathbf{H} , are macroscopic averages.

1-11. If the macroscopic boundary of a dielectric coincides with the face of the averaging cell of Fig. 1-3, then the equivalent bound charge density on the surface is $(\rho_s)_b = q'/d^2$, which by Eq. (1.23) is directly equal to the polarization magnitude P . More generally, when the physical boundary is tilted by the angle θ with respect to the surface of a cubical averaging cell, the cell can be deformed to match the boundary. The same charge q' is now distributed over an area that is larger by the factor $1/\cos\theta$. Hence the charge surface-density is reduced by $\cos\theta$, and $\mathbf{n} \cdot \mathbf{P}$ properly represents the charge density and its sign (where \mathbf{n} is the unit normal *outward* from the dielectric boundary).

Similarly, if the macroscopic boundary of a magnetic material coincides with a side wall of an averaging cell, Fig. 1-9, then the equivalent bound current density on the surface

is $K_b = l/d$, which equals cM by Eq. (1.58). If the physical boundary is tilted so that \mathbf{n} remains perpendicular to \mathbf{M} , the cell can be deformed to match with no change in K_b . But when the boundary normal \mathbf{n} tilts out of the plane perpendicular to \mathbf{M} , and the cell wall deformed to match, the same current I is distributed over a width that is larger by $1/\cos\theta$, where θ is the angle between \mathbf{n} and the plane perpendicular to \mathbf{M} . Thus the surface current-density is reduced by the *sine* of the angle between \mathbf{n} and \mathbf{M} , and $-\mathbf{n} \times \mathbf{M}$ properly represents the current density including its vector sense.

1-12. From Eqs. (1.25) and (A.50),

$$\rho_b = -\operatorname{div} \mathbf{P}(r) = -\frac{1}{r^2} \frac{d}{dr} [r^2(kr)] = 3k$$

At the surface $r = a$, by Eq. (1.34) or Prob. 1-11, there is a surface charge density

$$(\rho_s)_b = \mathbf{e}_r \cdot \mathbf{P}(a) = ka$$

We have spherical symmetry and can use Gauss' law. Using a spherical Gaussian surface of radius r with Eq. (1.6),

$$\oint \mathbf{E} \cdot d\mathbf{a} \rightarrow E_r(r) 4\pi r^2 = 4\pi q_{\text{encl}}$$

When $r < a$, the charge enclosed is

$$q = \int \rho_b dv = -3k \int_0^r 4\pi r^2 dr = -4\pi kr^3$$

$$\mathbf{E}(r < a) = -4\pi kr \mathbf{e}_r = -4\pi \mathbf{P}$$

When $r > a$, the charge enclosed is zero. (The dielectric dipoles consist of equal positive and negative charge. Formally, the volume integral of ρ is canceled by the surface integral of ρ_s .) Thus, $\mathbf{E}(r > a) = 0$.

Gauss' law for the \mathbf{D} field, Eq. (1.82), gives

$$\oint \mathbf{D} \cdot d\mathbf{a} = 4\pi q_{\text{free}} \rightarrow 0$$

That is, $\mathbf{D} = 0$ inside as well as out, since no free charge is present. As a check, note that Eq. (1.28) is satisfied both inside and outside the sphere.

1-13. (a) The bound surface charge is

$$(\rho_s)_b = \mathbf{n} \cdot \mathbf{P}_0 = P_0 \cos\theta$$

where θ is the polar angle with respect to the z axis. By symmetry, the net field at the center (the origin) will be in the z (or $\theta = 0$) direction. The surface analog of Eq. (1.20) gives:

$$\begin{aligned} E_z(0) &= \int \frac{(\rho_s)_b}{a^2} (-\mathbf{e}_r \cdot \mathbf{e}_z) 2\pi a^2 \sin\theta d\theta \\ &= -2\pi P_0 \int_0^\pi \cos^2\theta \sin\theta d\theta = -2\pi P_0 \int_{-1}^{+1} u^2 du = -\frac{4\pi}{3} P_0 \end{aligned}$$

That is, $\mathbf{E}(0) = -(4\pi/3)\mathbf{P}_0$.

(b) The total dipole moment of the polarized sphere is $p = P_0(4\pi a^3/3)$, where a is the radius. Since the external field of a spherical charge distribution is the same as an equivalent point charge at the origin (Prob. 1-4), the dipole moment of the superposed uniformly charged spheres is $p = q\delta = \rho_0(4\pi a^3/3)\delta$. These are equal (independent of a) when

$$P_0 = \rho_0 \delta$$

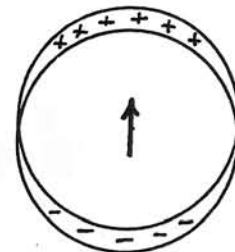
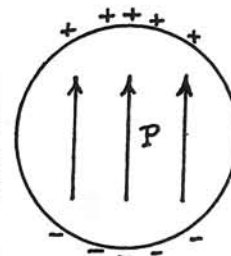
Now if we take the origin at the center of the negative sphere, with the center of the positive sphere at the vector position δ , we can write the total field within the superposed spheres as

$$\mathbf{E} = \frac{4\pi}{3} \rho_0 [-\mathbf{r} + (\mathbf{r} - \delta)] = -\frac{4\pi}{3} \rho_0 \delta = -\frac{4\pi}{3} \mathbf{P}$$

Thus the result of Part (a) extends to the *entire volume* of the polarized sphere. [Yet another approach to this problem uses the spherical harmonic expansion of Section 3.3.]

(c) Again we use superposition. If there were no cavity, the (spatial average) field in the uniform dielectric would be \mathbf{E} , as given. Superpose the polarized sphere of Parts (a) and (b) with its polarization equal and opposite to the polarization in the dielectric, producing the cavity, in which the net polarization is zero and the field is

$$\mathbf{E} - \frac{4\pi}{3}(-\mathbf{P}) = \mathbf{E} + \frac{4\pi}{3}\mathbf{P}$$



Note: The actual \mathbf{E} outside the cavity will have a dipole contribution (from the cavity) superposed on the postulated uniform field (from unspecified distant sources, such as a parallel-plate capacitor geometry). The \mathbf{E} in the formula is to be interpreted as the asymptotic uniform field at large distances from the cavity where its dipole perturbation can be neglected. Furthermore, the assumption in this problem of a strictly uniform \mathbf{P} , even close to the perturbing cavity, is rather artificial. If, instead, we assume a linear dielectric (with \mathbf{P} proportional to \mathbf{E}), then the \mathbf{P} just outside the cavity is modified by the dipole perturbation: this subtly different problem is addressed in Prob. 3-17.

1-14. We have axial symmetry as in Prob. 1-5. Using Gauss' law for \mathbf{D} and assuming a free charge per unit length ρ_l on the inner conductor, we have

$$\oint \mathbf{D} \cdot d\mathbf{a} \rightarrow D_r(r) 2\pi r b = 4\pi \rho_l b$$

where b is the length of the cylindrical Gaussian surface, and r lies between the inner and outer conductors. Thus

$$\mathbf{D} = \frac{2\rho_l}{r} \mathbf{e}_r$$

But if \mathbf{E} is to be constant, then $\mathbf{D} = \epsilon \mathbf{E} \rightarrow \epsilon(r) E_0 \mathbf{e}_r$. Consequently we require

$$\epsilon(r) = \frac{2\rho_l}{E_0 r} = \frac{\text{constant}}{r}$$

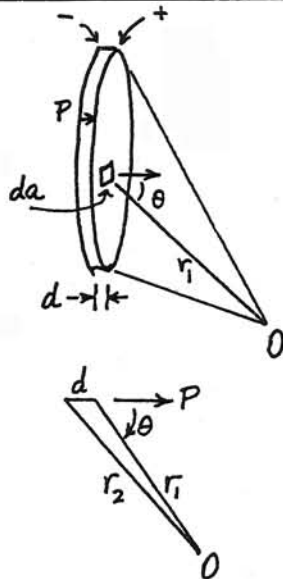
1-15. By Eq. (1.34) the system can be represented by two disks of surface charge density $(\rho_s)_b = P$, equal and opposite and separated by d . The potential at the observation point O , due to the charge on an element of area da of the positive face, is

$$d\Phi_+ = \frac{P da}{r_1}$$

That due to the corresponding element of area of the negative face is (using law of cosines)

$$\begin{aligned} d\Phi_- &= -\frac{P da}{r_2} \\ &= -\frac{P da}{\sqrt{r_1^2 + 2r_1 d \cos\theta + d^2}} \end{aligned}$$

where θ is the angle between \mathbf{P} and r_1 as shown in the sketch. Thus the total potential is



$$\begin{aligned} d\Phi &= \frac{P da}{r_1} \left[1 - \left(1 + \frac{2d}{r_1} \cos\theta + \frac{d^2}{r_1^2} \right)^{-1/2} \right] \\ &\approx \frac{P d da}{r_1^2} \cos\theta \end{aligned}$$

But $d\Omega = da \cos\theta / r_1^2$ is the solid angle subtended at O by this area element. Thus the integration over the face of the disk can be expressed in terms of the total solid angle subtended by the disk, $\Delta\Omega$, as

$$\Phi = P d \Delta\Omega$$

The sign convention for $\Delta\Omega$ can be taken that the solid angle is positive when the point O is in the half-space corresponding to the positive face of the disk, and negative when point O is in the half-space of the negative face.

The two sheets of surface charge density $\rho_s = \pm P$ comprise a parallel-plate capacitor geometry. By Gauss' law, the internal field magnitude is

$$E = 4\pi \rho_s = 4\pi P$$

in the sense opposite to \mathbf{P} . The \mathbf{D} field is, from its definition Eq. (1.28),

$$\mathbf{D} \equiv \mathbf{E} + 4\pi \mathbf{P} \rightarrow (-4\pi \mathbf{P}) + 4\pi \mathbf{P} = 0$$

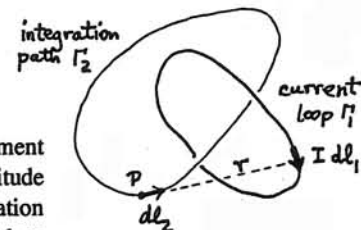
Note: For the electret the polarization \mathbf{P} is "frozen in" and the linear relation of Eq. (1.33) does not apply.

1-16. At a typical field point P , the magnetic field is given by the Biot-Savart integral

$$\mathbf{B}(P) = \oint_{\Gamma_1} \frac{I d\mathbf{l}_1 \times \mathbf{e}_r}{c r^2}$$

where \mathbf{e}_r is the unit vector from the source element $d\mathbf{l}_1$ to the field point P , and r is the scalar magnitude of the distance between $d\mathbf{l}_1$ and P . This integration is around the hardware current loop Γ_1 . We wish to evaluate the Ampèrian line integral of this field

$$\oint_{\Gamma_2} \mathbf{B} \cdot d\mathbf{l}_2$$



around the (mathematical) closed path Γ_2 . Thus the desired quantity is the double integral

$$\frac{I}{c} \oint_{\Gamma_2} \oint_{\Gamma_1} \frac{d\mathbf{l}_1 \times \mathbf{e}_r \cdot d\mathbf{l}_2}{r^2}$$

Now, at the point P the current loop subtends a certain solid angle Ω . When the point P advances by the step $d\mathbf{l}_2$, the subtended solid angle changes in a way that is equivalent to a displacement of all the elements of the current loop by $-d\mathbf{l}_2$ with respect to the original point P . Each $d\mathbf{l}_1$, displaced by $-d\mathbf{l}_2$, sweeps out an area of magnitude $|d\mathbf{l}_1 \times d\mathbf{l}_2|$. In general, this area is not normal to the direction of \mathbf{e}_r ; we need its normal projection to determine the solid angle. With due regard to sign, the increase in solid angle contributed by $d\mathbf{l}_1$ as P takes the step $d\mathbf{l}_2$ may thus be seen to be

$$d^2\Omega = \frac{[d\mathbf{l}_1 \times (-d\mathbf{l}_2)] \cdot \mathbf{e}_r}{r^2}$$

By the commutative properties of the triple scalar product [Eq. (A.18)], this differential solid angle is precisely the integrand of the previous integral. Hence

$$\oint_{\Gamma_2} \mathbf{B} \cdot d\mathbf{l}_2 = \frac{I}{c} \oint_{\Gamma_2} \oint_{\Gamma_1} d^2\Omega = \frac{I}{c} \oint_{\Gamma_2} d\Omega$$

where the first-order differential $d\Omega$ is the change in solid angle subtended by the *full* current loop Γ_1 when the observation point P takes the step $d\mathbf{l}_2$.

To evaluate this last integral, assume at first that the current loop Γ_1 is plane, and choose to begin and end the integration path Γ_2 where the integration path crosses the plane of the current loop, *outside* the area bounded by the loop. At that point the solid angle subtended by the current loop is then clearly zero. Let us further assume that the integration path *links* the current loop. Now, as the point P moves around the integration path, the solid angle grows from zero, to 2π (when P crosses the plane of the current loop, *inside* the loop's area), and finally to 4π (when P completes the circuit back to the starting point).

On the other hand, if the integration path *does not link* the current loop (i.e., the second crossing of the loop's plane is also *outside* the loop area), the solid angle rises to a positive maximum, returns to zero (when P crosses the plane, half-way around), rises to a negative maximum, and returns to zero (when P returns to the starting point). Thus the elapsed increment in solid angle is either 4π or zero, depending solely upon whether the integration path does or does not link the current loop.

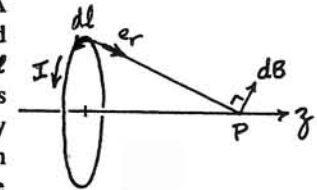
The special assumptions (a plane loop, and beginning and ending the integration in that plane) are not necessary so long as one handles the multivalued property of the solid

angle properly. But the three-dimensional spatial perceptions are difficult for most people!

As noted, it is then a relatively trivial matter to note that superposition allows Ampère's circuital law to apply to any number of linked current loops.

It is much more difficult to reverse the logic and derive the Biot-Savart law from Ampère's law. In the electrical analog the elementary electric source, a point charge q , permits invoking spherical-symmetry arguments (see Prob. 1-4) to "un-integrate" the flux integral of Gauss' law and find \mathbf{E} at a *point*—i.e., Coulomb's law for q . In the magnetic case, the analogous elementary source is the differential element $I d\mathbf{l}$, and Ampère's concept of "linking" fails. If one takes a full current loop as the magnetic source, there is no way to invoke symmetry to "un-integrate" Ampère's circulation integral. To accomplish this goal, therefore, one must convert Ampère's law to its differential-equation form, Eq. (1.41), and then find a way to solve it for the elementary source. The text does this, in a much broader context, in Section 9.3.

1-17. The geometry is shown in the figure. A typical current element $I d\mathbf{l}$ produces the vector field contribution $d\mathbf{B}$ at the point P . The angle between $d\mathbf{l}$ and \mathbf{e}_r is 90° , so Biot-Savart's cross product gives maximum magnitude. However, by symmetry, only the z component of \mathbf{B} will survive upon integration around the loop. With $d\ell = a d\varphi$, where φ is the azimuthal angle around the loop, the field is



$$\begin{aligned} B_z(z) &= \frac{I}{c} \int_0^{2\pi} \frac{a d\varphi}{(a^2+z^2)} \frac{a}{(a^2+z^2)^{1/2}} \\ &= \frac{I}{c} \frac{2\pi a^2}{(a^2+z^2)^{3/2}} \end{aligned}$$

(Note that the cosine of the angle between $d\mathbf{B}$ and the axis, to extract B_z , is the sine of the angle between \mathbf{e}_r and the axis.) The integral along the axis is then

$$\begin{aligned} \int_{-\infty}^{+\infty} B_z(z) dz &= \frac{2\pi a^2 I}{c} \int_{-\infty}^{+\infty} \frac{dz}{(a^2+z^2)^{3/2}} \\ &= \lim_{R \rightarrow \infty} \frac{2\pi a^2 I}{c} \left[\frac{z}{a^2(a^2+z^2)^{1/2}} \right]_{-R}^{+R} = \frac{4\pi I}{c} \end{aligned}$$

(The integral can be found in tables, or use the substitution $u = z/\sqrt{a^2+z^2}$.)

To make a closed path suitable for Ampère's circuital law, consider closing the z axis by a large semicircle of radius R . At large distances the loop looks like a dipole and therefore its field is of the order of a^2/R^3 [see Eq. (2.64)], while the semicircle's perimeter is proportional to R . Consequently the contribution of the semicircle to the line integral $\oint \mathbf{B} \cdot d\mathbf{l}$ is of order $(a/R)^2$, which can be made arbitrarily small.

1-18. Using the result of Prob. 1-17, develop a Taylor expansion about $z = h/2$. We will require the derivatives through order 4:

$$f(z) \equiv \frac{c}{2\pi a^2 I} B_z(z) = \frac{1}{(a^2+z^2)^{3/2}}$$

$$f' \equiv \frac{df}{dz} = -\frac{3z}{(a^2+z^2)^{5/2}}$$

$$f'' \equiv \frac{d^2f}{dz^2} = -\frac{3}{(a^2+z^2)^{5/2}} + \frac{15z^2}{(a^2+z^2)^{7/2}}$$

$$f''' \equiv \frac{d^3f}{dz^3} = \frac{(15+30)z}{(a^2+z^2)^{7/2}} - \frac{105z^3}{(a^2+z^2)^{9/2}}$$

$$f'''' \equiv \frac{d^4f}{dz^4} = \frac{45}{(a^2+z^2)^{7/2}} - \frac{(315+315)z^2}{(a^2+z^2)^{9/2}} + \frac{945z^4}{(a^2+z^2)^{11/2}}$$

Let the first loop be located in the plane $z = 0$. The Taylor expansion in the neighborhood of $z = h/2$ is (where $\zeta = z - h/2$)

$$\frac{c}{2\pi a^2 I} B_z\left(\frac{h}{2} + \zeta\right) = f\left(\frac{h}{2}\right) + \zeta f'\left(\frac{h}{2}\right) + \frac{\zeta^2}{2!} f''\left(\frac{h}{2}\right) + \frac{\zeta^3}{3!} f'''\left(\frac{h}{2}\right) + \frac{\zeta^4}{4!} f''''\left(\frac{h}{2}\right) + \dots$$

Now let the second loop be located in the plane $z = h$. Then its field at $z = +(h/2) + \zeta$ is equal to that of the first loop at $z = -(h/2) + \zeta$ (the loop currents are in the same sense). Observe that the odd-order derivatives are odd functions of z . Consequently all odd terms in the Taylor expansion for the second loop have opposite signs from the corresponding terms for the first loop, and these terms cancel when the two series are superposed. Thus we can write for the total field near $z = h/2$:

$$\begin{aligned} \frac{c}{2\pi a^2 I} B_z\left(\frac{h}{2} + \zeta\right) &= \frac{2}{[a^2+(h/2)^2]^{3/2}} \\ &+ \zeta^2 \left\{ -\frac{3}{[a^2+(h/2)^2]^{5/2}} + \frac{15(h/2)^2}{[a^2+(h/2)^2]^{7/2}} \right\} \\ &+ \frac{\zeta^4}{12} \left\{ \frac{45}{[a^2+(h/2)^2]^{7/2}} - \frac{630(h/2)^2}{[a^2+(h/2)^2]^{9/2}} + \frac{945(h/2)^4}{[a^2+(h/2)^2]^{11/2}} \right\} + \dots \end{aligned}$$

The first term is the one we want, a spatially constant field. The term proportional to ζ^2 can be made to *vanish* if we choose

$$a^2 + \left(\frac{h}{2}\right)^2 = 5 \left(\frac{h}{2}\right)^2 \quad \Rightarrow \quad h = a$$

The lowest-order *error* in this "uniform field" is now of 4th-order, proportional to ζ^4 . For this condition of optimum homogeneity, with N turns in each loop, the zeroth-order (nominal) field is

$$\begin{aligned} B_z\left(\frac{a}{2}\right) &= \frac{2\pi a^2 NI}{c} \frac{2}{[a^2+(a/2)^2]^{3/2}} = \frac{32\pi NI}{5^{3/2}ca} \quad (\text{Gaussian}) \\ &\rightarrow \frac{8\mu_0 NI}{5^{3/2}a} \quad (\text{SI units}) \end{aligned}$$

The ratio of the 4th-order (error) field to the nominal can be worked out to

$$\frac{B_4}{B_0} = -\frac{144}{125} \left(\frac{\zeta}{a}\right)^4$$

which remains small until ζ becomes comparable with a . The constraints on the three-dimensional magnetic field contained in the equations $\text{div } \mathbf{B} = 0$ and $\text{curl } \mathbf{B} = 0$ (no local currents near $z = a/2$) require that the field also remains very uniform as one moves out from the axis—that is, the error is no bigger than 4th-order throughout a spherical region centered on the axial point $z = a/2$.

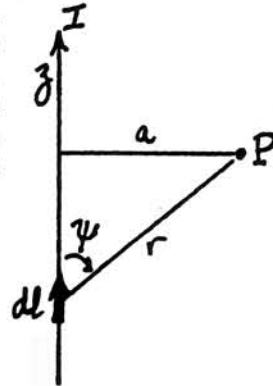
1-19. The Biot-Savart approach is straightforward but tedious because of the geometry of the integral, which becomes in this case:

$$\mathbf{B}(P) = \int \frac{I d\mathbf{l} \times \mathbf{e}_r}{cr^2} \rightarrow \frac{I}{c} \mathbf{e}_\phi \int \frac{\sin\psi dz}{r^2}$$

where ψ is the angle between the wire (z axis) and the radius vector (magnitude r) from the integration element ($d\ell \rightarrow dz$) to the field point P . The unit vector e_ϕ is in the right-handed azimuthal sense with respect to the current. Any one of the three variables z , r , and ψ is a candidate for the variable of integration. We will choose the angle ψ and express the other two in terms of it:

$$r = \frac{a}{\sin\psi}$$

$$z = \frac{a}{\tan\psi} \Rightarrow dz = \frac{a}{\sin^2\psi} d\psi$$



Therefore, the field is

$$\begin{aligned} \mathbf{B}(P) &= \frac{I}{c} e_\phi \int_0^\pi \sin\psi \left(\frac{\sin\psi}{a}\right)^2 \left(\frac{a d\psi}{\sin^2\psi}\right) \\ &= \frac{I}{ca} e_\phi \int_0^\pi \sin\psi d\psi = \frac{2I}{ca} e_\phi \end{aligned}$$

Ampère's law affords a much simpler analysis in this example because the system has axial symmetry. Paraphrasing Probs. 1-4 and 1-5, we can infer from the symmetry:

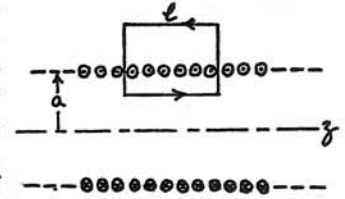
- (1) The *direction* of the magnetic field \mathbf{B} is azimuthal with respect to the wire.
- (2) The *magnitude* of the field depends only upon the radius (cylindrical coordinates).

Therefore if we choose a coaxial circle of radius a as the Ampèrian path of integration Γ (coinciding with a field-line of \mathbf{B}), the line integral reduces to scalar multiplication:

$$\oint_\Gamma \mathbf{B} \cdot d\ell \rightarrow \oint_\Gamma B_\phi(r) d\ell \rightarrow B_\phi(a) \oint_\Gamma d\ell = B_\phi(a) 2\pi a$$

Equating this value to $4\pi/c$ times the linked current I gives $B_\phi(a) = 2I/ca$, agreeing with the Biot-Savart result. [For the field *inside* a wire of finite radius, see Prob. 1-25.]

1-20. From the axial symmetry, we can argue that the magnetic field must be everywhere in the axial direction. The magnitude can be at most a function of radius. A visualization of the field-lines shows that they are dense (strong field) inside the solenoid, and very sparse ($\mathbf{B} \rightarrow 0$) outside. (A more complete argument for the vanishing of the exterior field is given in Section 2.7.)



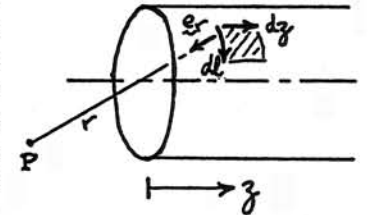
For the rectangular Ampèrian loop of length ℓ , shown in the sketch, we thus conclude that the only contribution to the line integral of \mathbf{B} is from the interior side parallel to z . Ampère's law then gives:

$$\oint \mathbf{B} \cdot d\ell \rightarrow B_z(r?) \ell = \frac{4\pi}{c} n \ell I$$

$$\mathbf{B} = \frac{4\pi n I}{c} e_z$$

In fact, there is no radial dependence—the field is uniform everywhere within the solenoid (except near the ends). Furthermore, this analysis is not restricted to solenoids of circular cross section. The cross section is arbitrary so long as it is constant with z .

1-21. The geometry of this problem is most easily perceived if we initially assume a solenoid of nearly circular cross section, and a field point P located so that it can "see" the inside surface and the far end of the solenoid. Consider a rectangular element of area on the surface of the solenoid, of dimensions dz in the axial direction by $d\ell$ in the azimuthal direction.



The orientation of this element of area is given by its (outward) normal, which is parallel to $d\ell \times dz$. The solid angle subtended at P by this element of area (seen from the inside) is then

$$d^2\Omega = \frac{(d\ell \times dz) \cdot (-e_r)}{r^2}$$

where e_r is the unit vector from the element to P . We can permute the triple scalar product [see Eq. (A.18)] to write this as

$$d^2\Omega = \frac{d\ell \times e_r \cdot dz}{r^2} \quad (1)$$

Now from the Biot-Savart law, Eq. (1.36), for a solenoid consisting of n turns per unit length, we have

$$d^2\mathbf{B} = \frac{n \, dz \, I}{c} \frac{d\mathbf{l} \times \mathbf{e}_r}{r^2} \quad (2)$$

which must be integrated over both z and the cross-sectional path Γ whose elements are $d\mathbf{l}$. Substituting (2) in (1), we have

$$\begin{aligned} d^2\Omega &= \frac{c}{n \, dz \, I} d^2\mathbf{B} \cdot d\mathbf{z} \\ &= \frac{c}{nI} d^2\mathbf{B} \cdot \frac{d\mathbf{z}}{dz} = \frac{c}{nI} d^2\mathbf{B} \cdot \mathbf{e}_z = \frac{c}{nI} d^2B_z \end{aligned}$$

That is,

$$d^2B_z = \frac{nI}{c} d^2\Omega$$

We see that integrating over the surface of the solenoid is equivalent simply to integrating over the aperture of the near end of the solenoid (if we assume that the solid angle subtended by the far end is negligible—if not, we will subtract that solid angle off). Thus

$$B_z(P) = \frac{nI}{c} \Delta\Omega \quad (3)$$

where $\Delta\Omega$ is the solid angle subtended at P by the near end (neglecting the far end).

When P is inside the solenoid (that is, within the cross section and with $z > 0$), $\Delta\Omega$ in (3) becomes larger than a half-space ($\Delta\Omega > 2\pi$). For this case, it may be more convenient to re-bookkeep $\Delta\Omega$ as the smaller solid angle looking "backwards" at the aperture of the end; that is, $\Delta\Omega(\text{new}) = 4\pi - \Delta\Omega(\text{old})$. When P moves a long way inside the semi-infinite solenoid, we obtain

$$B_z = \frac{4\pi nI}{c}$$

in agreement with Prob. 1-21.

Formula (3) is in fact general for any observation point P and any (constant) cross-sectional shape since the vector algebra remains valid. If the solid angle of the "far end" of the solenoid is not negligible, it can easily be subtracted out. Note that this calculation gives only the component B_z , not the full vector \mathbf{B} .

1-22. The function whose gradient we want is

$$f(\mathbf{r}, \mathbf{r}') \equiv \frac{1}{|\mathbf{r} - \mathbf{r}'|} = [(x-x')^2 + (y-y')^2 + (z-z')^2]^{-1/2}$$

Thus, for instance, by the chain rule of differentiation,

$$\frac{\partial}{\partial x} f(\mathbf{r}, \mathbf{r}') = - [\dots]^{-3/2} 2(x-x')(+1)$$

$$\frac{\partial}{\partial x'} f(\mathbf{r}, \mathbf{r}') = - [\dots]^{-3/2} 2(x-x')(-1)$$

The gradients, from Eq. (A.24), are then

$$\mathbf{grad}_{\mathbf{r}} f(\mathbf{r}, \mathbf{r}') = - \frac{(x-x')\mathbf{e}_x + \dots}{[\dots]^{3/2}} = - \frac{\mathbf{r} - \mathbf{r}'}{|\mathbf{r} - \mathbf{r}'|^3} = - \frac{\mathbf{e}_{\mathbf{r}-\mathbf{r}'}}{|\mathbf{r} - \mathbf{r}'|^2}$$

$$\mathbf{grad}_{\mathbf{r}'} f(\mathbf{r}, \mathbf{r}') = + \frac{(x-x')\mathbf{e}_x + \dots}{[\dots]^{3/2}} = + \frac{\mathbf{r} - \mathbf{r}'}{|\mathbf{r} - \mathbf{r}'|^3} = + \frac{\mathbf{e}_{\mathbf{r}-\mathbf{r}'}}{|\mathbf{r} - \mathbf{r}'|^2}$$

That is, switching between the source and field coordinates simply reverses the sign of the ∇ operator.

1-23. Without specified currents, we cannot use Eq. (1.46) to find \mathbf{A} , and so we must work backwards from Eq. (1.47). From Eq. (A.28), the z component of the curl is

$$(\mathbf{curl} \, \mathbf{A})_z \equiv \frac{\partial A_y}{\partial x} - \frac{\partial A_x}{\partial y} = B_z \rightarrow B_0$$

This differential equation is obviously satisfied by either of the candidate vector potentials:

$$\mathbf{A}_1: \quad A_{1x} = 0, \quad A_{1y} = B_0 x + f(y, z), \quad A_{1z} = 0$$

$$\mathbf{A}_2: \quad A_{2x} = -B_0 y + g(x, z), \quad A_{2y} = 0, \quad A_{2z} = 0$$

where f and g are arbitrary functions, and we omit the arbitrary constants that could be added to each of the six terms. However, the nonzero components are constrained by fact that the x and y components of the curl must vanish. For instance, f cannot be a function of z , because the derivative $\partial f / \partial z$ in $(\mathbf{curl} \, \mathbf{A})_x$ would give a nonzero component B_x . Likewise, g cannot depend upon z .

To further define \mathbf{A} , we are at liberty to choose a value for its divergence. For the conventional choice of $\text{div} \, \mathbf{A} = 0$ (see Section 4.5), we see that f cannot depend upon y , nor g upon x . Thus, f and g are at most constants. Even with this prescription of

the divergence, we still have the option of forming a linear combination of the two candidates,

$$\mathbf{A}_3 = a\mathbf{A}_1 + (1-a)\mathbf{A}_2$$

where a is an arbitrary constant. For instance, if $a = 1/2$, we can write the vector potential in coordinate-free style as

$$\mathbf{A} = -\frac{1}{2} \mathbf{r} \times \mathbf{B}_0$$

As noted in the text, the addition of the gradient of an arbitrary function will not change the curl of \mathbf{A} , and hence the resulting \mathbf{B} . If the arbitrary function is restricted to solutions of Laplace's equation, its gradient will not change $\text{div } \mathbf{A}$ either.

1-24. From Stokes' theorem, Eq. (A.54),

$$\oint_{\Gamma} \mathbf{A} \cdot d\boldsymbol{\ell} = \int_S \text{curl } \mathbf{A} \cdot d\mathbf{a} = \int_S \mathbf{B} \cdot d\mathbf{a}$$

where the closed line Γ (comprised of elements $d\boldsymbol{\ell}$) bounds the open surface S (comprised of elements $d\mathbf{a}$), in a right-handed sense with respect to the sense of $d\mathbf{a}$. The final integral is the conventional definition of the magnetic flux through a surface S [see Eq. (4.11)].

1-25. As in Prob. 1-19, we have axial symmetry and can use Ampère's circuital law, Eq. (1.37),

$$\oint \mathbf{B} \cdot d\boldsymbol{\ell} \rightarrow B_{\varphi}(r) 2\pi r$$

The current linked depends upon whether r is less or greater than a . Inside the wire,

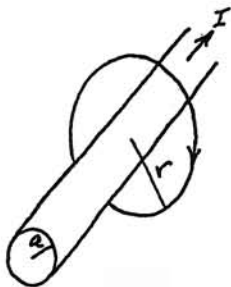
$$B_{\varphi}(r < a) 2\pi r = \frac{4\pi}{c} \left(\frac{I}{\pi a^2} \right) \pi r^2$$

$$\Rightarrow \mathbf{B} = \frac{2Ir}{ca^2} \mathbf{e}_{\varphi} \quad (r < a) \quad (1)$$

Outside the wire, as before,

$$B_{\varphi}(r < a) 2\pi r = \frac{4\pi}{c} I$$

$$\Rightarrow \mathbf{B} = \frac{2I}{cr} \mathbf{e}_{\varphi} \quad (r > a) \quad (2)$$



From Eq. (1.46) or (1.51), we know that the vector potential \mathbf{A} must be everywhere parallel (or antiparallel) to the straight current, i.e., the axis of the wire. By symmetry, the magnitude can depend at most upon r . Because \mathbf{A} is a potential, we can choose \mathbf{A} to be zero at an arbitrary point; for this geometry it is convenient to take this reference point at the surface of the wire (see Prob. 1-5).

As a Stokesian integration path, choose a rectangle in a plane containing the axis. One side coincides with the wire's surface; the opposite side is at a distance r from the axis. Let the length of these sides be ℓ . Then the line integral (circulation) of \mathbf{A} around this path is

$$\oint \mathbf{A} \cdot d\boldsymbol{\ell} \rightarrow \pm A_z(r) \ell$$

with the sign depending upon whether r is inside or outside the wire. From the circuital relation proved in Prob. 1-24, and formula (1) above, we have inside the wire

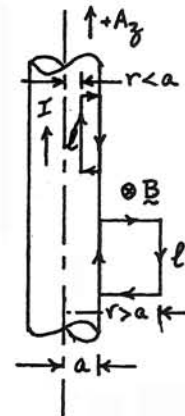
$$A_z(r) \ell = \int_r^a B_{\varphi}(r < a) \ell dr = \frac{I\ell}{ca^2} (a^2 - r^2)$$

$$\mathbf{A}(r) = \frac{I}{c} \left(1 - \frac{r^2}{a^2} \right) \mathbf{e}_z \quad (r < a)$$

And outside, using formula (2),

$$-A_z(r) \ell = \int_a^r B_{\varphi}(r < a) \ell dr = \frac{2I\ell}{c} \ln\left(\frac{r}{a}\right)$$

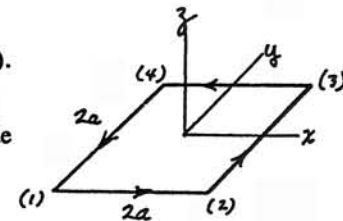
$$\mathbf{A}(r) = -\frac{I}{c} \ln\left(\frac{r^2}{a^2}\right) \mathbf{e}_z \quad (r > a)$$



1-26. The observation point is $\mathbf{r}_0 = (x_0, y_0, z_0)$.

The contribution to the vector potential from the side

between corners (1) and (2) is, from Eq. (1.46),



$$\begin{aligned}
 A_{x12} &= \frac{I}{c} \int_{-a}^{+a} \frac{dx}{|r_0 - r|} = \frac{I}{c} \int_{-a}^{+a} \frac{dx}{[(x_0 - x)^2 + (y_0 + a)^2 + z_0^2]^{1/2}} \\
 &= \frac{I}{cr_0} \int_{-a}^{+a} \left(1 - \frac{2x_0x}{r_0^2} + \frac{2y_0a}{r_0^2} + \frac{x^2}{r_0^2} + \frac{x^2}{r_0^2} \right)^{-1/2} dx \\
 &\approx \frac{I}{cr_0} \int_{-a}^{+a} \left(1 + \frac{x_0x}{r_0^2} - \frac{y_0a}{r_0^2} - \dots \right) dx \\
 &= \frac{I}{cr_0} \left(2a + 0 - \frac{2y_0a^2}{r_0^2} - \dots \right)
 \end{aligned}$$

Similarly, for the opposite side between corners (3) and (4),

$$A_{x34} = \frac{I}{cr_0} \left(-2a + 0 - \frac{2y_0a^2}{r_0^2} - \dots \right)$$

For the side between corners (2) and (3), we have

$$\begin{aligned}
 A_{y23} &= \frac{I}{c} \int_{-a}^{+a} \frac{dy}{[(x_0 - a)^2 + (y_0 - y)^2 + z_0^2]^{1/2}} \\
 &\approx \frac{I}{cr_0} \int_{-a}^{+a} \left(1 + \frac{x_0a}{r_0^2} + \frac{y_0y}{r_0^2} - \dots \right) dy \\
 &= \frac{I}{cr_0} \left(2a + \frac{2x_0a^2}{r_0^2} + 0 - \dots \right)
 \end{aligned}$$

And for the final side between corners (4) and (1),

$$= \frac{I}{cr_0} \left(-2a + \frac{2x_0a^2}{r_0^2} + 0 - \dots \right)$$

Thus to the lowest surviving order,

$$\mathbf{A} = \frac{4a^2I}{cr_0^3} (-y_0 \mathbf{e}_x + x_0 \mathbf{e}_y) \quad (1)$$

Now where \mathbf{e}_{r_0} is the unit vector in the r_0 direction, then

$$\mathbf{e}_z \times \mathbf{e}_{r_0} = \begin{vmatrix} \mathbf{e}_x & \mathbf{e}_y & \mathbf{e}_z \\ 0 & 0 & 1 \\ \frac{x_0}{r_0} & \frac{y_0}{r_0} & \frac{z_0}{r_0} \end{vmatrix} = -\frac{y_0}{r_0} \mathbf{e}_x + \frac{x_0}{r_0} \mathbf{e}_y$$

If we define the magnetic dipole moment in accord with Eq. (1.55) as

$$\mathbf{m} = \frac{I}{c} 4a^2 \mathbf{e}_z$$

then we can write

$$\mathbf{A} = \frac{\mathbf{m} \times \mathbf{e}_{r_0}}{r_0^2}$$

This formula is worked out for an arbitrary loop as Eq. (2.58). The field \mathbf{B} can be found by computing the curl of formula (1).

1-27. In the time Δt , the conduction electrons move with the average drift velocity u and advance by the distance $u \Delta t$ along the wire. That is, the number of electrons that cross a reference plane in the time Δt is the number that occupy the volume $(u \Delta t)(\Delta a)$, where Δa is the cross-sectional area of the wire. The current I is the rate at which charge crosses the reference plane, which is

$$I = q \frac{n(u \Delta t)(\Delta a)}{\Delta t} = nqu \Delta a$$

(a) The Lorentz force on one electron is

$$\mathbf{F}_q = \frac{q}{c} \mathbf{u} \times \mathbf{B}$$

In a wire element of length $d\ell$ and cross-sectional area Δa , there are $n d\ell \Delta a$ electrons. Consequently, the total force on all the conduction electrons in this element is

$$\begin{aligned}
 d\mathbf{F} &= (n d\ell \Delta a) \frac{q}{c} \mathbf{u} \times \mathbf{B} \\
 &= \frac{I d\ell}{c u} \mathbf{u} \times \mathbf{B}
 \end{aligned}$$

If we transfer the vector symbolism from the microscopic drift velocity \mathbf{u} to the wire element $d\ell$, then this simplifies to the standard macroscopic form,

$$d\mathbf{F} = \frac{1}{c} I d\ell \times \mathbf{B}$$

(b) On the model that the conduction electrons are free to move within the metal, the force just calculated will push the electrons sideways in the wire, but have no direct effect on the rigid lattice of copper atoms, which are positively charged but stationary. However, when the electrons are pushed sideways, they produce an excess of negative charge on one side and a deficiency of negative charge (i.e., an excess of positive

charge) on the other. This charge separation produces an *electric* field within the wire such that there is no net force on the electrons, $q\mathbf{E} = -q\mathbf{u} \times \mathbf{B}$. The electric field acts on the positively charged lattice to exert a force numerically equal to the Lorentz force. The existence of a sideways electric field, and the resulting difference of potential between the two sides of the wire, is known as the *Hall effect*.

1-28. From Prob. 1-19 the field of the long straight wire is

$$\mathbf{B}(r) = \frac{2I}{cr} \mathbf{e}_\phi$$

From Eq. (1.54) the force on the near side is

$$\begin{aligned} \mathbf{F}_{\text{near}} &= \frac{1}{c} \int_{\text{near}} I d\mathbf{l} \times \mathbf{B} \\ &= \frac{2I_1 I_2 a}{c^2 b} (\mathbf{e}_z \times \mathbf{e}_\phi) = \frac{2I_1 I_2 a}{c^2 b} (-\mathbf{e}_r) \end{aligned}$$

The outer side gives

$$\mathbf{F}_{\text{outer}} = \frac{2I_1 I_2 a}{c^2(a+b)} (+\mathbf{e}_r)$$

The sides perpendicular to the long wire involve an integration since B varies as $1/r$. However, it is easy to see that the forces on these two sides are equal and opposite, and contribute no net force to the rigid loop. Thus,

$$\begin{aligned} \mathbf{F}_{\text{total}} &= \frac{2I_1 I_2 a}{c^2} \left(-\frac{1}{b} + \frac{1}{a+b} \right) \mathbf{e}_r \\ &= \frac{2I_1 I_2 a^2}{c^2 b(a+b)} \mathbf{e}_r \end{aligned}$$

1-29. The force on element 1 due to the field of element 2 is

$$d^2\mathbf{F}_{12} = \frac{I_1 I_2}{c^2 r^2} d\mathbf{l}_1 \times [d\mathbf{l}_2 \times (-\mathbf{e}_r)]$$

where \mathbf{e}_r is the unit vector from element 1 to 2. Similarly, the force on 2 due to the field of 1 is

$$d^2\mathbf{F}_{21} = \frac{I_1 I_2}{c^2 r^2} d\mathbf{l}_2 \times [d\mathbf{l}_1 \times (+\mathbf{e}_r)]$$

Expanding the triple vector products using the "BAC-CAB" rule, Eq. (A.19), we have

$$d^2\mathbf{F}_{12} \propto -(\mathbf{e}_r \cdot d\mathbf{l}_1) d\mathbf{l}_2 + (d\mathbf{l}_1 \cdot d\mathbf{l}_2) \mathbf{e}_r$$

$$d^2\mathbf{F}_{21} \propto +(\mathbf{e}_r \cdot d\mathbf{l}_2) d\mathbf{l}_1 - (d\mathbf{l}_1 \cdot d\mathbf{l}_2) \mathbf{e}_r$$

The second terms are equal and opposite, but the first terms are not, in general. Now from Prob. 1-22,

$$\frac{\mathbf{e}_r}{r^2} = -\text{grad}_2 \left(\frac{1}{r} \right) = +\text{grad}_1 \left(\frac{1}{r} \right)$$

Thus

$$-d\mathbf{l}_2 \oint_1 \frac{\mathbf{e}_r \cdot d\mathbf{l}_1}{r^2} = -d\mathbf{l}_2 \oint_1 \text{grad}_1 \left(\frac{1}{r} \right) \cdot d\mathbf{l}_1$$



By extension of Eq. (A.25), the last integrand is the increment of $(1/r)$ over the step $d\mathbf{l}_1$, that is, it is an exact differential. Consequently upon traversing the closed loop 1, the total increment in $(1/r)$ is obviously zero. Thus the first term of the expansion of $d^2\mathbf{F}_{12}$ vanishes upon integration around circuit 1. Similarly the first term of $d^2\mathbf{F}_{21}$ vanishes upon integration around circuit 2. Since physical circuits carrying slowly varying currents must be closed loops, Newton's third law is satisfied.

1-30. (a) If the initial velocity is perpendicular to the magnetic field \mathbf{B} , the magnitude of the Lorentz force, Eq. (1.52), is

$$F = \frac{1}{c} |q\mathbf{u} \times \mathbf{B}| \rightarrow \frac{|q|}{c} u B$$

The direction of this force is perpendicular to the plane containing \mathbf{u} and \mathbf{B} . Thus the magnetic force does no work on the particle, and its speed $u = |\mathbf{u}|$ and kinetic energy $1/2 mu^2$ remain constant. Since the force is always perpendicular to the velocity, the particle moves in a circle, and its acceleration has the centripetal form u^2/R . Newton's equation of motion is

$$\frac{|q|}{c} u B = m \frac{u^2}{R}$$

The radius of the circular orbit is thus

$$R = \frac{mcu}{|q|B}$$

(b) The angular velocity has the magnitude

$$\omega = \frac{u}{R} = \frac{|q|B}{mc}$$

The sense of gyration is such that for a positive particle the vector angular velocity $\boldsymbol{\omega}$ is antiparallel to \mathbf{B} ; hence,

$$\boldsymbol{\omega} = -\frac{q}{mc} \mathbf{B}$$

(c) Any component of initial velocity parallel to \mathbf{B} produces no force and therefore remains constant. This general motion has the form of a *helix*.

1-31. Let \mathbf{E} be in the x direction, \mathbf{B} in the y direction; then $\mathbf{E} \times \mathbf{B}$ is in the z direction. Newton's equation of motion is

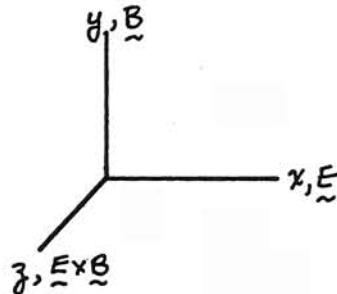
$$m \frac{d\mathbf{u}}{dt} = q \left(\mathbf{E} + \frac{\mathbf{u}}{c} \times \mathbf{B} \right) \quad (1)$$

We introduce the Galilean transformation such that

$$x' = x$$

$$y' = y$$

$$z' = z - c \frac{|\mathbf{E} \times \mathbf{B}|}{B^2} t$$



Using vector notation, we can write

$$\mathbf{u}' = \mathbf{u} - c \frac{\mathbf{E} \times \mathbf{B}}{B^2} \quad (2)$$

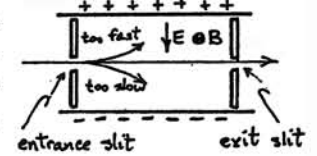
Substituting in (1),

$$\begin{aligned} m \frac{d\mathbf{u}'}{dt} &= q \left[\mathbf{E} + \frac{1}{c} \left(\mathbf{u}' + c \frac{\mathbf{E} \times \mathbf{B}}{B^2} \right) \times \mathbf{B} \right] \\ &= q \left[\mathbf{E} + \frac{\mathbf{u}'}{c} \times \mathbf{B} + \left(\frac{\mathbf{E} \cdot \mathbf{B}}{B^2} \right) \mathbf{B} - \left(\frac{\mathbf{B} \cdot \mathbf{B}}{B^2} \right) \mathbf{E} \right] \\ &= q \frac{\mathbf{u}'}{c} \times \mathbf{B} \end{aligned}$$

Thus in this reference frame the particle sees only the magnetic field, and the situation is that of Prob. 1-30. In the original reference frame, the motion appears as a *cycloid*

(see Prob. 1-32). Note that the "drift" direction $\mathbf{E} \times \mathbf{B}$ is independent of the sign of q . Note also that this nonrelativistic analysis is restricted to field magnitudes $E^2 \ll B^2$.

In the velocity selector, the collimated beam of particles enters the "crossed-field" region through a narrow slit. The particles leave the narrow exit slit when the electric and magnetic forces in Eq. (1.53) are precisely balanced, that is, when $u = cE/B$, independent of q or m .



1-32. For $\mathbf{B} = (0, B, 0)$,

$$\mathbf{u} \times \mathbf{B} = -\dot{z} B \mathbf{e}_x + \dot{x} B \mathbf{e}_z$$

And from Eq. (1) of Prob. 1-31,

$$m\ddot{x} = qE - \frac{q\dot{z}B}{c} \quad (1)$$

$$m\ddot{y} = 0 \quad (2)$$

$$m\ddot{z} = \frac{q\dot{x}B}{c} \quad (3)$$

For convenience, let the particle be located at the origin at $t = 0$, with the arbitrary initial velocity $\mathbf{u}_0 = (u_{0x}, u_{0y}, u_{0z})$. Equation (2) can be integrated immediately,

$$y = u_{0y} t \quad (4)$$

Now define:

$$\text{cyclotron frequency} \quad \omega_c \equiv \frac{qB}{mc}$$

$$\text{drift velocity} \quad V \equiv \frac{cE}{B}$$

Integrate Eq. (3) once, obtaining

$$\dot{z} = \omega_c x + u_{0z} \quad (5)$$

Substitute in Eq. (1), obtaining

$$\ddot{x} = \omega_c V - \omega_c(\omega_c x + u_{0z})$$

$$\ddot{x} + \omega_c^2 x = \omega_c(V - u_{0z})$$

The right-hand side being constant, this is the standard SHM equation for a displaced equilibrium. The solution for $x(t=0) = 0$, $\dot{x}(t=0) = u_{0x}$ is

$$x = \left(\frac{u_{0x}}{\omega_c}\right) \sin \omega_c t + \left(\frac{V - u_{0z}}{\omega_c}\right) (1 - \cos \omega_c t) \quad (6)$$

Substitute Eq. (6) in (5) and integrate,

$$\begin{aligned} \dot{z} &= u_{0x} \sin \omega_c t - (V - u_{0z}) \cos \omega_c t + V \\ z &= \left(\frac{u_{0x}}{\omega_c}\right) (1 - \cos \omega_c t) - \left(\frac{V - u_{0z}}{\omega_c}\right) \sin \omega_c t + Vt \end{aligned} \quad (7)$$

where the constant of integration has been added to make $z(t=0) = 0$. Equations (4), (6), and (7) describe the motion. Three constants of motion (the components of \mathbf{u}_0) appear; we could trivially add the components of an initial position \mathbf{r}_0 if we wished.

The oscillatory terms (sin and cos) average to zero, so the average velocity components are:

$$\begin{aligned} \langle \dot{x} \rangle &= 0 \\ \langle \dot{y} \rangle &= u_{0y} \\ \langle \dot{z} \rangle &= V \equiv \frac{cE}{B} \end{aligned}$$

An initial velocity component in the y direction (parallel to \mathbf{B}) is uninteresting. Consider initial velocities $\mathbf{u}_0 = (u_{0x}, 0, u_{0z})$, and rewrite Eqs. (6) and (7) in the form

$$\begin{aligned} x - \left(\frac{V - u_{0z}}{\omega_c}\right) &= \left(\frac{u_{0x}}{\omega_c}\right) \sin \omega_c t - \left(\frac{V - u_{0z}}{\omega_c}\right) \cos \omega_c t \\ z - \left(\frac{u_{0x}}{\omega_c}\right) &= Vt - \left(\frac{V - u_{0z}}{\omega_c}\right) \sin \omega_c t - \left(\frac{u_{0z}}{\omega_c}\right) \cos \omega_c t \end{aligned}$$

If we define the constants:

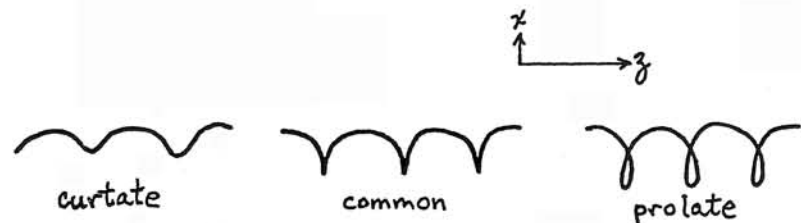
$$\begin{aligned} R &\equiv \left[\left(\frac{u_{0x}}{\omega_c}\right)^2 + \left(\frac{V - u_{0z}}{\omega_c}\right)^2 \right]^{1/2} \\ \tan \psi &\equiv \frac{V - u_{0z}}{\omega_c} \end{aligned}$$

then these equations can be put in the simpler form:

$$x - \left(\frac{V - u_{0z}}{\omega_c}\right) = R \sin(\omega_c t - \psi)$$

$$z - \left(\frac{u_{0x}}{\omega_c}\right) = Vt - R \cos(\omega_c t - \psi)$$

The constant offsets on the left could be eliminated by redefining the origin. The geometrical meaning of the right-hand sides can be seen by analogy with the motion of a lamp mounted on a wheel rolling in the $+z$ (or $\mathbf{E} \times \mathbf{B}$) direction, rotating at angular velocity ω_c . The wheel is of radius V/ω_c ; the lamp is mounted at radius R . When $\mathbf{u}_0 = (0, 0, V)$, the lamp is at the center of the wheel, and its trajectory is a straight line. When $R = V/\omega_c$ (for instance, when $\mathbf{u}_0 = 0$), the lamp is on the rim, and the motion is a common cycloid (with cusps). When the initial conditions are such that R is less than or greater than V/ω_c , the trajectory is a *curtate* or *prolate* cycloid, respectively:



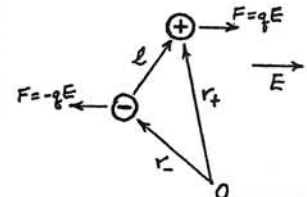
1-33. We model the electric dipole as a pair of charges $\pm q$ separated by the directed distance ℓ . In a uniform field, the two forces are equal and opposite, constituting a *couple*. The vector torque produced on a system by a set of forces is given by

$$\boldsymbol{\tau} = \sum_{\alpha} \mathbf{r}_{\alpha} \times \mathbf{F}_{\alpha}$$

Thus,

$$\begin{aligned} \boldsymbol{\tau}_e &= \mathbf{r}_+ \times q\mathbf{E} + \mathbf{r}_- \times (-q\mathbf{E}) \\ &= q(\mathbf{r}_+ - \mathbf{r}_-) \times \mathbf{E} = q\boldsymbol{\ell} \times \mathbf{E} = \mathbf{p} \times \mathbf{E} \end{aligned}$$

The magnetic dipole is modeled as a current loop of oriented (vector) area \mathbf{S} , with $\mathbf{m} = I\mathbf{S}/c$ as in Eq. (1.55). The force on an element $I d\boldsymbol{\ell}$ of the loop Γ is $d\mathbf{F} = (I/c)d\boldsymbol{\ell} \times \mathbf{B}$. Thus, recognizing that $d\boldsymbol{\ell} = d\mathbf{r}$ and using the "BAC-CAB" expansion of Eq. (A.19),



$$\begin{aligned}\tau_m &= \frac{I}{c} \oint_{\Gamma} \mathbf{r} \times (d\mathbf{r} \times \mathbf{B}) \\ &= \frac{I}{c} \oint_{\Gamma} (\mathbf{B} \cdot \mathbf{r}) d\mathbf{r} - \frac{I}{c} \oint_{\Gamma} \mathbf{B} (\mathbf{r} \cdot d\mathbf{r})\end{aligned}$$

For a spatially constant field \mathbf{B} , the second integrand is the exact differential $d(1/2r^2)$, which vanishes around a closed path. To evaluate the first integral, it is easiest to use the operator form of Stokes' theorem, Eq. (A.63),

$$\oint_{\Gamma} d\mathbf{r} [\dots] = \int_S d\mathbf{a} \times \nabla [\dots]$$

where $d\mathbf{a}$ is an element of any open surface S bounded by the closed loop Γ . In this case, the operand is $(\mathbf{B} \cdot \mathbf{r})$ [the identity has the form of Eq. (A.61)]:

$$\oint_{\Gamma} d\mathbf{r} (\mathbf{B} \cdot \mathbf{r}) = \int_S d\mathbf{a} \times \nabla (\mathbf{B} \cdot \mathbf{r})$$

But for a spatially constant \mathbf{B} , $\nabla (\mathbf{B} \cdot \mathbf{r}) = \nabla (B_x x + B_y y + B_z z) \rightarrow \mathbf{B}$. Using Eq. (1.55), the torque becomes

$$\tau_m = \frac{I}{c} \left(\int_S d\mathbf{a} \right) \times \mathbf{B} = \mathbf{m} \times \mathbf{B}$$

As noted, in a uniform field the net force on an electric dipole is zero because the forces on its constituents are equal and opposite. For the magnetic dipole, the net force is

$$\oint_{\Gamma} I d\mathbf{l} \times \mathbf{B} \rightarrow I \left(\oint_{\Gamma} d\mathbf{r} \right) \times \mathbf{B} = 0$$

where the integrand is again an exact differential.

1-34. Consider a cylindrical wire of radius a , length ℓ , carrying the current I . The current density is

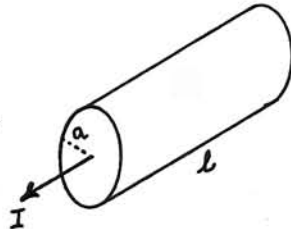
$$J = \frac{I}{\pi a^2}$$

and the potential difference (voltage) between the ends is

$$V = E \ell$$

The "microscopic" Ohm's law, $J = \sigma E$, becomes:

$$\frac{I}{\pi a^2} = \sigma \frac{V}{\ell}$$



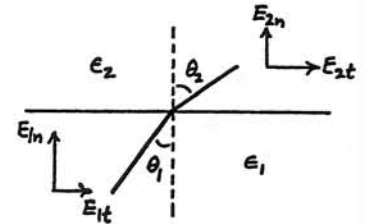
$$V = \left(\frac{\ell}{\sigma \pi a^2} \right) I = R I$$

where R is the macroscopic resistance, $R = \ell / \sigma \pi a^2$.

This analysis is elementary for the simple geometry of a long straight wire. It also applies to much more general "thin-wire" geometries (e.g., the wire wound into a coil) so long as the radius of curvature of the wire's axis is much larger than the wire's radius a , and any changes of radius with length ($da/d\ell$) are small. Under these assumptions, the current density J is essentially constant over an equipotential cross section, and the potential difference $V = \int \mathbf{E} \cdot d\mathbf{l}$ can be integrated along a path that coincides with a field-line of \mathbf{E} . The resistance is then given by the integral $\int d\ell / \sigma \pi a^2$.

1-35. The boundary conditions for the normal and tangential components of the electric field are, from Eqs. (1.85) and (1.89),

$$\begin{aligned}D_{1n} &= D_{2n} \Rightarrow \epsilon_1 E_{1n} = \epsilon_2 E_{2n} \\ E_{1t} &= E_{2t}\end{aligned}$$



(We assume that there is no free charge at the dielectric interface.) But from the geometry,

$$\tan \theta_1 = \frac{E_{1t}}{E_{1n}}$$

$$\tan \theta_2 = \frac{E_{2t}}{E_{2n}}$$

Thus

$$\frac{1}{\epsilon_1} \tan \theta_1 = \frac{1}{\epsilon_2} \tan \theta_2$$

The \mathbf{D} field-lines, being parallel to \mathbf{E} , obey the same rule. The \mathbf{D} field-lines are conserved across the interface so long as there is no free charge there; the \mathbf{E} lines can terminate on bound charges.

Snell's law for optical rays (see Section 6.2) is $n_1 \sin \theta_1 = n_2 \sin \theta_2$, where n_1 and n_2 are the refractive indices of the two media. For near-normal incidence (small angles θ), $\tan \theta \approx \sin \theta \approx \theta$. Thus the formulas have a similar form, with $(1/\epsilon) \leftrightarrow n$. Note that if one follows the analogy to make a "converging" dielectric lens for \mathbf{E} , it would be *concave* for typical dielectrics with $\epsilon > 1$ (compare the *convex* converging lens for optical media with $n > 1$).

The question of whether a dielectric lens can be used to "focus" an electric field is a subtle one. The short answer is "no". Light rays, which are a limiting solution of the wave equation, obey different rules from field-lines of \mathbf{E} , which relate to solutions of Laplace's equation. Light rays are determined by their source at one end of the system; they are not affected by the nature of the absorber at the output end. The electric field, pictorialized by field-lines, requires that both *sources* (positive charge) and *sinks* (negative charge) be specified, or the equivalent, on a *closed* surface surrounding the system. Field-lines do not necessarily travel in straight lines in a uniform medium. From the Maxwell stress tensor (Section 4.8) it can be shown that field-lines act like "furry rubber bands," which try to shrink along their length while pushing each other apart side-to-side. By contrast, the rays of geometrical optics do not interact with each other. Thus rays can cross each other at a focal point, whereas electric field-lines can cross only at those special points where the magnitude of the field happens to be zero (the field can't have two directions at the same point).

From Eqs. (1.92) and (1.95), for the magnetic field (with no free current on the interface),

$$B_{1n} = B_{2n}$$

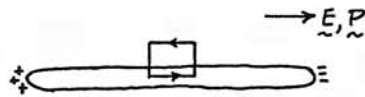
$$H_{1t} = H_{2t} \Rightarrow \frac{1}{\mu_1} B_{1t} = \frac{1}{\mu_2} B_{2t}$$

From the geometrical relations, as before, we obtain for a magnetic field-line,

$$\frac{1}{\mu_1} \tan \theta_1 = \frac{1}{\mu_2} \tan \theta_2$$

Both the \mathbf{B} and \mathbf{H} fields obey the same rule. The \mathbf{B} field-lines are conserved across the interface since there can be no magnetic monopoles, free or bound, on the interface; the \mathbf{H} lines can terminate on bound Coulomb-like sources (see Section 2.7).

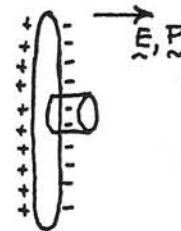
1-36. For the needle-shaped cavity, the surface charge density $(\rho_s)_b = \mathbf{n} \cdot \mathbf{P}$ on the boundary of the cavity is essentially restricted, by the dot product, to small areas at the two ends.



Because the cavity is long and thin, the small magnitude and large distance (squared) of these bound charges produce a negligible perturbation throughout most of the cavity. Thus the cavity \mathbf{E} -field remains equal to that in the medium. This fact can be seen more formally by constructing a Stokesian loop as shown and paraphrasing the argument leading to Eq. (1.89). The force on the test charge is $\mathbf{F} \equiv \delta q \mathbf{E}_{\text{cavity}} = \delta q \mathbf{E}_{\text{medium}}$.

For the disk-shaped cavity, the dielectric surface charges approximate a parallel-plate capacitor and contribute an \mathbf{E} -field of magnitude $4\pi\mathbf{P}$, parallel to the \mathbf{E} in the medium. The total \mathbf{E} -field in the cavity is the superposition of this cavity field and the global field produced by the unspecified distant sources,

$$\mathbf{E}_{\text{cavity}} = \mathbf{E} + 4\pi\mathbf{P}$$



But, by the definition of Eq. (1.28), this is just the \mathbf{D} -field in the medium. An argument using a Gaussian pillbox, as for Eq. (1.84), confirms that \mathbf{D} is the same in both cavity and medium. In this case, the force on the test charge is $\mathbf{F} \equiv \delta q \mathbf{E}_{\text{cavity}} = \delta q \mathbf{D}_{\text{medium}}$.

These arguments can be made rigorous for *ellipsoidal* cavities using methods analogous to those discussed in Section 3.3 (see Stratton St41, pp. 206-215). For ellipsoids of intermediate shape, between the limits of needle and disk, the cavity field turns out to be spatially *uniform*; it can be related to the medium field by geometrical coefficients known as the *depolarizing factor* [see Probs. 3-23 and 3-24].

1-37. For the vector potential \mathbf{A} , paraphrase the treatment of the vector fields in Section 1.8. For the tangential component (actually a two-dimensional vector), construct a rectangular Stokesian loop as shown in Fig. 1-12. The circulation of \mathbf{A} (line integral around a closed loop) is established in Prob. 1-24 as equal to the \mathbf{B} -field flux through the loop. As the width w of the rectangle shrinks to zero, the flux also goes to zero, and therefore the boundary condition for the tangential component is [paraphrasing Eqs. (1.89) and (1.94)]

$$(\mathbf{A}_2 - \mathbf{A}_1) \times \mathbf{n} = 0 \Rightarrow A_{1t} = A_{2t}$$

The normal component is found using a Gaussian pillbox as in Fig. 1-11. The flux of \mathbf{A} through a closed surface depends upon the choice of divergence of \mathbf{A} . If we take $\text{div } \mathbf{A} = 0$, then [paraphrasing Eqs.(1.84) and (1.92)],

$$(\mathbf{A}_2 - \mathbf{A}_1) \cdot \mathbf{n} = 0 \Rightarrow A_{1n} = A_{2n}$$

With this choice of divergence ("gauge"), the full three-dimensional vector potential is conserved across the interface [compare Eq. (1.90)],

$$\mathbf{A}_1 = \mathbf{A}_2$$

1-38. Consider the integral of the Gaussian function,

$$I = \int_{-\infty}^{+\infty} \exp\left(-\frac{x^2}{2a^2}\right) dx$$

Since x is a dummy variable, the *square* of this integral can be written in a way that allows a convenient change of variables:

$$\begin{aligned} I^2 &= \int_{-\infty}^{+\infty} \int_{-\infty}^{+\infty} \exp\left(-\frac{x^2+y^2}{2a^2}\right) dx dy \\ &= \int_0^{\infty} \exp\left(-\frac{r^2}{2a^2}\right) 2\pi r dr = \pi \int_0^{\infty} \exp\left(-\frac{u}{2a^2}\right) du \\ &= -2\pi a^2 \left[\exp\left(-\frac{u}{2a^2}\right) \right]_0^{\infty} = 2\pi a^2 \end{aligned}$$

Thus we conclude that the function as given has been *normalized* to unit area under the curve, for any value of a ,

$$\int_{-\infty}^{+\infty} F(x,a) dx = \frac{I}{\sqrt{2\pi} a} = 1$$

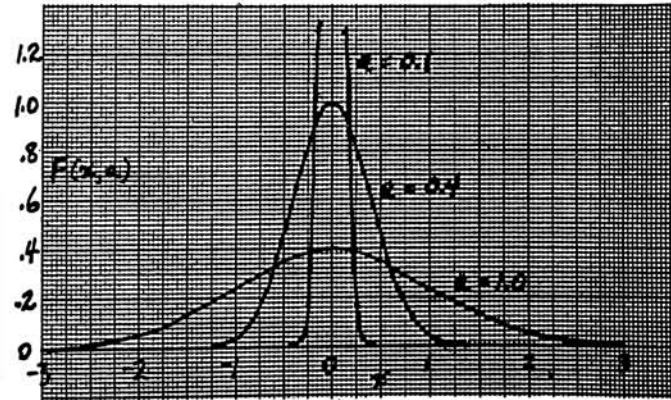
This is one of the defining properties of the Dirac delta function, stated in Eq. (1.97).

Changing the variable from x to $x-x_0$ simply shifts the center of the Gaussian from $x=0$ to x_0 , without changing the normalization. As seen in the graphs, the function $F(x-x_0,a)$ has a nonnegligible value only within approximately the range

$$x_0 - 3a \lesssim x \lesssim x_0 + 3a$$

(The parameter a is the *standard deviation* of the Gaussian function.) Thus the Δ function, incorporating the limit $a \rightarrow 0$, satisfies the other defining condition for the Dirac function, stated in Eq. (1.96).

When this limit of the Gaussian function appears as a factor in an integrand, as in Eq. (1.98), the integrand is essentially zero except when $x = x_0$. Therefore, by the mean-value theorem, the other factors in the integrand can be evaluated at $x = x_0$ and taken outside the integral.



Chapter 2

2-1. (a) On the *polar axis*,

$$E_{pa} = \frac{q}{(z-\ell)^2} - \frac{q}{(z+\ell)^2}$$

$$= \frac{q}{z^2} \left[\left(1 + \frac{2\ell}{z} + \dots\right) - \left(1 - \frac{2\ell}{z} + \dots\right) \right]$$

$$\rightarrow \frac{4q\ell}{z^3}$$

But $p = 2q\ell$, and \mathbf{E} is parallel to \mathbf{p} . Hence, vectorially,

$$\mathbf{E}_{pa} = \frac{2\mathbf{p}}{z^3}$$



(b) In the *equatorial plane*,

$$E_{ep} = 2 \frac{q}{(r^2 + \ell^2)} \cdot \frac{\ell}{(r^2 + \ell^2)^{3/2}}$$

$$= \frac{2q\ell}{r^3} \left(1 + \frac{\ell^2}{r^2}\right)^{-3/2} \rightarrow \frac{2q\ell}{r^3}$$

Or, vectorially,

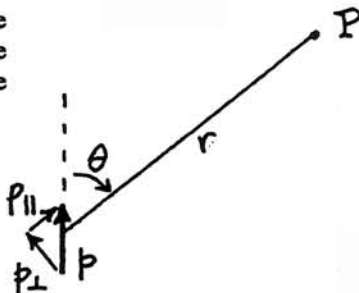
$$\mathbf{E}_{ep} = -\frac{\mathbf{p}}{r^3}$$

Note that both formulas are linear in (vector) \mathbf{p} , and inverse-cube in distance. One contains the factor 2, the other the negative sign.

(c) The field at the observation point P is the superposition of the polar-axis field of the component $p_{\parallel} = p \cos\theta$, and the equatorial-plane field of the component $p_{\perp} = p \sin\theta$. That is,

$$\mathbf{E}(r, \theta) = \frac{2p_{\parallel}}{r^3} \mathbf{e}_r + \frac{p_{\perp}}{r^3} \mathbf{e}_{\theta}$$

$$= \frac{p}{r^3} (2 \cos\theta \mathbf{e}_r + \sin\theta \mathbf{e}_{\theta})$$



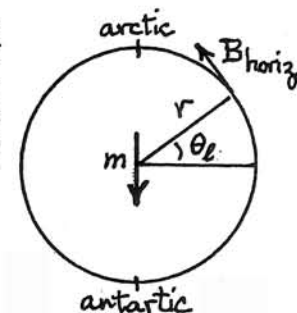
which is Eq. (2.29). Note that the direction of \mathbf{e}_{θ} is generally opposite to that of \mathbf{p} , so the negative sign is suppressed.

2-2. The geometry of the external fields of electric and magnetic dipoles is the same, so that the formulas of Prob. 2-1 can be adapted by simply replacing \mathbf{p} , \mathbf{E} by \mathbf{m} , \mathbf{B} . For a spherical Earth, the horizontal component is just the \mathbf{e}_{θ} component. However the latitude angle θ_l is measured from the equator instead of the pole. Thus

$$B_{\text{horiz}} = B_{\theta} = \frac{m \cos\theta_l}{R_E^3}$$

For $R_E = 6.37 \times 10^8$ cm,

$$m = \frac{(0.23)(6.37 \cdot 10^8)^3}{\cos 40^\circ} = 7.8 \times 10^{25} \text{ gauss-cm}^3$$



Note that the Earth's magnetic dipole points to Antarctica; the return field-lines point geographically north at the surface of the Earth. This corresponds to a current circulating in the opposite sense to the Earth's rotation. The magnitude for our very crude model can be found from Eq. (2.56) [Eq. (1.55)], $m = IS/c$:

$$I \sim \frac{mc}{\pi(R_E/3)^2} = \frac{(7.8 \cdot 10^{25})(3 \cdot 10^{10})}{\pi (2.12 \cdot 10^8)^2} = 1.7 \times 10^{19} \text{ statamperes}$$

$$= 5.5 \times 10^9 \text{ amperes}$$

(The conversion to SI units is found in Appendix D.)

2-3. Place the origin of a Cartesian coordinate system at the center of the dipole. Expand the field \mathbf{E} in a three-dimensional Taylor (Maclaurin) series about this origin:

$$\mathbf{E}(x, y, z) = \mathbf{E}_0 + \left(\frac{\partial \mathbf{E}}{\partial x}\right)_0 x + \left(\frac{\partial \mathbf{E}}{\partial y}\right)_0 y + \left(\frac{\partial \mathbf{E}}{\partial z}\right)_0 z + \dots$$

$$= \mathbf{E}_0 + (\mathbf{r} \cdot \mathbf{grad})\mathbf{E} + \dots$$

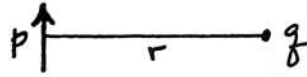
(This expression is shorthand for Taylor series for each of the three components E_x, E_y, E_z .) Now sum the (vector) forces on a model dipole consisting of charges $\pm q$ at positions $\pm \ell$, respectively:

$$\mathbf{F} = q [\mathbf{E}_0 + (\ell \cdot \mathbf{grad})\mathbf{E} + \dots] - q [\mathbf{E}_0 - (\ell \cdot \mathbf{grad})\mathbf{E} + \dots]$$

$$= 2q (\ell \cdot \mathbf{grad})\mathbf{E} + \dots \rightarrow (\mathbf{p} \cdot \mathbf{grad})\mathbf{E}$$

This leading term of the expansion gives the correct force so long as the \mathbf{E} field does not change appreciably over the dipole's structure size (ℓ in our model).

For the interaction of a point charge with a dipole, in case (1) the charge q is located in the "equatorial plane" of the dipole. Thus from Prob. 2-1(b), the force is



$$\mathbf{F}_{\text{on } q} = q \mathbf{E}_{\text{ep}}(p) = -\frac{qp}{r^3} \mathbf{e}_p \quad (1)$$

where \mathbf{e}_p is the unit vector in the direction of \mathbf{p} . In case (2) the force on \mathbf{p} is

$$\mathbf{F}_{\text{on } p} = (\mathbf{p} \cdot \mathbf{grad}) \mathbf{E}(q)$$

where of course $\mathbf{E}(q)$ is spherically symmetrical. The operator $(\mathbf{p} \cdot \mathbf{grad})$ is the spatial-derivative operator in the direction of \mathbf{e}_p . It might appear that the field due to q , at p , is changing only in the direction radial from q , and therefore that the derivative in the \mathbf{e}_p direction is zero. Not so!—although the field's magnitude does not change, its direction does change. In terms of a coordinate system with origin at q , x axis towards p , and y axis parallel to \mathbf{p} , the field near p is:

$$E_x = \frac{q}{(x^2+y^2)^{3/2}} \frac{x}{(x^2+y^2)^{1/2}} \approx \frac{q}{x^2}$$

$$E_y = \frac{q}{(x^2+y^2)^{3/2}} \frac{y}{(x^2+y^2)^{1/2}} \approx \frac{qy}{x^3}$$

$$E_z = \frac{q}{(x^2+y^2)^{3/2}} \frac{z}{(x^2+y^2)^{1/2}} \approx \frac{qz}{x^3}$$

The relevant operator is

$$\mathbf{p} \cdot \mathbf{grad} \rightarrow p \frac{\partial}{\partial y}$$

Thus q 's force on p is

$$\begin{aligned} \mathbf{F}_{\text{on } p} &= p \frac{\partial}{\partial y} \left(\frac{q}{x^2} \mathbf{e}_x + \frac{qy}{x^3} \mathbf{e}_y + \frac{qz}{x^3} \mathbf{e}_z \right) \\ &= p \frac{q}{x^3} \mathbf{e}_y \end{aligned} \quad (2)$$

which, with $x \rightarrow r$ and $\mathbf{e}_y \rightarrow \mathbf{e}_p$, is equal and opposite to (1), in agreement with Newton's action and reaction.

2-4. (a) The field of a unit source charge is $\mathbf{E}^{(1)} = \mathbf{e}_r/r^2$. Thus the rule gives

$$\mathbf{E}^{(2)} = -(\mathbf{p} \cdot \mathbf{grad}) \left(\frac{\mathbf{e}_r}{r^2} \right)$$

From Eq. (2.24), we have

$$\mathbf{E}^{(2)} = -\mathbf{grad} \left(\frac{\mathbf{p} \cdot \mathbf{r}}{r^3} \right) = -\mathbf{grad} \left(\mathbf{p} \cdot \frac{\mathbf{e}_r}{r^2} \right)$$

This has the form of $\mathbf{grad}(\mathbf{A} \cdot \mathbf{B})$, which can be expanded by the identity of Eq. (A.37). Since \mathbf{p} is a constant vector, the expansion gives

$$\mathbf{E}^{(2)} = -(\mathbf{p} \cdot \mathbf{grad}) \left(\frac{\mathbf{e}_r}{r^2} \right) - \mathbf{p} \times \mathbf{curl} \left(\frac{\mathbf{e}_r}{r^2} \right)$$

But the monopole field is conservative, and its curl vanishes [Eq. (1.12)]. Therefore the two expressions for $\mathbf{E}^{(2)}$ are equivalent, and work out to Eq. (2.28) or (2.29).

(b) The potential produced by a unit monopole is $\Phi^{(1)} = 1/r$. Thus

$$\Phi^{(2)} = -(\mathbf{p} \cdot \mathbf{grad}) \left(\frac{1}{r} \right)$$

which is equivalent to Eq. (2.21).

(c) The electrostatic potential at a point is the potential energy per unit test charge placed at that point, $\Phi = U^{(1)}/q_t$. The potential energy of the dipole is

$$U^{(2)} = +(\mathbf{p} \cdot \mathbf{grad}) \Phi = -\mathbf{p} \cdot \mathbf{E}$$

where $\mathbf{E} = -\mathbf{grad}\Phi$ is the field produced by other sources. This is the well-known formula for the potential energy of a dipole, which can be found by integrating the torque of Prob. 1-33 with respect to angle.

The meaning of this operator can be seen from the analysis of Prob. 2-3. Because the dipole charges are equal and opposite, their zero-order (monopole) effects cancel identically. The first-order terms of any Taylor expansion don't quite cancel, because of the slight offset between the dipole charges, and are expressed by this operation on whatever function is being Taylor-expanded. The sign results from whether the dipole is at the source or field (test) end of the radius vector, in the spirit of Prob. 1-22.

2-5. (a) From Eq. (2.7), the dipole potential is $\Phi = p \cos\theta/r^2$. Thus

$$r_\Phi = \sqrt{\frac{p \cos\theta}{\Phi}} = R_\Phi \sqrt{|\cos\theta|}$$

with the radius parameter $R_\Phi = \sqrt{p/|\Phi|}$, where Φ is the potential value on that surface.

(b) The dipole field is given in spherical coordinates by Eqs. (2-9) or (2-29). If the function $r_E(\theta)$ is to represent a field-line, then it must obey the differential equation

$$\begin{aligned} \frac{dr_E}{r_E d\theta} &= \frac{E_r}{E_\theta} = \frac{2 \cos\theta}{\sin\theta} \\ \int_{R_E}^{r_E} \frac{dr_E}{r_E} &= \int_{\pi/2}^{\theta} \frac{2 d(\sin\theta)}{\sin\theta} \\ \rightarrow \ln\left(\frac{r_E}{R_E}\right) &= 2 \ln\left(\frac{\sin\theta}{1}\right) \rightarrow r_E = R_E \sin^2\theta \end{aligned}$$

where we chose the lower θ limit of $\pi/2$ so that the integration constant R_E is the radius at which a particular field-line crosses the "equatorial plane" of the dipole.

In drawing quantitative plots of dipole field-lines, such as Fig. 2-11, it turns out to be a nontrivial matter to choose a set of R_E values so that the field-lines are spaced in a meaningful way. How would you choose them?

2-6. The diagram for the two-dimensional case is essentially the same as Fig. 2-1, except we now understand that the "charges" are *line* charges perpendicular to the page, and the vectors \mathbf{r} , \mathbf{R}_1 , and \mathbf{R}_2 lie in the plane of the diagram. The field of each line charge is inverse-first-power in r , and the potential is logarithmic (see Prob. 1-5). For one line charge, the equipotentials are of course concentric circles. For the pair of line charges, we expect something qualitatively like Fig. 2-2.

(a) The analog of Eq. (2.1) gives the potential as

$$\Phi(r, \theta) = -2\rho_\ell (\ln R_1 - \ln R_2) = 2\rho_\ell \ln\left(\frac{R_2}{R_1}\right)$$

From Fig. 2-1, in the limit $r \gg \ell$, we can approximate

$$R_1 \approx r - \ell \cos\theta, \quad R_2 \approx r + \ell \cos\theta$$

from which it follows that

$$\frac{R_2}{R_1} \approx 1 + 2 \frac{\ell}{r} \cos\theta$$

The power-series expansion for the natural logarithm is $\ln(1+x) = x - x^2/2 + \dots$. Therefore the lowest-order surviving term (the dipole approximation) is

$$\Phi_\ell^{(2)} = 2\rho_\ell \frac{\ell}{r} \cos\theta = p_\ell \frac{\cos\theta}{r} = \frac{\mathbf{p}_\ell \cdot \mathbf{e}_r}{r}$$

where $\mathbf{p}_\ell = 2\rho_\ell \ell$ is the dipole moment per-unit-length, and $\mathbf{r} = r \mathbf{e}_r$ is the radius vector in cylindrical coordinates. This compares with Eq. (2.7) for the three-dimensional dipole. The potential is zero everywhere in the midplane ($\theta = \pi/2$), as well as at large cylindrical radius.

(b) The field components (in cylindrical coordinates) are

$$\begin{aligned} E_r &= -\frac{\partial\Phi}{\partial r} = p_\ell \frac{\cos\theta}{r^2} \\ E_\theta &= -\frac{\partial\Phi}{r \partial\theta} = p_\ell \frac{\sin\theta}{r^2} \\ (\mathbf{E})_\ell^{(2)} &= \frac{p_\ell}{r^2} (\cos\theta \mathbf{e}_r + \sin\theta \mathbf{e}_\theta) \end{aligned}$$

This differs from the 3-d Eq. (2.29) by the omission of the factor of 2 in the radial component.

(c) Paraphrasing Prob. 2-5, the function $r_\Phi(\theta)$ representing an equipotential is, from Part (a),

$$r_\Phi = \frac{p_\ell}{\Phi_\ell} \cos\theta = R_\Phi |\cos\theta|$$

where again the parameter $R_\Phi = p_\ell/|\Phi_\ell|$ is the intersection distance along the "polar axis" of the dipole. Here there is no square-root as there was for the 3-d dipole.

For the 2-d field-line,

$$\begin{aligned} \frac{dr_E}{r_E d\theta} &= \frac{E_r}{E_\theta} = \frac{\cos\theta}{\sin\theta} \\ \int_{R_E}^{r_E} \frac{dr_E}{r_E} &= \int_{\pi/2}^{\theta} \frac{d(\sin\theta)}{\sin\theta} \\ \rightarrow \ln\left(\frac{r_E}{R_E}\right) &= \ln\left(\frac{\sin\theta}{1}\right) \rightarrow r_E = R_E \sin\theta \end{aligned}$$

where again the integration constant R_E is the radius at which a particular field-line crosses the "equatorial plane" of the dipole. The $\sin\theta$ is no longer squared as it was for the 3-d dipole's field-lines. In this 2-d case, the equipotentials and field-lines have the same form (sine equals cosine rotated by 90°). Both formulas create *circles* of radius $R/2$, all passing through the dipole origin. The 3-d curves are flattened and elongated as shown in Fig. 2-2.

2-7. (a) From the preceding problem, the potential is

$$\Phi = 2\rho\ell \ln\left(\frac{R_2}{R_1}\right) = -2\rho\ell \ln(\Gamma)$$

$$\Gamma = \exp\left(-\frac{\Phi}{2\rho\ell}\right)$$

Thus an equipotential is a locus of constant Γ . For the Cartesian coordinates suggested, the R radii are given by:

$$R_1^2 = (x - \ell)^2 + y^2$$

$$R_2^2 = (x + \ell)^2 + y^2$$

Thus

$$\Gamma^2 = \left(\frac{R_1}{R_2}\right)^2 = \frac{(x - \ell)^2 + y^2}{(x + \ell)^2 + y^2}$$

$$\Gamma^2 x^2 + 2\ell\Gamma^2 x + \ell^2\Gamma^2 + \Gamma^2 y^2 = x^2 - 2\ell x + \ell^2 + y^2$$

$$\left[x - \ell\left(\frac{1+\Gamma^2}{1-\Gamma^2}\right)\right]^2 + y^2 = \left(\frac{2\ell\Gamma}{1-\Gamma^2}\right)^2$$

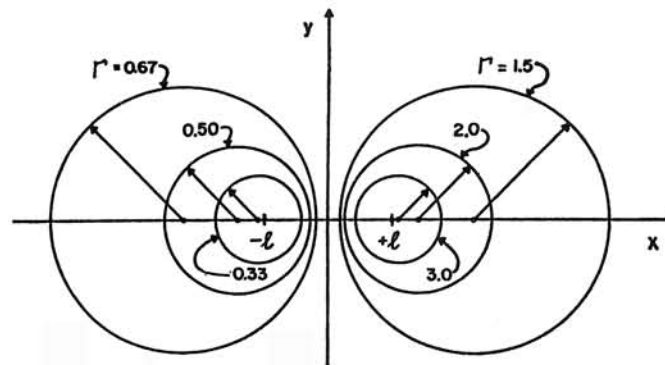
This is the equation of a displaced circle (cylinder in 3-d), with center at $(X_c, 0)$ and radius R_Φ given by:

$$X_c = \ell\left(\frac{1+\Gamma^2}{1-\Gamma^2}\right) = \ell \coth\left(\frac{\Phi}{2\rho\ell}\right)$$

$$R_\Phi = \frac{2\ell\Gamma}{|1-\Gamma^2|} = \ell \frac{1}{|\sinh(\Phi/2\rho\ell)|}$$

For $\Gamma < 1$, corresponding to $\Phi > 0$, the circles are nested about the positive line charge, with $\Gamma \rightarrow 0$ and $\Phi \rightarrow +\ln(\infty)$ at the line. For $\Gamma = 1$ and $\Phi = 0$, the equipotential circle becomes the line (plane) of symmetry at $x = 0$ (with

$X_c \approx R_\Phi \rightarrow \infty$). For $\Gamma > 1$ and $\Phi < 0$, the circles are nested about the negative line charge.



(b) To apply to parallel wires of radius a , center-to-center separation $2d$, we first note that equal and opposite potentials, $\pm\Delta\Phi_0/2$, correspond to reciprocal values of Γ :

$$\Gamma_+ = \frac{1}{\Gamma_-} = \exp\left(-\frac{\Delta\Phi_0}{4\rho\ell}\right)$$

Then

$$a = R_\Phi = 2\ell\left(\frac{\Gamma_+}{1-\Gamma_+^2}\right) = \ell \frac{1}{\sinh(\Delta\Phi_0/4\rho\ell)}$$

$$d = X_c = \ell\left(\frac{1+\Gamma_+^2}{1-\Gamma_+^2}\right) = \ell \coth(\Delta\Phi_0/4\rho\ell)$$

Hence

$$\frac{\Delta\Phi_0}{4\rho\ell} = \cosh^{-1}\left(\frac{d}{a}\right)$$

and the capacitance per unit length of the parallel wires is

$$C_\ell \equiv \frac{\rho\ell}{\Delta\Phi_0} = \frac{1}{4 \cosh^{-1}(d/a)}$$

Further applications are discussed by Edmonds and Corson, *Am.J.Phys.* **54**, 811 (1986).

2-8. By Eq. (2.22) the dipole moment of a system of charges is

$$\mathbf{p} = \sum_{\alpha} q_{\alpha} \mathbf{r}'_{\alpha}$$

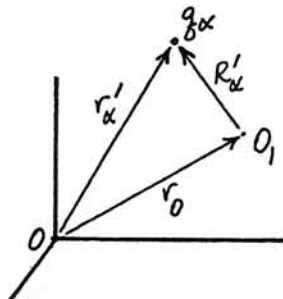
Express the position vectors in terms of an intermediate origin O' , located from the original origin O by the vector \mathbf{r}_0 ,

$$\mathbf{r}'_{\alpha} = \mathbf{r}_0 + \mathbf{R}'_{\alpha}$$

Then,

$$\mathbf{p} = \sum q_{\alpha} (\mathbf{r}_0 + \mathbf{R}'_{\alpha}) = \mathbf{r}_0 \sum q_{\alpha} + \sum q_{\alpha} \mathbf{R}'_{\alpha}$$

If the system has zero net charge ($\sum q_{\alpha} = 0$), the dipole moment is independent of the location \mathbf{r}_0 of the origin.



2-9. From Eq. (2.35) the quadrupole tensor in full glory is

$$\{\mathbf{Q}\} = \begin{pmatrix} \sum q(2x^2 - y^2 - z^2) & \sum q(3xy) & \sum q(3xz) \\ \sum q(3xy) & \sum q(-x^2 + 2y^2 - z^2) & \sum q(3yz) \\ \sum q(3xz) & \sum q(3yz) & \sum q(-x^2 - y^2 + 2z^2) \end{pmatrix}$$

For a single charge $+q$ at $(0, 0, +\ell)$,

$$\{\mathbf{Q}\} = \begin{pmatrix} -q\ell^2 & 0 & 0 \\ 0 & -q\ell^2 & 0 \\ 0 & 0 & +2q\ell^2 \end{pmatrix}$$

For an equal-and-opposite charge $-q$ at $(0, 0, -\ell)$, the quadrupole tensor is exactly the negative. Thus the total $\{\mathbf{Q}\}$ vanishes for the pair, constituting a finite-size dipole. If, however, the origin is chosen somewhere other than the center of the dipole, the dipole's $\{\mathbf{Q}\}$ does not vanish, in general. The dipole moment \mathbf{p} , being the lowest-order moment of this system, is independent of origin, as shown in Prob. 2-8.

2-10. When x_3 is the symmetry axis of the charge distribution, the quadrupole moment is [discrete form of Eq. (2.42)]

$$Q \equiv Q_{33} = \sum_{\alpha} q_{\alpha} (3x'_{\alpha 3} x'_{\alpha 3} - r'_{\alpha 3}{}^2)$$

The quadrupole tensor is diagonal and, by Eq. (2.38),

$$Q_{11} = Q_{22} = -\frac{1}{2}Q_{33}$$

Thus Eq. (2.34) gives

$$\begin{aligned} \Phi^{(4)} &= \frac{1}{6} \sum_{ij} Q_{ij} \left(\frac{3x_i x_j - r^2 \delta_{ij}}{r^5} \right) \\ &= \frac{1}{6} \left(-\frac{1}{2}Q \right) \left(\frac{3x_1^2 - r^2}{r^5} \right) + \frac{1}{6} \left(-\frac{1}{2}Q \right) \left(\frac{3x_2^2 - r^2}{r^5} \right) + \frac{1}{6} (+Q) \left(\frac{3x_3^2 - r^2}{r^5} \right) \\ &= \frac{Q}{r^5} \left(-\frac{1}{4}x_1^2 - \frac{1}{4}x_2^2 + \frac{1}{2}x_3^2 \right) = \frac{Q}{r^5} \left(\frac{3}{4}x_3^2 - \frac{1}{4}r^2 \right) \end{aligned}$$

But with the polar axis of spherical coordinates aligned with the symmetry axis x_3 ,

$$\cos\theta = \frac{x_3}{r}$$

so that

$$\Phi^{(4)}(r, \theta) = \frac{1}{2} \frac{Q}{r^3} \left(\frac{3}{2} \cos^2\theta - \frac{1}{2} \right)$$

This peculiar factoring of the numerical coefficient anticipates the conventional normalization of the second-order Legendre polynomial, $P_2(\cos\theta)$ [see Eqs. (3.39) and (3.41)].

2-11. We wish to recast Eq. (2.34),

$$\Phi^{(4)} = \frac{1}{6} \sum_{ij} Q_{ij} \left(\frac{3x_i x_j - r^2 \delta_{ij}}{r^5} \right)$$

By Eq. (A.88),

$$\mathbf{r} \cdot \{\mathbf{Q}\} \cdot \mathbf{r} = \sum_{ij} x_i Q_{ij} x_j = \sum_{ij} Q_{ij} x_i x_j$$

With $\mathbf{e}_r = \mathbf{r}/r$, the first term of the potential is

$$\frac{1}{6} \sum_{ij} Q_{ij} \left(\frac{3x_i x_j}{r^5} \right) = \frac{1}{2} \frac{\mathbf{e}_r \cdot \{\mathbf{Q}\} \cdot \mathbf{e}_r}{r^3}$$

The second term is, using Eq. (2.40),

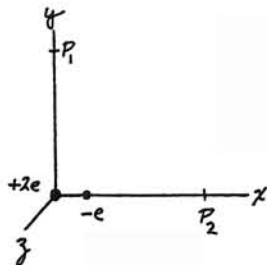
$$-\frac{1}{6r^3} \sum_{ij} Q_{ij} \delta_{ij} = -\frac{1}{6r^3} \sum_i Q_{ii} = 0$$

Thus the new form of the first term is a complete expression for $\Phi^{(4)}$.

2-12. (a) Direct calculation from Eq. (1.21):

$$\Phi(P_1) = \frac{2e}{5} - \frac{e}{\sqrt{26}} = 0.2039 e$$

$$\Phi(P_2) = \frac{2e}{5} - \frac{e}{4} = 0.1500 e$$



(b) The general multipole expansion is given in Eqs. (2.19–20).

$$\text{monopole moment: } q = 2e - e = +e$$

$$\Phi^{(1)}(P_1) = \Phi^{(1)}(P_2) = \frac{q}{r} = \frac{e}{5} = 0.200 e$$

From Eqs. (2.22–23),

$$\text{dipole moment: } p_x = (+2e)(0) + (-e)(1) = -e \Rightarrow \mathbf{p} = -e \mathbf{e}_x$$

$$\Phi^{(2)}(P_1) = \frac{\mathbf{p} \cdot \mathbf{e}_r}{r^2} = \frac{e \cos 90^\circ}{25} = 0$$

$$\Phi^{(2)}(P_2) = \frac{\mathbf{p} \cdot \mathbf{e}_r}{r^2} = \frac{e \cos 180^\circ}{25} = -0.040 e$$

From Eqs. (2.34–35),

$$\text{quadrupole tensor: } \{\mathbf{Q}\} = \begin{pmatrix} -2e & 0 & 0 \\ 0 & +e & 0 \\ 0 & 0 & +e \end{pmatrix}$$

$$\Phi^{(4)}(P_1) = \frac{1}{6} \sum_i Q_{ii} \frac{3x_i^2 - r^2}{r^5} = \frac{1}{6} e \frac{(2 + 2 - 1)}{5^3} = 0.004 e$$

$$\Phi^{(4)}(P_2) = \frac{1}{6} e \frac{(-4 - 1 - 1)}{5^3} = -0.008 e$$

[Since the charge distribution is axially symmetric about the $x = x_1$ axis, the quadrupole potentials could be found from Eq. (2.43), with $Q = Q_{11} = -2e$, and $\theta_1 = 90^\circ$, $\theta_2 = 0$.] Thus the first three terms of the multipole series are:

$$\Phi(P_1) = e (0.200 + 0 + 0.004 + \dots) \approx e (0.204)$$

$$\Phi(P_2) = e (0.200 - 0.040 - 0.008 + \dots) \approx e (0.152)$$

Because the finite size of the charge distribution extends in the x direction from the origin, P_2 is effectively closer than P_1 , and its series converges somewhat more slowly.

2-13. Using Eq. (2.35) in the given coordinate system, we have

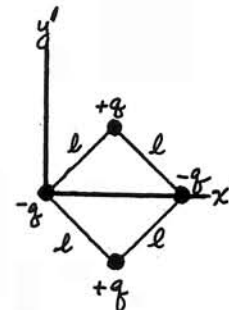
$$\{\mathbf{Q}\} = \begin{pmatrix} 0 & -3q\ell^2 & 0 \\ -3q\ell^2 & 0 & 0 \\ 0 & 0 & 0 \end{pmatrix}$$

The symmetry of the charge distribution suggests a rotation by 45° about the z axis. [This transformation can be found formally by the method outlined in Sec. A.7. See also Marion and Thornton (Ma95, Sec. 11.4).]

In the new system with axes as shown,

$$\{\mathbf{Q}\} = \begin{pmatrix} -3q\ell^2 & 0 & 0 \\ 0 & +3q\ell^2 & 0 \\ 0 & 0 & 0 \end{pmatrix}$$

Because the system is not a figure of revolution, the relationship of Eq. (2.41) for the diagonal elements does not apply here.



2-14. Equation (3) of Example 2.4 gives

$$\Phi^{(4)} = 2p\ell \frac{3\cos^2\theta - 1}{r^3}$$

The field components are:

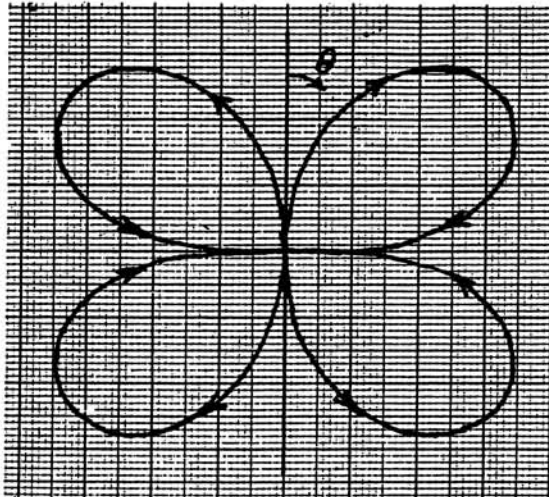
$$E_r = -\frac{\partial\Phi}{\partial r} = 6p\ell \frac{3\cos^2\theta - 1}{r^4}$$

$$E_\theta = -\frac{\partial\Phi}{r\partial\theta} = 12p\ell \frac{\cos\theta \sin\theta}{r^4}$$

Clearly the field-lines are radial ($E_\theta = 0$) at $\theta = 0, 90, 180^\circ$, and reach their maximum radius ($E_r = 0$) at $\theta = \cos^{-1}(\pm 1/\sqrt{3}) \approx 55, 125^\circ$. To find the quantitative shape $r_E(\theta)$ of the field-lines, we have the differential equation (see Prob. 2-5)

$$\begin{aligned} \frac{dr_E}{r_E d\theta} &= \frac{E_r}{E_\theta} = \frac{3\cos^2\theta - 1}{2\cos\theta \sin\theta} \\ \int_{R_E}^{r_E} \frac{dr_E}{r_E} &= \frac{3}{2} \int_{\cos^{-1}1/\sqrt{3}}^{\theta} \frac{\cos\theta}{\sin\theta} d\theta - \frac{1}{2} \int_{\cos^{-1}1/\sqrt{3}}^{\theta} \frac{1}{\cos\theta \sin\theta} d\theta \\ &= \left[\frac{3}{2} \ln |\sin\theta| - \frac{1}{2} \ln |\tan\theta| \right]_{\cos^{-1}1/\sqrt{3}}^{\theta} \end{aligned}$$

The lower limits of the definite integrals are chosen to be at the maximum radius R_E . The first angular integral is obvious; the second may be found in tables. Thus,

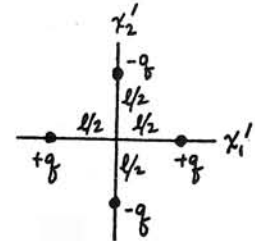


$$\begin{aligned} \ln\left(\frac{r_E}{R_E}\right) &= \left[\ln\left(\frac{\sin^{3/2}\theta}{|\tan\theta|^{1/2}}\right) \right]_{\cos^{-1}1/\sqrt{3}}^{\theta} = \ln\left[\frac{\sin\theta |\cos\theta|^{1/2}}{(2/3)^{1/2} (1/3)^{1/4}}\right] \\ r_E &= R_E \frac{\sin\theta |\cos\theta|^{1/2}}{(4/27)^{1/4}} \end{aligned}$$

All field-lines are similar to each other, that is, the same function of θ scaled by the maximum radius R_E . Note that since we have used only the quadrupole potential (the lowest-order term for the configuration of Fig. 2-4), these field-lines do not take into account the finite size of the charge distribution.

2-15. Evaluating Eq. (2.35), we have

$$\{Q\} = \begin{pmatrix} +\frac{3}{2}q\ell^2 & 0 & 0 \\ 0 & -\frac{3}{2}q\ell^2 & 0 \\ 0 & 0 & 0 \end{pmatrix}$$



Now, from Eq. (2.34),

$$\begin{aligned} \Phi^{(4)}(x_1, x_2, x_3) &= \frac{1}{6} \left(+\frac{3}{2}q\ell^2 \right) \left(\frac{3x_1^2 - r^2}{r^5} \right) + \frac{1}{6} \left(-\frac{3}{2}q\ell^2 \right) \left(\frac{3x_2^2 - r^2}{r^5} \right) \\ &= \frac{3}{4}q\ell^2 \left(\frac{x_1^2 - x_2^2}{r^5} \right) \end{aligned}$$

For spherical coordinates such that

$$x_1 = r \sin\theta \cos\varphi$$

$$x_2 = r \sin\theta \sin\varphi$$

$$x_3 = r \cos\theta$$

we have

$$\begin{aligned} \Phi^{(4)}(r, \theta, \varphi) &= \frac{3}{4}q\ell^2 \left[\frac{\sin^2\theta (\cos^2\varphi - \sin^2\varphi)}{r^3} \right] \\ &= \frac{3}{4}q\ell^2 \left(\frac{\sin^2\theta \cos 2\varphi}{r^3} \right) \end{aligned}$$

as quoted in Eq. (4) of Example 2.4. Because of the φ dependence, the potential and field are not axially symmetric. The field components are:

$$E_r = -\frac{\partial\Phi}{\partial r} = \frac{3}{4}q\ell^2 \left(\frac{3\sin^2\theta \cos 2\varphi}{r^4} \right)$$

$$E_\theta = -\frac{\partial\Phi}{r\partial\theta} = -\frac{3}{4}q\ell^2 \left(\frac{\sin 2\theta \cos 2\varphi}{r^4} \right)$$

$$E_\varphi = -\frac{\partial\Phi}{r\sin\theta\partial\varphi} = \frac{3}{4}q\ell^2 \left(\frac{2\sin^2\theta \sin 2\varphi}{r^4} \right)$$

In the equatorial plane ($\theta = 90^\circ$, the x_1 - x_2 plane), E_θ vanishes and the field-lines are found from the differential equation (see Prob. 2-5):

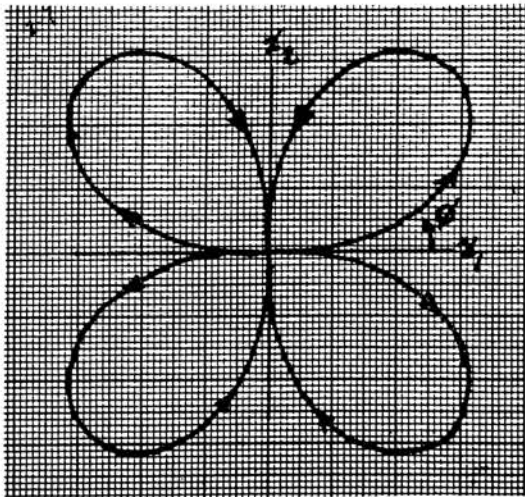
$$\frac{dr_E}{r_E d\varphi} = \frac{E_r}{E_\varphi} = \frac{3\cos 2\varphi}{2\sin 2\varphi}$$

$$\int_{R_E}^{r_E} \frac{dr_E}{r_E} = \frac{3}{4} \int_{2(45^\circ)}^{2\varphi} \frac{\cos 2\varphi}{\sin 2\varphi} d(2\varphi)$$

$$\ln\left(\frac{r_E}{R_E}\right) = \frac{3}{4} \ln|\sin 2\varphi|$$

$$r_E = R_E |\sin 2\varphi|^{3/4}$$

In this plane the field-line looks much like that of Prob. 2-14, but of course there is no longer an axis of symmetry.



2-16. The monopole moment is, trivially, q . From Eq. (2.22) the dipole moment is

$$\mathbf{p} = \int \rho(\mathbf{r}') \mathbf{r}' dv'$$

$$\rightarrow e_z \int \rho_\ell z dz = e_z \frac{q}{2h} \int_{-h}^{+h} z dz = 0$$

From Eq. (2.42), since the system is symmetric about the z axis,

$$Q = Q_{zz} = \int \rho(\mathbf{r}') (3z'^2 - r'^2) dv'$$

$$\rightarrow \int \rho_\ell (2z^2) dz = \frac{q}{h} \int_{-h}^{+h} z^2 dz = \frac{2}{3}qh^2$$

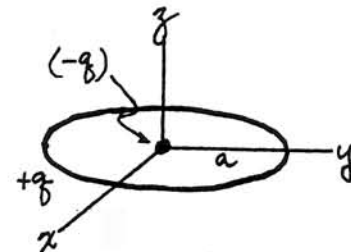
By Eq. (2.41),

$$Q_{xx} = Q_{yy} = -\frac{1}{2}Q_{zz} = -\frac{1}{3}qh^2$$

Thus the full quadrupole tensor is

$$\{\mathbf{Q}\} = \begin{pmatrix} -\frac{1}{3}qh^2 & 0 & 0 \\ 0 & -\frac{1}{3}qh^2 & 0 \\ 0 & 0 & +\frac{2}{3}qh^2 \end{pmatrix}$$

2-17. The monopole moment is zero only with the added point charge at the center. When added, the dipole moment vanishes for any origin (see Prob. 2-8). Without the central charge, the dipole moment depends upon the choice of origin. For the obvious origin, at the center, the dipole moment vanishes anyhow, by symmetry.



Both systems are symmetric about the z axis, so Eqs. (2.41-42) apply for the quadrupole moment. With the origin at the center,

$$Q_{\text{ring}} = Q_{zz} = \int \rho(\mathbf{r}') (3z'^2 - r'^2) dv'$$

$$\rightarrow \oint \rho_\ell (-a^2) d\ell = \left(\frac{q}{2\pi a}\right)(-a^2)(2\pi a) = -qa^2$$

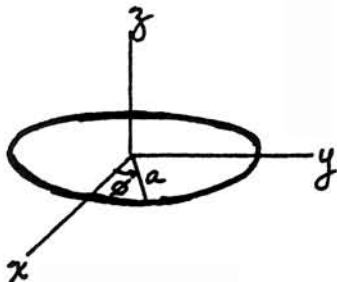
The point charge at the origin adds no contribution. Thus, in either case,

$$\{\mathbf{Q}\} = \begin{pmatrix} \frac{1}{2}qa^2 & 0 & 0 \\ 0 & \frac{1}{2}qa^2 & 0 \\ 0 & 0 & -qa^2 \end{pmatrix}$$

2-18. It is instructive in this problem to keep separate account of the two components of the given linear charge density. Note that we might regard these as two terms in a Fourier series.

The monopole moment is:

$$\begin{aligned} q &= \oint \rho_\ell d\ell \\ &= \frac{q}{a} \int_0^{2\pi} (\cos\varphi)(a d\varphi) - \frac{q}{a} \int_0^{2\pi} (\sin 2\varphi)(a d\varphi) = 0 - 0 = 0 \end{aligned}$$



That is, for each term there is an equal quantity of positive and negative charge. The components of the dipole moment are, from Eq. (2.22),

$$\begin{aligned} p_x &= \oint \rho_\ell x d\ell = \frac{q}{a} \int_0^{2\pi} (\cos\varphi - \sin 2\varphi)(a \cos\varphi)(a d\varphi) \\ &= qa \left(\int_0^{2\pi} \cos^2\varphi d\varphi - 2 \int_0^{2\pi} \sin\varphi \cos^2\varphi d\varphi \right) = qa(\pi + 0) \\ p_y &= \oint \rho_\ell y d\ell = \frac{q}{a} \int_0^{2\pi} (\cos\varphi - \sin 2\varphi)(a \sin\varphi)(a d\varphi) \\ &= qa \left(\int_0^{2\pi} \sin\varphi \cos\varphi d\varphi - 2 \int_0^{2\pi} \sin^2\varphi \cos\varphi d\varphi \right) = qa(0 + 0) \\ \Rightarrow \mathbf{p} &= \pi qa \mathbf{e}_x \end{aligned}$$

The dipole moment arises only from the $\cos\varphi$ term in the charge density. [Note: To evaluate integrals of the form $\int \cos^2\varphi d\varphi$, recall that $\cos 2\varphi \equiv \frac{1}{2}(1 + \cos 2\varphi)$, and thus that the average value of the integrand is $\frac{1}{2}$. Therefore when the integration span $\Delta\varphi$ covers integral periods of the integrand, the integral is simply $\frac{1}{2}\Delta\varphi$.]

Since we do not have axial symmetry, we must calculate each element of the quadrupole tensor from Eq. (2.35):

$$Q_{ij} = \oint \rho_\ell (3x_i x_j - r^2) d\ell$$

$$\begin{aligned} Q_{xx} &= \frac{q}{a} \int_0^{2\pi} (\cos\varphi - \sin 2\varphi)(3a^2 \cos^2\varphi - a^2)(a d\varphi) \\ &= qa^2 \left[\int_0^{2\pi} \cos\varphi (3\cos^2\varphi - 1) d\varphi - 2 \int_0^{2\pi} \sin\varphi \cos\varphi (3\cos^2\varphi - 1) d\varphi \right] \\ &= qa^2(0 - 0) \end{aligned}$$

$$\begin{aligned} Q_{yy} &= \frac{q}{a} \int_0^{2\pi} (\cos\varphi - \sin 2\varphi)(3a^2 \sin^2\varphi - a^2)(a d\varphi) \\ &= qa^2 \left[\int_0^{2\pi} \cos\varphi (3\sin^2\varphi - 1) d\varphi - 2 \int_0^{2\pi} \sin\varphi \cos\varphi (3\sin^2\varphi - 1) d\varphi \right] \\ &= qa^2(0 - 0) \end{aligned}$$

$$Q_{zz} = \frac{q}{a} \int_0^{2\pi} (\cos\varphi - \sin 2\varphi)(-a^2)(a d\varphi) = qa^2(0 - 0)$$

$$\begin{aligned} Q_{xy} &= Q_{yx} = \frac{q}{a} \int_0^{2\pi} (\cos\varphi - \sin 2\varphi)(3a^2 \sin\varphi \cos\varphi)(a d\varphi) \\ &= 3qa^2 \left[\int_0^{2\pi} \sin\varphi \cos^2\varphi d\varphi - \frac{1}{2} \int_0^{2\pi} \sin^2 2\varphi d\varphi \right] = 3qa^2(0 - \frac{\pi}{2}) \end{aligned}$$

The other off-diagonal elements are zero because $z = 0$ for all charge. Thus the quadrupole tensor is:

$$\{\mathbf{Q}\} = \begin{pmatrix} 0 & -\frac{3}{2}\pi qa^2 & 0 \\ -\frac{3}{2}\pi qa^2 & 0 & 0 \\ 0 & 0 & 0 \end{pmatrix}$$

Thus the quadrupole contribution arises only from the $\sin 2\varphi$ term in the charge density. Note the qualitative similarity with the discrete charge distribution in Prob. 2-13. If the axes were rotated 45° , or if the phase of the term were shifted to $\cos 2\varphi$, $\{\mathbf{Q}\}$ would have come out in diagonal form.

Using Eqs. (2.23) and (2.34), the terms in the potential expansion are:

$$\begin{aligned}\Phi^{(1)} &= 0 \\ \Phi^{(2)} &= \pi q a \frac{\mathbf{e}_x \cdot \mathbf{e}_r}{r^2} = \frac{\pi q a x}{r^3} \\ \Phi^{(4)} &= \frac{1}{6r^5} (Q_{xy} + Q_{yx}) (3xy) = -\frac{3\pi q a^2 xy}{2r^5} \\ \Rightarrow \Phi &= \pi q a \left(\frac{x}{r^3} - \frac{3axy}{2r^5} + \dots \right)\end{aligned}$$

2-19. (a) Note that one cannot integrate a vector field over volume in anything but Cartesian coordinates, because non-Cartesian unit vectors (such as $\mathbf{e}_r, \mathbf{e}_\theta, \mathbf{e}_\varphi$ of spherical coordinates) have different orientations in different places. With the axial symmetry of a dipole, we need be concerned only with the integral of the field component parallel to the dipole axis. Hence, choosing Eq. (2.29) because it is more transparent,

$$\begin{aligned}\int_R \mathbf{E} d\mathbf{v} &\rightarrow \int_R E_z d\mathbf{v} = \iint \mathbf{e}_z \cdot \frac{p(2\cos\theta \mathbf{e}_r + \sin\theta \mathbf{e}_\theta)}{r^3} 2\pi r^2 \sin\theta d\theta dr \\ &= 2\pi p \int_0^R \frac{dr}{r} \int_0^\pi (2\cos^2\theta - \sin^2\theta) \sin\theta d\theta\end{aligned}$$

The θ integral is

$$\int_{-1}^{+1} (3\cos^2\theta - 1) d(\cos\theta) = [\cos^3\theta - \cos\theta]_{-1}^{+1} = 0$$

However, the r integral is

$$\int_0^R \frac{dr}{r} = [\ln r]_0^R \rightarrow \ln\left(\frac{R}{0}\right) \sim \ln(\infty)$$

Thus the three-dimensional integral (including the trivial integration over φ) is

indeterminate ($0 \times \infty$) when the lower limit is at the origin. However, if we take the lower limit at some small finite radius ϵ , then R/ϵ and its logarithm are bounded and the zero of the θ integration stands, independent of the value of R . That is, if the integral has any nonzero value, it comes only from the volume element right at the origin.

(b) Expressing the field as the gradient of the dipole potential, Eq. (2.23), we have

$$\begin{aligned}\int_R \mathbf{E} d\mathbf{v} &= -\int_V \mathbf{grad} \left(\frac{\mathbf{p} \cdot \mathbf{e}_r}{r^3} \right) d\mathbf{v} \\ &= -\oint_S \left(\frac{\mathbf{p} \cdot \mathbf{e}_r}{r^3} \right) d\mathbf{a}\end{aligned}$$

using Eq. (A.58) to transform to an integral over the surface S (with vector elements $d\mathbf{a}$) enclosing the volume V . Again, it is only the \mathbf{e}_z component we want, so that

$$\begin{aligned}\int_R E_z d\mathbf{v} &= -\oint_S \left(\frac{p \cos\theta}{R^3} \right) (\mathbf{e}_z \cdot \mathbf{e}_r) 2\pi R^2 \sin\theta d\theta \\ &= -2\pi p \int_0^\pi \cos^2\theta \sin\theta d\theta = -2\pi p \int_{-1}^{+1} u^2 du = -\frac{4\pi}{3} p \\ \Rightarrow \int_R \mathbf{E} d\mathbf{v} &= -\frac{4\pi}{3} \mathbf{p}\end{aligned}$$

The volume integral includes the origin (there is no bounding surface there), and the r dependence cancels identically on the surface at $r=R$. The three-dimensional Dirac delta function, $\delta(\mathbf{r})$ of Eq. (1.99), is precisely the quantity that is zero everywhere except at the origin, and has a finite integral (of unity) over any volume that encloses the origin. Thus we modify the field formulas of Eqs. (2.28–29) by adding the term $-(4\pi/3)\mathbf{p}\delta(\mathbf{r})$.

(c) Equation (2.64) for the magnetic dipole has exactly the same form as Eq. (2.29), and so the mathematics of integration is identical. Paraphrasing Part (b) using the vector potential, Eq. (2.58), and the identity of Eq. (A.59), we have

$$\begin{aligned}\int_R \mathbf{B} d\mathbf{v} &= \int_V \mathbf{curl} \left(\frac{\mathbf{m} \times \mathbf{e}_r}{r^3} \right) d\mathbf{v} = \\ &= -\oint_S \left(\frac{\mathbf{m} \times \mathbf{e}_r}{r^3} \right) \times d\mathbf{a}\end{aligned}$$

Therefore, noting that $\mathbf{m} \times \mathbf{e}_r$ is in the \mathbf{e}_φ direction, and $\mathbf{e}_z \cdot (\mathbf{e}_\varphi \times \mathbf{e}_r) = -\sin\theta$:

$$\begin{aligned} \int_R B_z dv &= -\oint_S \left(\frac{m \sin\theta}{R^3} \right) [\mathbf{e}_z \cdot (\mathbf{e}_\varphi \times \mathbf{e}_r)] 2\pi R^2 \sin\theta d\theta \\ &= +2\pi m \int_0^\pi \sin^3\theta d\theta = 2\pi m \int_{-1}^{+1} (1-u^2) du = +\frac{8\pi}{3} m \\ &\Rightarrow \int_R \mathbf{B} dv = +\frac{8\pi}{3} \mathbf{m} \end{aligned}$$

Therefore we add the term $+(4\pi/3)\mathbf{m}\delta(\mathbf{r})$ to Eqs. (2.63–64).

Since the "logarithmic infinity" of Eqs. (2.29) and (2.64) is weaker than the delta-function's infinity, it is not necessary to exclude the origin from the domain of the original formulas. Real dipoles of finite size have complicated but finite fields within their structure, and the idealized Eqs. (2.29) and (2.64) [or (2.28), (2.63)] will surely fail as $r \rightarrow 0$. However, this problem shows how to finesse this complication by working with the potentials and converting to surface integrals, at a large enough radius that the structural details are irrelevant.

2-20. The time-average of the first term of Eq. (2.45), when written as a discrete sum, is

$$\begin{aligned} \langle \mathbf{A}^{(1)} \rangle &= \frac{1}{\tau} \int_0^\tau \left(\frac{1}{cr} \sum_\alpha q_\alpha \mathbf{u}_\alpha \right) dt \\ &= \frac{1}{cr} \sum_\alpha q_\alpha \int_0^\tau \dot{\mathbf{r}}_\alpha dt = \frac{1}{cr} \sum_\alpha q_\alpha \frac{\mathbf{r}_\alpha(\tau) - \mathbf{r}_\alpha(0)}{\tau} \end{aligned}$$

[The denominator r , representing the distance from origin to the *field* point, is not a function of time, nor the charge index α .] If the charges are restricted to a bounded region of space, as postulated, then the term $[\mathbf{r}_\alpha(\tau) - \mathbf{r}_\alpha(0)]$ remains finite as $\tau \rightarrow \infty$, and $\langle \mathbf{A}^{(1)} \rangle$ goes to zero.

2-21. Stokes' theorem, Eq. (A.54), is

$$\int_S \mathbf{curl} \mathbf{V} \cdot d\mathbf{a} = \oint_\Gamma \mathbf{V} \cdot d\mathbf{s}$$

where the closed curve Γ bounds the open surface S , and the vector elements $d\mathbf{s}$ and $d\mathbf{a}$ are related in a right-handed sense. Let $\mathbf{V} = \mathbf{r} \times \mathbf{k}$, where \mathbf{k} is a constant vector. On the right, using Eq. (A.18),

$$\oint_\Gamma \mathbf{V} \cdot d\mathbf{s} \rightarrow \oint_\Gamma \mathbf{r} \times \mathbf{k} \cdot d\mathbf{s} = -\mathbf{k} \cdot \oint_\Gamma \mathbf{r} \times d\mathbf{s} \quad (1)$$

On the left, using Eq. (A.39) and the fact that \mathbf{k} is a constant vector,

$$\mathbf{curl} \mathbf{V} \rightarrow \mathbf{curl} (\mathbf{r} \times \mathbf{k}) = \mathbf{k} \cdot \mathbf{grad} \mathbf{r} - \mathbf{k} \operatorname{div} \mathbf{r}$$

Now, for example, if $\mathbf{k} = \mathbf{e}_x$,

$$\mathbf{e}_x \cdot \mathbf{grad} \mathbf{r} = \frac{\partial}{\partial x} \mathbf{r} = \mathbf{e}_x$$

Thus for an arbitrary constant \mathbf{k} ,

$$\mathbf{k} \cdot \mathbf{grad} \mathbf{r} = \mathbf{k}$$

[This result could also be obtained by noting that $\mathbf{grad} \mathbf{r}$ is the identity tensor, Eq. (A.72).] Also, we have $\operatorname{div} \mathbf{r} = 3$. Consequently the left side of Stokes' theorem becomes

$$\int_S \mathbf{curl} (\mathbf{r} \times \mathbf{k}) \cdot d\mathbf{a} = -2\mathbf{k} \cdot \int_S d\mathbf{a} \quad (2)$$

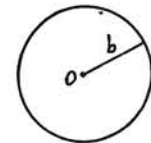
Since the equality between Eqs. (1) and (2) must hold for arbitrary \mathbf{k} , it follows that

$$2 \int_S d\mathbf{a} = \oint_\Gamma \mathbf{r} \times d\mathbf{s}$$

(a) Specifically for a circle of radius b with origin at the center,

$$2 \int_S |d\mathbf{s}| = 2 \int_0^b 2\pi b da = 2\pi b^2$$

$$\oint_\Gamma |\mathbf{r} \times d\mathbf{s}| = b \oint_\Gamma ds = 2\pi b^2$$

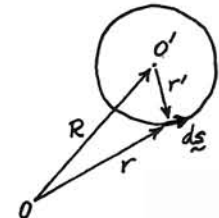


The vector direction of both integrals is perpendicular to the plane of the circle.

(b) For an arbitrary origin O , express \mathbf{r} in terms of a secondary origin O' at the center. Then,

$$\oint_\Gamma \mathbf{r} \times d\mathbf{s} = \oint_\Gamma (\mathbf{R} + \mathbf{r}') \times d\mathbf{s}$$

$$= \mathbf{R} \times \oint_\Gamma d\mathbf{s} + \oint_\Gamma \mathbf{r}' \times d\mathbf{s}$$



But $\oint ds = 0$ for the closed loop, and the second integral is identical with that in case (a).

2-22. (a) Using Eq. (2.51) and $I ds \rightarrow q\mathbf{u}$ [Eq. (1.49)], we define the (instantaneous) magnetic moment for a discrete charge as

$$\mathbf{m} = \frac{I}{2c} \oint \mathbf{r} \times d\mathbf{s} \rightarrow \frac{1}{2c} \mathbf{r} \times q\mathbf{u}$$

The vector angular momentum of a particle is defined as [see (Ma95, Sec. 2.5)]

$$\mathbf{L} = \mathbf{r} \times m\mathbf{u}$$

The two expressions differ only by *scalar* coefficients, and the gyromagnetic ratio is $m/L = q/2mc$, which depends only upon the particle's charge-to-mass ratio.

(b) For a collection of particles,

$$\mathbf{m} = \frac{1}{2c} \sum_{\alpha} \mathbf{r}_{\alpha} \times q_{\alpha} \mathbf{u}_{\alpha}$$

$$\mathbf{L} = \sum_{\alpha} \mathbf{r}_{\alpha} \times m_{\alpha} \mathbf{u}_{\alpha}$$

Now if all particles have the same charge-to-mass ratio (even though the individual charges, and masses, may differ), these vector sums are directly proportional in the ratio $(q/m)/2c$. If a system consists of electrons with $q = -e$ and $m = m_e$, and the angular momentum of the system is quantized with $L = \ell\hbar$ ($\ell = 0, 1, 2, \dots$), then the magnetic moment of the system is quantized as

$$m_{\ell} = \ell \frac{e\hbar}{2m_e c}$$

where the constant is known as the Bohr magneton. In this example with *negative* charges, the magnetic moment is *antiparallel* to the angular momentum.

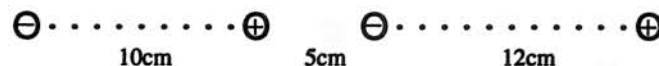
This classical analysis works for the *orbital* behavior of elementary particles. It fails notoriously for the *spin* behavior, where, for electrons, it is found that their spin magnetic moment is (very nearly) one Bohr magneton even though their spin angular momentum is only *one-half* of \hbar . That is, the electron gyromagnetic ratio for spin is twice as large as the classical value.

2-23. It would be a forbidding task to integrate the Biot-Savart law, Eq. (1.36), over Solenoid 1 to find the magnetic field that it produces at many points throughout the volume occupied by the windings of Solenoid 2, and then to integrate the Lorentz force law, Eq. (1.54), to find the net force exerted on Solenoid 2.

However, we can replace each solenoid by its equivalent (fictitious) magnetic poles (see Fig. 2-12). Strictly, these are *disks* of magnetic charge (pole-strength) at the ends of the solenoids, with charge density given by Eq. (2.77). For the geometry of this problem (with $d^2 \gg A/\pi$), we can neglect the spatial extent of the disks and treat them as *point* charges of magnitude

$$q^* = \rho_s^* A = \frac{nIA}{c}$$

The configuration thus reduces to:



The net force between the solenoids is now given by the algebraic sum of Coulomb forces between the four possible pairs of charges. From Eqs. (2.69) and (2.72), counting attractive forces as positive and repulsive as negative,

$$F = \sum \frac{q_i^* q_j^*}{r_{ij}^2} = q^{*2} \left(\frac{1}{5^2} - \frac{1}{15^2} - \frac{1}{17^2} + \frac{1}{27^2} \right) \\ \approx q^{*2} (0.03347 \text{ cm}^{-2})$$

To evaluate q^* , we note from Appendix D that 1 ampere = $3 \cdot 10^9$ esu/s; thus

$$q^* = \frac{nIA}{c} = \frac{(600 \text{ A/cm})(3 \cdot 10^9 \text{ esu/A-s})(2 \text{ cm}^2)}{(3 \cdot 10^{10} \text{ cm/s})} = 120 \text{ esu}$$

(note the canceling factors of "c = 3"), and the force is attractive with magnitude

$$F = (120)^2 (0.03347) = 482 \text{ dynes}$$

(From Coulomb's force law in Gaussian units, dyne \equiv esu²/cm².) Alternatively, one can convert the algebra to SI:

$$q^* \rightarrow nIA \quad F \rightarrow \frac{\mu_0}{4\pi} \sum \frac{q_i^* q_j^*}{r_{ij}^2}$$

with $\mu_0/4\pi = 10^{-7}$ henry/meter.

2-24. (a) If we represent the magnetized material by its equivalent pole strength, it has a surface pole density of $(\rho_s^*)_b = \mathbf{n} \cdot \mathbf{M}_0 = M_0 \cos\theta$. Paraphrasing the solution for Prob. 1-13(a) (sphere radius = a), we find the field at the center (and indeed throughout the sphere) to be:

$$\begin{aligned} H_z(0) &= \int \frac{(\rho_s^*)_b}{a^2} (-\cos\theta) 2\pi a^2 \sin\theta d\theta \\ &= -2\pi M_0 \int_{-1}^{+1} u^2 du = -\frac{4\pi}{3} M_0 \\ \Rightarrow \mathbf{H} &= -\frac{4\pi}{3} \mathbf{M}_0 \end{aligned}$$

We use \mathbf{H} here because Eq. (2.67) shows that magnetic pole strength is a Coulomb-like source of \mathbf{H} , not of \mathbf{B} .

(b) However, if we represent the magnetized material by its equivalent bound current, it has a surface current density of $\mathbf{K}_b = -c\mathbf{n} \times \mathbf{M}_0 = cM_0 \sin\theta \mathbf{e}_\phi$. A simple Biot-Savart integration (Prob. 1-17) finds the field on the axis of a circular current loop (of radius a_1) to be

$$B_z(z) = \frac{2\pi a_1^2 I}{c(a_1^2 + z^2)^{3/2}}$$

Now the surface current on the sphere (of radius a) can be considered to be divided into the elementary loops that lie between θ and $\theta + d\theta$. The current is $I(\theta) \rightarrow K_b(\theta) a d\theta$; the radius is $a_1 \rightarrow a \sin\theta$; and the axial distance to the sphere's center is $z \rightarrow a \cos\theta$. The field contributions of all loops at the sphere's center are in the direction of the polar axis ($\mathbf{e}_z = \mathbf{e}_M$). Thus:

$$\begin{aligned} B_z(0) &= \int_0^\pi \frac{2\pi (a \sin\theta)^2 (cM_0 \sin\theta)}{ca^3 (\sin^2\theta + \cos^2\theta)^{3/2}} a d\theta \\ &= 2\pi M_0 \int_{-1}^{+1} (1 - \cos^2\theta) d(\cos\theta) = \frac{8\pi}{3} M_0 \\ \Rightarrow \mathbf{B} &= +\frac{8\pi}{3} \mathbf{M}_0 \end{aligned}$$

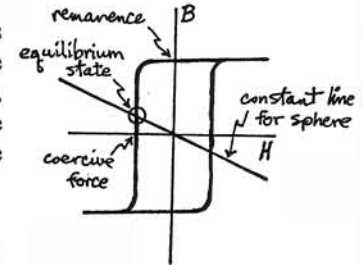
(c) The two fields thus calculated give $\mathbf{B} - \mathbf{H} = 4\pi\mathbf{M}_0$, which does indeed satisfy the definition of \mathbf{H} in Eq. (1.65). They are related as

$$\mathbf{B} = -2\mathbf{H}$$

—that is, in opposite directions, with magnitude ratio of 2.

(d) The ratio of the intercepts for Alnico V's hysteresis "rectangle" is $13000/600 \approx 22$, more than ten times the constrained slope of 2. That is, the intersection of the constraint line for the spherical shape will be relatively close to the "coercive-force" H -intercept. Thus:

$$(H, B)_{\text{Alnico V sphere}} \approx (-600 \text{ oersted}, 1200 \text{ gauss})$$



[It is conventional to use the different names, oersted and gauss, for the units of \mathbf{H} and \mathbf{B} even though they are dimensionally the same in Gaussian units. In SI units, \mathbf{H} and \mathbf{B} differ dimensionally by the constant μ_0 .]

For a magnet in the shape of a *long bar*, magnetized parallel to its axis with its "poles" at the ends, the internal fields are $\mathbf{H} \rightarrow 0$, and $\mathbf{B} \rightarrow 4\pi\mathbf{M}$. In this case, the B/H constraint line has a very large (but still negative) slope, and the intersection with the hysteresis curve is close to the "remanence" B -intercept. If the "long bar" is a right-circular cylinder (or anything other than a *prolate ellipsoid*), the internal fields are not spatially uniform, and the B/H ratio varies within the sample. Thus, the equilibrium magnetization \mathbf{M} is likely to be somewhat nonuniform, especially near the ends. See Probs. 3-23 and 24 for related dependency on the shape of a dielectric or magnetic object.

2-25. (a) The magnetic circuit consists of the length $(\ell + d)$ of soft iron, plus the air-gap of thickness δ , all with cross-sectional area A . From Eq. (2.81) the reluctance in Gaussian units is

$$\mathcal{R}(\delta) = \frac{c}{4\pi} \left(\frac{\ell + d}{\mu A} + \frac{\delta}{A} \right)$$

Of the two terms, the air-gap completely dominates the reluctance unless $\delta \lesssim (\ell + d)/\mu = 16/5000 \approx 3 \cdot 10^{-3} \text{ cm}$ —that is, a very tiny gap. Thus, in the analogy to the usual Ohm's law, the iron is "hookup wire" of negligible "resistance" and the air-gap constitutes the entire "load resistor" of the circuit, unless the air-gap is essentially zero as in this example. Have you noticed how a magnet tends to "grab" its keeper just as the gap closes?

From Eq. (2.81), the magnetic field in the circuit is simply:

$$B(\delta) = \frac{\Phi_m(\delta)}{A} = \frac{NI}{A\mathcal{R}(\delta)}$$

(b) The force is

$$\begin{aligned} F &= \left(\frac{\partial U_m}{\partial \delta} \right)_{\delta \rightarrow 0} = \left[\frac{\partial}{\partial \delta} \left(\frac{N^2 I^2}{2c\mathcal{R}(\delta)} \right) \right]_{\delta \rightarrow 0} \\ &= - \frac{N^2 I^2}{2c\mathcal{R}_0^2} \frac{\partial \mathcal{R}}{\partial \delta} = - \frac{2\pi\mu^2 N^2 I^2 A}{c^2(\ell + d)^2} \\ &= \frac{2\pi(5000)^2(300)^2(20A)^2(0.8\text{cm}^2)}{(3 \cdot 10^{10}\text{cm/s})^2 (12+4)^2\text{cm}^2} \left(\frac{3 \cdot 10^9\text{esu/s}}{A} \right)^2 = 1.96 \cdot 10^6 \text{ dynes} \end{aligned}$$

(Note the cancellation of the factors of " $c = 3$ ".) Alternatively, the algebra can be converted to SI by replacing the coefficient $1/c^2$ by $\mu_0/4\pi = 10^{-7}$ H/m, and interpreting μ in the formula as the *relative permeability*, $\mu_{\text{rel}} = 5000$, of the iron.

The negative sign indicates that the force is in the direction of *decreasing* air-gap δ —that is, the force is attractive (as any schoolchild knows). This is the force at one end of the keeper; if a load is placed symmetrically at the center of the keeper, the two poles would provide twice this force.

Chapter 3

3-1. From symmetry, the potential is a function of the cylindrical-coordinate radius only. From Eq. (A.47),

$$\frac{1}{r} \frac{d}{dr} \left(r \frac{d\Phi}{dr} \right) = 0$$

The first integration gives

$$d \left(r \frac{d\Phi}{dr} \right) = 0 \quad \Rightarrow \quad r \frac{d\Phi}{dr} = C \text{ (a constant)}$$

The second gives

$$\begin{aligned} \int_0^\Phi d\Phi &= C \int_a^r \frac{dr}{r} \\ \Phi(r) &= C \ln \left(\frac{r}{a} \right) \end{aligned}$$

The integration constant C is now determined by

$$\Phi_0 = \Phi(b) = C \ln \left(\frac{b}{a} \right)$$

Therefore,

$$\Phi(r) = \Phi_0 \frac{\ln(r/a)}{\ln(b/a)}$$

The result can be checked by the use of Gauss' law as in Prob. 1-5.

3-2. The problem is identical to Prob. 3-1 except that the symmetry is spherical. Using Eq. (A.52), with Φ a function of the spherical-coordinate radius only,

$$\begin{aligned} \frac{1}{r^2} \frac{d}{dr} \left(r^2 \frac{d\Phi}{dr} \right) &= 0 \quad \Rightarrow \quad r^2 \frac{d\Phi}{dr} = C \\ \Phi(r) &= C \int_a^r \frac{dr}{r^2} = C \left(\frac{1}{a} - \frac{1}{r} \right) \end{aligned}$$

The integration constant C is determined by

$$\Phi_0 = \Phi(b) = C \left(\frac{1}{a} - \frac{1}{b} \right)$$

Therefore,

$$\Phi(r) = \Phi_0 \frac{\left(\frac{1}{a} - \frac{1}{r} \right)}{\left(\frac{1}{a} - \frac{1}{b} \right)} = \Phi_0 \left(\frac{b}{b-a} \right) \left(\frac{r-a}{r} \right)$$

3-3. The potential averaged over the surface of a sphere of radius R is

$$\langle \Phi \rangle_R = \frac{1}{4\pi R^2} \oint_{\theta, \varphi} \Phi(R, \theta, \varphi) R^2 \sin\theta \, d\theta \, d\varphi$$

If we can show that this quantity is independent of radius, then as a special case it must equal the value of Φ at the point $R \rightarrow 0$. Although the explicit R dependence cancels out, Φ remains a function of R in the integrand. Thus we need to evaluate

$$\frac{d}{dR} \langle \Phi \rangle_R = \frac{1}{4\pi} \oint_{\theta, \varphi} \left(\frac{\partial \Phi}{\partial r} \right)_{r=R} \sin\theta \, d\theta \, d\varphi$$

But by Eq. (A.25),

$$\left(\frac{\partial \Phi}{\partial r} \right)_{r=R} = (\mathbf{e}_r \cdot \mathbf{grad} \Phi)_{r=R}$$

and we can write

$$\frac{d}{dR} \langle \Phi \rangle_R = \frac{1}{4\pi R^2} \oint_{\text{surface of sphere}} \mathbf{grad} \Phi \cdot \mathbf{e}_r \, da$$

By the divergence theorem, Eq. (A.53), this can be transformed to a volume integral,

$$= \frac{1}{4\pi R^2} \int_{\text{volume}} \text{div} \, \mathbf{grad} \, \Phi \, dv = \frac{1}{4\pi R^2} \int_{\text{volume}} \nabla^2 \Phi \, dv$$

By assumption, there is no charge within the sphere, and Laplace's equation, Eq. (3.2), makes the integral vanish. Thus the derivative $d\langle \Phi \rangle/dR$ is indeed zero, and the theorem is proved. Note that we have made no assumption concerning the symmetry of $\Phi(R, \theta, \varphi)$, nor of any charge distribution outside the sphere.

This theorem is a manifestation of the smoothing property of Sec. 3.1, and is closely related to the relaxation algorithm discussed in Sec. 3.6.

3-4. If a positive charge is to be in stable equilibrium at a point, then (1) the electric field must be zero at that point, and (2) at any nearby point, there must be a nonzero field pointing back toward the stable point. (We are speaking here of the externally imposed field; we do not count the field of the hypothetically confined particle itself.) Thus, if we enclose the point with a Gaussian surface, stability demands that there be *inward* electric flux everywhere over the surface. By Gauss' law, Eq. (1.8), this inward flux must be matched by enclosed negative charge. But, by assumption, the proposed confining field is to be produced by external charges only. This contradiction proves that no such stable point is possible.

It is possible to confine the particle in two dimensions, but it will then be unstable in the third.

An alternative argument invoking Laplace's equation is frequently given. In one dimension, a charge is in equilibrium when $E = -d\Phi/dx = 0$. This equilibrium is stable (i.e., there is a restoring force) if, for positive particles,

$$\frac{d^2\Phi}{dx^2} = -\frac{dE}{dx} > 0$$

In three dimensions, stability would require that all three second-order derivatives be positive,

$$\frac{\partial^2\Phi}{\partial x^2}, \frac{\partial^2\Phi}{\partial y^2}, \frac{\partial^2\Phi}{\partial z^2} > 0$$

But this would violate Laplace's equation—at least *one* of the derivatives must be negative (unstable). This argument, while applicable in the typical case of potential functions $\Phi(x, y, z)$ with "normal" Taylor expansions in the vicinity of the confinement point, fails in the unusual circumstance where the second-order Taylor derivatives all happen to be zero. One must then test for stability in the higher-order terms. See Weinstock, *Am.J.Phys.* **44**, 392 (1976).

Problems 3-5 through 3-8 have Cartesian geometry in two or three dimensions. The method of separation of variables discussed in Sec. 3.2 is appropriate.

3-5. In two dimensions, the separation constants, α^2 and β^2 of Eq. (3.13), are equal and opposite, and the resulting harmonic functions are oscillatory in one dimension, and exponential in the other. For the boundary conditions of this problem, $X(x)$ is easily identified as the oscillatory function, and $Y(y)$ as exponential. Since only a finite range of y is involved, the linear combination of positive and negative exponentials known as the hyperbolic sine is appropriate, adjusted so that $Y(y_0) = 0$,

$$Y(y) = \frac{\sinh[\beta(y_0 - y)]}{\sinh(\beta y_0)}$$

The denominator normalizes the function so that $Y(0) = 1$. The phase of the square-wave potential along the x axis suggests that its Fourier series is comprised of sine functions [Eq. (B.1)],

$$X(x) = \sum_r B_r \sin(r\beta x)$$

The spatial periodicity β must match that of the given problem, that is, $\beta a = \pi$. From Eq. (B.2), we have

$$\begin{aligned} B_r &= \frac{1}{\pi} \int_{-\pi}^{+\pi} \Phi(x,0) \sin\left(\frac{r\pi x}{a}\right) d\left(\frac{\pi x}{a}\right) \\ &= \frac{2}{\pi} \int_0^\pi \Phi_0 \sin\left(\frac{r\pi x}{a}\right) d\left(\frac{\pi x}{a}\right) \\ &= \frac{2\Phi_0}{\pi} \left[-\frac{1}{r} \cos(ru) \right]_0^\pi = \begin{cases} \frac{4\Phi_0}{\pi r} & (r = 1, 3, 5, \dots) \\ 0 & (r = 2, 4, 6, \dots) \end{cases} \end{aligned}$$

Note that we used the odd symmetry of the two factors in the integrand to integrate over half the domain and double the result. Thus we have

$$\Phi(x,y) = \frac{4\Phi_0}{\pi} \sum_{\text{odd } r} \frac{\sin(r\pi x/a)}{r} \frac{\sinh[\beta(y_0 - y)]}{\sinh(\beta y_0)}$$

Note that $\cosh u$ and $\sinh u$ are the linear combinations of $\exp(\pm u)$ that have even and odd symmetry, respectively.

3-6. (a) The boundary conditions of this problem differ from Example 3.2(b) only in that the top face of the cube, in addition to the bottom face, is maintained at the potential Φ_0 . Thus given the Example's solution, Eq. (10), we can immediately write out the desired result:

$$\begin{aligned} \Phi(x,y,z) &= \frac{16\Phi_0}{\pi^2} \sum_{r,s \text{ odd}} \frac{1}{rs} \left[\frac{\sinh \gamma_{rs}(c-z)}{\sinh \gamma_{rs}c} \right] \sin\left(\frac{r\pi x}{a}\right) \sin\left(\frac{s\pi y}{b}\right) \\ &+ \frac{16\Phi_0}{\pi^2} \sum_{r,s \text{ odd}} \frac{1}{rs} \left[\frac{\sinh \gamma_{rs}z}{\sinh \gamma_{rs}c} \right] \sin\left(\frac{r\pi x}{a}\right) \sin\left(\frac{s\pi y}{b}\right) \end{aligned}$$

where γ_{rs} is defined in Eq. (4) of the Example. The first term, reproducing Eq. (10), gives the value Φ_0 on the bottom, and zero on the other five sides. The added second term is a simple revision of the first (replacing $c-z$ by z), which gives the value Φ_0 on the top face, and zero on all other sides (including the bottom). The sum matches the new boundary conditions.

(b) For the cube, $\gamma_{rs} = (\pi/a)\sqrt{r^2 + s^2}$, and the potential at the center is:

$$\Phi\left(\frac{a}{2}, \frac{a}{2}, \frac{a}{2}\right) = \frac{32\Phi_0}{\pi^2} \sum_{r,s \text{ odd}} \frac{1}{rs} \left[\frac{\sinh \frac{1}{2}\pi\sqrt{r^2 + s^2}}{\sinh \pi\sqrt{r^2 + s^2}} \right] \sin\left(\frac{r\pi}{2}\right) \sin\left(\frac{s\pi}{2}\right)$$

The sine functions are of magnitude unity, alternating in sign as the index advances 1, 3, 5, ... Numerically,

r	s	$\frac{1}{rs} \left[\frac{\sinh \frac{1}{2}\pi\sqrt{r^2 + s^2}}{\sinh \pi\sqrt{r^2 + s^2}} \right]$	$\sin\left(\frac{r\pi}{2}\right)$	$\sin\left(\frac{s\pi}{2}\right)$
1	1	0.10719	+	+
1	3	0.00232	+	-
3	1		-	+
3	3	0.00014	-	-
1	5	0.00007	+	+
5	1		+	+
3	5	0.00001	-	+
5	3		+	-

Beyond the first term, $\sinh(u/2)/\sinh(u)$ can be approximated by $\exp(-u/2)$. Thus,

$$\begin{aligned} \Phi(\text{center}) &= \Phi_0 \frac{32}{\pi^2} [0.10719 - 2(0.00232) + 0.00014 + 2(0.00007) - 2(0.00001) - \dots] \\ &\approx \Phi_0 \frac{32}{\pi^2} [0.10281 \dots] \approx 0.33334 \Phi_0 \end{aligned}$$

This value coincides with the average potential over the walls of the box (compare Prob. 3-3):

$$\langle \Phi \rangle_{\text{walls}} = \frac{2\Phi_0}{6} = \frac{1}{3} \Phi_0$$

The numerical terms in the table were evaluated by the following BASIC program:

```

REM Numerical factor for Problem 3-6
INPUT PROMPT "r, s, = ": R,S
LET RT = SQR(R^2+S^2)
LET E = EXP(PI*RT/2)
LET F = (E - 1/E)/((E^2 - 1/E^2)*(R*S))
PRINT F
END

```

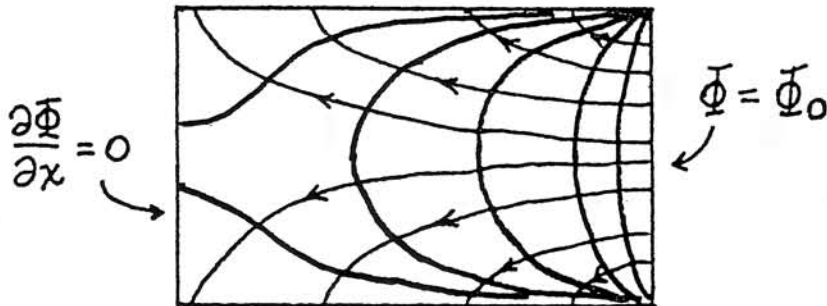
3-7. The oscillatory functions will be in the y direction, restricted to terms that vanish at both $y=0$ and b . The exponential functions are in the x direction; since the x derivative must vanish for $x=0$, the hyperbolic cosine is appropriate. Thus we construct a solution of the form:

$$\Phi(x,y) = \sum_{r \text{ odd}} A_r \left(\frac{\cosh r\pi x/b}{\cosh r\pi a/b} \right) \sin\left(\frac{r\pi y}{b}\right)$$

Note that *even* values of the index r , which also satisfy the requirement that $\Phi=0$ at $y=0, b$, nevertheless would violate the symmetry of the boundary conditions about the center-line $y=b/2$.

The potential at $x=a$ can be considered to be the first half-period of a square-wave, for which the Fourier series was found in Prob. 3-5. That is, $A_r = 4\Phi_0/\pi r$, and we have:

$$\Phi(x,y) = \frac{4\Phi_0}{\pi} \sum_{r \text{ odd}} \left(\frac{\cosh r\pi x/b}{\cosh r\pi a/b} \right) \left(\frac{\sin r\pi y/b}{r} \right)$$



3-8. As in Prob. 3-6, we invoke superposition in order to deal separately with the two arbitrary functions. Putting $\partial\Phi/\partial x=0$ along $x=0$, we modify the solution for Prob. 3-7,

$$\Phi_1 = \sum_r \left(\frac{\cosh r\pi x/b}{\cosh r\pi a/b} \right) \left[A_r \cos\left(\frac{r\pi y}{b}\right) + B_r \sin\left(\frac{r\pi y}{b}\right) \right] \quad (1)$$

where the Fourier coefficients A_r and B_r are to be determined such that

$$(\Phi)_{x=a} = \eta(y) = \sum_r \left[A_r \cos\left(\frac{r\pi y}{b}\right) + B_r \sin\left(\frac{r\pi y}{b}\right) \right]$$

Both the cosine and sine series are needed because we have assumed no special symmetry of the function $\eta(y)$ about the center-line $y=b/2$. Multiply through by $\cos(s\pi y/b)$ [or \sin] and integrate over y from 0 to b . Because of the orthogonality of the sine and cosine functions, as for example

$$\int_0^b \cos\left(\frac{r\pi y}{b}\right) \cos\left(\frac{s\pi y}{b}\right) dy = \frac{1}{2} b \delta_{rs}$$

we can thus determine the coefficients from [equivalent to Eq. (B.2)]

$$\left. \begin{aligned} A_r &= \frac{2}{b} \int_0^b \eta(y) \cos\left(\frac{r\pi y}{b}\right) dy \\ B_r &= \frac{2}{b} \int_0^b \eta(y) \sin\left(\frac{r\pi y}{b}\right) dy \end{aligned} \right\} \quad (2)$$

The second partial solution is for the boundary conditions $\Phi(x=a)=0$, and $\partial\Phi/\partial x = \xi(y)$ along $x=0$. The x -dependent factor must vanish at $x=a$, and have a first derivative normalizable to unity at $x=0$. The appropriate function is $\sinh[\alpha(x-a)]$, and so our second partial solution is of the form

$$\Phi_2 = \sum_r \left(\frac{\sinh r\pi(x-a)/b}{(r\pi/b) \cosh r\pi a/b} \right) \left[C_r \cos\left(\frac{r\pi y}{b}\right) + D_r \sin\left(\frac{r\pi y}{b}\right) \right] \quad (3)$$

The boundary condition at $x=0$ is

$$\left(\frac{\partial\Phi}{\partial x} \right)_{x=0} = \xi(y) = \sum_r \left[C_r \cos\left(\frac{r\pi y}{b}\right) + D_r \sin\left(\frac{r\pi y}{b}\right) \right]$$

By the same procedure as above, we can find the Fourier coefficients from:

$$\left. \begin{aligned} C_r &= \frac{2}{b} \int_0^b \xi(y) \cos\left(\frac{r\pi y}{b}\right) dy \\ D_r &= \frac{2}{b} \int_0^b \xi(y) \sin\left(\frac{r\pi y}{b}\right) dy \end{aligned} \right\} \quad (4)$$

Thus the problem is solved in full generality by adding together (superposing) the solutions (1) and (3), with the coefficients calculated from (2) and (4).

3-9. (a) The zero-order function is uniquely $F_0 = 1$. The first-order function, $F_1 = x + a$, must be orthogonal to F_0 , that is,

$$0 = \int_{-1}^{+1} F_0(x) F_1(x) dx = \int_{-1}^{+1} (x + a) dx = \left[\frac{1}{2}x^2 + ax \right]_{-1}^{+1} = 2a$$

Therefore, $a = 0$, and $F_1 = x$. Now, $F_2 = x^2 + bx + c$ must be orthogonal to both F_0 and F_1 , that is,

$$0 = \int_{-1}^{+1} (1)(x^2 + bx + c) dx = \left[\frac{1}{3}x^3 + \frac{1}{2}bx^2 + cx \right]_{-1}^{+1} = \frac{2}{3} + 2c$$

$$0 = \int_{-1}^{+1} (x)(x^2 + bx + c) dx = \left[\frac{1}{4}x^4 + \frac{1}{3}bx^3 + \frac{1}{2}cx^2 \right]_{-1}^{+1} = \frac{2}{3}b$$

Therefore $b = 0$, $c = -\frac{1}{3}$, and $F_2 = x^2 - \frac{1}{3}$. This sequence of computations can be continued in a straightforward manner. Note that even[odd] orders of F_n contain only even[odd] powers of x , respectively. Since each higher order adds one more coefficient to be determined, but also provides one more orthogonality integral with lower orders, the whole set of polynomials is unique.

(b) The normalization constants are:

$$C_0 = \int_{-1}^{+1} (1)^2 dx = 2$$

$$C_1 = \int_{-1}^{+1} (x)^2 dx = \left[\frac{1}{3}x^3 \right]_{-1}^{+1} = \frac{2}{3}$$

$$C_2 = \int_{-1}^{+1} (x^2 - \frac{1}{3})^2 dx = \left[\frac{1}{5}x^5 - \frac{2}{9}x^3 + \frac{1}{9}x \right]_{-1}^{+1} = \frac{8}{45}$$

(c) Clearly F_0 and F_1 are identical to the corresponding Legendre polynomials of Eqs. (3.41), while $F_2 = \frac{2}{3}P_2$. Because the orthogonality integral, Eq. (3.43), has the same form as the F 's condition (4), we can infer that the whole set of F functions is in fact the same as the set of Legendre functions except for their normalization. For the Legendre polynomials, the normalization condition, replacing (3), is given by Eq. (3.40): *the function has the value of unity at the upper end of its domain, $x = +1$.* For this choice, it turns out that the coefficient of the highest power, x^l , in the Legendre P_l is

$$\frac{(2l-1)(2l-3) \cdots 1}{l!}$$

That is, this is the factor that one must multiply our F functions by to turn them into the conventional Legendre functions. The normalization constants for the Legendre functions are given in Eq. (3.43) as $C_l = 2/(2l+1)$.

3-10. Any polynomial of degree n ,

$$F_n(x) = \sum_{i=0}^n a_i x^i \quad (1)$$

can be regrouped as a sum of Legendre polynomials,

$$F_n(x) = \sum_{l=0}^n A_l P_l(x) \quad (2)$$

There is a unique transformation between the $n+1$ coefficients a_i and the $n+1$ coefficients A_l . Now, the conventional least-squares method for approximating a given function $f(x)$ is to solve the $n+1$ simultaneous algebraic equations

$$\frac{\partial}{\partial a_i} \int_{-1}^{+1} \left[f(x) - \sum_{i=0}^n a_i x^i \right]^2 dx = 0 \quad (0 \leq i \leq n) \quad (3)$$

for the $n+1$ a_i 's. An equivalent operation is to solve the $n+1$ equations

$$\frac{\partial}{\partial A_l} \int_{-1}^{+1} \left[f(x) - \sum_{l=0}^n A_l P_l(x) \right]^2 dx = 0 \quad (0 \leq l \leq n) \quad (4)$$

for the $n+1$ A_l 's. The integral in (4) can be expanded out to

$$\int_{-1}^{+1} [\dots]^2 dx = \int_{-1}^{+1} [f(x)]^2 dx - 2 \sum_{l=0}^n A_l \int_{-1}^{+1} f(x) P_l(x) dx$$

$$+ \sum_{l=0}^n A_l^2 \int_{-1}^{+1} [P_l(x)]^2 dx + \sum_{l \neq l'} A_l A_{l'} \int_{-1}^{+1} P_l(x) P_{l'}(x) dx$$

The last integral vanishes by orthogonality, and the next-to-last integral can be evaluated by Eq. (3.43) as $2/(2l+1)$. Thus, setting the derivatives with respect to A_l equal to zero as in (4), we obtain the $n+1$ independent equations:

$$-2 \int_{-1}^{+1} f(x) P_l(x) dx + 2 A_l \left(\frac{2}{2l+1} \right) = 0$$

$$A_l = \frac{2l+1}{2} \int_{-1}^{+1} f(x) P_l(x) dx \quad (0 \leq l \leq n) \quad (5)$$

which is Eq. (3.45). Although the least-squares approximations of the function $f(x)$ by the series (1) and by the series (2) are numerically identical (for the same degree n), the computation of the coefficients in (2) does *not* involve solving simultaneous equations, because the P_l 's are orthogonal whereas the x_i 's are not. Moreover, if one wishes to improve an already-computed approximation by extending the series to a higher order n' , all $n'+1$ coefficients in (1) would have to be recomputed, while only the additional $n'-n$ coefficients in (2) are needed.

3-11. Expand the generating function, Eq. (3.46), in a binomial series, and then regroup in powers of μ :

$$\frac{1}{(1-2\mu x + \mu^2)^{1/2}} = [1 + (-2\mu x + \mu^2)]^{-1/2}$$

$$= 1 - \frac{1}{2}(-2\mu x + x^2) + \frac{3}{8}(-2\mu x + x^2)^2$$

$$- \frac{5}{16}(-2\mu x + x^2)^3 + \frac{35}{128}(-2\mu x + x^2)^4 - \dots$$

$$= 1 + \mu(x) + \mu^2 \left(-\frac{1}{2} + \frac{3}{2}x^2 \right)$$

$$+ \mu^3 \left(-\frac{3}{2}x + \frac{5}{2}x^3 \right) + \mu^4 \left(\frac{3}{8} - \frac{15}{4}x^2 + \frac{35}{8}x^4 \right) + \dots$$

The coefficients of successive powers of μ are the Legendre polynomials, Eqs. (3.41).

3-12. (a) For $x = +1$, the generating function reduces to:

$$\frac{1}{(1-2\mu x + \mu^2)^{1/2}} \rightarrow \frac{1}{[(1-\mu)^2]^{1/2}} = (1-\mu)^{-1}$$

$$= 1 + \mu + \mu^2 + \mu^3 + \mu^4 + \dots$$

All the coefficients of this binomial expansion are unity. Therefore, the P_l of Eq. (3.47) go to unity for all l when $x = +1$.

(b) We wish to substitute the given function

$$F(x, \mu) = \frac{1}{(1-2\mu x + \mu^2)^{1/2}}$$

in the equation

$$(1-x^2) \frac{\partial^2 F}{\partial x^2} - 2x \frac{\partial F}{\partial x} + \mu \frac{\partial^2}{\partial \mu^2}(\mu F) = 0$$

First we compute:

$$\frac{\partial F}{\partial x} = \left(-\frac{1}{2}\right) \frac{1}{(1-2\mu x + \mu^2)^{3/2}} (-2\mu)$$

$$\frac{\partial^2 F}{\partial x^2} = \left(-\frac{3}{2}\right) \frac{\mu}{(1-2\mu x + \mu^2)^{5/2}} (-2\mu)$$

$$\frac{\partial}{\partial \mu}(\mu F) = F + \mu \frac{\partial F}{\partial \mu}$$

$$= \frac{1}{(1-2\mu x + \mu^2)^{1/2}} + \left(-\frac{1}{2}\mu\right) \frac{1}{(1-2\mu x + \mu^2)^{3/2}} (-2x + 2\mu)$$

$$\frac{\partial^2}{\partial \mu^2}(\mu F) = \frac{\partial}{\partial \mu} \left[\frac{\partial}{\partial \mu}(\mu F) \right]$$

$$= \left(-\frac{1}{2}\right) \frac{1}{(1-2\mu x + \mu^2)^{3/2}} (-2x + 2\mu) + \frac{1}{(1-2\mu x + \mu^2)^{3/2}} (x - 2\mu)$$

$$+ \mu(x - \mu) \left(-\frac{3}{2}\right) \frac{1}{(1-2\mu x + \mu^2)^{5/2}} (-2x + 2\mu)$$

To substitute the derivatives in the proposed identity, it helps to organize the algebra by collecting terms according to the power of F that appears as a factor:

$$\begin{aligned}
 & F^3 [(1-x^2)(0) - (2x)(\mu) + (\mu)((x-\mu) + (x-2\mu))] \\
 & \quad + F^5 [(1-x^2)(3\mu^2) - (2x)(0) + (\mu)(3\mu(x-\mu)^2)] \\
 & = F^5 [(-3\mu^2)(1-2\mu x + \mu^2) + 3\mu^2(1-x^2) + 3\mu^2(x-\mu)^2] = 0
 \end{aligned}$$

Yes, the generating function F satisfies the given equation. Now express F in the form of Eq. (3.47), that is, as a power series in μ with the coefficients $P_l(x)$. Substitution in the identity gives a sum of three infinite series, each of which is a power series in μ . Select out from each of the three series the particular term involving μ^l . The explicit factors of μ in the third term compensate for the second derivative—that is, we start with the term $P_l \mu^l$. Multiply it by μ [$\mu^l \rightarrow \mu^{l+1}$], differentiate twice [$\rightarrow (l+1)l \mu^{l-1}$], and multiply by μ once more [$\rightarrow (l+1)l \mu^l$]. Then we can rewrite the three-term identity in the form:

$$\sum_l \left[(1-x^2) \frac{\partial^2 P_l}{\partial x^2} - 2x \frac{\partial P_l}{\partial x} + l(l+1) P_l \right] \mu^l = 0$$

Since this sum must vanish identically for all μ , the coefficient of each μ^l must be zero. Therefore the $P_l(x)$ functions defined from the generating function F do indeed satisfy Legendre's differential equation, Eq. (3.37).

3-13. For $Q_0 = \frac{1}{2} \ln(1+x)/(1-x)$, calculate the derivatives:

$$\frac{dQ_0}{dx} = \frac{1}{2} \left(\frac{1}{1+x} + \frac{1}{1-x} \right) = \frac{1}{1-x^2}$$

$$\frac{d^2 Q_0}{dx^2} = \frac{2x}{(1-x^2)^2}$$

Substitute in Legendre's differential equation, Eq. (3.37), with $l=0$:

$$(1-x^2) \frac{2x}{(1-x^2)^2} - 2x \frac{1}{1-x^2} = 0$$

The equation is satisfied. Similarly for $Q_1 = \frac{1}{2} x \ln(1+x)/(1-x) - 1$, and $l=1$:

$$\frac{dQ_1}{dx} = \frac{1}{2} \ln\left(\frac{1+x}{1-x}\right) + \frac{x}{1-x^2}$$

$$\frac{d^2 Q_1}{dx^2} = \frac{2}{1-x^2} + \frac{2x^2}{(1-x^2)^2} = \frac{2}{(1-x^2)^2}$$

$$\begin{aligned}
 (1-x^2) \frac{2}{(1-x^2)^2} - 2x \left[\frac{1}{2} \ln\left(\frac{1+x}{1-x}\right) + \frac{x}{1-x^2} \right] \\
 + 2 \left[\frac{1}{2} x \ln\left(\frac{1+x}{1-x}\right) - 1 \right] = 0
 \end{aligned}$$

Again the equation is satisfied. From the recursion relation of Eq. (3.48),

$$(l+1) Q_{l+1} = (2l+1)x Q_l - l Q_{l-1}$$

we can compute

$$\begin{aligned}
 Q_2 &= \frac{1}{2} \left[3x \left(\frac{1}{2} x \ln\frac{1+x}{1-x} - 1 \right) - \left(\frac{1}{2} \ln\frac{1+x}{1-x} \right) \right] \\
 &= \frac{1}{2} \left(\frac{3}{2} x^2 - \frac{1}{2} \right) \ln\left(\frac{1+x}{1-x}\right) - \frac{3}{2} x
 \end{aligned}$$

The coefficient of the logarithm looks familiar. In fact, continuing this process, one can show that

$$Q_l = \frac{1}{2} P_l \ln\left(\frac{1+x}{1-x}\right) - \left(\frac{2l-1}{1 \cdot l}\right) P_{l-1} - \left(\frac{2l-5}{3(l-1)}\right) P_{l-3} - \dots$$

The presence of the logarithm makes this solution independent of the P_l 's (but also makes this solution blow up at $x = \pm 1$).

3-14. In Eq. (3.39) the A_2 term contributes the potential

$$\Phi(r, \theta) = A_2 r^2 P_2(\cos \theta) = A_2 r^2 \left(\frac{3}{2} \cos^2 \theta - \frac{1}{2} \right)$$

Remember that we are assuming axial symmetry—that is, the potential is independent of the azimuthal angle φ . The potential is zero on the cones given by

$$\cos \theta = \pm \frac{1}{\sqrt{3}} \quad \Rightarrow \quad \theta \approx 55^\circ, 125^\circ \quad (1)$$

Positive potentials exist within each of the cones (near the axis); negative potentials exist between the cones (near the equator). Let the equipotential of value $+\Delta\Phi_0/2$ intersect the polar axis at $r = R_+$, which sets $A_2 = \Delta\Phi_0/2R_+^2$. The cross section of this equipotential in the x - z plane ($z = \text{polar axis}$) has the equation

$$2R_+^2 = r^2 (3\cos^2 \theta - 1) \rightarrow 3z^2 - r^2 = 2z^2 - x^2$$

This represents a pair of hyperbolas ("hyperboloid of two sheets" when revolved about the symmetry axis), and we imagine a pair of conducting electrodes made in this shape. Both of these "polar electrodes" are at the positive potential—we could call one the "north polar electrode" ($z > 0$) and the other the "south polar electrode" ($z < 0$), if you like, but they are physically indistinguishable.

The negative equipotential of matching value $-\Delta\Phi/2$, for the same A_2 , has the equation

$$2R_+^2 = -r^2(3\cos^2\theta - 1) \rightarrow -3z^2 + r^2 = -2z^2 + x^2$$

This is again a hyperbola ("hyperboloid of one sheet" in 3-d), which intersects the "equatorial plane" ($\theta = 90^\circ$) at $R_- = x(z=0) = \sqrt{2}R_+$. So we make a conducting ring in this shape to form the negative "equatorial electrode." Mathematically, all three electrodes extend to infinity; in the real world they must be truncated somewhere out along the asymptotic cones of (1). Except for these edge effects, the potential distribution in the space between the electrodes is described by the A_2 term alone. Intermediate equipotentials are of course hyperboloids with the same topology as the electrodes.

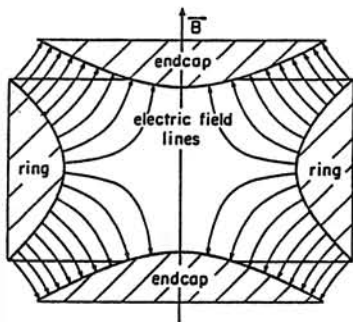
The corresponding field components are

$$E_r = -\frac{\partial\Phi}{\partial r} = -A_2 r(3\cos^2\theta - 1)$$

$$E_\theta = -\frac{\partial\Phi}{r\partial\theta} = A_2 r(3\cos\theta\sin\theta)$$

If desired, we could find an analytical formula for the field-lines by the method of Prob. 2-5. The general topology is shown in the sketch. There is a null field at the origin, and the magnitude $|E|$ increases as one goes out radially in any direction.

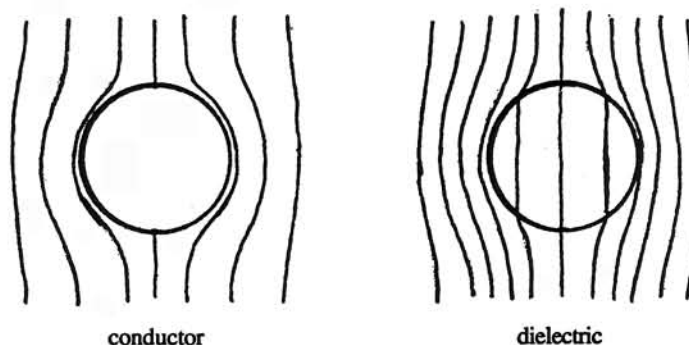
This configuration is sometimes called a "quadrupole field" in reference to the B_2 term in the Legendre-polynomial (or axial multipole) expansion. By the same logic, one would call the uniform field in a parallel-plate capacitor a "dipole field."



The addition of a uniform axial magnetic field to the "quadrupole" electric field produces an important configuration known as a *Penning trap* for charged particles [see Brown and Gabrielse, *Rev.Mod.Phys.* 58, 233 (1986)]. The cylindrical analog [the A_2 term of Eq. (3.79)] is used as an electrostatic lens to focus the beam in particle accelerators.

Problems 3-15 through 3-27 involve geometries for which spherical coordinates are convenient. Moreover the systems are axially symmetric and call for solutions in terms of Legendre polynomials (zonal harmonics), as discussed in Sec. 3.3.

3-15. The electric field-lines of Example 3.3(a) are shown in Fig. 3-4; those of Example 3.3(b), in Fig. 3-5. The equipotentials are everywhere perpendicular to the field-lines:



3-16. The problem is identical to Example 3.3(a) except for the presence of the net charge Q on the conducting sphere. Clearly, at large distances this charge produces the monopole potential Q/r of Eq. (2.20a) [= Eq. (1.18)]. The solution at all points external to the sphere must, however, be expressible in the form of Eq. (5) of the Example. Since Q/r is exactly of the form of the B_0 term in (5), all we need to do is add this term to the previous solution, obtaining

$$\Phi(r, \theta) = \frac{Q}{r} - E_0 r \cos\theta + \frac{a^3 E_0}{r^2} \cos\theta$$

If it is desired that the potential of the charged sphere still be defined to be zero, we can also add an A_0 term [in Eq. (3.39)] equal to $-Q/a$. Note that A_0 is just the arbitrary constant that can always be added to the potential function [see paragraph following Eq. (1.18)].

3-17. As in Example 3.3(b), there are two regions separated by the spherical boundary at $r = a$. The causal agent in this problem is the dipole at the origin, whose potential is given by Eq. (2.23) as $\Phi = (p_0 \cos\theta)/r^2$. The θ dependence suggests that we will need only the $l = 1$ terms in the zonal-harmonic expansion, Eq. (3.39), which involve $P_1(\cos\theta) = \cos\theta$. Therefore, the expansions reduce to:

$$\Phi_{\text{int}} = \left[(A_1)_{\text{int}} r + (B_1)_{\text{int}} \frac{1}{r^2} \right] \cos\theta$$

$$\Phi_{\text{ext}} = \left[(A_1)_{\text{ext}} r + (B_1)_{\text{ext}} \frac{1}{r^2} \right] \cos\theta$$

Clearly, $(B_1)_{\text{int}} = p_0$ because of the causal dipole, and $(A_1)_{\text{ext}} \rightarrow 0$ because there is no applied field at infinity. This leaves two coefficients to be determined by the two boundary conditions at $r = a$:

$$\Phi_{\text{int}} = \Phi_{\text{ext}} \quad (E_{\theta\text{int}} = E_{\theta\text{ext}}) :$$

$$(A_1)_{\text{int}} a + p_0 \frac{1}{a^2} = (B_1)_{\text{ext}} \frac{1}{a^2}$$

$$\left(\frac{\partial\Phi}{\partial r} \right)_{\text{int}} = \epsilon \left(\frac{\partial\Phi}{\partial r} \right)_{\text{ext}} \quad (D_{r\text{int}} = D_{r\text{ext}}) :$$

$$(A_1)_{\text{int}} - 2p_0 \frac{1}{a^3} = -2\epsilon (B_1)_{\text{ext}} \frac{1}{a^3}$$

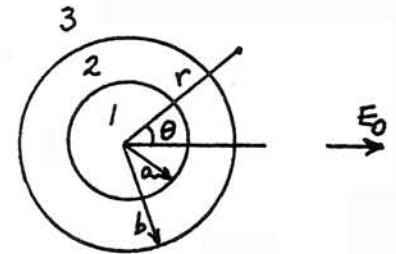
$$\begin{pmatrix} a^3 & -1 \\ a^3 & 2\epsilon \end{pmatrix} \begin{pmatrix} (A_1)_{\text{int}} \\ (B_1)_{\text{ext}} \end{pmatrix} = \begin{pmatrix} -p_0 \\ 2p_0 \end{pmatrix}$$

$$(A_1)_{\text{int}} = -\frac{2(\epsilon-1)p_0}{a^3(2\epsilon+1)}; \quad (B_1)_{\text{ext}} = \frac{3p_0}{2\epsilon+1}$$

Physically, the dipole p_0 polarizes the dielectric, which now has a bound surface charge [Eq. (1.34)] on the cavity wall. This surface charge produces a *uniform field* within the cavity of magnitude $-(A_1)_{\text{int}} = +2(\epsilon-1)p_0/a^3(2\epsilon+1)$. The surface charge also modifies the field in the dielectric, the net field being that of a dipole of strength $(B_1)_{\text{ext}} = 3p_0/(2\epsilon+1)$.

3-18. Label the three regions as shown. Only those terms in the zonal-harmonic expansion that contain $P_1 = \cos\theta$ are needed to satisfy boundary conditions consistent with the prescribed potential at large distances,

$$\Phi_3(r \rightarrow \infty) = -E_0 r \cos\theta$$



Consequently the potentials in the three regions will be of the form:

$$\Phi_1 = -E_1 r \cos\theta$$

$$\Phi_2 = A_2 r \cos\theta + B_2 \frac{1}{r^2} \cos\theta$$

$$\Phi_3 = -E_0 r \cos\theta + B_3 \frac{1}{r^2} \cos\theta$$

where E_1 is the desired (uniform) field inside the shell. The potential, and the normal component of $\mathbf{D} = \epsilon\mathbf{E}$ (i.e., $-\epsilon \partial\Phi/\partial r$) must be continuous across both boundary surfaces (the factor $\cos\theta$ cancels out throughout):

$$-E_1 a = A_2 a + \frac{B_2}{a^2}$$

$$A_2 b + \frac{B_2}{b^2} = -E_0 b + \frac{B_3}{b^2}$$

$$E_1 = -\epsilon A_2 + \frac{2\epsilon B_2}{a^3}$$

$$-\epsilon A_2 + \frac{2\epsilon B_2}{b^3} = E_0 + \frac{2B_3}{b^3}$$

In matrix form the simultaneous equations are:

$$\begin{pmatrix} 1 & 1 & 1/a^3 & 0 \\ 0 & -1 & -1/b^3 & 1/b^3 \\ 1 & \epsilon & -2\epsilon/a^3 & 0 \\ 0 & -\epsilon & 2\epsilon/b^3 & -2/b^3 \end{pmatrix} \begin{pmatrix} E_1 \\ A_2 \\ B_2 \\ B_3 \end{pmatrix} = E_0 \begin{pmatrix} 0 \\ 1 \\ 0 \\ 1 \end{pmatrix}$$

We can use Cramer's rule to solve for E_1 :

denominator determinant:

$$\begin{aligned} & \frac{1}{a^3 b^3}(-4\varepsilon - 2\varepsilon^2 - \varepsilon - 2) + \frac{1}{b^6}(2\varepsilon^2 - 2\varepsilon + 2 - 2\varepsilon) \\ &= \frac{1}{b^3} \left[-\frac{(2\varepsilon + 1)(\varepsilon + 2)}{a^3} + \frac{2(\varepsilon - 1)^2}{b^3} \right] \end{aligned}$$

E_1 numerator determinant:

$$\frac{1}{a^3 b^3}(-4\varepsilon - 2\varepsilon - \varepsilon - 2\varepsilon) = -\frac{1}{a^3 b^3} 9\varepsilon E_0$$

Thus,

$$E_1 = E_0 \frac{9\varepsilon}{(2\varepsilon + 1)(\varepsilon + 2) - \frac{2a^3}{b^3}(\varepsilon - 1)^2}$$

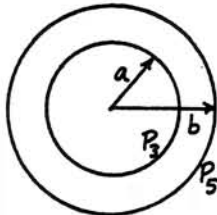
This configuration is a useful model for the shielding effect of a dielectric layer surrounding a region of space. A more practical application is the analogous problem for an approximately linear ferromagnetic material with $\mu \sim 5000$. Substituting μ, B for ε, E , and assuming $\mu \gg 1$,

$$\frac{B_1}{B_0} \rightarrow \frac{9}{2\mu(1 - a^3/b^3)}$$

For a thin shield, $(b - a) \ll b$,

$$\frac{B_1}{B_0} \rightarrow \frac{3b}{2\mu(b - a)}$$

3-19. In the region $a < r < b$, only terms involving P_3 and P_5 in Eq. (3.39) are required to match the prescribed boundary conditions. Moreover, their coefficients must vanish respectively on the outer and inner surfaces. This fact suggests that we set up the potential in the form:



$$\Phi(a \leq r \leq b) = C_3 \left(\frac{b^7}{r^4} - r^3 \right) P_3(\cos\theta) + C_5 \left(r^5 - \frac{a^{11}}{r^6} \right) P_5(\cos\theta)$$

At $r = a$,

$$C_3 \left(\frac{b^7}{a^4} - a^3 \right) = \Phi_a \quad \Rightarrow \quad C_3 = \frac{a^4}{b^7 - a^7} \Phi_a$$

At $r = b$,

$$C_5 \left(b^5 - \frac{a^{11}}{b^6} \right) = \Phi_b \quad \Rightarrow \quad C_5 = \frac{b^6}{b^{11} - a^{11}} \Phi_b$$

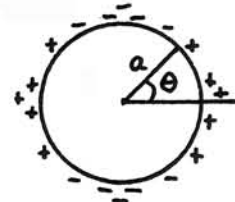
Therefore,

$$\Phi(r, \theta) = \Phi_a \left(\frac{b^7 - r^7}{b^7 - a^7} \right) \frac{a^4}{r^4} P_3(\cos\theta) + \Phi_b \left(\frac{r^{11} - a^{11}}{b^{11} - a^{11}} \right) \frac{b^6}{r^6} P_5(\cos\theta)$$

The uniqueness theorem (Sec. 3.1) assures us that we need look no further.

3-20. The surface charge density is

$$\begin{aligned} \rho_s(\theta) &= \rho_{s0} \cos 2\theta = \rho_{s0} (2\cos^2\theta - 1) \\ &= \rho_{s0} \left[-\frac{1}{3} P_0(\cos\theta) + \frac{4}{3} P_2(\cos\theta) \right] \end{aligned}$$



where we have expressed the angular dependence in terms of Legendre polynomials. Since the charge density is not an equilibrium one for a conducting sphere, we must assume that it is "pasted" on an inert insulating structure, the interior of which has the properties of free space ($\varepsilon = 1$).

The potential must remain finite at the origin and at infinity, and can only contain terms of the form:

$$\Phi(r < a) = A_0 P_0 + A_2 r^2 P_2$$

$$\Phi(r > a) = B_0 \frac{1}{r} P_0 + B_2 \frac{1}{r^3} P_2$$

The boundary conditions at $r = a$ require continuity of potential,

$$A_l a^l P_l = B_l \frac{1}{a^{l+1}} P_l$$

and a discontinuity in E_r proportional to ρ_s [Eq. (1.85)],

$$l A_l a^{l-1} P_l + (l + 1) B_l \frac{1}{a^{l+2}} P_l = 4\pi (\rho_s)_l P_l$$

where $(\rho_s)_l$ is the coefficient of P_l in the given charge density. Eliminate A_l to solve for B_l :

$$l \frac{B_l}{a^{2l+1}} a^{l-1} + (l+1) \frac{B_l}{a^{l+2}} = 4\pi (\rho_s)_l$$

$$B_l = \left(\frac{a^{l+2}}{2l+1} \right) 4\pi (\rho_s)_l$$

Thus, with $l = 0$ and 2 , we have

$$\Phi(r > a) = 4\pi\rho_{s0} \left[-\frac{a^2}{3r} P_0(\cos\theta) + \frac{4a^4}{15r^3} P_2(\cos\theta) \right]$$

With the potential expressed in terms of zonal harmonics, it is easy to see that the given charge distribution has a monopole moment of $q = -4\pi a^2 \rho_{s0}/3$, and a quadrupole moment of $Q_{33} = 32\pi a^4 \rho_{s0}/15$ [see Eq. (2.61)].

3-21. Since the potential must remain finite

at the origin and at infinity, we can write the

potential in the two regions in the forms:

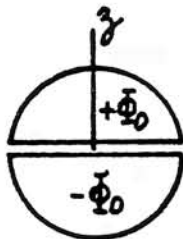
$$\Phi_1(r < a) = A_0 + A_1 \left(\frac{r}{a} \right) P_1 + A_2 \left(\frac{r}{a} \right)^2 P_2 + \dots + A_n \left(\frac{r}{a} \right)^n P_n + \dots$$

$$\Phi_2(r > a) = A_0 \left(\frac{a}{r} \right) + A_1 \left(\frac{a}{r} \right)^2 P_1 + A_2 \left(\frac{a}{r} \right)^3 P_2 + \dots + A_n \left(\frac{a}{r} \right)^{n+1} P_n + \dots$$

That is, we have arranged the terms so that the two series are identical at the prescribed boundary at $r = a$. On the boundary the potential is proportional to the "squarewave" function,

$$f_{sw}(\theta) = \begin{cases} +1 & 0 < \theta < \frac{\pi}{2} \\ -1 & \frac{\pi}{2} < \theta < \pi \end{cases}$$

Substitute this function for the left side of either series above, and let $r = a$ on the right side. Multiply through by $P_n(\cos\theta) d(\cos\theta)$, and integrate. By orthogonality, only the P_n^2 term survives on the right. Using the normalization from Eq. (3.43), we have then



$$A_n = \left(\frac{2n+1}{2} \right) \Phi_0 \int_{\theta=0}^{\pi} f_{sw}(\theta) P_n(\cos\theta) d(\cos\theta)$$

Since f_{sw} is an odd function, all coefficients for even n vanish. For odd n (even integrand), double the integral from 0 to $\pi/2$,

$$A_{n(\text{odd})} = (2n+1) \Phi_0 \int_0^1 P_n(x) dx$$

Specifically, using Eqs. (3.41),

$$A_1 = 3 \Phi_0 \int_0^1 x dx = \frac{3}{2} \Phi_0$$

$$A_3 = \frac{7}{2} \Phi_0 \int_0^1 (5x^3 - 3x) dx = -\frac{7}{8} \Phi_0$$

$$A_5 = \frac{11}{8} \Phi_0 \int_0^1 (63x^5 - 70x^3 + 15x) dx = \frac{11}{16} \Phi_0$$

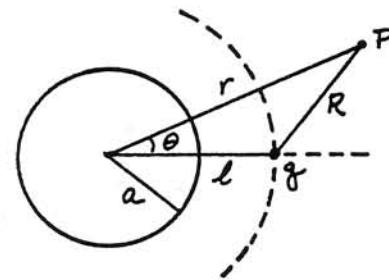
These coefficients now substitute in (1) and (2); for instance,

$$\Phi_2(r > a) = \Phi_0 \left[\frac{3}{2} \left(\frac{a}{r} \right)^2 P_1 - \frac{7}{8} \left(\frac{a}{r} \right)^4 P_3 + \frac{11}{16} \left(\frac{a}{r} \right)^6 P_5 - \dots \right]$$

Incidentally, it can be shown that, for odd n ,

$$\int_0^1 P_n(x) dx = \frac{(-1)^{\frac{n-1}{2}}}{n} \left[\frac{1 \cdot 3 \cdot 5 \cdots n}{2 \cdot 4 \cdot 6 \cdots (n+1)} \right]$$

3-22. We must superpose an expansion of the potential due to q on that due to the induced charge on the sphere. From Eqs. (2.3) and (3.46), we can write the potential at the point P due to q as:



$$\begin{aligned}\Phi_q &= \frac{q}{R} \rightarrow \frac{q}{\ell} \left(1 - 2 \frac{r}{\ell} \cos\theta + \frac{r^2}{\ell^2}\right)^{-1/2} \\ &= \frac{q}{\ell} \sum_n \left(\frac{r}{\ell}\right)^n P_n(\cos\theta) \quad (r < \ell) \\ &\rightarrow \frac{q}{r} \left(1 - 2 \frac{\ell}{r} \cos\theta + \frac{\ell^2}{r^2}\right)^{-1/2} \\ &= \frac{q}{r} \sum_n \left(\frac{\ell}{r}\right)^n P_n(\cos\theta) \quad (r > \ell)\end{aligned}$$

Since the induced charge on the sphere has axial symmetry, we can represent its potential by the B series of Eq. (3.39). The superposition thus has the form:

$$\Phi(a < r < \ell) = \frac{q}{\ell} \left(P_0 + \frac{r}{\ell} P_1 + \frac{r^2}{\ell^2} P_2 + \dots\right) + \left(\frac{B_0}{r} P_0 + \frac{B_1}{r^2} P_1 + \frac{B_2}{r^3} P_2 + \dots\right)$$

$$\Phi(\ell < r < \infty) = \frac{q}{r} \left(P_0 + \frac{\ell}{r} P_1 + \frac{\ell^2}{r^2} P_2 + \dots\right) + \left(\frac{B_0}{r} P_0 + \frac{B_1}{r^2} P_1 + \frac{B_2}{r^3} P_2 + \dots\right)$$

At $r = \ell$ the two series coincide, as they must, except when $\cos\theta \rightarrow 1$ (at the point charge) where the series do not converge. To determine the coefficients B_n , we invoke the boundary condition at $r = a$,

$$\begin{aligned}\Phi(r=a) &= 0 \\ &= \frac{q}{\ell} \left(P_0 + \frac{a}{\ell} P_1 + \frac{a^2}{\ell^2} P_2 + \dots\right) + \left(\frac{B_0}{a} P_0 + \frac{B_1}{a^2} P_1 + \frac{B_2}{a^3} P_2 + \dots\right)\end{aligned}$$

Because of the orthogonality of the P_n 's, we know that the coefficients must vanish individually:

$$B_0 = -\frac{qa}{\ell} \quad B_1 = -\frac{qa^3}{\ell^2} \quad B_2 = -\frac{qa^5}{\ell^3} \quad \text{etc.}$$

That is,

$$B_n = -\frac{q a^{2n+1}}{\ell^{n+1}}$$

The surface charge distribution on the sphere can now be found from:

$$\begin{aligned}4\pi \rho_s &= (E_r)_{r \rightarrow a} = -\left(\frac{\partial\Phi}{\partial r}\right)_{r \rightarrow a} = -\left[\frac{q n a^{n-1}}{\ell^{n+1}} - \frac{n+1}{a^{n+2}} \left(-\frac{q a^{2n+1}}{\ell^{n+1}}\right)\right] P_n \\ &= -\frac{q}{\ell} \sum_n (2n+1) \left(\frac{a}{\ell}\right)^{n-1} P_n(\cos\theta)\end{aligned}$$

The integral of the $n = 0$ term over the sphere gives the net induced charge,

$$q' = \frac{1}{4\pi} \int_0^\pi \left(-\frac{q}{a\ell}\right) 2\pi a^2 \sin\theta d\theta = -q \frac{a}{\ell}$$

This is a well-known problem that is neatly treated by the method of images. See, for instance, Reitz-Milford-Christy (Re93, Sec. 3-9).

3-23. (a) Example 3.3(b), Eq. (9), finds the field within the dielectric sphere to be uniform and related to the (asymptotic) externally applied field \mathbf{E}_0 by

$$\mathbf{E}_{\text{int}} = \frac{3\epsilon_0}{\epsilon_1 + 2\epsilon_0} \mathbf{E}_0 \rightarrow \frac{3}{\epsilon + 2} \mathbf{E}_0$$

Within the sphere, $\mathbf{D} = \mathbf{E} + 4\pi\mathbf{P} = \epsilon\mathbf{E}$, from which it follows that $\mathbf{P} = (\epsilon - 1)\mathbf{E}_{\text{int}}/4\pi$. Therefore, by straightforward algebra, we can express the internal field as the superposition of the applied field and the incremental field produced by the induced polarization:

$$\begin{aligned}\mathbf{E}_{\text{int}} &= \mathbf{E}_0 \left[1 - \left(1 - \frac{3}{\epsilon + 2}\right)\right] \\ &= \mathbf{E}_0 - \left(\frac{\epsilon + 2 - 3}{\epsilon + 2}\right) \left(\frac{\epsilon + 2}{3}\right) \left(\frac{4\pi\mathbf{P}}{\epsilon - 1}\right) = \mathbf{E}_0 - \left(\frac{1}{3}\right) 4\pi\mathbf{P}\end{aligned}$$

(b) For a needle-shaped dielectric aligned with the applied field, the induced polarization is parallel to the needle's long axis. The only significant bound charge-per-unit-area [$\mathbf{P} \cdot \mathbf{n}$ of Eq. (1.34)] occurs at the ends, which by hypothesis have negligible area. Therefore the incremental field associated with the polarization is negligible, and the depolarizing factor L approaches zero.

(c) For a disk-shaped dielectric perpendicular to the applied field, the induced polarization is normal to the disk faces, and bound surface charges $(\rho_s)_b = \pm P$ appear on the two surfaces. This is a parallel-plate capacitor geometry, and these charges contribute the incremental field $E_P = 4\pi|\rho_s| = 4\pi P$. The direction of this contribution is opposite to the applied field. Therefore the depolarizing factor L for this limiting case is unity.

3-24. (a) For a cavity in a surrounding dielectric medium, the result of Example 3.3(b) becomes

$$\mathbf{E}_{\text{int}} = \frac{3\epsilon_0}{\epsilon_1 + 2\epsilon_0} \mathbf{E}_0 \rightarrow \frac{3\epsilon}{1 + 2\epsilon} \mathbf{E}_0$$

Although the field in the spherical cavity is spatially uniform, the electric field \mathbf{E} in the medium near the cavity is not: it is perturbed by the dipole field due to the dielectric's bound charge on the surface of the cavity. Far away from the cavity, where the external field is uniform, the polarization in the medium is $\mathbf{P}_0 = (\epsilon - 1)\mathbf{E}_0/4\pi$. We can express the cavity field in terms of this \mathbf{P}_0 as

$$\begin{aligned} \mathbf{E}_{\text{cav}} &\equiv \mathbf{E}_{\text{int}} = \mathbf{E}_0 \left[1 + \left(\frac{3\epsilon}{1 + 2\epsilon} - 1 \right) \right] \\ &= \mathbf{E}_0 + \left(\frac{3\epsilon - 1 - 2\epsilon}{1 + 2\epsilon} \right) \left(\frac{4\pi\mathbf{P}_0}{\epsilon - 1} \right) = \mathbf{E}_0 + \left(\frac{1}{1 + 2\epsilon} \right) 4\pi\mathbf{P}_0 \end{aligned}$$

Qualitatively, it is easy to see that the bound charge on the cavity surface now *aids* the applied field, rather than opposing it when a dielectric sphere is surrounded by free space. But the factor of $L = 1/3$ that is characteristic of spheres is hidden in this formula.

Problem 1-13(c) refers to a cavity cut in a *uniformly polarized* medium—that is, \mathbf{P} is spatially constant right up to the cavity surface. However, the local \mathbf{E} field in the medium surrounding the cavity is perturbed by the bound charge on the cavity wall—that is, \mathbf{E} is *not* spatially constant, \mathbf{P} and \mathbf{E} are not linearly proportional, and the medium cannot be described by a dielectric constant. (Perhaps the polarization was "frozen" in the dielectric before the cavity was cut in it.) Thus, in Prob. 1-13(c), the bound charge on the cavity surface is due to the same $\mathbf{P} = \mathbf{P}_0$ that exists at a large distance from the perturbing cavity. By contrast, the present problem assumes a linear medium, with the local \mathbf{P} , near the cavity, readjusting in response to the perturbed \mathbf{E} . Therefore the bound charge, which affects both the internal uniform field and the external dipole field, is determined by the local \mathbf{P} at the cavity wall rather than the value \mathbf{P}_0 that pertains at large distances from the cavity. The surface charge can be found from Eq. (7) of the Example:

$$\begin{aligned} (\rho_s)_b &= \mathbf{n} \cdot \mathbf{P} = \frac{\epsilon - 1}{4\pi} (-E_r)_{\text{ext}} = + \frac{\epsilon - 1}{4\pi} \left(\frac{\partial \Phi_{\text{ext}}}{\partial r} \right)_{r \rightarrow a} \\ &= \frac{\epsilon - 1}{4\pi} \left[-E_0 \cos\theta - \frac{1 - \epsilon}{1 + 2\epsilon} 2E_0 \cos\theta \right] \\ &= -P_0 \cos\theta \left(1 - 2 \frac{\epsilon - 1}{1 + 2\epsilon} \right) = -P_0 \cos\theta \left(\frac{3}{1 + 2\epsilon} \right) \end{aligned}$$

That is, the $(\rho_s)_b$ of the "frozen" uniform \mathbf{P}_0 is reduced by the factor $3/(1 + 2\epsilon)$.

(b) Once more we massage Eq. (9) of Example 3.3(b):

$$\mathbf{E}_{\text{int}} = \frac{3\epsilon_0}{\epsilon_1 + 2\epsilon_0} \mathbf{E}_0 = \frac{1}{\frac{\epsilon_1}{3\epsilon_0} + \frac{2}{3}} \mathbf{E}_0 = \frac{1}{1 + \frac{1}{3} \left(\frac{\epsilon_1}{\epsilon_0} - 1 \right)} \mathbf{E}_0$$

which shows that $L \rightarrow 1/3$ for a sphere in the given formula.

In Prob. 1-36 we show, using a Stokesian loop, that \mathbf{E}_{int} in the aligned needle-shaped cavity is equal to \mathbf{E}_0 in the external medium. This equality holds when the "cavity" medium has an arbitrary dielectric constant ϵ_1 . Thus the formula applies to the needle shape when $L \rightarrow 0$.

For the oriented disk-shaped "cavity" we find, using a Gaussian pillbox, that the \mathbf{D} -field in the "cavity" ($= \mathbf{E}_{\text{int}}$ when $\epsilon_1 \rightarrow 1$) is equal to the \mathbf{D} -field in the external medium. Thus, for arbitrary ϵ_1 , we have $\mathbf{D}_{\text{int}} = \epsilon_1 \mathbf{E}_{\text{int}} = \epsilon_0 \mathbf{E}_0$, and the given formula is correct when $L \rightarrow 1$.

These three special cases (sphere, needle, disk) are usually the geometries of interest and are the easiest to treat. A more general analysis [see (St41)] shows that the concept of a depolarizing factor L applies to ellipsoids of all ratios among the principal axes, so that it is no accident that the same formula works in the three special cases. This analysis also applies in the magnetic analog, where L is called the *demagnetizing factor*.

3-25. The surface current divides the world into two current-free regions, inside and outside the sphere of radius a . The magnetic field is derivable from a (magnetic) scalar potential in each of the regions,

$$\mathbf{B} = - \text{grad } \Phi_m$$

where Φ_m is a solution of Laplace's equation and can be expanded in the zonal-harmonic series of Eq. (3.39). [Since there are no magnetic materials involved, we do not need to be careful to distinguish the \mathbf{B} and \mathbf{H} fields.]

The goal of the problem is to find a surface current distribution $K(\theta)$ that will produce a uniform field within the sphere. This implies a potential in the region $r < a$ of

$$\Phi_m(r < a) = -B_0 z = -B_0 r \cos\theta$$

which is just the A_1 term of Eq. (3.39). Outside the sphere, since the potential must not blow up at infinity, we have:

$$\Phi_m(r > a) = \sum_l C_l \frac{1}{r^{l+1}} P_l(\cos\theta)$$

where we have renamed the " B_l " coefficients in Eq. (3.39) to avoid confusion.

We must now investigate the boundary conditions that hold at $r = a$. From Eqs. (1.92) and (1.94), we conclude that the radial (normal) component of \mathbf{B} must be continuous,

$$B_r(\text{inside}) = B_r(\text{outside})$$

and that the θ (tangential) components differ by $4\pi K/c$ according to

$$B_\theta(\text{outside}) - B_\theta(\text{inside}) = \frac{4\pi}{c} K_\varphi$$

These boundary conditions couple the inside and outside regions together, and allow us to make the important inference that, because of the orthogonality of the Legendre polynomials, only the term involving $P_1 = \cos\theta$ is acceptable for $\Phi_m(\text{outside})$. Accordingly, we can write the two boundary conditions explicitly as

$$B_r = - \frac{\partial\Phi_m}{\partial r} \Rightarrow B_0 \cos\theta = \frac{2C_1}{a^3} \cos\theta$$

$$B_\theta = - \frac{\partial\Phi_m}{r \partial\theta} \Rightarrow \frac{C_1}{a^3} \sin\theta + B_0 \sin\theta = \frac{4\pi}{c} K_\varphi(\theta)$$

These simultaneous equations can be solved for

$$C_1 = \frac{a^3 B_0}{2}; \quad K_\varphi(\theta) = \frac{3c}{8\pi} B_0 \sin\theta$$

The current density varies as $\sin\theta$, flowing azimuthally on the surface of the sphere. Translated into discrete turns of wire, this is equivalent to a coil with *constant axial pitch*. The external field of the coil is that of a pure dipole.

This problem is closely related to Probs. 1-13 and 2-24. For instance, the magnetic analog of Prob. 1-13, which showed that the internal field of a uniformly polarized sphere is constant, gives the internal field of a uniformly magnetized sphere as

$$\mathbf{H} = - \frac{4\pi}{3} \mathbf{M}$$

from which

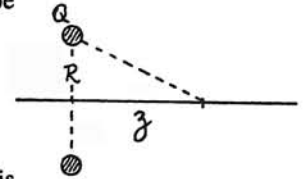
$$\mathbf{B} = \mathbf{H} + 4\pi\mathbf{M} = + \frac{8\pi}{3} \mathbf{M}$$

Then from Eq. (1.69),

$$\mathbf{K} = -c \mathbf{n} \times \mathbf{M} \rightarrow \frac{3c}{8\pi} B_0 \sin\theta \mathbf{e}_\varphi$$

3-26. The potential on the symmetry axis can be written down immediately:

$$\Phi(z) = \frac{Q}{(z^2 + R^2)^{1/2}}$$



For regions where z is less than or greater than R , this function can be expanded in the respective power series:

$$\left. \begin{aligned} \Phi_1(z < R) &= \frac{Q}{R} \left[1 - \frac{1}{2} \left(\frac{z}{R}\right)^2 + \frac{3}{8} \left(\frac{z}{R}\right)^4 + \dots \right] \\ \Phi_2(z > R) &= \frac{Q}{z} \left[1 - \frac{1}{2} \left(\frac{R}{z}\right)^2 + \frac{3}{8} \left(\frac{R}{z}\right)^4 + \dots \right] \end{aligned} \right\} (1)$$

Now imagine a spherical surface of radius R dividing all space into two regions. The inner region, $r < R$, contains no charge (we neglect the thickness of the ring, which lies on the surface $r = R$). Therefore the potential in this region is a solution of Laplace's equation and can be written in the form

$$\Phi_1(r < R) = A_0 + A_1 \left(\frac{r}{R}\right) P_1 + A_2 \left(\frac{r}{R}\right)^2 P_2 + \dots$$

Similarly for $r > R$,

$$\Phi_2(r > R) = A_0 \left(\frac{R}{r}\right) + A_1 \left(\frac{R}{r}\right)^2 P_1 + A_2 \left(\frac{R}{r}\right)^3 P_2 + \dots$$

Note that we have labeled the terms so that the two series coincide at $r = R$. On the z (polar) axis, $r \rightarrow z$, $\theta \rightarrow 0$, and these series reduce to:

$$\left. \begin{aligned} \Phi_1 &= A_0 + A_1 \left(\frac{z}{R}\right) + A_2 \left(\frac{z}{R}\right)^2 + \dots \\ \Phi_2 &= A_0 \left(\frac{R}{z}\right) + A_1 \left(\frac{R}{z}\right)^2 + A_2 \left(\frac{R}{z}\right)^3 + \dots \end{aligned} \right\} (3)$$

Comparing Eqs. (3) with (1), we can evaluate the coefficients as:

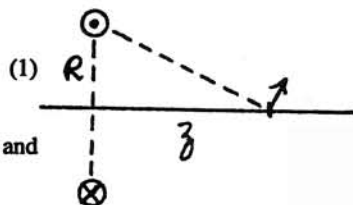
$$A_0 = \frac{Q}{R}; \quad A_1 = A_3 = A_{\text{all odd}} = 0$$

$$A_2 = -\frac{1}{2} \frac{Q}{R}; \quad A_4 = +\frac{3}{8} \frac{Q}{R}; \quad \text{etc.}$$

Substituting these values in Eq. (2) gives us a complete solution at all points in space, except in the immediate vicinity of the ring where the series do not converge.

3-27. From Prob. 1-17 the magnetic field on the axis of a circular loop is

$$B_z = \frac{I 2\pi R^2}{c(z^2 + R^2)^{3/2}} \quad (1)$$



Except at the loop, there are no magnetic sources and the field is related to a scalar potential such that

$$\mathbf{B} = -\text{grad } \Phi_m$$

On the axis this reduces to

$$B_z = -\frac{\partial \Phi_m(z)}{\partial z} \Rightarrow \Phi_m(z) = -\int_{\infty}^z B_z(z) dz$$

Expand Eq. (1) for $z > R$,

$$B_z(z) = \frac{2\pi I R^2}{c z^3} \left[1 - \frac{3}{2} \left(\frac{R}{z}\right)^2 + \frac{15}{8} \left(\frac{R}{z}\right)^4 - \dots \right]$$

Integrate term by term to get

$$\Phi_m(z) = \frac{2\pi I}{c} \left[\frac{1}{2} \left(\frac{R}{z}\right)^2 - \frac{3}{8} \left(\frac{R}{z}\right)^4 + \frac{5}{16} \left(\frac{R}{z}\right)^6 - \dots \right]$$

As argued in the preceding problem, the scalar potential for $r > R$ must be of the form

$$\Phi_m(r > R) = A_0 \left(\frac{R}{r}\right) + A_1 \left(\frac{R}{r}\right)^2 P_1 + A_2 \left(\frac{R}{r}\right)^3 P_2 + \dots$$

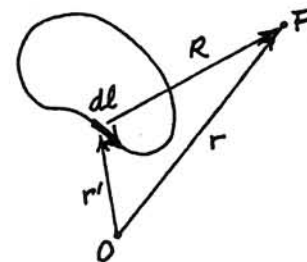
Matching coefficients when $r \rightarrow z$ and $\theta \rightarrow 0$, we have:

$$A_0 = A_2 = A_{\text{all even}} = 0; \quad A_1 = \frac{\pi I}{c}$$

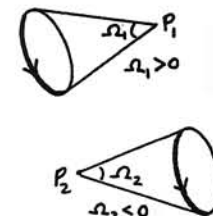
$$A_3 = -\frac{3}{4} \frac{\pi I}{c}; \quad A_5 = +\frac{5}{8} \frac{\pi I}{c}; \quad \text{etc.}$$

Thus the potential is of the form given. The numerical coefficients in the A 's turn out to be the Legendre polynomial values $P_1(\cos \frac{\pi}{2}) = P_1(0)$ [see (Ja75, p.93)]. The potential series for $r < R$ can now be written out trivially, as seen in the preceding problem. One or the other series converges at all points in space except at the current loop. Series expansions for the field components, B_z and B_θ , can easily be found by differentiating the potential. Direct calculation of the off-axis fields from the Biot-Savart law produces the transcendental functions known as *elliptic integrals*.

3-28. (a) When the observation point P is displaced by the vector increment $d\mathbf{r}$, the change in solid angle subtended at P by the loop is equivalent to the change holding P fixed and displacing the loop by the increment $(-d\mathbf{r})$. From this point of view the element $d\mathbf{l}$ of the loop sweeps out the area $|d\mathbf{l} \times d\mathbf{r}|$. To compute the change of solid angle from this area element, we must project its area onto a plane normal to the line-of-sight vector, $\mathbf{R} = \mathbf{r} - \mathbf{r}' = R \mathbf{e}_R$, and then divide by R^2 .



To make this argument fully quantitative, we must establish a *sign convention* for measuring solid angles. When viewed from P , if the current circulates counter-clockwise, we will take the solid angle as positive; and if clockwise, negative. (This convention will make our results consistent with the potential of an electrostatic dipole.)



With this sign convention, we now complete the evaluation of change of solid angle for a displacement of P by $d\mathbf{r}$. Refer to the sketch showing P_1 and imagine that $d\mathbf{r}$ is toward the loop. By our convention this will be a positive increment of solid angle, equivalent to a displacement of $d\mathbf{l}$ parallel to $(-d\mathbf{r})$. The projected area with correct sign may then be seen to be:

$$d\mathbf{l} \times (-d\mathbf{r}) \cdot (-\mathbf{e}_R)$$

Thus

$$d\Omega = \oint_{\Gamma} \frac{d\mathbf{l} \times d\mathbf{r} \cdot \mathbf{e}_R}{R^2}$$

where Γ is the current loop, whose elements are $d\ell = dr'$. By permuting the triple scalar product [see Eqs. (A.18) and (A.25)],

$$d\Omega = \mathbf{grad} \Omega \cdot d\mathbf{r} = - \oint_{\Gamma} \frac{d\ell \times \mathbf{e}_R}{R^2} \cdot d\mathbf{r}$$

$$\mathbf{grad} \Omega = - \oint_{\Gamma} \frac{d\ell \times \mathbf{e}_R}{R^2}$$

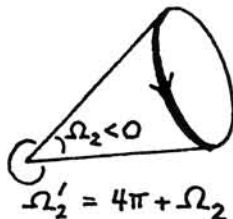
But this is just the integrand of the Biot-Savart law, Eq. (1.36); accordingly,

$$\mathbf{B} = - \frac{I}{c} \mathbf{grad} \Omega$$

Thus $I\Omega/c$ is the magnetic scalar potential for a current loop.

The multiple-valued nature of solid angles (as with plane angles) imposes a subtlety of measurement that can cause trouble. Our convention defined above imposes a discontinuity from $\Omega = +2\pi$ to -2π as the observation point moves across the "plane" of the loop, inside the loop. However, there is a smooth change, with Ω passing through zero, when the point crosses the "plane" outside the loop.

Alternatively we could define the solid angle for points on the " P_2 " side of the loop (negative by our original convention) as the *exterior* solid angle $\Omega'_2 = 4\pi + \Omega_2 < 4\pi$ (see sketch). In this case the crossing is continuous within the loop, but there is now a discontinuity from 0 to 4π when crossing outside.



A discontinuity somewhere in the solid-angle bookkeeping is a necessary result of the circulation of \mathbf{B} in Ampère's law, Eq. (1.37), and one must arrange things so that it does not occur at the point where one is computing the gradient of Ω .

Problems 3-29 through 3-31 use spherical coordinates but no longer have azimuthal symmetry. The full spherical harmonics of Eq. (3.66) are needed.

3-29. The potential as calculated in the Example is

$$\Phi^{(4)} = \frac{3}{4} q \ell^2 \frac{\sin^2 \theta \cos 2\varphi}{r^3}$$

In the table, Eqs. (3.59–62) [using the Euler identity, $\exp(\pm 2i\varphi) \equiv \cos 2\varphi \pm i \sin 2\varphi$], we find a suitable linear combination of the spherical harmonics,

$$\frac{1}{2}(Y_2^{+2} + Y_2^{-2}) = \sqrt{\frac{15}{32\pi}} \sin^2 \theta \cos 2\varphi$$

In this notation the potential is explicitly in the form of two terms of Eq. (3.66),

$$\Phi^{(4)} = \sqrt{\frac{3\pi}{10}} q \ell^2 \frac{Y_2^{+2} + Y_2^{-2}}{r^3}$$

3-30. The prescribed potential is

$$\Phi(\theta, \varphi) = \Phi_0 \sin 3\theta \cos \varphi = \Phi_0 (3 \sin \theta - 4 \sin^3 \theta) \cos \theta \quad (1)$$

We propose to construct the required solution in the form of Eq. (3.66) by finding the appropriate linear combination from the table of spherical harmonics, Eqs. (3.59–62). We observe that terms proportional to $\cos \varphi$ can be constructed from linear combinations of $Y_l^{\pm 1}$,

$$-\frac{1}{2}(Y_l^{+1} - Y_l^{-1}) \propto -\frac{1}{2}(-e^{i\varphi} - e^{-i\varphi}) = \cos \varphi$$

Furthermore, we note that the spherical harmonics of order l contain $\sin \theta$ and/or $\cos \theta$ to the power l .

The θ -dependent factor in $Y_3^{\pm 1}$ is

$$4 \cos^2 \theta \sin \theta - \sin^3 \theta = 4 \sin \theta - 5 \sin^3 \theta \quad (2)$$

Thus to match the coefficient of the $\sin^3 \theta \cos \varphi$ term in (1) we require the term:

$$\Phi_0 \frac{4}{5} \sqrt{\frac{64\pi}{21}} \left(-\frac{1}{2}\right) (Y_3^{+1} - Y_3^{-1})$$

But we see in (2) that this term includes also the term $4\left(\frac{4}{5}\right)\sin \theta \cos \varphi$, the coefficient of which is $1/5$ more than required by (1). Thus we must add (negatively) the term:

$$-\Phi_0 \frac{1}{5} \sqrt{\frac{8\pi}{3}} \left(-\frac{1}{2}\right) (Y_1^{+1} - Y_1^{-1})$$

In order to keep the potential finite at the origin, the solution for $r < a$ will include only the A_l^m terms in Eq. (3.66). To keep the potential finite at infinity, the solution for $r > a$ will include only the B_l^m terms. Therefore our full solution, consistent with the boundary conditions on the spherical surface, is simply:

$$\Phi(r < a, \theta, \varphi) = \Phi_0 \sqrt{\frac{2\pi}{3}} \left[\frac{1}{5} \left(\frac{r}{a}\right) (Y_1^{+1} - Y_1^{-1}) + \frac{4}{5} \sqrt{\frac{8}{7}} \left(\frac{r}{a}\right)^3 (Y_3^{+1} - Y_3^{-1}) \right]$$

$$\Phi(r > a, \theta, \varphi) = \Phi_0 \sqrt{\frac{2\pi}{3}} \left[\frac{1}{5} \left(\frac{a}{r}\right) (Y_1^{+1} - Y_1^{-1}) + \frac{4}{5} \sqrt{\frac{8}{7}} \left(\frac{a}{r}\right)^3 (Y_3^{+1} - Y_3^{-1}) \right]$$

Note the introduction of the factors of a , matching the powers of r . If the given potential is such that the required set of spherical harmonics is not obvious, then the coefficients can be found by direct integration of Eq. (3.65) for each pair of quantum numbers l, m .

3-31. The problem is an analog of Example 3.3(a). From Eqs. (3.59–62) and (3.66), and the identity $\sin 2\theta \equiv 2\sin\theta\cos\theta$, the given r , θ , and φ dependence can be seen to be consistent with $l = 2$, $m = \pm 1$. Specifically, the distant (asymptotic) potential can be written as

$$\Phi_0 = r^2 2 \sqrt{\frac{8\pi}{15}} \left(-\frac{1}{2}\right) (Y_2^1 - Y_2^{-1})$$

Because of the orthogonality of the spherical harmonics, the only term in Eq. (3.66) that can cancel this A_7^{η} term, to produce zero potential at $r = a$, is the corresponding B_7^{η} term. Thus the required full solution is immediately:

$$\Phi(r, \theta, \varphi) = \sqrt{\frac{8\pi}{15}} \left(-r^2 + \frac{a^5}{r^3}\right) (Y_2^1 - Y_2^{-1})$$

3-32. Expanding the derivative in Eq. (3.76) gives

$$r^2 \frac{d^2 R}{dr^2} + r \frac{dR}{dr} - n^2 R = 0$$

Paraphrasing the solution of Eq. (3.30), we substitute the trial power-law function $R = r^\alpha$:

$$r^2 \alpha(\alpha - 1) r^{\alpha-2} + r \alpha r^{\alpha-1} - n^2 r^\alpha = 0$$

$$\alpha^2 - n^2 = 0 \quad \Rightarrow \quad \alpha = \pm n$$

So long as $n \neq 0$, the two functions, r^n and $1/r^n$, are independent. A general solution of a second-order, *linear* differential equation is then given by an arbitrary linear combination of the two solutions, as expressed by the summation in Eq. (3.77). Because of the symmetry in $+n$ and $-n$, in both the $Q(\theta)$ solution of Eq. (3.71) and the $R(r)$ solutions in Eq. (3.77), it is only necessary to sum over positive n 's.

We must look more closely at the special case where $n = 0$, and the two power-law solutions collapse to only one. The differential equation, Eq. (3.76), can be integrated twice by elementary means:

$$r \frac{d}{dr} \left(r \frac{dR}{dr} \right) = 0 \quad \Rightarrow \quad r \frac{dR}{dr} = B_0 \quad \Rightarrow \quad R = B_0 \ln r + A_0$$

where the constants of integration in each step have been named to match Eq. (3.77).

3-33. (a) In two dimensions, introduce the complex variables $u \equiv x + iy$ and $v \equiv x - iy$. Compute the derivatives of the complex function $F_1(u)$:

$$\frac{\partial F_1}{\partial x} = \frac{dF_1}{du} \frac{\partial u}{\partial x} = F_1'; \quad \frac{\partial^2 F_1}{\partial x^2} = \frac{d^2 F_1}{du^2} \frac{\partial u}{\partial x} = F_1''$$

$$\frac{\partial F_1}{\partial y} = \frac{dF_1}{du} \frac{\partial u}{\partial y} = i F_1'; \quad \frac{\partial^2 F_1}{\partial y^2} = i \frac{d^2 F_1}{du^2} \frac{\partial u}{\partial y} = -F_1''$$

where the primes signify differentiation of a function with respect to its argument. Thus, the two-dimensional Laplace's equation is satisfied:

$$\nabla^2 F_1 = \frac{\partial^2 F_1}{\partial x^2} + \frac{\partial^2 F_1}{\partial y^2} = F_1'' - F_1'' = 0$$

By the same argument, the function $F_2(v)$ is also a solution. In order for complex functions to have unique derivatives, they must be continuous and *analytic*. That is, they must satisfy the *Cauchy-Riemann conditions*:

$$\frac{\partial \text{Re}(F)}{\partial x} = \frac{\partial \text{Im}(F)}{\partial y}; \quad \frac{\partial \text{Re}(F)}{\partial y} = -\frac{\partial \text{Im}(F)}{\partial x}$$

See Boas (Bo83, Chap. 14).

(b) An analytic function of a complex variable can be broken into its real and imaginary parts. If the complex argument is complex-conjugated (sign of i reversed), the imaginary part of the function changes sign. Thus,

$$\Phi_1(x, y) \equiv \text{Re}[F_1(x + iy)] = \frac{1}{2} [F_1(x + iy) + F_1(x - iy)]$$

$$\Phi_2(x, y) \equiv \text{Im}[F_1(x + iy)] = \frac{1}{2i} [F_1(x + iy) - F_1(x - iy)]$$

Since we have shown that $F_1(u)$ and $F_1(v)$ are both solutions of Laplace's equation, and the equation is *linear*, it follows that these pure-real combinations are also solutions. It can be shown from the Cauchy-Riemann conditions that Φ_1 and Φ_2 are orthogonal functions in the sense that, if $\text{Re}(F) = \text{constant}$ represents an *equipotential* of a system, then $\text{Im}(F) = \text{constant}$ represents an *E field-line* of the system, or vice versa.

(c) Using the Euler identity, the summed terms in Eq. (3.79) can be recognized as the real and imaginary parts of

$$F_n \equiv (x + iy)^n = r^n e^{in\theta} = r^n (\cos n\theta + i \sin n\theta)$$

The A_n terms are generated when n is a positive integer, and the B_n terms when n is a negative integer. For $n = 0$, this function contributes the A_0 term. The B_0 term is generated by

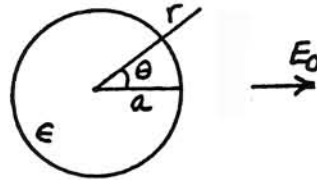
$$F_{0B} \equiv \ln(x + iy) = \ln(r e^{i\theta}) = \ln r + i\theta$$

The linear term in θ is omitted from Eq. (3.79) because it violates the requirement that angular functions must be periodic (i.e., single-valued).

Problems 3-34 through 3-38 are in cylindrical-coordinate geometry. The first two are two-dimensional (without z dependence) and use the cylindrical-harmonic expansion of Eq. (3.79). The latter three are three-dimensional and require the Fourier-Bessel expansion of Eq. (3.107).

3-34. This is the cylindrical analog of the spherical geometry of Example 3.3(b). If we take $\theta = 0$ in the direction of the applied \mathbf{E}_0 , then the asymptotic potential is

$$\Phi(r \rightarrow \infty) = -E_0 r \cos\theta$$



As in the Example, we find solutions for $r < a$ and for $r > a$ that satisfy the boundary conditions at $r = a$, remain finite at the origin, and have the assumed limit as $r \rightarrow \infty$.

(a) Since there is no z dependence, we use the general solution of Eq. (3.79). The functions $\cos n\theta$ (and $\sin n\theta$) form an orthogonal set analogous to the Legendre polynomials $P_l(\cos\theta)$ in spherical coordinates—indeed, they are just the familiar Fourier series. Consequently, we require only those terms having the same angular dependence as that imposed by the asymptotic field:

$$\Phi_1(r < a) = A_1 r \cos\theta$$

$$\Phi_2(r > a) = -E_0 r \cos\theta + B_1 \frac{1}{r} \cos\theta$$

At $r = a$ the potentials must match (this condition is equivalent to the tangential \mathbf{E} -fields being equal), and the normal \mathbf{D} -fields are equal:

$$A_1 a = -E_0 a + B_1 \frac{1}{a}$$

$$-\epsilon A_1 = E_0 + B_1 \frac{1}{a^2}$$

Thus the coefficients are:

$$A_1 = -\frac{2}{\epsilon + 1} E_0$$

$$B_1 = \frac{1}{2}(1 - \epsilon)a^2 A_1 = \frac{\epsilon - 1}{\epsilon + 1} a^2 E_0$$

The resulting potentials are:

$$\Phi_1(r < a) = -\frac{2}{\epsilon + 1} E_0 r \cos\theta$$

$$\Phi_2(r > a) = -E_0 r \cos\theta + \frac{\epsilon - 1}{\epsilon + 1} E_0 \frac{a^2}{r} \cos\theta$$

The fields are:

$$\mathbf{E}(r < a) = -\text{grad } \Phi_1 = (+) \frac{2}{\epsilon + 1} \mathbf{E}_0$$

$$\mathbf{E}(r > a) = -\text{grad } \Phi_2 = \mathbf{E}_0 + \left(\frac{\epsilon - 1}{\epsilon + 1} \frac{E_0 a^2}{r^2} \right) (\mathbf{e}_r \cos\theta + \mathbf{e}_\theta \sin\theta)$$

As in Example 3.3(b), the field inside the dielectric is uniform, now with the magnitude $(2/\epsilon+1)E_0$. The field outside is perturbed by a pure (two-dimensional) dipole field.

(b) As in Prob. 3-23, using the relation $4\pi\mathbf{P} = (\epsilon - 1)\mathbf{E}$, we have

$$\begin{aligned} \mathbf{E}(r < a) &= \mathbf{E}_0 \left[1 - \left(1 - \frac{2}{\epsilon + 1} \right) \right] \\ &= \mathbf{E}_0 - \left(\frac{\epsilon + 1 - 2}{\epsilon + 1} \right) \left(\frac{\epsilon + 1}{2} \right) \left(\frac{4\pi\mathbf{P}}{\epsilon - 1} \right) = \mathbf{E}_0 - \left(\frac{1}{2} \right) 4\pi\mathbf{P} \end{aligned}$$

The depolarizing factor for a dielectric object in the shape of a long cylinder (or needle), with the field *perpendicular* to its axis, is $L = 1/2$.

3-35. The magnetic analog follows directly except that, in the presence of magnetic materials, one must be very careful to distinguish between the \mathbf{B} and \mathbf{H} fields. It is the \mathbf{H} field that is *formally* (mathematically) analogous to the electrical \mathbf{E} field, whereas it is \mathbf{B} that is *physically* analogous to \mathbf{E} as the fundamental field (i.e., the space-time average field within a medium). As worked out in Sec. 1.8, at an interface

the *tangential* \mathbf{E} and \mathbf{H} are continuous (with no free current), and the *normal* $\mathbf{D} = \epsilon\mathbf{E}$ and $\mathbf{B} = \mu\mathbf{H}$ are continuous (no free charge).

(a) The magnetic paraphrase of Prob. 3-34 gives the internal fields within the cylinder of magnetic material as:

$$\mathbf{H}_{\text{int}} = \frac{2}{\mu + 1} \mathbf{B}_0 \Rightarrow \mathbf{B}_{\text{int}} = \mu \mathbf{H}_{\text{int}} = \frac{2\mu}{\mu + 1} \mathbf{B}_0$$

Note that $\mathbf{B}_0 = \mathbf{H}_0$ since we assume $\mu = 1$ outside the cylinder. In the limit of large permeability, clearly $\mathbf{B}_{\text{int}} \rightarrow 2\mathbf{B}_0$.

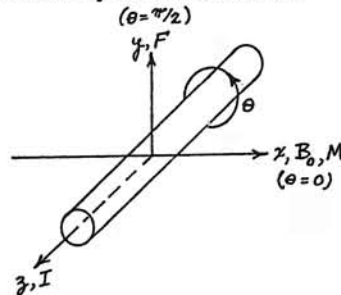
(b) By Eq. (1.54), the force on a current-carrying wire is $c d\mathbf{F} = I d\boldsymbol{\ell} \times \mathbf{B}$, where the relevant \mathbf{B} is the field within the wire. Thus, at first glance, it appears that the force-per-length \mathbf{F}_L on the current I in an iron wire would be approximately twice the force on a copper wire:

$$(\mathbf{F}_L)_{\mu=\mu} = \frac{2\mu}{\mu + 1} \frac{IB_0}{c} \mathbf{e}_I \times \mathbf{e}_{B_0} \xrightarrow{\mu \gg 1} 2(\mathbf{F}_L)_{\mu=1} \quad (1)$$

The unit vectors are perpendicular, and their cross product represents a unit vector in the third dimension.

But there is an additional magnetic force that arises in this situation. The iron's magnetization is equivalent to a bound current density \mathbf{K}_b on the surface of the wire, and this current experiences a force from the \mathbf{B} field produced by the wire's current I .

The geometry of this effect is complicated. The sketch defines Cartesian coordinates with the current I in the z direction, \mathbf{B}_0 and \mathbf{M} in the x direction, and the force of Eq. (1) in the y direction. There are also cylindrical coordinates sharing the z axis and with $x = r \cos\theta$ and $y = r \sin\theta$.



The magnetization in the iron wire is

$$\mathbf{M} = \frac{\mu - 1}{4\pi} \mathbf{H}_{\text{int}} = \frac{\mu - 1}{\mu + 1} \frac{B_0}{2\pi} \mathbf{e}_x$$

By Eq. (1.69), the magnetization is equivalent to the surface current density on the surface of the wire of

$$\mathbf{K}_b = -c \mathbf{n} \times \mathbf{M} = \frac{\mu - 1}{\mu + 1} \frac{cB_0}{2\pi} \sin\theta \mathbf{e}_z \xrightarrow{\mu \gg 1} \frac{cB_0}{2\pi} \sin\theta \mathbf{e}_z$$

This is in the $+z$ direction on the $+y$ side of the wire ($0 < \theta < \pi$), and in the $-z$ direction on the $-y$ side ($\pi < \theta < 2\pi$). From an elementary Ampère's-law calculation, the magnetic field produced by the current I at the wire's surface (radius a) is

$$\mathbf{B}_I = \frac{2I}{ca} \mathbf{e}_\theta$$

Therefore the force-per-length on the magnetization due to the current I is

$$\begin{aligned} (\mathbf{F}_L)_{\mu>1} &= \frac{1}{c} \int \mathbf{K}_b(\theta) \times \mathbf{B}_I a d\theta = \frac{a}{c} \left(\frac{\mu - 1}{\mu + 1} \frac{cB_0}{2\pi} \right) \left(\frac{2I}{ca} \right) \int_0^{2\pi} \sin\theta (-\mathbf{e}_r) d\theta \\ &= \frac{\mu - 1}{\mu + 1} \frac{IB_0}{\pi c} \int_0^{2\pi} \sin\theta (-\cos\theta \mathbf{e}_x - \sin\theta \mathbf{e}_y) d\theta = -\frac{\mu - 1}{\mu + 1} \frac{IB_0}{c} \mathbf{e}_y \quad (2) \end{aligned}$$

Since $\mathbf{e}_y = \mathbf{e}_I \times \mathbf{e}_{B_0}$, this force when added to Eq. (1) neatly removes the dependence on μ :

$$\mathbf{F}_L(\text{total}) = \mathbf{F}_L(1) + \mathbf{F}_L(2) = \left(\frac{2\mu}{\mu + 1} - \frac{\mu - 1}{\mu + 1} \right) \frac{IB_0}{c} \mathbf{e}_y = \frac{IB_0}{c} \mathbf{e}_y$$

That is, the net force on the current-carrying wire is independent of its magnetic properties. The force of Eq. (2) is, in fact, an *internal* force on the wire (the force of the conduction current on the magnetization), and you might think it shouldn't count. But Eq. (1) includes the internal force of the magnetization on the conduction current. We must either include *both* internal forces (an action-reaction pair, canceling out), or omit both.

That this is a treacherous problem is shown by the inclusion of an erroneous statement of it in a highly respected textbook: see (Re93, Prob. 9-12).

3-36. From Gauss' law, Eq. (1.6), the charge density on a conducting surface is related to the normal component of electric field by

$$\rho_s = \frac{E_n}{4\pi}$$

On the cylindrical walls of the system treated in Example 3.5,

$$E_n = -E_r = + \left(\frac{\partial\Phi}{\partial r} \right)_{r=a}$$

Using Eq. (3.109a),

$$\frac{d}{dr} J_0(k_m r) = -k_m J_1(k_m r)$$

Thus from the solution given in Eq. (8) of the Example,

$$\rho_s(r=a; z) = -\frac{\Phi_0}{2\pi a} \sum_m e^{-k_m z}$$

where the allowed k_m values are determined by the roots of $J_0(k_m a) = 0$, denoted by the index m .

On the endplate at $z = 0$,

$$E_n = +E_z = -\left(\frac{\partial \Phi}{\partial z}\right)_{z=0}$$

and

$$\rho_s(r; z=0) = \frac{\Phi_0}{2\pi a} \sum_m \frac{J_0(k_m r)}{J_1(k_m a)}$$

The total charge on the side walls, for a given mode k_m , is

$$q_{\text{sides}} = \int_0^\infty \rho_s(a, z) 2\pi a dz = -\frac{\Phi_0}{k_m}$$

Similarly the total charge on the endplate is, using Eq. (3.111),

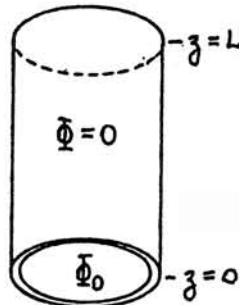
$$q_{\text{end}} = \int_0^a \rho_s(r, 0) 2\pi r dr = \frac{\Phi_0}{ak_m^2 J_1(k_m a)} \int_0^{k_m a} u J_0(u) du = +\frac{\Phi_0}{k_m}$$

Thus all field-lines originating on the endplate terminate on the side walls, as they should.

3-37. The problem is similar to Example 3.5 except for the finite length L . It is the cylindrical analog of the rectangular system of Example 3.2(b).

Let $z = 0$ at the endplate of potential Φ_0 , and $z = L$ at the endplate of potential zero. In place of the decaying exponential $\exp(-k_m z)$, we substitute

$$\frac{\sinh[k_m(L-z)]}{\sinh(k_m L)}$$



which goes to zero for $z = L$, and is normalized to unity at $z = 0$. The rest of the calculation of Example 3.6 remains unchanged. Thus,

$$\Phi(r, z) = 2\Phi_0 \sum_m \frac{1}{k_m a} \frac{\sinh[k_m(L-z)]}{\sinh(k_m L)} \frac{J_0(k_m r)}{J_1(k_m a)}$$

where again the index m denotes the roots of $J_0(k_m a) = 0$.

3-38. The fact that both endplates are at $\Phi = 0$ suggests $Z(z)$ functions that are periodic. Let the separation constant for Eq. (3.72) be $+k^2$. The appropriate solution of Eq. (3.73) is then

$$Z(z) \propto \sin(k_n z)$$

with the k_n restricted by

$$k_n L = n\pi \quad (n = 1, 3, 5, \dots)$$

Only odd values of n are consistent with the symmetry about the midplane.

The radial equation, Eq. (3.74), is now modified by the change of sign of k^2 . In effect, the independent variable r is replaced by ir (where $i = \sqrt{-1}$). From the series solutions, Eqs. (3.95), it can be seen that real solutions of the modified equation are of the form

$$I_n(kr) = i^{-n} J_n(ikr)$$

These functions are commonly known as *modified Bessel functions of the first kind*. They increase monotonically, rather than oscillating like the ordinary J_n Bessel functions—the I_n 's are related to the J_n 's as the exponential (or hyperbolic) functions are to the sinusoidal functions. [The second, independent solutions of the modified differential equation are customarily represented by the symbol K_n ("modified Bessel functions of the second kind"). Like the Neumann functions N_n of Eq. (3.100), the K_n 's diverge for $r \rightarrow 0$.]

In the given problem, there is no azimuthal dependence. Thus $n = 0$, and the solution has the form

$$\Phi(r, z) = \sum_{m \text{ odd}} A_m \sin(k_m z) \frac{I_0(k_m r)}{I_1(k_m a)}$$

We have already chosen a form that satisfies the condition $\Phi = 0$ on the endplates. At $r = a$ we require $\Phi = \Phi_0$, which is accomplished by the familiar Fourier analysis for a squarewave. From Prob. 3-5,

$$A_m = \frac{4\Phi_0}{m\pi}$$

Thus, with $k_m = m\pi/L$,

$$\Phi(r, z) = 4\Phi_0 \sum_{m \text{ odd}} \left(\frac{\sin k_m z}{k_m L} \right) \frac{I_0(k_m r)}{I_1(k_m a)} \quad (1)$$

Physically, the problem would be unchanged if we took the cylindrical wall to be at $\Phi = 0$, and the endplates at $\Phi = -\Phi_0$. This bookkeeping is more directly analogous to Example 3.5 and Prob. 3-37. The solution in that case has the form

$$\Phi(r, z) = \sum_m B_m \frac{\cosh[k_m(z - L/2)]}{\cosh(k_m L)} J_0(k_m r)$$

Now the k_m values are determined by the m th root of $J_0(k_m a) = 0$. To satisfy the boundary condition $\Phi = -\Phi_0$ at $r = 0$ and L , we require

$$-\Phi_0 = \sum_m B_m J_0(k_m r)$$

The coefficients B_m are just the negative of those in Eq. (7) of Example 3.5. Therefore,

$$\Phi(r, z) = -2\Phi_0 \sum_{\text{all } m} \frac{1}{k_m a} \frac{\cosh[k_m(z - L/2)]}{\cosh(k_m L)} \frac{J_0(k_m r)}{J_1(k_m a)} \quad (2)$$

The two solutions (1) and (2) have different forms and different definitions of the parameters k_m , but the respective series sum to values that differ only by the additive constant Φ_0 . We see that the *algebraic form* of series solutions of Laplace's equation may not be unique even though the *potential* itself is unique (except for the additive constant—see Sec. 3.1).

3-39. (a) The following relaxation program is written interactively (in TrueBASIC dialect) to allow the user to monitor the decrease of the maximum change (E) in each iteration, and terminate the sequence by hand when E is sufficiently small. Alternatively, in place of the manual control, one could do the "WHILE" test on the increment E to terminate the iterations automatically when E falls below a predetermined value. Convergence can be speeded up by including an "over-relaxation coefficient" (≈ 1.4) multiplying DV in the "update V(i,j)" line.

```

REM Relaxation solution for Prob.3-39(a).
REM Square grid in X-Z plane, sides A=C=10.
REM Potential=0 on X and Z axes.
REM Potential=+200 at Z=10; -100 at X=10.
DIM V(11,11)
OPEN #1: NAME "Relax3-39A", CREATE NEWOLD !create output file
ERASE #1
FOR I = 2 TO 10 !set boundary values
  LET V(I,1) = 0
  LET V(1,I) = 0
  LET V(I,11) = +200
  LET V(11,I) = -100
NEXT I
LET T = 0 !flag for repeat, exit
LET N = 0 !initialize iteration counter
DO WHILE T<1 !iteration loop
  LET E=0 !initialize maximum increment
  LET N = N+1
  FOR I = 2 TO 10
    FOR J = 2 TO 10
      LET S = V(I-1,J)+V(I+1,J)+V(I,J-1)+V(I,J+1)
      LET DV = (S/4) - V(I,J) !increment in V(i,j)
      LET E = MAX(E,ABS(DV)) !update max increment
      LET V(I,J) = V(I,J) + 1.0*DV !update V(i,j)
    NEXT J
  NEXT I
  PRINT "Maximum increment = ";E
  INPUT PROMPT "Enter 0 to repeat, 1 to exit: ":T
LOOP
PRINT #1: "Problem 3-39A: Potential relaxation
after";N;"iterations"
PRINT #1
FOR J = 11 TO 1 STEP -1 !print out values
  FOR I = 1 TO 11
    PRINT USING "----#": V(I,J);
    PRINT #1, USING "----#": V(I,J); !write to file
  NEXT I
  PRINT
  PRINT #1
NEXT J
CLOSE #1
END

```

The output file after enough iterations to reduce the maximum increment to $E < 0.3V$ is:

Problem 3-39A: Potential relaxation after 29 iterations

0	200	200	200	200	200	200	200	200	200	0
0	97	133	147	152	151	146	133	107	49	-100
0	54	87	104	110	108	99	79	46	-11	-100
0	33	57	71	76	72	61	40	7	-40	-100
0	21	37	47	49	45	33	13	-16	-55	-100
0	13	23	29	30	25	13	-5	-31	-63	-100
0	8	14	18	17	11	1	-16	-39	-67	-100
0	5	8	10	8	3	-6	-21	-41	-68	-100
0	3	4	5	3	-1	-8	-19	-37	-63	-100
0	1	2	2	1	-1	-5	-12	-24	-47	-100
0	0	0	0	0	0	0	0	0	0	0

(b) The adaptation of Eq. (10) of Example 3.2(b) gives:

$$\Phi(x,z) = \sum_{\text{odd } r} \frac{4}{r\pi \sinh(r\pi)} \times \left[(+200) \sinh(r\pi z/a) \sin(r\pi x/a) + (-100) \sinh(r\pi x/a) \sin(r\pi z/a) \right]$$

where $\Phi = 0$ on the x and z axes, $\Phi = +200V$ at $z = c$, $\Phi = -100V$ at $x = a$, and $a = c = 10$. An interactive program follows, which again allows the user to monitor the size of the largest term (E) as each order r (R) is added to the summation:

```

REM Series solution for Prob.3-39(b).
REM Square grid in X-Z plane, sides A=C=10.
REM Potential=0 on X and Z axes.
REM Potential=+200 at Z=10; -100 at X=10.
DIM V(11,11)
MAT V = 0 !initialize potential grid
OPEN #1: NAME "Series3-39B", CREATE NEWOLD !create output file
ERASE #1
FOR I = 2 TO 10 !set boundary values
  LET V(I,1) = 0
  LET V(1,I) = 0
  LET V(I,11) = +200
  LET V(11,I) = -100
NEXT I
LET T = 0 !flag for repeat, exit
LET R = -1 !initialize summation index
DO WHILE T<1 !iteration loop
  LET E = 0 !initialize maximum increment
  LET R = R+2
  LET D = PI*R*(EXP(PI*R)-EXP(-PI*R))/4
  FOR I = 2 TO 10
    FOR J = 2 TO 10
      LET RI = PI*R*(I-1)/10 !gamma*x

```

```

      LET RJ = PI*R*(J-1)/10 !gamma*z
      LET N1 = (200)*(EXP(RJ)-EXP(-RJ))*SIN(RI)
      LET N2 = (-100)*(EXP(RI)-EXP(-RI))*SIN(RJ)
      LET DV = (N1+N2)/D !increment in V(i,j)
      LET E = MAX(E,ABS(DV)) !update max increment
      LET V(I,J) = V(I,J) + DV !update V(i,j)
    NEXT J
  NEXT I
  PRINT "Maximum increment = ";E
  INPUT PROMPT "Enter 0 to repeat, 1 to exit: ":T
LOOP
PRINT #1: "Problem 3-39B: Potential series up to R =";R;
PRINT #1: " (i.e.,";(R+1)/2;"terms)"
PRINT #1
FOR J = 11 TO 1 STEP -1 !print out values
  FOR I = 1 TO 11
    PRINT USING "----#": V(I,J);
    PRINT #1, USING "----#": V(I,J); !write to file
  NEXT I
  PRINT
  PRINT #1
NEXT J
CLOSE #1
END

```

The output file after enough iterations to reduce the maximum term to $E \approx 0.15V$ is:

Problem 3-39B: Potential series up to R = 15 (i.e., 8 terms)

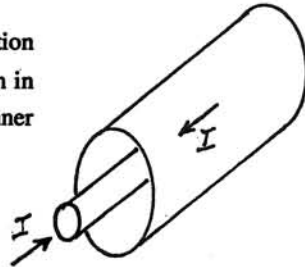
0	200	200	200	200	200	200	200	200	200	0
0	97	134	148	153	152	147	134	109	49	-100
0	53	87	104	111	109	99	80	46	-13	-100
0	32	56	71	76	73	62	40	7	-41	-100
0	20	37	47	49	45	33	13	-17	-56	-100
0	13	23	29	30	25	13	-6	-32	-64	-100
0	8	14	18	17	11	1	-16	-39	-68	-100
0	5	8	10	8	3	-6	-21	-41	-68	-100
0	3	4	5	3	-1	-8	-19	-37	-64	-100
0	1	2	2	1	-1	-5	-12	-23	-47	-100
0	0	0	0	0	0	0	0	0	0	0

The agreement between the two calculations is seen to be good. The "4th-order error" [see Eq. (3.118)] in the relaxation calculation turns out to be of the order of 1V for the grid size used here. The series calculation is subject to the "Gibbs phenomenon" of Fig. 3-10. One could go on and write a routine (or use commercial software) to draw equipotentials and field-lines determined by the grid values of potential.

Chapter 4

4-1. (a) Assume a current I flows in one direction in the inner conductor, and in the reverse direction in the outer. In the space between conductors, the inner current produces the magnetic field (Prob. 1-19)

$$B_\theta = \frac{2I}{cr}$$



The outer current produces no field in this space because of its symmetry. The magnetic flux, Eq. (4.11), passing between the conductors in a length ℓ is

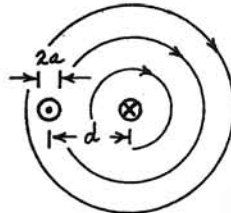
$$\Phi_m = \int \mathbf{B} \cdot \mathbf{n} \, da = \frac{2I\ell}{c} \int_a^b \frac{dr}{r} = \frac{2I\ell}{c} \ln\left(\frac{b}{a}\right)$$

From Eq. (4.9), the ratio of emf-per-unit-length to dI/dt is

$$L_{\mathcal{A}(\text{coax})} = \frac{2}{c^2} \ln\left(\frac{b}{a}\right)$$

(b) In this case, each wire contributes flux to the space between the wires, giving (in length ℓ)

$$\Phi_m = 2 \times \frac{2I\ell}{c} \int_a^d \frac{dr}{r} = \frac{4I\ell}{c} \ln\left(\frac{d}{a}\right)$$



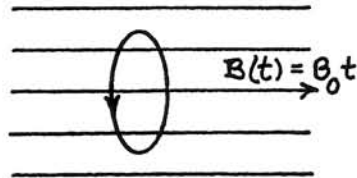
and hence

$$L_{\mathcal{A}(\text{parallel wire})} = \frac{4}{c^2} \ln\left(\frac{d}{a}\right)$$

4-2. From Prob. 1-24 we have

$$\oint \mathbf{A} \cdot d\boldsymbol{\ell} = \int \mathbf{B} \cdot \mathbf{n} \, da$$

Choose a Stokesian path in the form of a circle centered on the x_3 axis. The axial symmetry allows this relation to be evaluated as:



Chapter 4

$$(A_\theta)(2\pi r) = (B_\theta t)(\pi r^2) \Rightarrow \mathbf{A}(r) = \frac{1}{2} B_0 t r \mathbf{e}_\theta$$

where \mathbf{e}_θ is the azimuthal unit vector of cylindrical coordinates. Then, from Eq. (4.42),

$$\mathbf{E} = -\frac{1}{c} \frac{\partial \mathbf{A}}{\partial t} = -\frac{B_0 r}{2c} \mathbf{e}_\theta$$

An alternative approach for \mathbf{E} is to apply Faraday's law in the form of Eq. (4.12),

$$\oint \mathbf{E} \cdot d\boldsymbol{\ell} = -\frac{1}{c} \int \frac{\partial \mathbf{B}}{\partial t} \cdot \mathbf{n} \, da$$

to the same circular Stokesian loop:

$$(E_\theta)(2\pi r) = -\frac{1}{c}(B_0)(\pi r^2) \Rightarrow \mathbf{E}(r) = -\frac{B_0 r}{2c} \mathbf{e}_\theta$$

4-3. (a) Ampere's law and the Biot-Savart law are essentially inverses of each other: Ampere differentiates the field to find the sources, while Biot-Savart integrates the sources to find the field. Omitting the Maxwell displacement current in Ampere's law, the equations are:

$$\text{curl } \mathbf{B} = \frac{4\pi}{c} \mathbf{J} \quad (1) \quad \mathbf{B} = \frac{1}{c} \int \frac{\mathbf{J} \times \mathbf{e}_r}{r^2} d\nu \quad (2)$$

where \mathbf{J} is the total microscopic current and we have substituted $I d\boldsymbol{\ell} \rightarrow \mathbf{J} d\nu$ by Eq. (1.49). Faraday's law,

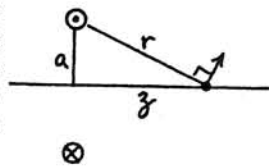
$$\text{curl } \mathbf{E} = -\frac{1}{c} \frac{\partial \mathbf{B}}{\partial t} \quad (3)$$

has a mathematical form identical to Ampere's law, with $\mathbf{B} \rightarrow \mathbf{E}$ and $4\pi\mathbf{J} \rightarrow -\partial\mathbf{B}/\partial t$. Consequently, the integral relation analogous to Biot-Savart is

$$\mathbf{E} = -\frac{1}{4\pi c} \int \frac{(\partial\mathbf{B}/\partial t) \times \mathbf{e}_r}{r^2} d\nu \quad (4)$$

Note: Under slowly varying conditions, the Maxwell term $(\partial\mathbf{E}/\partial t)/4\pi$ can be included within the "J" in both (1) and (2) [see Eq. (4.18)]. However, it will integrate to a null resultant in (2), because \mathbf{E} is derivable from a scalar potential in this limit. Under rapidly varying conditions, (2) is no longer correct, because of retardation effects. Then the proper formulas are Eqs. (8.26) and (8.30), which express the fields entirely in terms of the ultimate charge and current sources, without using "induction" terms involving $\partial\mathbf{B}/\partial t$ and $\partial\mathbf{E}/\partial t$.

(b) The time-varying magnetic flux in the ring constitutes a "magnetic current" producing an electric field according to (4). The situation is analogous to the circular electric current producing a magnetic field in Prob. 1-17. Only the components of $d\mathbf{E}$ parallel to the axis contribute to the net field, and the integration is elementary:



$$\begin{aligned} \mathbf{E}(z) &= -\frac{1}{4\pi c} \left[\frac{(\partial \mathbf{B} / \partial t)(S)(2\pi a)}{r^2} \right] \left(\frac{a}{r} \right) \mathbf{e}_z \\ &= -\frac{a^2 S}{2c(a^2+z^2)^{3/2}} \left(\frac{\partial \mathbf{B}}{\partial t} \right) \mathbf{e}_z \end{aligned}$$

4-4. The voltmeter V_1 measures $I_R R_1$, and V_2 measures $I_R R_2$. That is, the two meters read different values (for $R_1 \neq R_2$) even though connected to the same points a, b , because the electric field is not conservative (its line integral is not independent of path). Moreover, the meters read opposite polarities: i.e., one meter will indicate that Point a is "positive" relative to b , at the same instant that the other meter indicates the reverse).

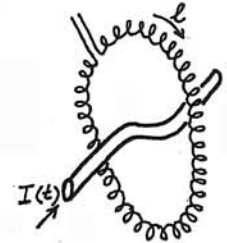
The point of this famous example is to clarify the distinction between conservative (Coulomb) and nonconservative (Faraday) electric fields. Because of the time-varying magnetic flux, a Faraday electric field exists both within the solenoid (where $\text{curl } \mathbf{E} \neq 0$) and in the space outside (where $\text{curl } \mathbf{E} \rightarrow 0$). Strictly, a vector field is conservative only if the curl vanishes *everywhere*. More to the point, one must be able to carry out the line integral $\int \mathbf{E} \cdot d\mathbf{l}$ around *any* closed path and get a null result. In this sense, the Faraday \mathbf{E} is nonconservative outside the solenoid, as well as inside.

However, in the present example, the Faraday contribution to the total \mathbf{E} acts as if it were conservative when we limit attention to a circuit-integration-loop that does *not* encircle the solenoid (e.g., the loop containing V_1 and R_1). That is, although there is a Faraday component of the total \mathbf{E} in the region occupied by this loop, both this component as well as the conservative Coulomb component of \mathbf{E} integrate to zero around the loop. Therefore we can pretend that the total \mathbf{E} is conservative, apply the Kirchhoff rule (sum of "potential-differences" equals zero) to the loop, and conclude that the voltmeter V_1 measures the magnitude, and the polarity, of the "voltage drop" $I_R R_1$. On the other hand, the loop containing V_1 and R_2 links the solenoid and therefore is acted on by the Faraday emf: in this loop, V_1 equals the sum/difference (depending on sign conventions) of $I_R R_2$ and $d\Phi/cdt$. Likewise, for the loop containing the two voltmeters, we have $|V_1| + |V_2| = |d\Phi/cdt|$, independent of the R s.

The underlying physics can be understood in more detail by noting that a conservative (Coulomb) component of \mathbf{E} exists, produced by charge on the circuit wires. This charge is distributed in such a way that the *total* field steers the current along the wire. That is, the line integral of the total field, $\int \mathbf{E} \cdot d\mathbf{l}$, must be zero along a piece of (resistanceless) hookup wire, and has the value IR through a resistor (see Prob. 1-34). The integral through a voltmeter is the "voltage" indicated by the voltmeter. The term "potential difference" (between Points a and b) refers to the integral of the conservative component, $\Delta\Phi = -\int_a^b \mathbf{E}_{\text{con}} \cdot d\mathbf{l}$ [Eq. (1.13)], while one uses the term "emf" for the nonconservative component, $\mathcal{E} = +\int_a^b \mathbf{E}_{\text{non}} \cdot d\mathbf{l}$. Since the total field, $\mathbf{E} = \mathbf{E}_{\text{con}} + \mathbf{E}_{\text{non}}$, is negligible along a piece of hookup wire (e.g., between Point a and the upper terminal of R_1), it follows that $\mathbf{E}_{\text{con}} = -\mathbf{E}_{\text{non}}$ within the wire. That is, the potential difference $\Delta\Phi$ and the emf \mathcal{E} are nonzero and equal for a piece of hookup wire. Because they cancel, they can both be ignored as indicated above.

See Romer, *Am.J.Phys.* **50**, 1089 (1982), and Purcell (Pu85, Problem 7.27).

4-5. We can regard the coordinate ℓ as a vector quantity directed normal to the turns of the toroidal winding. Then the emf induced in the turns within the element $d\ell$ is



$$d\mathcal{E} = (-) \frac{nS}{c} \frac{\partial \mathbf{B}}{\partial t} \cdot d\mathbf{\ell} = (-) \frac{nS}{c} \frac{d}{dt} (\mathbf{B} \cdot d\mathbf{\ell})$$

where we assume that \mathbf{B} is spatially uniform over the (thin) cross section S , but make no restriction on the orientation of \mathbf{B} or its variation along ℓ . Now, integrating around the loop, Ampere's law gives

$$\oint \mathbf{B} \cdot d\mathbf{\ell} = \frac{4\pi}{c} I_{\text{linked}}$$

Therefore, the induced emf is

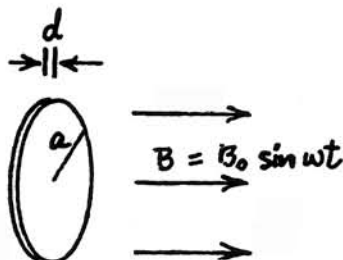
$$\mathcal{E}(t) = (-) \frac{4\pi nS}{c^2} \frac{dI}{dt}$$

A discussion of experiments using this device is given by Heller, *Am.J.Phys.* **60**, 17 and 274 (1992), and **61**, 1045 (1993). Note that the actual device requires the return lead to be threaded back through the solenoid to cancel the signal induced in the axial component of the helical winding.

4-6. We have axial symmetry. Paraphrasing the solution for Prob. 4-2, we have

$$E_{\theta}(r, t) = -\frac{r}{2c} \frac{\partial B}{\partial t}$$

$$\xrightarrow{\text{(first-order } B)} -\frac{\omega B_0}{2c} r \cos \omega t$$



From Ohm's law, Eq. (1.81), the current density is

$$\mathbf{J}(r, t) = \sigma \mathbf{E} \approx -\frac{\sigma \omega B_0}{2c} r \cos \omega t \mathbf{e}_{\theta}$$

Note: From Prob. 1-17, the *second-order* magnetic field at the center of the disk, due to the induced current, is

$$B_z^{(2)} = \frac{2\pi d}{c} \int_0^a \frac{J_{\theta}(r)}{r} dr = -\frac{\pi a d \sigma \omega}{c^2} B_0 \cos \omega t$$

Thus if $\pi a d \sigma \omega / c^2$ is not small compared to unity, the current density will be modified from that driven by the (first-order) externally applied field $B^{(1)} = B_0 \sin \omega t$. The system is then subject to the "skin effect" discussed in Section 5.6. For an extensive discussion of *eddy currents*, see Smythe (Sm89, Chapter 10).

4-7. (a) The mobile charge carriers (electrons) carried along within the wire are subject to the Lorentz force $\mathbf{F} = q\mathbf{u} \times \mathbf{B}/c$ [Eq. (1.52)]. The work done on a charge q as it is pumped through the element is $dW = \mathbf{F} \cdot d\mathbf{l}$, and the emf is defined as the work done per unit charge. Thus,

$$d\mathcal{E} = \frac{dW}{q} = \frac{\mathbf{u}}{c} \times \mathbf{B} \cdot d\mathbf{l}$$

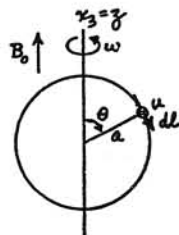
Note: There is a seeming paradox here because magnetic forces, being perpendicular to the displacement of a moving charge, can in fact do no work on the charge! When this primitive "generator" drives a current, the current experiences a magnetic force, and the agent causing the motion does the work against this force. See Griffiths (Gr89, Section 7.1.3).

(b) For the rotating spherical shell,

$$\mathbf{u} = \omega a \sin \theta \mathbf{e}_{\phi}$$

$$d\mathbf{l} = a d\theta \mathbf{e}_{\theta}$$

$$\mathbf{e}_{\phi} \times \mathbf{e}_z \cdot \mathbf{e}_{\theta} = \cos \theta$$



and the emf between pole and equator is

$$\text{emf} = \frac{\omega a^2 B_0}{c} \int_0^{\pi/2} \sin \theta \cos \theta d\theta = \frac{\omega a^2 B_0}{2c}$$

Positive charge is pumped from the poles to the equator—i.e., the equator is the "positive" terminal of the generator.

4-8. The charge carriers (conduction electrons) are in equilibrium between the magnetic force $q\mathbf{u} \times \mathbf{B}/c$ and the electrostatic force $q\mathbf{E}$ produced by charge distributed on the sphere. Consequently the difference of potential between the pole ($\theta = 0$) and a point on the surface at polar angle θ is

$$\begin{aligned} \Phi(r=a; \theta) &= -\int \mathbf{E} \cdot d\mathbf{l} = +\frac{1}{c} \int \mathbf{u} \times \mathbf{B} \cdot d\mathbf{l} \\ &= \frac{\omega a^2 B_0}{c} \int_0^{\theta} \sin \theta \cos \theta d\theta \\ &= \frac{\omega a^2 B_0}{2c} (1 - \cos^2 \theta) \\ &= \frac{\omega a^2 B_0}{3c} [P_0(\cos \theta) - P_2(\cos \theta)] \end{aligned} \quad (1)$$

The final expression is cast in terms of Legendre polynomials using Eqs. (3.41). The potential at the equator ($\theta = \pi/2$) equals the emf calculated in Prob. 4-7.

From Eq. (3.39), the potentials inside and outside the sphere that match this boundary condition are:

$$\Phi(r < a) = \frac{\omega a^2 B_0}{3c} \left[P_0 - \left(\frac{r}{a}\right)^2 P_2 \right] \quad (2)$$

$$\Phi(r > a) = \frac{\omega a^2 B_0}{3c} \left[\left(\frac{a}{r}\right) P_0 - \left(\frac{a}{r}\right)^3 P_2 \right] \quad (3)$$

Now, equation (3) represents the external potential of an axially symmetric charge distribution composed of a monopole and a quadrupole. In the context of this problem, we assume that the rotating sphere has no net charge, and therefore there can be no P_0 term. It was an arbitrary choice to take $\Phi = 0$ at the pole. If, instead, we take the potential zero at the zero of P_2 (that is, where $\cos^2 \theta = 1/3$, or $\theta \approx 55^\circ$), then (1)–(3) reduce to:

$$\Phi(r=a) = -\frac{\omega a^2 B_0}{3c} P_2(\cos\theta) \quad (1')$$

$$\Phi(r<a) = -\frac{\omega a^2 B_0}{3c} \left(\frac{r}{a}\right)^2 P_2 \quad (2')$$

$$\Phi(r>a) = -\frac{\omega a^2 B_0}{3c} \left(\frac{a}{r}\right)^3 P_2 \quad (3')$$

Adding a constant to the boundary condition at $r = a$ does not change differences of potential between any two points on the sphere. The exterior potential is now that of a pure quadrupole.

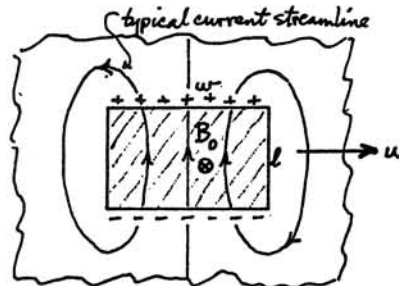
The charge density on the spherical surface is now, from Eqs. (1.14) and (1.85),

$$\begin{aligned} \rho_s(\theta) &= \frac{1}{4\pi} [E_r(r>a) - E_r(r<a)]_{r=a} \\ &= -\frac{\omega a B_0}{12\pi c} (+3P_2 + 2P_2) = -\frac{5\omega a B_0}{12\pi c} P_2 \end{aligned} \quad (4)$$

The rotating charge constitutes a system of current loops, which turn out to have dipole and octupole magnetic moments. The associated ("second-order") magnetic field produces an increment in emf and potential, which is negligible so long as $(\omega a)^2 \ll c^2$.

4-9. Each element of width dw and length l constitutes a "moving wire" which, from Prob. 4-7, generates the emf

$$\mathcal{E} = \frac{u B_0 \ell}{c}$$



which pumps charge through the magnetic-field region. The conductivity of the sheet allows this pumped charge to flow as an eddy current around the magnet's "footprint" in the manner indicated in the sketch. To proceed further, we need an estimate of the effective resistance of this distributed array of current paths. The current density *within* the footprint should be fairly uniform (except for fringing effects near the " ℓ " sides), and the effective "internal resistance" (within the "battery") can be estimated as

$$R_{\text{int}} = \frac{(\text{length})}{\sigma(\text{cross section})} = \frac{\ell}{\sigma w h}$$

We may guess that the effective resistance of the *external* portion of the circuit is of this same order of magnitude (the paths are longer, but wider). Since the internal and external resistances are in series, we can write the total effective circuit resistance as $R_{\text{tot}} = R_{\text{int}}/\alpha$, where the coefficient α is of the order of $1/2$. Thus the total magnitude of the eddy current is

$$I = \frac{\mathcal{E}}{R_{\text{int}}/\alpha} = \frac{\alpha \sigma h w B_0 u}{c}$$

As this current flows through the footprint, it experiences the Lorentz force [Eq. (1.54)], in the direction opposing the velocity \mathbf{u} ,

$$\mathbf{F} = \frac{I \boldsymbol{\ell} \times \mathbf{B}}{c} = -\frac{\alpha \sigma h \ell w B_0^2}{c^2} \mathbf{u}$$

It turns out that the fringing fields, and the resulting distribution of current density, can be calculated for this geometry with some rigor, giving

$$\alpha = 1 - \frac{1}{2\pi} \left[4 \tan^{-1} A + A \ln \left(1 + \frac{1}{A^2} \right) - \frac{1}{A} \ln(1 + A^2) \right]$$

where $A = w/\ell$, the aspect ratio of the footprint. For a square footprint ($w = \ell$), indeed $\alpha = 1/2$, precisely. See the paper cited.

4-10. (a) Using a Gaussian pillbox with one face within the field-free interior of one of the capacitor plates [see Fig. 1-11 and Eq. (1.84)], the uniform D -field inside the capacitor is related to the surface charge density by $D = \epsilon E = 4\pi\rho_s = 4\pi Q/A$. Thus the displacement current density is

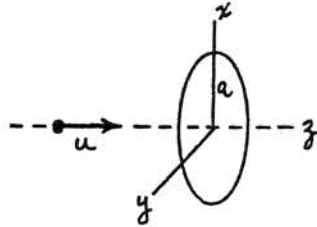
$$\frac{1}{4\pi} \frac{\partial D}{\partial t} = \frac{1}{A} \frac{dQ}{dt}$$

Integrating over area (and neglecting edge effects!) gives the total displacement current as dQ/dt , which by definition is the current I flowing into the capacitor.

(b) If Q is the total charge on one plate of the capacitor, however distributed, then by Gauss' law the total D -flux through a *closed* surface surrounding the plate is $(1/4\pi) \int \mathbf{D} \cdot \mathbf{n} da$. And hence the time derivative of the total flux is $dQ/dt = I$. However, the surface S in Fig. 4-2 is not closed. To close it, construct a conical surface S' extending from the contour Γ to the point where the circuit wire connects to the left-hand capacitor plate. The displacement current through S' will be less than I to the degree that there is displacement current through S' . If there is a significant electric field outside the capacitor, then there is a corresponding displacement-current correction for the surface in Fig. 4-1.

The existence of "fringe" fields outside a capacitor, and indeed in the vicinity of the "hookup wire" of a circuit, can be tricky. See Solution for Prob. 4-13.

4-11. We assume the medium is free space, $\epsilon = \mu = 1$. Calculate the electric flux at the instant when the particle is at $z = -z_0$ by integrating the Coulomb field over a spherical cap bounded by the circle and of radius $(a^2 + z_0^2)^{1/2}$:



$$\begin{aligned} \int \mathbf{D} \cdot \mathbf{n} \, da &= \int_0^{\tan^{-1} a/z_0} \frac{q}{(a^2 + z_0^2)} 2\pi(a^2 + z_0^2) \sin\theta \, d\theta \\ &= 2\pi q \int_{z_0/(a^2+z_0^2)^{1/2}}^1 d(\cos\theta) = 2\pi q \left[1 - \frac{z_0}{(a^2 + z_0^2)^{1/2}} \right] \end{aligned}$$

Now generalize this result, noting that as the particle moves from $z = -\infty$ through 0 to $+\infty$, the flux

$$\int \mathbf{D} \cdot \mathbf{n} \, da = 2\pi q \left[1 + \frac{z}{(a^2 + z^2)^{1/2}} \right]$$

grows continuously from 0, through $2\pi q$, to $4\pi q$. Therefore the displacement current is proportional to

$$\begin{aligned} \frac{d}{dt} \int \mathbf{D} \cdot \mathbf{n} \, da &= 2\pi q \left[\frac{1}{(a^2 + z^2)^{1/2}} - \frac{z^2}{(a^2 + z^2)^{3/2}} \right] \frac{dz}{dt} \\ &= 2\pi q \frac{a^2}{(a^2 + z^2)^{3/2}} u \end{aligned}$$

For nonmagnetic materials and in the absence of conduction current, the integral form of the Ampere-Maxwell law, Eq. (4.17), reduces to

$$\oint \mathbf{B} \cdot d\boldsymbol{\ell} = \frac{1}{c} \frac{d}{dt} \int \mathbf{D} \cdot \mathbf{n} \, da$$

Using the usual symmetry arguments (see Prob. 1-19: because the *direction* of the magnetic field is azimuthal, and its *magnitude* depends only upon radius, the line integral reduces to elementary multiplication), the magnetic field at the circle is given by

$$(B_\theta)(2\pi a) = \frac{2\pi q}{c} \frac{a^2}{(a^2 + z^2)^{3/2}} u$$

$$\mathbf{B} = \frac{q}{c} \frac{au}{(a^2 + z^2)^{3/2}} \mathbf{e}_\theta \quad (1)$$

The moving-particle form of the Biot-Savart law is [Eqs. (1.36) and (1.49)]

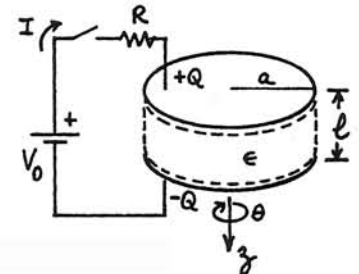
$$\mathbf{B} = \frac{q\mathbf{u} \times \mathbf{e}_r}{c r^2}$$

Here, $r = (a^2 + z^2)^{1/2}$, and the sine of the angle between \mathbf{u} and \mathbf{e}_r , implicit in the cross product, is a/r . Thus Biot-Savart reduces to

$$\mathbf{B} = \frac{q}{c} \frac{u}{r^2} \frac{a}{r} \mathbf{e}_\theta = \frac{q}{c} \frac{au}{(a^2 + z^2)^{3/2}} \mathbf{e}_\theta \quad (2)$$

in agreement with (1).

4-12. If the time-variations are slow enough that we can neglect Faraday induction, the electric field is essentially conservative and $\oint \mathbf{E} \cdot d\boldsymbol{\ell} = 0$. That is, the potential differences must sum to zero around the circuit (Kirchhoff loop rule):



$$V_0 - RI - \frac{Q}{C} = 0$$

where $C = \epsilon\pi a^2/4\pi h$ (see Prob. 1-7), and $I = dQ/dt$. Thus we have the differential equation

$$R \frac{dQ}{dt} + \frac{1}{C} Q = V_0$$

The solution satisfying the given initial condition ($Q = 0$ at $t = 0$) is

$$Q(t) = CV_0 (1 - e^{-t/RC})$$

(a) Since $C = Q/\Delta\Phi$ and $\Delta\Phi = Eh$, the electric field within the capacitor (neglecting edge corrections) is

$$\mathbf{E}(t) = \frac{Q}{Ch} \mathbf{e}_z = \frac{V_0}{h} (1 - e^{-t/RC}) \mathbf{e}_z$$

where \mathbf{e}_z is the unit vector along the axis of the capacitor as shown in the sketch.

(b) The magnetic field is azimuthal within the capacitor and can be found from the displacement current using Eq. (4.17) and symmetry arguments (see Solutions for Probs. 1-19 and 4-11):

$$(B_\theta)(2\pi r) = \frac{\epsilon}{c} \frac{\partial E_z}{\partial t} (\pi r^2)$$

$$\mathbf{B}(r,t) = \frac{\epsilon V_0}{2chRC} r e^{-t/RC} \mathbf{e}_\theta = \frac{2V_0}{cRa^2} r e^{-t/RC} \mathbf{e}_\theta$$

Our neglect of induction neglects the electric field associated with this time-varying magnetic field, as well as the magnetic field produced by the current dQ/dt in the circuit leads. In circuit terms, we are assuming that the circuit has negligible inductance.

(c) The Poynting vector, Eq. (4.66), is

$$\begin{aligned} \mathbf{S}(r,t) &= \frac{c}{4\pi} \mathbf{E} \times \mathbf{B} = \frac{c}{4\pi} \frac{V_0}{h} \frac{2V_0}{cRa^2} r (1 - e^{-t/RC}) e^{-t/RC} \mathbf{e}_z \times \mathbf{e}_\theta \\ &= \frac{V_0^2}{4\pi Rha^2} r (e^{-t/RC} - e^{-2t/RC}) (-\mathbf{e}_r) \end{aligned}$$

The exponential factor rises from zero at $t=0$ to a maximum of $1/4$ at $t=RC \ln 2$, and then decays back to zero as $t \rightarrow \infty$. The Poynting flux carries the field energy *radially inward* as the capacitor charges. The Poynting flux-lines outside the capacitor originate at the battery, following paths determined by the geometry of the circuit leads.

(d) The field energy stored in the capacitor is found by integrating Eq. (4.70):

$$\begin{aligned} U(t) &= \frac{1}{8\pi} \int (\epsilon E^2 + \frac{B^2}{\mu}) dv \\ &= \frac{\epsilon V_0^2 \pi a^2}{8\pi h} (1 - e^{-t/RC})^2 + \frac{h}{8\pi \mu} \left(\frac{\epsilon V_0}{2chRC} \right)^2 e^{-2t/RC} \int_0^a r^2 2\pi r dr \\ &= \frac{1}{2} CV_0^2 \left[(1 - e^{-t/RC})^2 + \frac{\epsilon}{8\mu} \left(\frac{a}{cRC} \right)^2 e^{-2t/RC} \right] \\ &\rightarrow \frac{1}{2} CV_0^2 (1 - e^{-t/RC})^2 \end{aligned}$$

Dropping the magnetic-energy term follows from our neglect of magnetic induction, i.e., treating the electric field as conservative. We see here that this is equivalent to assuming that the transit time for electromagnetic effects to cross the capacitor, a/c , is small compared to the time constant RC .

(e) The "ground" point of the circuit has not been specified. For convenience, we can define the positive plate of the capacitor as $\Phi = 0$, and as the origin of the z axis (see sketch; the negative plate is at $z = +h$). Then, within the capacitor,

$$\Phi(z,t) = -E_z z = -\frac{V_0}{h} z (1 - e^{-t/RC})$$

(f) Since we have axial symmetry, it is convenient to use the circuital law of Prob. 1-24,

$$\oint \mathbf{A} \cdot d\boldsymbol{\ell} = \int \mathbf{B} \cdot d\mathbf{a}$$

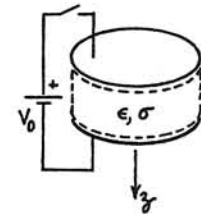
The magnetic field is azimuthal and varies only with radius r . We can take the vector potential to be axial, likewise varying with r , and choose $\mathbf{A} = 0$ at the axis. Use a Stokesian rectangle with one side coinciding with the axis, the opposite side at radius r (within the capacitor), and the two radial sides coinciding with the surface of the capacitor plates. Then, only one of the four sides contributes (negatively) to the loop integral, giving:

$$\begin{aligned} -A_z(r) h &= \int_0^r B_\theta(r) h dr \\ &= \frac{\epsilon V_0}{2cRC} e^{-t/RC} \int_0^r r dr \end{aligned}$$

$$\mathbf{A}(r,t) = -\frac{\epsilon V_0}{4chRC} r^2 e^{-t/RC} \mathbf{e}_z$$

It is easy to calculate $(1/c)\partial\mathbf{A}/\partial t$ to show that there is a negligible nonconservative contribution to \mathbf{E} in Eq. (4.42) in the limit $a/c \ll RC$. The divergence of \mathbf{A} is zero (Coulomb gauge), which is appropriate in the "slowly varying" limit. We could add to this \mathbf{A} the gradient of any function of space and time so long as its time derivative contributes negligibly to \mathbf{E} .

4-13. (a) To the extent that we can neglect edge corrections, the electric field within the capacitor is uniform, $E = \Delta\Phi/h = Q/Ch$. This field drives the current density $J = \sigma E$, which is related to the time-rate-of-change of the charge by



$$\frac{dQ}{dt} = -(J)(\pi a^2) = -\frac{\sigma Q}{Ch} \pi a^2 = -\frac{Q}{RC}$$

In the final form we have introduced the resistance, $R = h/\sigma\pi a^2$, of the leaky dielectric filling the capacitor. The solution of this differential equation, for the given initial condition, is

$$Q(t) = CV_0 e^{-t/RC} \quad (1)$$

This is, of course, identical to the charge decay of a nonleaky capacitor connected to an external resistor R .

(b) The classes of current density are explicit in the right-hand side of Eq. (4.18). The conduction (free) current density is

$$\mathbf{J} = -\frac{1}{\pi a^2} \frac{dQ}{dt} \mathbf{e}_z = \frac{V_0}{R\pi a^2} e^{-t/RC} \mathbf{e}_z$$

The polarization current density is, using Eqs. (1.28) and (1.33),

$$\begin{aligned} \frac{\partial \mathbf{P}}{\partial t} &= \left(\frac{\epsilon - 1}{4\pi} \right) \frac{\partial \mathbf{E}}{\partial t} = \left(\frac{\epsilon - 1}{4\pi} \right) \frac{1}{hC} \frac{dQ}{dt} \mathbf{e}_z \\ &= -\left(\frac{\epsilon - 1}{4\pi} \right) \frac{V_0}{hRC} e^{-t/RC} \mathbf{e}_z \\ &= -\left(\frac{\epsilon - 1}{\epsilon} \right) \frac{V_0}{R\pi a^2} e^{-t/RC} \mathbf{e}_z \end{aligned}$$

(There is no current density associated with magnetization here.) The \mathbf{E} -field displacement current density is

$$\frac{1}{4\pi} \frac{\partial \mathbf{E}}{\partial t} = \left(\frac{1}{\epsilon - 1} \right) \frac{\partial \mathbf{P}}{\partial t} = -\frac{1}{\epsilon} \frac{V_0}{R\pi a^2} e^{-t/RC} \mathbf{e}_z$$

(c) We use the integral form of the Ampere-Maxwell law, Eq. (4.17), and the usual symmetry arguments (see Probs. 1-19 and 4-11), to find

$$(B_\theta)(2\pi r) = \frac{4\pi}{c} \left(1 - \frac{\epsilon - 1}{\epsilon} - \frac{1}{\epsilon} \right) \frac{V_0}{R\pi a^2} e^{-t/RC} (\pi r^2) = 0 \quad (2)$$

The three terms in parentheses are coefficients of the three current densities found in Part (b). The conduction and \mathbf{D} -field displacement currents cancel identically and there is no magnetic field.

This is not the whole story however. If we assume that the conducting dielectric ends at the edge of the capacitor (i.e., it is a disk of radius a and thickness h), then the conduction current is confined within the material, whereas the displacement current "fringes" out around the edges. Now the total Ampere-Maxwell currents no longer quite cancel. The magnitude of this residual magnetic field is surprisingly large—it turns out to be of the order of h/a times the field that would be calculated from *either* the conduction current *or* the displacement current alone. On the other hand, if we completely immerse the capacitor in a homogeneous leaky dielectric, outside and in,

then the currents do cancel identically, and there is no magnetic field. See the papers by Bartlett and by French; also Carlson and Illman, *Am.J.Phys.* **62**, 1099 (1994).

(d) When the capacitor discharges through an external resistor R , the Kirchhoff loop rule gives

$$R \frac{dQ}{dt} + \frac{1}{C} Q = 0$$

the solution of which is identical to (1) even though the current dQ/dt is in a different place. There is no longer a conduction current within the capacitor, but the polarization and displacement currents remain as calculated in Part (b). Revising (2), we have

$$(B_\theta)(2\pi r) = \frac{4\pi}{c} \left(0 - \frac{\epsilon - 1}{\epsilon} - \frac{1}{\epsilon} \right) \frac{V_0}{R\pi a^2} e^{-t/RC} (\pi r^2) \quad (2')$$

$$\mathbf{B}(r,t) = -\frac{2V_0}{cRa^2} r e^{-t/RC} \mathbf{e}_\theta$$

This field during discharge is in the reverse sense from that during the charging process, found in Prob. 4-12(b).

4-14. The fields are related to the potentials by Eqs. (4.40) and (4.42),

$$\mathbf{E} = -\mathbf{grad} \Phi - \frac{1}{c} \frac{\partial \mathbf{A}}{\partial t}$$

$$\mathbf{B} = \mathbf{curl} \mathbf{A}$$

Use of these potentials automatically satisfies the homogeneous Maxwell equations, Eqs. (4.22–23). Substituting in the inhomogeneous equations, Eqs. (4.21) and (4.24), written for vacuum ($\epsilon = \mu = 1$; ρ, \mathbf{J} represent *total* charges and currents), we get

$$\mathbf{div} \mathbf{E} = -\nabla^2 \Phi - \frac{1}{c} \frac{\partial}{\partial t} \mathbf{div} \mathbf{A} = 4\pi \rho \quad (1)$$

$$\begin{aligned} \mathbf{curl} \mathbf{B} - \frac{1}{c} \frac{\partial \mathbf{E}}{\partial t} \\ = -\nabla^2 \mathbf{A} + \mathbf{grad} \mathbf{div} \mathbf{A} + \frac{1}{c} \mathbf{grad} \frac{\partial \Phi}{\partial t} + \frac{1}{c^2} \frac{\partial^2 \mathbf{A}}{\partial t^2} = \frac{4\pi}{c} \mathbf{J} \end{aligned} \quad (2)$$

[We have used Eqs. (A.29), (A.40), and (A.41), and the commutivity of space and time derivatives.] In the Coulomb gauge, $\mathbf{div} \mathbf{A} = 0$, (1) reduces to Poisson's equation, Eq. (1.15),

$$\nabla^2 \Phi = -4\pi \rho$$

The solution of this equation is the *instantaneous* Coulomb potential,

$$\Phi(\mathbf{r}, t) = \int \frac{\rho(\mathbf{r}', t)}{|\mathbf{r} - \mathbf{r}'|} dv' \quad (3)$$

Compare the *retarded* potential of Eq. (8.4). Similarly, for $\text{div } \mathbf{A} = 0$, (2) reduces to

$$\nabla^2 \mathbf{A} - \frac{1}{c^2} \frac{\partial^2 \mathbf{A}}{\partial t^2} = -\frac{4\pi}{c} \mathbf{J} + \frac{1}{c} \text{grad} \frac{\partial \Phi}{\partial t} \quad (4)$$

Now let

$$\mathbf{J} = \mathbf{J}_1 + \mathbf{J}_2$$

where

$$\text{curl } \mathbf{J}_1 = 0, \quad \text{div } \mathbf{J}_2 = 0$$

Take the time derivative of (3) and use the equation of continuity, Eq. (4.4), to obtain

$$\frac{\partial \Phi}{\partial t} = - \int \frac{\text{div}' \mathbf{J}(\mathbf{r}', t)}{|\mathbf{r} - \mathbf{r}'|} dv'$$

Now we know that if any vector field obeys the relations

$$\text{div } \mathbf{J}_1 = 4\pi a(\mathbf{r}), \quad \text{curl } \mathbf{J}_1 = 0$$

then by analogy with the electrostatic field [see Eqs. (1.14) and (1.21)],

$$\begin{aligned} \mathbf{J}_1 &= -\text{grad} \int \frac{a(\mathbf{r}')}{|\mathbf{r} - \mathbf{r}'|} dv' \\ &= -\frac{1}{4\pi} \text{grad} \int \frac{\text{div}' \mathbf{J}_1(\mathbf{r}')}{|\mathbf{r} - \mathbf{r}'|} dv' \end{aligned}$$

Thus, since $\text{div } \mathbf{J} = \text{div } \mathbf{J}'$,

$$\text{grad} \frac{\partial \Phi}{\partial t} = 4\pi \mathbf{J}_1$$

and (4) reduces to

$$\nabla^2 \mathbf{A} - \frac{1}{c^2} \frac{\partial^2 \mathbf{A}}{\partial t^2} = -\frac{4\pi}{c} \mathbf{J}_2$$

4-15. (a) As suggested, the partially inserted slab amounts to two capacitors in parallel, so the total capacitance [Prob. 1-7] is

$$C = \frac{1}{4\pi} \epsilon \frac{wx}{h} + \frac{1}{4\pi} 1 \frac{w(w-x)}{h} = \frac{w}{4\pi h} [(\epsilon - 1)x + w]$$

(b) Define the potential of the negatively charged plate as $\Phi_- = 0$; the positively charged plate then has the potential $\Phi_+ = \Delta\Phi = Q/C$ and surface charge such that $\int \rho_s da = +Q$. Equation (4.83) integrates trivially to

$$U_e = \frac{1}{2} \int \rho_s \Phi da \rightarrow \frac{1}{2} Q \Phi_+ = \frac{Q^2}{2C}$$

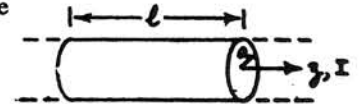
(c) Now, the force on the slab is

$$\begin{aligned} F_x &= -\frac{d}{dx} \left(\frac{Q^2}{2C} \right) = +\frac{Q^2}{2C^2} \frac{dC}{dx} \\ &= \frac{1}{2} \Delta\Phi^2 \frac{w}{4\pi h} (\epsilon - 1) \end{aligned}$$

The force is in the $+x$ direction, that is, toward larger insertion of the slab. Note that the force is independent of the insertion distance x , so long as the insertion is sufficient to reach the uniform field in the interior of the capacitor. See the cited paper by Margulies for a more complete discussion.

4-16. Consider a length ℓ of the wire, whose radius is a . The resistance is (see Prob. 1-34)

$$R = \frac{\ell}{\sigma\pi a^2}$$



Since the current density is $\mathbf{J} = I/\pi a^2$, the electric field required to drive the current is, from Eq. (1.81),

$$\mathbf{E} = \frac{\mathbf{J}}{\sigma} = \frac{I}{\sigma\pi a^2} \mathbf{e}_z$$

which integrates to a difference of potential $\Delta\Phi = E\ell$ between the ends of the wire. By Eq. (1.89) the *tangential* component of \mathbf{E} must be continuous across the surface of the wire. The magnetic field at the surface of the wire is, from Ampere's law [Prob. 1-19],

$$\mathbf{B} = \frac{2I}{ca} \mathbf{e}_\theta$$

Consequently the Poynting vector, Eq. (4.66), is *radially inward* at the surface,

$$\mathbf{S} = \frac{c}{4\pi} \mathbf{E} \times \mathbf{B} = \frac{1}{4\pi} \frac{2I^2}{\sigma a^3} (-\mathbf{e}_r)$$

Integrating this over the surface area $2\pi a\ell$ gives the total power flow

$$P = (S)(2\pi a\ell) = \frac{1}{4\pi} \frac{2I^2}{\sigma a^3} 2\pi a\ell = I^2 R$$

The Poynting vector associated with the *normal* component of \mathbf{E} , due to charge on the surface of the wire, represents power flow *parallel* to the wire and is the mechanism by which the wire can transmit power from one end to the other. From the Poynting point of view, the wire acts as a guide for electromagnetic energy. The energy is transported *outside* the wire, only flowing into the wire as needed to provide the Joule heating. See Heald, *Am.J.Phys.* 52, 522 (1984).

4-17. The relation

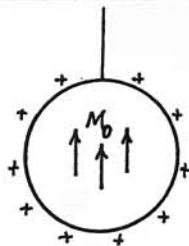
$$\frac{d}{dt} \left(\frac{1}{2} LI^2 + \frac{1}{2} \frac{Q^2}{C} \right) + RI^2 - \mathcal{E}I = 0$$

is the circuit analog of the integral form of Poynting's theorem, Eq. (4.69). The time derivative is the rate of change of energy stored in the inductor and capacitor. The familiar I^2R term represents the rate of energy dissipation from the circuit by conversion to heat in the resistor. The $\mathcal{E}I$ term is the power delivered to the circuit by the driving emf \mathcal{E} . The sign of this last term is reversed from that of the Poynting-vector term in Eq. (4.69) because, by convention, the surface integral of \mathbf{S} is calculated for power flowing *out* of the system.

4-18. (a) From the definition of the magnetization \mathbf{M} [Sec. 1-6], a uniformly magnetized sphere has the total dipole moment $\mathbf{m} = \frac{4\pi}{3} a^3 \mathbf{M}_0$. Its external field is then given by Eq. (2.64) as

$$\mathbf{B}(r, \theta) = \frac{4\pi a^3 M_0}{3} \frac{1}{r^3} (2\cos\theta \mathbf{e}_r + \sin\theta \mathbf{e}_\theta)$$

where θ is the polar angle from the axis defined by \mathbf{M}_0 . This formula turns out to be valid *everywhere* outside the sphere, not just at large distances. To prove this in full detail, apply the Legendre-polynomial expansion, Eq. (3.39), of the magnetic scalar



potential [Sec. 2.7] to the regions inside and outside the spherical surface. Observe that the magnetic surface charge, $\rho_s^* = \mathbf{n} \cdot \mathbf{M}_0 = M_0 \cos\theta$, which provides the boundary condition at the interface, implies a *uniform* field inside ($\mathbf{H} = -\frac{4\pi}{3} \mathbf{M}_0$, $\mathbf{B} = +\frac{8\pi}{3} \mathbf{M}_0$), and the given *pure-dipole* field outside [see Probs. 1-13, 2-24, and 3-25].

With the charge Q distributed symmetrically over the conducting sphere, the external electric field is the same as the field of a point charge,

$$\mathbf{E}(r) = \frac{Q}{r^2} \mathbf{e}_r$$

Therefore, the Poynting vector [Eq. (4.66)] is

$$\mathbf{S}(r, \theta) = \frac{c}{4\pi} \mathbf{E} \times \mathbf{B} = \frac{1}{3} c Q M_0 a^3 \frac{1}{r^5} \sin\theta \mathbf{e}_\phi$$

That is, electromagnetic energy is flowing *azimuthally* in the space outside the sphere. (Inside the sphere, $\mathbf{S} = 0$ because $\mathbf{E} = 0$.)

(b) Where there is energy flow, there is also momentum. By Eq. (4.108), the density of the field momentum is $\mathbf{g} = \mathbf{S}/c^2$, which in this case constitutes the *angular momentum*

$$\begin{aligned} \mathbf{L} &= \int \mathbf{r} \times \mathbf{g} \, dV = \mathbf{e}_z \iint (r \sin\theta) \left(\frac{Q M_0 a^3}{3c} \frac{1}{r^5} \sin\theta \right) (2\pi r^2 \sin\theta \, dr \, d\theta) \\ &= \mathbf{e}_z \frac{2\pi Q M_0 a^3}{3c} \int_a^\infty \frac{1}{r^2} \, dr \int_0^\pi \sin^3\theta \, d\theta \\ &= \frac{8\pi Q M_0 a^2}{9c} \mathbf{e}_z \end{aligned} \quad (1)$$

If angular momentum is to be conserved about the suspension (z) axis, then when Q is changed, the sphere itself must acquire mechanical angular momentum. That is, if we remove the charge Q through the fine wire (moderately quickly), then the sphere will start rotating about the vertical axis. (Because of the elasticity of the supporting wire, the sphere would subsequently undergo torsional oscillations.)

To see how the torque is delivered to the sphere, consider the forces on the surface current created by the changing charge. Assume that, at any instant, the charge is distributed uniformly over the sphere. The amount of charge below the co-latitude θ is then

$$Q_\theta(\theta) = \frac{Q}{4\pi} 2\pi(1 + \cos\theta)$$

The total current crossing this latitude is then $I = dQ/dt$, and the surface current density is

$$\mathbf{K}(\theta) = \frac{dQ/dt}{2\pi a \sin\theta} \mathbf{e}_\theta$$

This distributed current experiences a Lorentz force in the magnetic field, producing the torque

$$\begin{aligned} \mathcal{T} &= \frac{1}{c} \int \mathbf{r} \times (\mathbf{K} \times \mathbf{B}) da \\ &= -\frac{\mathbf{e}_z}{c} \int (a \sin\theta) \left(\frac{\frac{1}{2}(1+\cos\theta)dQ/dt}{2\pi a \sin\theta} \right) \left(\frac{8\pi M_0 \cos\theta}{3} \right) (2\pi a^2 \sin\theta d\theta) \\ &= -\mathbf{e}_z \frac{4\pi a^2 M_0}{3c} \frac{dQ}{dt} \int_0^\pi (1+\cos\theta) \cos\theta \sin\theta d\theta = \frac{8\pi a^2 M_0}{9c} \left(-\frac{dQ}{dt} \right) \mathbf{e}_z \quad (2) \end{aligned}$$

Since $\mathcal{T} = d\mathbf{L}_{\text{sph}}/dt$, this torque drives the sphere to acquire the angular momentum (1) lost by the electromagnetic field.

This is a version of the famous "Feynman disk paradox." As noted in the text (footnote, end of Sec. 4.6), there are many discussions in the literature of similar systems with Poynting energy and momentum arising from "static" electric and magnetic fields. The particular geometry chosen here allows relatively simple quantitative evaluation, but it leaves some loose ends [see Pugh and Pugh, *Am.J.Phys.* 35, 153 (1967)]. Since the mass (moment of inertia) of the sphere is an independent parameter, there is no automatic conservation of energy between field and matter; presumably this is accomplished by Poynting energy flowing axially in or out of the system along the suspension wire. Also, the symmetry of the system does not give a simple mechanism by which the torque, which acts on the "free" conduction electrons, is communicated to the rigid atomic lattice of the sphere.

4-19. Using Gauss' law, Eq. (1.6), with symmetry arguments (see Solution for Prob. 1-4), we find the electric field:

$$\oint \mathbf{E} \cdot d\mathbf{a} \rightarrow E_r(r) (4\pi r^2) = \begin{cases} 4\pi\rho_0 \frac{4\pi}{3} r^3 & (r \leq a) \\ 4\pi\rho_0 \frac{4\pi}{3} a^3 & (r \geq a) \end{cases}$$

$$\mathbf{E} = \begin{cases} \frac{4\pi}{3} \rho_0 r \mathbf{e}_r & (r \leq a) \\ \frac{4\pi}{3} \rho_0 \frac{a^3}{r^2} \mathbf{e}_r & (r \geq a) \end{cases}$$

(a) By integrating Eq. (4.70), the electrostatic energy is

$$\begin{aligned} U_{es} &= \int \frac{E^2}{8\pi} dv = \frac{1}{8\pi} \left(\frac{4\pi}{3} \rho_0 \right)^2 \left[\int_0^a r^2 4\pi r^2 dr + \int_a^\infty \frac{a^6}{r^4} 4\pi r^2 dr \right] \\ &= \frac{8\pi^2 \rho_0^2}{9} \left(\frac{a^5}{5} + a^5 \right) = \frac{16\pi^2 \rho_0^2 a^5}{15} \quad (1) \end{aligned}$$

(b) The potential *inside* the sphere is, taking $\Phi = 0$ at infinity as required,

$$\begin{aligned} \Phi(r) &= - \int_\infty^r \mathbf{E} \cdot d\mathbf{r} = - \frac{4\pi\rho_0}{3} \left[\int_\infty^a \frac{a^3}{r^2} dr + \int_a^r r dr \right] \\ &= \frac{4\pi\rho_0}{3} \left[a^2 - \frac{1}{2}(r^2 - a^2) \right] \\ &= \frac{4\pi\rho_0}{3} (3a^2 - r^2) \quad (r < a) \end{aligned}$$

Now, using Eq. (4.82), the energy is

$$\begin{aligned} U_{es} &= \frac{1}{2} \int \rho\Phi dv = \frac{\pi\rho_0^2}{3} \int_0^a (3a^2 - r^2) 4\pi r^2 dr \\ &= \frac{4\pi^2 \rho_0^2}{3} \left(a^5 - \frac{a^5}{5} \right) = \frac{16\pi^2 \rho_0^2 a^5}{15} \quad (2) \end{aligned}$$

which agrees with (1). In Case (b) all the energy is localized *within* the charge distribution since $\rho(r)$ is zero elsewhere. In Case (a), $5/6$ of the energy is *outside* the charge distribution.

4-20. From Eqs. (4.70) and (4.40), the magnetic energy is

$$U_m = \frac{1}{8\pi} \int_V \mathbf{H} \cdot \mathbf{B} dv = \frac{1}{8\pi} \int_V \mathbf{H} \cdot \text{curl } \mathbf{A} dv$$

The identity of Eq. (A.38) gives

$$\mathbf{H} \cdot \text{curl } \mathbf{A} = \mathbf{A} \cdot \text{curl } \mathbf{H} + \text{div}(\mathbf{A} \times \mathbf{H})$$

The volume integral of the second term on the right can be transformed to a surface integral by the divergence theorem,

$$\int_V \text{div}(\mathbf{A} \times \mathbf{H}) dv = \oint_S (\mathbf{A} \times \mathbf{H}) \cdot \mathbf{n} da$$

If we assume that there are no radiation fields at infinity, then at large distances $H \propto 1/r^2$ and $A \propto 1/r$, with $da \propto r^2$. Thus when we let the volume V include all space, the surface integral vanishes. Using Ampere's law [Eq. (4.24) with negligible Maxwell induction], the surviving term gives

$$U_m = \frac{1}{8\pi} \int_V \mathbf{A} \cdot \text{curl } \mathbf{H} \, dV = \frac{1}{2c} \int_V \mathbf{A} \cdot \mathbf{J}_f \, dV$$

4-21. The electromagnetic momentum density is

$$\begin{aligned} \mathbf{g} &= \frac{1}{4\pi c} \mathbf{E} \times \mathbf{B} = \frac{1}{4\pi c} \frac{e^2}{cr^4} \sin\theta \mathbf{e}_r \times (\mathbf{u} \times \mathbf{e}_r) \\ &= \frac{e^2}{4\pi c^2 r^4} (\mathbf{u} - \cos\theta \mathbf{e}_r) \end{aligned}$$

where θ is the angle between the velocity \mathbf{u} and the radial unit vector \mathbf{e}_r . When we integrate this expression over all space, the transverse components of the \mathbf{e}_r term will cancel out, while the components in the direction of \mathbf{u} survive. Thus,

$$\mathbf{g} \rightarrow g_u \mathbf{e}_u = \frac{e^2}{4\pi c^2 r^4} \mathbf{u} (1 - \cos^2\theta) = \frac{e^2}{4\pi c^2 r^4} \mathbf{u} \sin^2\theta$$

Then integrating, the total electromagnetic momentum is

$$\begin{aligned} \mathbf{p}_{\text{field}} &= \mathbf{e}_u \iint g_u 2\pi r^2 \sin\theta \, d\theta \, dr \\ &= \frac{e^2}{2c^2} \mathbf{u} \int_0^\pi \sin^3\theta \, d\theta \int_{R_e}^\infty \frac{1}{r^2} \, dr = \frac{2e^2}{3c^2 R_e} \mathbf{u} \end{aligned}$$

If we now equate this to the observed "mechanical" momentum, $m_e \mathbf{u}$, we find

$$(R_e)_{\text{dynamic}} = \frac{2e^2}{3m_e c^2} = \frac{2}{3} r_0$$

where $r_0 = e^2/m_e c^2$ is the parameter defined following Eq. (4.87), such that $(R_e)_{\text{static}} = \frac{1}{2} r_0$. The slightly different numerical coefficients are dependent on our model putting all of the electron's charge on its "surface" [see Feynman (Fe89, Vol. 2, Chap. 28)].

4-22. (a) Equation (4.91) reduces to

$$\begin{pmatrix} \Phi_a \\ \Phi_b \\ \Phi_c \end{pmatrix} = \begin{pmatrix} p_{aa} & p_{ab} & p_{ac} \\ p_{ba} & p_{bb} & p_{bc} \\ p_{ca} & p_{cb} & p_{cc} \end{pmatrix} \begin{pmatrix} q_a \\ q_b \\ q_c \end{pmatrix}$$

The given quantities are $\Phi_a = \Phi_c = 0$, and $q_b = Q$. The unknowns are q_a and q_c . The matrix equation stands for three simultaneous equations, of which we only care about the first and third (the middle equation, for Φ_b , is not useful because Φ_b and p_{bb} blow up to infinity in our idealization of a "point" charge at b). Thus, we need to evaluate the six p 's in the first and third rows.

The diagonal elements, p_{aa} and p_{cc} , are easy because we have spherical symmetry when the charge on the "point" at b is assumed to be zero. Put a charge Q_a on the inner sphere, with no charge elsewhere, and find the potential of the inner sphere to be $\Phi_a = Q_a/a$. Do the same for the outer sphere (which we can assume to be of zero thickness). Thus, immediately,

$$p_{aa} = \frac{1}{a} \quad \text{and} \quad p_{cc} = \frac{1}{c}$$

The elements p_{ac} and p_{ca} are also easy. Put the charge on a and find the potential of c , or vice versa. Either way,

$$p_{ac} = p_{ca} = \frac{1}{c}$$

The tricky ones are p_{ab} and p_{cb} , which call for a charge placed at the asymmetrical point b . But because of the reciprocity (symmetry of the p matrix, which is not to be confused with the symmetry of the geometry!), we can instead find p_{ba} and p_{bc} . That is, we can put the charge symmetrically on one or the other of the spheres and find the potential at the mathematical point b . Thus,

$$p_{ba} = p_{ab} = \frac{1}{b} \quad \text{and} \quad p_{bc} = p_{cb} = \frac{1}{c}$$

The first and third equations can now be written out explicitly as:

$$\begin{aligned} 0 &= \frac{1}{a} q_a + \frac{1}{b} Q + \frac{1}{c} q_c \\ 0 &= \frac{1}{c} q_a + \frac{1}{c} Q + \frac{1}{c} q_c \end{aligned}$$

These equations are readily solved to give:

$$q_a = -\frac{a(c-b)}{b(c-a)} Q \quad \text{and} \quad q_c = -\frac{c(b-a)}{b(c-a)} Q$$

Note that the sum of the induced charges is equal and opposite to the given Q —that is, the total system is electrically neutral. The system has no external field, outside the outer sphere. Therefore, to compute the potentials with respect to infinity (as required in this formalism), we do not need the assumption that the outer sphere is "thin" so long as we understand that c is its *inner* radius.

(b) Using the limits suggested, with a/b and $c/b \rightarrow 1$, the solutions reduce to:

$$q_a = -\frac{h-x}{h}Q \quad \text{and} \quad q_c = -\frac{x}{h}Q$$

This geometry appears to lend itself to the method of images, but summing the infinite series of images-of-images turns out to be difficult. For yet another approach, see Purcell (Pu85, Prob. 3.24).

4-23. Let the charges have equal magnitude Q , with the separation $2d$. To find the force on the right-hand charge, enclose the charge with a Maxwellian surface in the shape of a hemisphere of very large radius, with the plane face lying in the midplane between the charges, as shown in the sketches.

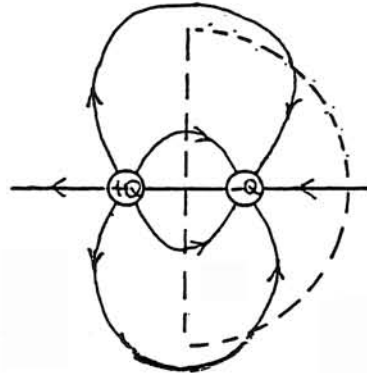
(a) For charges of opposite signs, the field in the midplane is normal to the surface. Using cylindrical coordinates (r, θ, z) with origin midway between the charges, the vector sum of the fields of the two point charges is

$$\mathbf{E}(z=0) = \frac{2Qd}{(r^2 + d^2)^{3/2}} \mathbf{e}_z$$

where the axial unit vector \mathbf{e}_z points to the right in the sketch. The midplane's contribution to the force on the contents of the Maxwellian surface (i.e., on the right-hand charge) is

$$\begin{aligned} \mathbf{F}_{\text{midplane}} &= \int_{\text{midplane}} \mathbf{T} \cdot \mathbf{n} \, da = -\mathbf{e}_z \int_0^\infty \frac{E^2}{8\pi} 2\pi r \, dr \\ &= -\mathbf{e}_z Q^2 d^2 \int_0^\infty \frac{r \, dr}{(r^2 + d^2)^3} = -\mathbf{e}_z \frac{Q^2}{(2d)^2} \end{aligned}$$

The corresponding integral over the hemispherical surface goes to zero because $T \propto 1/r^4$ while $da \propto r^2$ at large distances. Thus $\mathbf{F}_{\text{midplane}}$ is the entire force on the right-hand charge, in agreement with the elementary Coulomb force law.



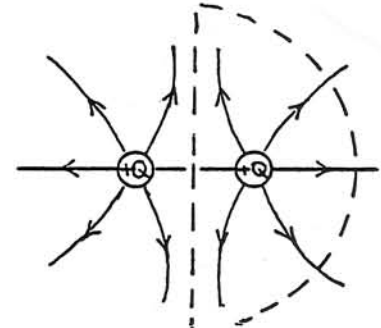
The direction of this force is easily inferred by the "furry rubber band" analogy (at the midplane, the field-lines want to shrink along their length, hence the enclosed right-hand charge is attracted to the left). Formally, the *outward* surface normal \mathbf{n} points in the negative z direction at the midplane. In Eq. (4.110), the stress tensor has been diagonalized by assuming that the field is aligned with the " x_3 " direction, and the T_{33} element has the positive sign. Therefore, the direction of the $\mathbf{T} \cdot \mathbf{n}$ vector in this case is parallel to $+\mathbf{n} = -\mathbf{e}_z$. If, instead, we were to surround the *left-hand* charge with the Maxwellian surface, then the outward normal \mathbf{n} would be in the *positive* z direction—the integrated force would now have the same magnitude, but (correctly) the opposite sense.

(b) For the same-sign case, the midplane field is radial (in cylindrical coordinates),

$$\mathbf{E}(z=0) = \frac{2Qr}{(r^2 + d^2)^{3/2}} \mathbf{e}_r$$

The midplane contribution is now

$$\mathbf{F}_{\text{midplane}} = +\mathbf{e}_z Q^2 \int_0^\infty \frac{r^3 \, dr}{(r^2 + d^2)^3} = +\mathbf{e}_z \frac{Q^2}{(2d)^2}$$



The magnitude is straightforward (except perhaps for an unfamiliar integral). In this case, the outward normal \mathbf{n} remains in the negative z direction (for right-hand charge enclosed). But now, since the local field is *tangential* to the midplane, a *negative* element, T_{11} or T_{22} in Eq. (4.110), applies. Because these are diagonal elements, the operation $\mathbf{T} \cdot \mathbf{n}$ gives back a vector in the negative- \mathbf{n} direction, i.e., the direction of $+\mathbf{e}_z$. Much more simply, one can invoke the "furry rubber bands" (in this case, the "fur" wants to push the field-lines apart, and hence the charges repel).

4-24. The magnetic field at the surface of a column of radius a carrying current I is, by Ampere's law (see Prob. 1-19),

$$\mathbf{B} = \frac{2I}{ca} \mathbf{e}_\theta$$

where \mathbf{e}_θ is the azimuthal unit vector of cylindrical coordinates. The Maxwell stress tensor, Eq. (4.111), says that this field conveys a stress of magnitude

$$\frac{B^2}{8\pi} = \frac{\rho}{2\pi c^2 a^2}$$

Because the field-lines are tangential to the surface of the column, the magnetic stress is a pressure, not a tension—that is, the field exerts an *inward* force on the column. The system is in equilibrium when this external magnetic pressure equals the internal particle pressure—that is, for the special current I_{equil} such that

$$\frac{I_{\text{equil}}^2}{2\pi c^2 a^2} = nkT \quad \Rightarrow \quad I_{\text{equil}} = \sqrt{2\pi c^2 a^2 nkT} = \sqrt{2c^2 nSkT}$$

where $S = \pi a^2$, and nS is the number of particles per unit length of the column.

Now suppose an external power supply drives a current larger than I_{equil} . If the initial particle density and radius are n_0 and a_0 , the column will be compressed such that $nS = n_0\pi a_0^2$ remains constant (conservation of particles—density goes up as radius decreases). This adiabatic compression raises the temperature T of the particles. In principle, the compression continues until the temperature rises enough to reach the equilibrium $I = I_{\text{equil}}$. More practically, the system is vulnerable to *instabilities*. For instance, if there is an initial perturbation along the column where the radius a is less than nominal, the locally greater field pressure makes this dimple grow larger ("sausage instability"). If the axis of the column is slightly curved, the magnetic pressure is larger on the inside of the curve than the outside and the deformation increases ("kink instability"). For further discussion, see Reitz-Milford-Christy (Re93, Sec. 14-6).

4-25. (a) As worked out for Prob. 2-25, the reluctance of the electromagnet is, with no gap,

$$\mathcal{R} = \frac{c}{4\pi} \frac{\ell + d}{\mu A}$$

where ℓ is the length of the U-shaped magnet, d is the length of the "keeper" between the magnet's poles, A is the cross-sectional area of both, and μ is the permeability of the soft iron. According to the magnetic "Ohm's law" [Eq. (2.81)], the field produced within the iron circuit is

$$B = \frac{NI}{A\mathcal{R}}$$

where NI is the "magnetomotive force" (ampere-turns) in the winding.

The Maxwell stress tensor, Eq. (4.111), gives the stress communicated across a free-space gap (of negligible thickness) between a magnet pole and the keeper. Thus, the magnitude is

$$F = \frac{B^2}{8\pi} A = \frac{N^2 I^2}{8\pi A} \frac{1}{\mathcal{R}^2}$$

$$= \frac{N^2 I^2}{8\pi A} \left[\frac{4\pi\mu A}{c(\ell + d)} \right]^2 \quad (= 1.96 \times 10^6 \text{ dynes})$$

which agrees with the result found for Prob. 2-25. The direction of the force is of course attractive, as can be seen by imagining the field-lines, perpendicular to the gap, to be stretched rubber bands.

[Note: The analysis leading to Eq. (4.111) assumed the absence of any magnetic materials. More generally, the elements of the magnetic stress tensor have the magnitude $BH/8\pi$, as can be inferred from the more general energy-density formula of Eq. (4.70). Usually, as in the present example, we are interested in the force *between*, not *within*, ferromagnetic objects.]

(b) We assume that the permanent magnet has uniform magnetization \mathbf{M}_0 parallel to the axis of the rod, which has length ℓ and cross-sectional area A . With no keeper, there are fictitious magnetic poles, $q^* = \pm M_0 A$, at the *ends* of the rod (elsewhere, $\text{div}\mathbf{M}$ and $\mathbf{M}\cdot\mathbf{n}$ are negligible). With the highly permeable keeper in place, an essentially equal magnetization is induced in the keeper, producing poles that cancel those of the permanently magnetized rod. That is, with the keeper in place, there is a negligible pole strength anywhere. With no free currents present, it follows that the \mathbf{H} -field is very small throughout the system. (What residual \mathbf{H} -field there is, is in opposite directions in magnet and keeper: "backwards" in the magnet, and "forwards" in the keeper.) The \mathbf{B} -field, created by strong Amperian currents, $\mathbf{M}\times\mathbf{n}$, at the surface of the iron, is by no means negligible, and is essentially equal in both magnet and keeper. (\mathbf{B} is "forward" —i.e., continuous—in both regions.)

Therefore, the *constraint line* on the state of the permanent-magnet's iron, which was found in Prob. 2-24 to be $B/H = -2$ for a spherical specimen, here becomes $B/H \rightarrow -\infty$. Thus, in the present problem, the relevant parameter of the permanent magnet's hysteresis graph is its *remanence* [i.e., the B intercept of Fig. 1-10(b)]. We conclude that, $B = B_{\text{rem}} \approx 4\pi M_0 \approx 1.3 \times 10^4$ gauss throughout the magnetic circuit, including the (vanishingly small) airgap between magnet pole and keeper.

Now it is easy to use the stress tensor to find the force with which the magnet holds one end of the keeper:

$$\begin{aligned} F &= \frac{B_{\text{rem}}^2}{8\pi} A = \frac{(1.3 \times 10^4 \text{ gauss})^2}{8\pi} (0.8 \text{ cm}^2) \\ &= 5.4 \times 10^6 \text{ dynes} \end{aligned}$$

which can be compared with the 1.96×10^6 dynes found for Part (a).

Chapter 5

5-1. Substitution of the assumed fields in Eq. (5.1) gives

$$P' = 0$$

where the prime denotes differentiation with respect to the argument $(x - Vt)$. Thus P is at most a constant, which is not a wave field of the assumed form; hence $P = 0$. Equation (5.2) gives a similar conclusion for S .

Substitution in Eq. (5.3) gives

$$\begin{aligned} \text{curl } \mathbf{E} &= \begin{vmatrix} \mathbf{e}_x & \mathbf{e}_y & \mathbf{e}_z \\ \partial/\partial x & 0 & 0 \\ P & Q & R \end{vmatrix} = -R' \mathbf{e}_y + Q' \mathbf{e}_z \\ &= \frac{\sqrt{\epsilon\mu}}{c} V (T' \mathbf{e}_y + U' \mathbf{e}_z) \end{aligned} \quad (1)$$

Similarly, Eq. (5.4) gives

$$\sqrt{\epsilon\mu} (-U' \mathbf{e}_y + T' \mathbf{e}_z) = -\frac{\epsilon\mu}{c} V (Q' \mathbf{e}_y + R' \mathbf{e}_z) \quad (2)$$

The y components of (1) and the z components of (2) require

$$\frac{R'}{T'} = -\frac{\sqrt{\epsilon\mu} V}{c} = -\frac{c}{\sqrt{\epsilon\mu} V}$$

Thus the propagation velocity V is required to be equal to $c/\sqrt{\epsilon\mu}$, and the relation between R' and T' integrates to

$$R = -T$$

Similarly, the z components of (1) and the y components of (2) require the same V , and

$$Q = U$$

Thus only two of the six functions are nonzero and independent.

5-2. Maxwell's equations (5.1-4) are replaced by (4.25-28). (With no material medium, there is no distinction between *total* and *free* charges and currents.) Taking the curl of Eq. (4.27) and using the expansion identity of Eq. (A.40), we have

$$\begin{aligned} \text{curl curl } \mathbf{E} &\equiv \text{grad div } \mathbf{E} - \nabla^2 \mathbf{E} \\ &= -\frac{1}{c} \text{curl } \frac{\partial \mathbf{B}}{\partial t} = -\frac{1}{c} \frac{\partial}{\partial t} \text{curl } \mathbf{B} \end{aligned}$$

Invoking Eqs. (4.25) and (4.28), this becomes

$$\text{grad}(4\pi\rho) - \nabla^2 \mathbf{E} = -\frac{1}{c} \frac{\partial}{\partial t} \left[\frac{1}{c} \left(\frac{\partial \mathbf{E}}{\partial t} + 4\pi \mathbf{J} \right) \right]$$

Rearranging,

$$\nabla^2 \mathbf{E} - \frac{1}{c^2} \frac{\partial^2 \mathbf{E}}{\partial t^2} = 4\pi \left(\text{grad } \rho + \frac{1}{c^2} \frac{\partial \mathbf{J}}{\partial t} \right) \quad (1)$$

Similarly, taking the curl of Eq. (4.28),

$$\begin{aligned} \text{curl curl } \mathbf{B} &\equiv \text{grad div } \mathbf{B} - \nabla^2 \mathbf{B} \\ &= \frac{1}{c} \text{curl } \frac{\partial \mathbf{E}}{\partial t} + \frac{4\pi}{c} \text{curl } \mathbf{J} = \frac{1}{c} \frac{\partial}{\partial t} \text{curl } \mathbf{E} + \frac{4\pi}{c} \text{curl } \mathbf{J} \end{aligned}$$

Invoking Eqs. (4.26) and (4.27), and rearranging, we have

$$\begin{aligned} 0 - \nabla^2 \mathbf{B} &= \frac{1}{c} \frac{\partial}{\partial t} \left(-\frac{1}{c} \frac{\partial \mathbf{B}}{\partial t} \right) + \frac{4\pi}{c} \text{curl } \mathbf{J} \\ \Rightarrow \nabla^2 \mathbf{B} - \frac{1}{c^2} \frac{\partial^2 \mathbf{B}}{\partial t^2} &= -\frac{4\pi}{c^2} \text{curl } \mathbf{J} \end{aligned} \quad (2)$$

These are the *inhomogeneous* wave equations, with the source terms involving ρ and \mathbf{J} on the right-hand sides. In Sec. 8.1 it is shown that a general solution of such equations [such as Eq. (8.6)] can be written in the form of a volume integral over the sources [such as Eq. (8.4) or (8.21)], provided that the integrand is evaluated at the *retarded time*. That is, we can immediately write down solutions of (1) and (2) as

$$\begin{aligned} \mathbf{E}(\mathbf{r}, t) &= -\int_V \frac{\text{grad}' \rho(\mathbf{r}', \tau) + \frac{1}{c} \frac{\partial \mathbf{J}(\mathbf{r}', \tau)}{\partial t}}{|\mathbf{r} - \mathbf{r}'|} dv' \\ \mathbf{B}(\mathbf{r}, t) &= \int_V \frac{\frac{1}{c} \text{curl}' \mathbf{J}(\mathbf{r}', \tau)}{|\mathbf{r} - \mathbf{r}'|} dv' \end{aligned}$$

where \mathbf{r}' and \mathbf{r} are the *source* and *field* coordinates, respectively, and $\tau = t - |\mathbf{r} - \mathbf{r}'|/c$ is the so-called retarded time. Better solutions of this sort are discussed in Sec. 8.2.

5-3. (a) The divergence of all four wavefunctions vanishes because the vector components are in the x and y directions, while the magnitude depends (spatially) only upon z . For \mathbf{E}_A ,

$$\begin{aligned} \mathbf{curl} \mathbf{E}_A &= E_0 \sin \omega t \begin{vmatrix} \mathbf{e}_x & \mathbf{e}_y & \mathbf{e}_z \\ 0 & 0 & \partial/\partial z \\ \sin kz & \cos kz & 0 \end{vmatrix} \\ &= E_0 \sin \omega t (k \sin kz \mathbf{e}_x + k \cos kz \mathbf{e}_y) \end{aligned}$$

while for \mathbf{B}_A ,

$$-\frac{1}{c} \frac{\partial \mathbf{B}_A}{\partial t} = -\frac{1}{c} E_0 (-\omega \sin \omega t) (\sin kz \mathbf{e}_x + \cos kz \mathbf{e}_y)$$

Thus, Eq. (5.3) is satisfied so long as $k = \omega/c$, which is what was implicitly assumed. A similar calculation verifies the Maxwell curl equations for \mathbf{B}_A and for both Case-B fields.

For the wave equation, the operator ∇^2 simply multiplies each wavefunction by $-k^2$, and the second time derivative multiplies each by $-\omega^2$. Thus, again, the wave equation [Eq. (5.5) or (5.6), with $\epsilon = \mu = 1$] is satisfied for each field so long as $k = \omega/c$.

(b) Since \mathbf{E} and \mathbf{B} are parallel, the Poynting vector ($c/4\pi\mu$) $\mathbf{E} \times \mathbf{B}$ [Eq. (4.66)] is zero in each case. The energy density [Eq. (4.70)] is

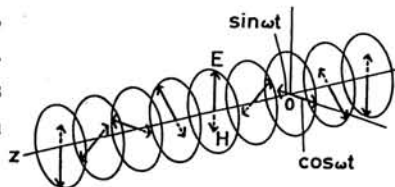
$$\begin{aligned} \mathcal{E}_A &= \frac{1}{8\pi} (E_A^2 + B_A^2) \\ &= \frac{1}{8\pi} E_0^2 (\sin^2 \omega t + \cos^2 \omega t) = \frac{1}{8\pi} E_0^2 \end{aligned}$$

and

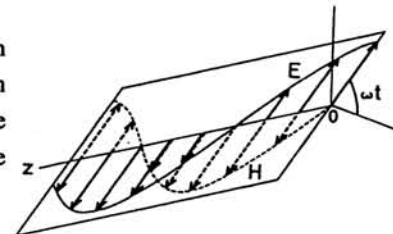
$$\mathcal{E}_B = \frac{1}{8\pi} E_0^2 (\cos^2 kz + \sin^2 kz) = \frac{1}{8\pi} E_0^2$$

That is, in both cases the energy density is a constant, independent of space and time.

(c) Case A is circularly polarized in space, with \mathbf{E} and \mathbf{B} 90° out-of-phase in time. That is, at a given position z , both fields oscillate in a fixed direction; this direction describes a corkscrew as z varies.



Case B is circularly polarized in time, with \mathbf{E} and \mathbf{B} 90° out-of-phase in space. At an instant of time, both fields lie in a plane independent of z ; this plane rotates in time at angular frequency ω .



Both cases represent *standing waves*. With a little imagination, or exercise with trigonometric identities, they can be written in the forms:

$$\begin{cases} \mathbf{E}_A = \frac{E_0}{2} [\cos(\omega t - kz) \mathbf{e}_x + \sin(\omega t - kz) \mathbf{e}_y \\ \quad - \cos(\omega t + kz) \mathbf{e}_x + \sin(\omega t + kz) \mathbf{e}_y] \\ \mathbf{B}_A = \frac{E_0}{2} [\cos(\omega t - kz) \mathbf{e}_y - \sin(\omega t - kz) \mathbf{e}_x \\ \quad \cos(\omega t + kz) \mathbf{e}_y + \sin(\omega t + kz) \mathbf{e}_x] \end{cases}$$

$$\begin{cases} \mathbf{E}_B = \frac{E_0}{2} [\cos(\omega t - kz) \mathbf{e}_x - \sin(\omega t - kz) \mathbf{e}_y \\ \quad \cos(\omega t + kz) \mathbf{e}_x - \sin(\omega t + kz) \mathbf{e}_y] \\ \mathbf{B}_B = \frac{E_0}{2} [\cos(\omega t - kz) \mathbf{e}_y + \sin(\omega t - kz) \mathbf{e}_x \\ \quad - \cos(\omega t + kz) \mathbf{e}_y - \sin(\omega t + kz) \mathbf{e}_x] \end{cases}$$

These forms can be recognized as the superposition of two plane traveling waves, each of which are *circularly polarized* [compare Eqs. (5.26–27)], but which are propagating in *opposite* directions. The terms with the argument $(\omega t - kz)$ advance in the $+z$ direction; the corresponding terms of \mathbf{E} and \mathbf{B} are equal in magnitude with vector directions such that $\mathbf{e}_E \times \mathbf{e}_B = +\mathbf{e}_z$. The terms with $(\omega t + kz)$ advance in the $-z$ direction, with vector directions such that $\mathbf{e}_E \times \mathbf{e}_B = -\mathbf{e}_z$.

Circularly polarized traveling waves have the property that their instantaneous Poynting vector is constant in time (the Poynting vector of linearly polarized traveling waves is "lumpy"—it rises and falls each half-cycle). Thus counter-propagating circularly polarized waves, of equal amplitude, carry energy continuously in opposite directions, and the net Poynting vector cancels to zero, as we have already seen. On the other hand, the energy density of each traveling wave doubles in the superposition.

For further discussion of these special cases, see Zaghoul and Buckmaster, *Am.J.Phys.* **56**, 801 (1988), and Shimoda, et al., *Am.J.Phys.* **58**, 394 (1990).

5-4. (a) The scalar wave equation is

$$\nabla^2 \Psi - \frac{1}{c^2} \frac{\partial^2 \Psi}{\partial t^2} = 0$$

Saying that the wavefunction Ψ is spherically symmetric means that it is a function only of r in spherical coordinates; therefore the Laplacian operator reduces to [Eq. (A.52)]

$$\nabla^2 \rightarrow \frac{1}{r^2} \frac{\partial}{\partial r} \left(r^2 \frac{\partial \Psi}{\partial r} \right)$$

Applying this to the given function,

$$\begin{aligned} \nabla^2 \Psi_s &= \frac{1}{r^2} \frac{\partial}{\partial r} \left[r^2 \left(-\frac{C}{r^2} + \frac{ikC}{r} \right) e^{i(kr-\omega t)} \right] \\ &= \frac{1}{r^2} [(0 + ikC) + ik(-C + ikCr)] e^{i(kr-\omega t)} = -k^2 \Psi_s \end{aligned}$$

The second time derivative is easily seen to be $-\omega^2 \Psi_s$. Therefore the given function does indeed satisfy the wave equation so long as $k = \omega/c$. To construct a solution of the vector wave equation in the form $\mathbf{e}_z \Psi_s$, we must use a Cartesian unit vector because non-Cartesian unit vectors (such as \mathbf{e}_r , \mathbf{e}_θ , and \mathbf{e}_ϕ of spherical coordinates) do not commute through the spatial derivatives in ∇^2 .

(b) We take the vector function $\mathbf{A}_s = \mathbf{e}_z \Psi_s(r)$ to be a solution of the wave equation for the vector potential, Eq. (4.57b). Note the mixed bookkeeping, that the vector component is in Cartesian (or cylindrical?) coordinates, while the functional dependence is in spherical coordinates. To work out the curl, it is easiest to express the unit vector as $\mathbf{e}_z = \cos\theta \mathbf{e}_r - \sin\theta \mathbf{e}_\theta$. Then, using Eq. (A.50), the corresponding magnetic field is

$$\begin{aligned} \mathbf{B}_s &= \mathbf{curl} \mathbf{A}_s = \begin{vmatrix} \mathbf{e}_r & \mathbf{e}_\theta & \mathbf{e}_\phi \\ \frac{1}{r^2 \sin\theta} & \frac{1}{r \sin\theta} & \frac{1}{r} \\ \frac{\partial}{\partial r} & \frac{\partial}{\partial \theta} & 0 \\ \Psi_s(r) \cos\theta & -r \Psi_s(r) \sin\theta & 0 \end{vmatrix} \\ &= \frac{\mathbf{e}_\phi}{r} \left[\frac{\partial}{\partial r} (-C e^{i(kr-\omega t)} \sin\theta) - \frac{\partial}{\partial \theta} \left(\frac{C}{r} e^{i(kr-\omega t)} \cos\theta \right) \right] \\ &= \frac{\mathbf{e}_\phi}{r} C \left(-ik + \frac{1}{r} \right) \sin\theta e^{i(kr-\omega t)} = -ik^2 C \left[\frac{1}{kr} + \frac{i}{(kr)^2} \right] \sin\theta e^{i(kr-\omega t)} \mathbf{e}_\phi \end{aligned}$$

And then the associated electric field is

$$\begin{aligned} \mathbf{E}_s &= \frac{ic}{\omega} \mathbf{curl} \mathbf{B}_s = \frac{i}{k} \begin{vmatrix} \frac{\mathbf{e}_r}{r^2 \sin\theta} & \frac{\mathbf{e}_\theta}{r \sin\theta} & \frac{\mathbf{e}_\phi}{r} \\ \frac{\partial}{\partial r} & \frac{\partial}{\partial \theta} & 0 \\ 0 & 0 & r \sin\theta B_s(r, \theta) \end{vmatrix} \\ &= \frac{i}{k} \left[\frac{\mathbf{e}_r}{r^2 \sin\theta} \frac{\partial}{\partial \theta} - \frac{\mathbf{e}_\theta}{r \sin\theta} \frac{\partial}{\partial r} \right] \left[C \left(-ik + \frac{1}{r} \right) \sin^2\theta e^{i(kr-\omega t)} \right] \\ &= \frac{iC}{kr^2} \left(-ik + \frac{1}{r} \right) 2 \cos\theta e^{i(kr-\omega t)} \\ &\quad - \frac{iC}{kr} \left[\left(0 - \frac{1}{r^2} \right) + ik \left(-ik + \frac{1}{r} \right) \right] \sin\theta e^{i(kr-\omega t)} \\ &= iCk^2 \left[-\frac{i}{(kr)^2} + \frac{1}{(kr)^3} \right] 2 \cos\theta e^{i(kr-\omega t)} \mathbf{e}_r \\ &\quad + iCk^2 \left[-\frac{1}{kr} - \frac{i}{(kr)^2} + \frac{1}{(kr)^3} \right] \sin\theta e^{i(kr-\omega t)} \mathbf{e}_\theta \end{aligned}$$

With $iC \rightarrow p_0 k$, these are precisely the fields found in Eqs. (8.42–44) for an oscillating electric dipole. See also Souza, *Am.J.Phys.* **51**, 54 (1983).

5-5. From Eqs. (5.3–4), so long as ε is not time-dependent (and $\mu = 1$),

$\mathbf{curl} \mathbf{curl} \mathbf{E}$

$$= -\frac{1}{c} \mathbf{curl} \frac{\partial \mathbf{B}}{\partial t} = -\frac{1}{c} \frac{\partial}{\partial t} (\mathbf{curl} \mathbf{B}) = -\frac{\varepsilon}{c^2} \frac{\partial^2 \mathbf{E}}{\partial t^2}$$

The expansion of the double curl is given by Eq. (A.40),

$$\mathbf{curl} \mathbf{curl} \mathbf{E} = \mathbf{grad} \operatorname{div} \mathbf{E} - \nabla^2 \mathbf{E}$$

When the medium is inhomogeneous, $\operatorname{div} \mathbf{E}$ is no longer zero [Eq. (5.1)]. In order to invoke the more general Eq. (4.21), use the expansion of Eq. (A.35),

$$\varepsilon \operatorname{div} \mathbf{E} = \operatorname{div}(\varepsilon \mathbf{E}) - \mathbf{E} \cdot \mathbf{grad} \varepsilon \rightarrow -\mathbf{E} \cdot \mathbf{grad} \varepsilon$$

Thus the wave equation for \mathbf{E} becomes, replacing Eq. (5.5),

$$\nabla^2 \mathbf{E} - \frac{\varepsilon}{c^2} \frac{\partial^2 \mathbf{E}}{\partial t^2} = -\mathbf{grad} \left(\frac{\mathbf{grad} \varepsilon}{\varepsilon} \cdot \mathbf{E} \right) \quad (1)$$

Similarly, using Eqs. (A.40), (A.36), and (5.2-4), we have

$$\begin{aligned}\mathbf{curl\,curl\,B} &= \mathbf{grad\,div\,B} - \nabla^2\mathbf{B} \rightarrow -\nabla^2\mathbf{B} \\ &= \frac{1}{c} \mathbf{curl}\left(\varepsilon \frac{\partial\mathbf{E}}{\partial t}\right) = \frac{\varepsilon}{c} \frac{\partial}{\partial t}(\mathbf{curl\,E}) - \frac{1}{c} \frac{\partial\varepsilon}{\partial t} \times (\mathbf{grad\,E}) \\ &= -\frac{\varepsilon}{c^2} \frac{\partial^2\mathbf{B}}{\partial t^2} - \frac{1}{\varepsilon} (\mathbf{curl\,B}) \times (\mathbf{grad\,\varepsilon})\end{aligned}$$

Thus the wave equation for \mathbf{B} becomes, replacing Eq. (5.6),

$$\nabla^2\mathbf{B} - \frac{\varepsilon}{c^2} \frac{\partial^2\mathbf{B}}{\partial t^2} = -\left(\frac{\mathbf{grad\,\varepsilon}}{\varepsilon}\right) \times (\mathbf{curl\,B}) \quad (2)$$

When either (1) or (2) is written out as three scalar equations for the Cartesian components of the vector field, the right-hand sides couple the otherwise-independent simultaneous equations.

When $\varepsilon = \varepsilon(z)$ and \mathbf{E}, \mathbf{B} have no components in the z direction, then $\mathbf{grad\,\varepsilon} \rightarrow (d\varepsilon/dz)\mathbf{e}_z$. The right-hand side of (1) now vanishes, and the right-hand side of (2) reduces to

$$-\frac{1}{\varepsilon} \frac{d}{dz} \mathbf{e}_z \times \begin{vmatrix} \mathbf{e}_x & \mathbf{e}_y & \mathbf{e}_z \\ 0 & 0 & \partial/\partial z \\ B_x & B_y & 0 \end{vmatrix} = \frac{1}{\varepsilon} \frac{d\varepsilon}{dz} \frac{\partial\mathbf{B}}{\partial z}$$

5-6. The proof is essentially trivial: the right-hand side is the distributed multiplication of the complex function F with the real quantity $(G + G^*)$ —that is, twice the real part of G . Then the (implicit) real part of the product picks up only the real part of F . With the explicit factor of $1/2$, the result is indeed the product of $\text{Re}[F]$ times $\text{Re}[G]$, which is the intended meaning of the left-hand side. The point of the problem is to display the notational code whereby an algebraic expression with *one* implicit real operator (the right-hand side) stands in the place of an expression with *two* implicit real operators (the left-hand side). These shorthand conventions are used glibly in the literature, often with idiosyncratic variations. Readers must be prepared to supply the proper interpretation from the context.

5-7. (a) Using the time-average product theorem [Eq. (5.42)] in the form of Eq. (5.50), with $\mathbf{H} \rightarrow \mathbf{B}$ for a nonmagnetic medium, we have for the superposition of Waves 1 and 2:

$$\begin{aligned}\langle \mathbf{S}_{12} \rangle &= \frac{c}{8\pi} (\mathbf{e}_x E_1^0 + \mathbf{e}_y E_2^0 e^{+i\alpha}) \times (\mathbf{e}_y E_1^0 - \mathbf{e}_x E_2^0 e^{-i\alpha}) \\ &= \frac{c}{8\pi} (\mathbf{e}_x E_1^0 \times \mathbf{e}_y E_1^0 - \mathbf{e}_x E_1^0 \times \mathbf{e}_x E_2^0 e^{-i\alpha} \\ &\quad + \mathbf{e}_y E_2^0 e^{+i\alpha} \times \mathbf{e}_y E_1^0 - \mathbf{e}_y E_2^0 e^{+i\alpha} \times \mathbf{e}_x E_2^0 e^{-i\alpha}) \\ &= \frac{c}{8\pi} \mathbf{e}_x [(E_1^0)^2 + (E_2^0)^2] = \langle \mathbf{S}_1 \rangle + \langle \mathbf{S}_2 \rangle\end{aligned}$$

That is, the two cross-terms vanish because $\mathbf{e}_x \times \mathbf{e}_x = \mathbf{e}_y \times \mathbf{e}_y = 0$, and the remaining terms correspond to the Poynting vector of the two waves taken separately. (Remember, we want only the *real part* of the result of the calculation, which in this case is trivially the result itself.)

Because these two waves are linearly polarized at right angles, they propagate independently of each other. However, depending upon the phase difference α , the *superposition* can represent *linear* [$\alpha = 0$ or π , Eq. (5.34)], *circular* [$\alpha = \pm\pi/2$ with $E_1^0 = E_2^0$, Eqs. (5.35-37)], or *elliptical* polarization [Eqs. (5.38-41)].

(b) For Waves 1 and 3 (using the identity $e^{+i\alpha} + e^{-i\alpha} = 2\cos\alpha$),

$$\begin{aligned}\langle \mathbf{S}_{13} \rangle &= \frac{c}{8\pi} (\mathbf{e}_x E_1^0 + \mathbf{e}_x E_3^0 e^{+i\alpha}) \times (\mathbf{e}_y E_1^0 + \mathbf{e}_y E_3^0 e^{-i\alpha}) \\ &= \frac{c}{8\pi} (\mathbf{e}_x E_1^0 \times \mathbf{e}_y E_1^0 + \mathbf{e}_x E_1^0 \times \mathbf{e}_y E_3^0 e^{-i\alpha} \\ &\quad + \mathbf{e}_x E_3^0 e^{+i\alpha} \times \mathbf{e}_y E_1^0 + \mathbf{e}_x E_3^0 e^{+i\alpha} \times \mathbf{e}_y E_3^0 e^{-i\alpha}) \\ &= \frac{c}{8\pi} \mathbf{e}_z [(E_1^0)^2 + E_1^0 E_3^0 (e^{+i\alpha} + e^{-i\alpha}) + (E_3^0)^2] \\ &= \langle \mathbf{S}_1 \rangle + \langle \mathbf{S}_3 \rangle + \frac{c}{8\pi} \mathbf{e}_z 2E_1^0 E_3^0 \cos\alpha\end{aligned}$$

The two waves in this case have the same linear polarization, and interfere constructively or destructively depending upon the phase difference α . The resultant amplitude is related to the amplitudes of the component waves by the law of cosines (see Fig. 11-4).

(c) In this case the complex-exponential wavefunction is not the same in the two cases, and we must include the spatial factor $e^{\pm ikz}$ explicitly in the time-average product theorem:

$$\begin{aligned}\langle \mathbf{S}_{14} \rangle &= \frac{c}{8\pi} (\mathbf{e}_x E_1^0 e^{+ikz} + \mathbf{e}_x E_1^0 e^{-ikz}) \times (\mathbf{e}_y E_1^0 e^{-ikz} - \mathbf{e}_y E_1^0 e^{+ikz}) \\ &= \frac{c}{8\pi} (\mathbf{e}_x E_1^0 e^{+ikz} \times \mathbf{e}_y E_1^0 e^{-ikz} - \mathbf{e}_x E_1^0 e^{+ikz} \times \mathbf{e}_y E_1^0 e^{+ikz} \\ &\quad + \mathbf{e}_x E_1^0 e^{-ikz} \times \mathbf{e}_y E_1^0 e^{-ikz} - \mathbf{e}_x E_1^0 e^{-ikz} \times \mathbf{e}_y E_1^0 e^{+ikz})\end{aligned}$$

$$\begin{aligned}
 &= \frac{c}{8\pi} \mathbf{e}_z [(E_1^0)^2 - (E_1^0)^2 (e^{+i2kz} - e^{-i2kz}) - (E_1^0)^2] \\
 &= \langle S_1 \rangle - \langle S_4 \rangle - \frac{c}{8\pi} \mathbf{e}_z 2i (E_1^0)^2 \sin(2kz) \xrightarrow{\text{real part}} 0
 \end{aligned}$$

In this case we have two waves of the same amplitude and polarization, but traveling in opposite directions. The superposition is a *standing wave*. Thus their individual Poynting vectors cancel, and the "interference" term contributes no time-average because there is no real part of a pure-imaginary quantity.

To find the *time-dependent* energy density, we use the result of Prob. 5-6. The electric portion of Eq. (4.70) is:

$$\begin{aligned}
 \frac{1}{8\pi} E^2 &= \frac{1}{16\pi} (\mathbf{E}_1 + \mathbf{E}_4) \cdot (\mathbf{E}_1 + \mathbf{E}_4 + \mathbf{E}_1^* + \mathbf{E}_4^*) \\
 &= \frac{1}{16\pi} [\mathbf{e}_x E_1^0 (2 \cos kz) e^{-i\omega t}] \cdot [\mathbf{e}_x E_1^0 (2 \cos kz) (2 \cos \omega t)] \\
 &\xrightarrow{\text{real part}} \frac{1}{2\pi} (E_1^0)^2 \cos^2 kz \cos^2 \omega t
 \end{aligned}$$

Similarly, the magnetic portion of the energy density is:

$$\begin{aligned}
 \frac{1}{8\pi} B^2 &= \frac{1}{16\pi} (\mathbf{B}_1 + \mathbf{B}_4) \cdot (\mathbf{B}_1 + \mathbf{B}_4 + \mathbf{B}_1^* + \mathbf{B}_4^*) \\
 &= \frac{1}{16\pi} [\mathbf{e}_y E_1^0 (2i \sin kz) e^{-i\omega t}] \cdot [\mathbf{e}_y E_1^0 (2i \sin kz) (-2i \sin \omega t)] \\
 &\xrightarrow{\text{real part}} \frac{1}{2\pi} (E_1^0)^2 \sin^2 kz \sin^2 \omega t
 \end{aligned}$$

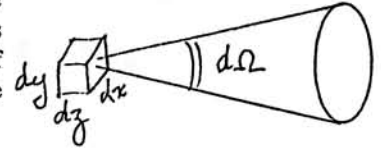
The electric and magnetic portions are out-of-phase by $\pi/2$ in both space and time. The sum is:

$$\begin{aligned}
 \mathcal{E} &= \frac{1}{8\pi} (E^2 + B^2) \\
 &= \frac{1}{8\pi} (E_1^0)^2 [(1 + \cos 2kz)(1 + \cos 2\omega t) + (1 - \cos 2kz)(1 - \cos 2\omega t)] \\
 &= \frac{1}{4\pi} (E_1^0)^2 (1 + \cos 2kz \cos 2\omega t)
 \end{aligned}$$

Similarly, the time-dependent Poynting vector is:

$$\begin{aligned}
 \mathbf{S}(z, t) &= \frac{1}{8\pi} (\mathbf{E}_1 + \mathbf{E}_4) \times (\mathbf{B}_1 + \mathbf{B}_4 + \mathbf{B}_1^* + \mathbf{B}_4^*) \\
 &= \frac{1}{8\pi} [\mathbf{e}_x E_1^0 (2 \cos kz) e^{-i\omega t}] \times [\mathbf{e}_y E_1^0 (2i \sin kz) (-2i \sin \omega t)] \\
 &\xrightarrow{\text{real part}} \frac{1}{4\pi} \mathbf{e}_z (E_1^0)^2 \sin 2kz \sin 2\omega t
 \end{aligned}$$

5-8. (a) Consider a Cartesian volume element of dimensions dx by dy by $dz = c dt$ (see diagram), through which radiation flows isotropically. In the time dt , the amount of energy that flows out of the dx - dy face, into the element of solid angle $d\Omega$ in the z direction, is



$$\langle \mathcal{E} \rangle dx dy c dt \left(\frac{d\Omega}{4\pi} \right)$$

That is, the wave Poynting vector [energy per time per cross-sectional area] in any particular direction in this region of space, has the magnitude $d\langle S \rangle = (c/4\pi)\langle \mathcal{E} \rangle d\Omega$. Thus,

$$\frac{d\langle S \rangle}{d\Omega} = \frac{c}{4\pi} \langle \mathcal{E} \rangle \quad (1)$$

Note that there is *no* power flowing in *exactly* a given direction, but there is a finite amount into a small-but-finite solid angle $\Delta\Omega$.

Now consider an element of area dA in this region. For radiation flowing at angle θ with respect to the element's normal, the area projects as $\cos\theta dA$. Therefore this portion of the radiation contributes the power

$$d^2P_{\theta}(\theta) = dS (\cos\theta dA)$$

The total power flowing in one direction is, using (1) and $d\Omega = 2\pi \sin\theta d\theta$,

$$\begin{aligned}
 dP &= \int_{\text{hemisphere}} d^2P_{\theta}(\theta) \\
 &= \frac{c}{4\pi} \langle \mathcal{E} \rangle \int_0^{\pi/2} (\cos\theta dA) 2\pi \sin\theta d\theta = \frac{c}{4} \langle \mathcal{E} \rangle dA
 \end{aligned}$$

That is, the power-per-area for isotropic radiation crossing a surface in one direction is

$$\frac{dP}{dA} = \frac{c}{4} \langle \mathcal{E} \rangle \quad (2)$$

Equation (5.54) says $\langle S \rangle = c \langle \mathcal{E} \rangle$. Now this dP/dA is *almost* the same quantity as the Poynting vector $\langle S \rangle$ —the difference being that dP/dA represents radiation flowing in all directions within a hemisphere whereas $\langle S \rangle$ is the time-averaged magnitude of the vector \mathbf{S} which represents collimated radiation flowing in a particular direction. Equation (2) differs from (5.54) by the factor of $1/4$.

(b) At the distance of the Earth, the Sun's radiation is essentially *collimated* (i.e., the Poynting vector has a well-defined direction), and the Poynting vector and energy density are related by Eq. (5.54), $\langle S \rangle = c\langle \mathcal{E} \rangle$. Close to the surface of the Sun, for an element of area dA parallel to the Sun's surface, the radiation can be assumed to be isotropic over the *outbound* hemisphere, but zero over the *inbound* hemisphere. Since only half of the fully isotropic radiation is present, the $\langle \mathcal{E} \rangle$ in Eq. (2) is only *half* as large for the *same* outbound dP/dA . Thus, with r_S = radius of Sun,

$$\begin{aligned} \langle \mathcal{E} \rangle_{\text{Sun's surface}} &= \frac{2}{c} \frac{dP}{dA} = \frac{2}{c} \frac{\langle S_E \rangle 4\pi r_E^2}{4\pi r_S^2} \\ &= \frac{2(1.4 \times 10^6 \text{ erg/cm}^2\text{-s})(1.5 \times 10^{13} \text{ cm})^2}{(3 \times 10^{10} \text{ cm/s})(7 \times 10^{10} \text{ cm})^2} = 4.3 \text{ erg/cm}^3 \end{aligned}$$

A quick approximation to this result can be got by simply pretending that the radiation at the Sun's surface is radially outward, and using Eq. (5.54) with $\langle S \rangle_{\text{Sun}} = \langle S_E \rangle r_E^2 / r_S^2$. This just misses the factor of 2.

(c) The root-mean-square amplitude of the electric field is, from Eqs. (5.53) and (5.55),

$$E_{rms} = \sqrt{4\pi\langle \mathcal{E} \rangle} = \sqrt{4\pi(4.3 \text{ erg/cm}^3)} = 7.3 \text{ statvolts/cm}$$

In Gaussian units, the magnetic amplitude is the same although reckoned in different units,

$$B_{rms} = 7.3 \text{ gauss}$$

(d) From Appendix D,

$$E_{rms} = 7.3 \text{ statvolts/cm} \left(\frac{300 \text{ volts}}{1 \text{ statvolt}} \right) \left(\frac{10^2 \text{ cm}}{1 \text{ meter}} \right) = 2.2 \times 10^5 \text{ volts/m}$$

$$B_{rms} = 7.3 \text{ gauss} \left(\frac{1 \text{ tesla}}{10^4 \text{ gauss}} \right) = 7.3 \times 10^{-4} \text{ tesla}$$

As a check, for SI units (see footnotes near end of Section 5.1),

$$\left(\frac{E_{rms}}{B_{rms}} \right)_{SI} = \frac{2.2 \times 10^5}{7.3 \times 10^{-4}} = 3 \times 10^8 \text{ m/s} = c$$

Note: The component waves in different directions (near the Sun), and of different frequencies, interfere with each other, so that the *instantaneous* amplitude of E and B at a particular point can be very large (or small). However, the components add *incoherently*, which allows us to treat the *time-averaged* total energies (in $\langle \mathcal{E} \rangle$ and $\langle S \rangle$) as simply the sum of the component energies (see the discussion in Sec. 11.2). That

is, the *rms* amplitudes E_{rms} and B_{rms} [Eq. (5.55)] are well-defined in this case, but *peak* values E_0 and B_0 [as in Eqs. (5.51) and (5.53)] would not be.

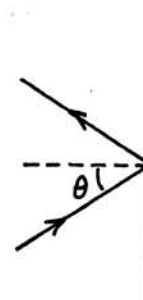
5-9. (a) From Eq. (5.60), the radiation pressure for a wave at normal incidence is

$$p = \frac{1}{c} \langle S \rangle$$

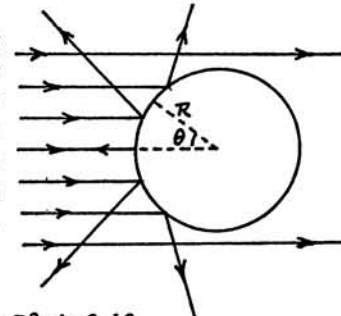
When the wave is incident obliquely on a target surface, at angle θ from the normal, then a unit area of the *surface* intercepts an area $\cos\theta$ of the *wavefront*. The component of the resulting force normal to the surface brings in a second factor of $\cos\theta$. And the force is doubled by the reaction from the reflected radiation. Thus the pressure normal to the perfectly reflecting surface is

$$p_n(\theta) = 2 \cos^2\theta p = \frac{2\langle S \rangle}{c} \cos^2\theta$$

There is no tangential force on the patch of area: the reflecting wave undergoes no change of momentum in the tangential direction (the incident wave tends to push the patch forward, while the reaction to the reflected wave pushes it equally backward).



(b) When the plane wave is incident on a reflecting sphere, the radiation pressure on an area element da produces the force of Part (a) in the inward-radial direction. From symmetry, the only contribution to the *net* force on the sphere is the component of this radial force in the direction of travel of the incident wave, which brings in yet another factor of $\cos\theta$. Thus



$$\begin{aligned} F_{\text{sphere}}^{\text{reflecting}} &= \int p_n(\theta) \cos\theta \, 2\pi R^2 \sin\theta \, d\theta \\ &= \frac{4\pi R^2 \langle S \rangle}{c} \int_0^{\pi/2} \cos^3\theta \sin\theta \, d\theta = \frac{\pi R^2 \langle S \rangle}{c} \end{aligned}$$

(c) For a perfectly absorbing sphere, the wave momentum is completely transferred to the sphere. The easiest approach in this case is to observe that the sphere presents the cross-sectional area πR^2 to the incoming wave, and therefore the total force is simply

$$F_{\text{sphere}}^{\text{absorbing}} = p \pi R^2 = \frac{\pi R^2 \langle S \rangle}{c}$$

which is the same result as the reflecting case. More laboriously, we can paraphrase Part (a) to see that the normal force on a surface element da is $dF_n = \cos^2\theta p da$ [no factor of 2], and the tangential force is $dF_t = \sin\theta \cos\theta p da$. Then paraphrasing Part (b) the net force on the sphere is

$$\int (\cos\theta dF_n + \sin\theta dF_t) = \frac{\langle S \rangle}{c} \int_0^{\pi/2} (\cos^3\theta + \sin^2\theta \cos\theta) 2\pi R^2 \sin\theta d\theta$$

which agrees with the simpler calculation.

It may seem strange that the same force is obtained for both the reflecting and absorbing cases. The reflecting sphere reflects the incoming radiation in the "backward" sense for polar angles less than $\pi/4$, but in the "forward" sense for angles between $\pi/4$ and $\pi/2$. The *net* momentum of the reflected radiation turns out to be zero. So the net momentum exchange between wave and sphere is the same in both cases.

To extend this analysis to cases other than the idealized limits of perfect reflection and absorption, one needs to take into account the fact that the reflection may be *diffuse* to some degree, rather than *specular*. That is, the incoming plane wave, from a well-defined direction, may be reflected as an ensemble of partial waves in various directions (within a solid angle of 2π). See discussions of *Lambert's law* in an optics textbook.

5-10. (a) The gravitational force on the particle of radius R and density ρ is

$$F_g = \frac{GM}{r_p^2} \left(\frac{4\pi R^3}{3} \right) \rho$$

where r_p is the particle's distance from the Sun, G is the universal gravitational constant, and M is the Sun's mass. From Prob. 5-9, the force due to radiation pressure is

$$F_r = \frac{\pi R^2 \langle S \rangle}{c} = \frac{\pi R^2}{c} \left(\frac{P}{4\pi r_p^2} \right)$$

where P is the total power radiated by the Sun. The ratio of radiation to gravitational force is then

$$\frac{F_r}{F_g} = \frac{3P}{16\pi c GM \rho R}$$

Note that the particle's distance from the Sun cancels out; both forces are inverse-square. Thus, the (outward) radiation force dominates only for

$$R < \frac{3P}{16\pi c GM \rho}$$

(b) To evaluate the constants, Newton's second law for a gravitational circular orbit gives

$$m \left(\frac{2\pi}{T} \right)^2 r = \frac{GMm}{r^2}$$

from which we obtain Kepler's third law in the form $GM = (2\pi/T)^2 r_E^3$ where $T = 1 \text{ yr} = 3.16 \times 10^7 \text{ s}$, and r_E is the Earth-Sun distance. Also, $P = S_E 4\pi r_E^2$ where S_E is the Poynting flux at the Earth's orbit (see data given in Prob. 5-8). The condition for radiation dominance is then:

$$\begin{aligned} R &< \frac{3S_E T^2}{16\pi^2 c \rho r_E} \\ &= \frac{3(1.4 \times 10^6 \text{ erg/cm}^2\text{-s})(3.16 \times 10^7 \text{ s})^2}{16\pi^2 (3 \times 10^{10} \text{ cm/s})(2.5 \text{ g/cm}^3)(1.5 \times 10^{13} \text{ cm})} = 2.4 \times 10^{-5} \text{ cm} \end{aligned}$$

The gravitational force dominates unless the particle's diameter is less than the wavelength of visible light. Alternatively, instead of a sphere, suppose the object is in the form of a very thin sail, ...

5-11. The Joule-heating term of Poynting's theorem, Eq. (4.67), is

$$\mathbf{J} \cdot \mathbf{E} = \mathbf{J} \cdot \left(\frac{\mathbf{J}}{\sigma} \right) = \frac{J^2}{\sigma}$$

This result can also be found from $\nabla \cdot \mathbf{J}$ by the arguments of Prob. 1-34.

In terms of the complex propagation constant, $\hat{k} = \alpha + i\beta$, using Eqs. (5.71-72) and (5.80), we can write the wave fields as

$$\begin{aligned} \mathbf{E} &\rightarrow \mathbf{E}_0 e^{-\beta \zeta} \\ \mathbf{B} &\rightarrow \frac{c\hat{\mathbf{k}}}{\omega} \times \mathbf{E}_0 e^{-\beta \zeta} \end{aligned}$$

where it is understood that each expression is multiplied by the complex wavefunction $\exp[i(\alpha\zeta - \omega t)]$. Using the time-average product theorem, Eq. (5.46), the Poynting vector for waves in a conducting medium is then

$$\begin{aligned} \langle \mathbf{S} \rangle &= \frac{c}{4\pi} \mathbf{E} \times \mathbf{H}^* \\ &= \frac{c}{4\pi} (\mathbf{E}_0 e^{-\beta \zeta}) \times \left(\frac{c}{\mu \omega} \hat{\mathbf{k}}^* e_{\zeta} \times \mathbf{E}_0 e^{-\beta \zeta} \right) \end{aligned}$$

$$= \frac{c^2}{8\pi\mu\omega} \hat{k}^* E_0^2 e^{-2\beta\zeta} e_\zeta$$

$$\xrightarrow{\text{real part}} \frac{c^2}{8\pi\mu\omega} \alpha E_0^2 e^{-2\beta\zeta} e_\zeta$$

Evaluating at $\zeta = 0$ where the peak field amplitude is E_0 , and using Eq. (5.74b),

$$\text{div}(\mathbf{S}) \rightarrow \frac{d\langle \mathbf{S} \rangle}{d\zeta} = -2\alpha\beta \frac{c^2}{8\pi\mu\omega} E_0^2 e^{-2\beta\zeta} \xrightarrow{\zeta=0} -\frac{1}{2}\sigma E_0^2$$

The root-mean-square current density is related to the peak electric field of the wave by

$$J_{\text{rms}} = \frac{1}{\sqrt{2}} J_{\text{peak}} = \frac{1}{\sqrt{2}} \sigma E_0$$

so that $\text{div}(\mathbf{S}) = -J_{\text{rms}}^2/\sigma$, the time-average Joule heating. The $\partial\langle \mathcal{E} \rangle/\partial t$ term in Eq. (4.67) is zero because the time-average energy density $\langle \mathcal{E} \rangle$ for a damped wave is constant in time (but not in space).

5-12. If $\xi = i\sqrt{i}x = i(1+i)x/\sqrt{2}$, then

$$\xi^2 = -ix^2 \quad \xi^4 = -x^4 \quad \xi^6 = +ix^6 \quad \xi^8 = +x^8, \text{ etc.}$$

Substituting in the given J_0 series and separating real and imaginary parts, we have

$$J_0(i\sqrt{i}x) = \left[1 - \frac{(x/2)^4}{(2!)^2} + \frac{(x/2)^8}{(4!)^2} - \dots \right] + i \left[\frac{(x/2)^2}{(1!)^2} - \frac{(x/2)^6}{(3!)^2} + \dots \right]$$

$$\equiv \text{ber}(x) + i \text{bei}(x)$$

If, instead, $\xi = \sqrt{i}x = (1+i)x/\sqrt{2}$, then

$$\xi^2 = +ix^2 \quad \xi^4 = -x^4 \quad \xi^6 = -ix^6 \quad \xi^8 = +x^8, \text{ etc.}$$

That is, the even powers are just the complex conjugates of the former values. Thus,

$$J_0(\sqrt{i}x) = \text{ber}(x) - i \text{bei}(x)$$

5-13. From Eq. (3.103), for $kr \gg 1$,

$$J_0(kr) \approx \sqrt{\frac{2}{\pi kr}} \cos\left(kr - \frac{\pi}{4}\right)$$

When $kr \rightarrow \sqrt{i}u = (1+i)u/\sqrt{2}$,

$$J_0(\sqrt{i}u) \xrightarrow{u \gg 1} \sqrt{\frac{2}{\pi u}} (e^{i\pi/2})^{-1/4} \left\{ \frac{e^{+i[(1+i)u/\sqrt{2} - \pi/4]} + e^{-i[(1+i)u/\sqrt{2} - \pi/4]}}{2} \right\}$$

$$\rightarrow \sqrt{\frac{1}{2\pi u}} e^{u/\sqrt{2}} e^{-i(u/\sqrt{2} - \pi/8)}$$

which is equivalent to the complex conjugate of Eq. (5.121). Putting $u \rightarrow \sqrt{2}r/\delta$, and wiping off the phase, we have

$$\left| J_0\left(\sqrt{i}\frac{\sqrt{2}r}{\delta}\right) \right| \approx \sqrt{\frac{\delta}{2\sqrt{2}\pi r}} e^{r/\delta}$$

Therefore, the ratio of the current density at radius r to that at the surface, $r = r_0$, is

$$\left| \frac{J_s(r)}{J_s} \right| \approx \sqrt{\frac{r_0}{r}} e^{-(r_0-r)/\delta} \approx e^{-(r_0-r)/\delta}$$

The final approximation follows because, when $\delta \ll r_0$, the current density is negligible unless $r \approx r_0$. The result is identical in form to Eq. (5.103) with x replaced by the radial penetration, $r_0 - r$.

5-14. From Eq. (5.121), for $u \gg 1$,

$$\text{ber } u \approx \frac{1}{\sqrt{2\pi u}} e^{u/\sqrt{2}} \cos\left(\frac{u}{\sqrt{2}} - \frac{\pi}{8}\right)$$

$$\text{bei } u \approx \frac{1}{\sqrt{2\pi u}} e^{u/\sqrt{2}} \sin\left(\frac{u}{\sqrt{2}} - \frac{\pi}{8}\right)$$

$$\text{ber}' u \approx \frac{1}{\sqrt{2\pi u}} \frac{e^{u/\sqrt{2}}}{\sqrt{2}} \left[\cos\left(\frac{u}{\sqrt{2}} - \frac{\pi}{8}\right) - \sin\left(\frac{u}{\sqrt{2}} - \frac{\pi}{8}\right) \right]$$

$$\text{bei}' u \approx \frac{1}{\sqrt{2\pi u}} \frac{e^{u/\sqrt{2}}}{\sqrt{2}} \left[\sin\left(\frac{u}{\sqrt{2}} + \frac{\pi}{8}\right) - \cos\left(\frac{u}{\sqrt{2}} - \frac{\pi}{8}\right) \right]$$

Substituting these asymptotic forms in the quantity in parentheses on the right-hand side of Eq. (5.120), we note that the common factors of $e^{u/\sqrt{2}}/\sqrt{2\pi u}$ cancel, leaving

$$(\dots) \approx \sqrt{2} \frac{\cos(\cdot)[\sin(\cdot) + \cos(\cdot)] - \sin(\cdot)[\cos(\cdot) - \sin(\cdot)]}{[\sin(\cdot) + \cos(\cdot)]^2 + [\cos(\cdot) - \sin(\cdot)]^2}$$

$$= \sqrt{2} \frac{1}{2} = \frac{1}{\sqrt{2}}$$

5-15. The algebra is easier if we use the complex-exponential notation, writing the magnitude of the applied field as $B(t) = B_0 e^{-i\omega t}$ (with B_0 a real number). The field within the tube is $\tilde{B}_{in} e^{-i\omega t}$, with \tilde{B}_{in} understood to be a complex quantity because in general it will be phase-shifted with respect to B_0 . This oscillating field induces an emf driving current azimuthally around the wall of the tube,

$$\mathcal{E}(t) = -\frac{1}{c} \frac{d\Phi_m}{dt} = +\frac{i\omega}{c} \pi a^2 \tilde{B}_{in} e^{-i\omega t}$$

The resistance of a length ℓ of the tube is $R = 2\pi a/\sigma h \ell$. Therefore the current per-unit-length is $K(t) = \mathcal{E}/R\ell = (i\omega\sigma ah/2c) \tilde{B}_{in} e^{-i\omega t}$. The current-bearing tube is like a solenoid, the field of which is (Prob. 1-20)

$$\tilde{B}_{tube} e^{-i\omega t} = \frac{4\pi K}{c} = i \frac{2\pi\omega\sigma ah}{c^2} \tilde{B}_{in} e^{-i\omega t}$$

Now the applied and induced fields superpose to produce the net internal field, that is,

$$\tilde{B}_{in} = B_0 + \tilde{B}_{tube} = B_0 + i \frac{2\pi\omega\sigma ah}{c^2} \tilde{B}_{in}$$

Therefore,

$$\frac{\tilde{B}_{in}}{B_0} = \frac{1}{1 - i 2\pi\omega\sigma ah/c^2} = \frac{1}{1 - i ah/\delta^2}$$

where $\delta = c/\sqrt{2\pi\sigma\omega}$ is the skin depth. In magnitude,

$$|\tilde{B}_{in}| = \frac{1}{\sqrt{1 + (ah/\delta^2)^2}} B_0 \xrightarrow{ah \gg \delta^2} \frac{\delta^2}{ah} B_0$$

This shielding is only algebraically small, compared with the exponential shielding of Eq. (5.103). Further details are discussed by Fahy, Kittel, and Louie, *Am.J.Phys.* **56**, 989 (1988).

Chapter 6

6-1. From Eqs. (6.10) and (6.12), the power reflection and transmission coefficients are

$$R = \left(\frac{n_2 - n_1}{n_2 + n_1} \right)^2; \quad T = \frac{n_2}{n_1} \left(\frac{2n_1}{n_2 + n_1} \right)^2$$

These are equal when

$$(n_2 - n_1)^2 = 4n_1 n_2 \Rightarrow n_2^2 - 6n_2 n_1 + n_1^2 = 0$$

$$\frac{n_2}{n_1} = 3 \pm 2\sqrt{2} = \begin{cases} 5.83 \\ 0.172 \end{cases}$$

The two ratios are reciprocals of each other, so they represent the same relation looked at from opposite sides of the interface. Transparent materials with such a large ratio of refractive indices are not generally available at optical frequencies. And also, in practice, there are usually at least *two* interfaces, with air as the common medium on both the input and output sides. More practical schemes use a thin layer of a very good conductor (Ag or Al—see Sec. 6.4), or multiple layers of dielectric spaced so that the weak reflections at each interface interfere constructively.

6-2. Now $\underline{H} = \underline{B}/\mu$, and Eq. (6.3) is replaced by $\underline{H} = (1/\eta)\mathbf{e}_3 \times \underline{E}$, where $\eta = \mu/n = \sqrt{\mu/\epsilon}$ is the wave impedance of the medium [Eq. (5.29)]. Therefore, we simply substitute $n \rightarrow 1/\eta$ in Eqs. (6.6) and (6.7), to obtain the amplitude coefficients:

$$\frac{E_1^0}{E_0^0} = \frac{\frac{1}{\eta_2} - \frac{1}{\eta_1}}{\frac{1}{\eta_2} + \frac{1}{\eta_1}} = \frac{\eta_1 - \eta_2}{\eta_1 + \eta_2}$$

$$\frac{E_2^0}{E_0^0} = \frac{\frac{2}{\eta_1}}{\frac{1}{\eta_2} + \frac{1}{\eta_1}} = \frac{2\eta_2}{\eta_1 + \eta_2}$$

The same substitution in Eqs. (6.10) and (6.12) gives the power coefficients:

$$R = \left(\frac{\frac{1}{\eta_2} - \frac{1}{\eta_1}}{\frac{1}{\eta_2} + \frac{1}{\eta_1}} \right)^2 = \left(\frac{\eta_1 - \eta_2}{\eta_1 + \eta_2} \right)^2$$

$$T = \frac{1}{\eta_1} \left(\frac{\frac{2}{\eta_1}}{\frac{1}{\eta_2} + \frac{1}{\eta_1}} \right)^2 = \frac{4\eta_1\eta_2}{(\eta_1 + \eta_2)^2}$$

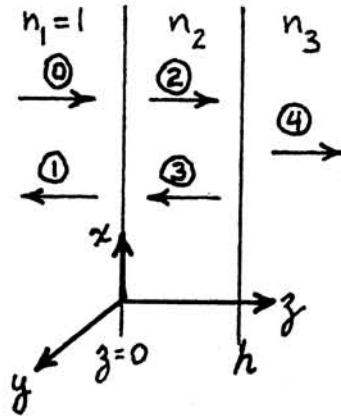
6-3. We analyze the system in terms of five waves, labeled as shown, as an extension of Fig. 6-1. Choose the sign convention that all **H**-fields have the same sense. To Eqs. (6.1) and (6.4) we add

$$\mathbf{E}_3 = -\mathbf{e}_x E_3^0 e^{i(-k_2 z - \omega t)}$$

$$\mathbf{E}_4 = +\mathbf{e}_x E_4^0 e^{i(+k_3 z - \omega t)}$$

$$\mathbf{H}_3 = \mathbf{e}_x n_2 E_3^0 e^{i(-k_2 z - \omega t)}$$

$$\mathbf{H}_4 = \mathbf{e}_x n_3 E_4^0 e^{i(+k_3 z - \omega t)}$$



The boundary conditions at $z = 0$ are

$$E_0^0 - E_1^0 = E_2^0 - E_3^0 \quad (1)$$

$$n_1 (E_0^0 + E_1^0) = n_2 (E_2^0 + E_3^0) \quad (2)$$

And those at $z = h$ are

$$E_2^0 e^{+ik_2 h} - E_3^0 e^{-ik_2 h} = E_4^0 e^{+ik_3 h} \quad (3)$$

$$n_2 (E_2^0 e^{+ik_2 h} + E_3^0 e^{-ik_2 h}) = n_3 E_4^0 e^{+ik_3 h} \quad (4)$$

We have four simultaneous equations from which we wish to calculate the reflection coefficient $R = |E_1^0/E_0^0|^2$. Eliminate E_4^0 from (3)–(4) to obtain

$$E_3^0 = E_2^0 \left(\frac{n_3 - n_2}{n_3 + n_2} \right) e^{+i2k_2 h} \quad (5)$$

Add and subtract (1)–(2) to obtain:

$$2 E_2^0 = \left(1 + \frac{n_1}{n_2} \right) E_0^0 - \left(1 - \frac{n_1}{n_2} \right) E_1^0 \quad (6)$$

$$2 E_3^0 = - \left(1 - \frac{n_1}{n_2} \right) E_0^0 + \left(1 + \frac{n_1}{n_2} \right) E_1^0 \quad (7)$$

Equate the ratios E_2^0/E_3^0 from (5) and (6)–(7) and rearrange to obtain

$$\frac{E_1^0}{E_0^0} = \frac{\left(\frac{n_2 - n_1}{n_2 + n_1} \right) + \left(\frac{n_3 - n_2}{n_3 + n_2} \right) e^{+i2k_2 h}}{1 + \left(\frac{n_2 - n_1}{n_2 + n_1} \right) \left(\frac{n_3 - n_2}{n_3 + n_2} \right) e^{+i2k_2 h}} \quad (8)$$

Define the single-interface amplitude reflection coefficients:

$$r_{12} \equiv \frac{n_2 - n_1}{n_2 + n_1}; \quad r_{23} \equiv \frac{n_3 - n_2}{n_3 + n_2} \quad (9)$$

And finally calculate the power reflection coefficient of the slab by multiplying (8) by its complex conjugate to obtain

$$R = \left| \frac{E_1^0}{E_0^0} \right|^2 = \frac{r_{12}^2 + r_{23}^2 + 2r_{12}r_{23}\cos 2k_2 h}{1 + r_{12}^2 r_{23}^2 + 2r_{12}r_{23}\cos 2k_2 h} \quad (10)$$

Now, both numerator and denominator have extreme values when $\cos 2k_2 h = \pm 1$. In particular, the reflection goes to zero when $2k_2 h$ is an odd multiple of π and $r_{12} = r_{23}$. That is, when

$$2k_2 h = 2n_2 \frac{2\pi}{\lambda_0} h = m\pi \implies h = m \frac{\lambda_0}{4n_2} \quad (m \text{ odd})$$

$$\frac{n_2 - n_1}{n_2 + n_1} = \frac{n_3 - n_2}{n_3 + n_2} \implies n_2 = \sqrt{n_1 n_3}$$

where $\lambda_0 = 2\pi c/\omega$ is the free-space wavelength. The slab thickness h needs to be an odd number of quarter-wavelengths (in the medium), and the refractive index of the slab needs to be the geometric mean of the indices of the input and output media. The suppression of reflection is least wavelength- (frequency-) sensitive for $m = 1$. This of course is the principle of coated optical lenses.

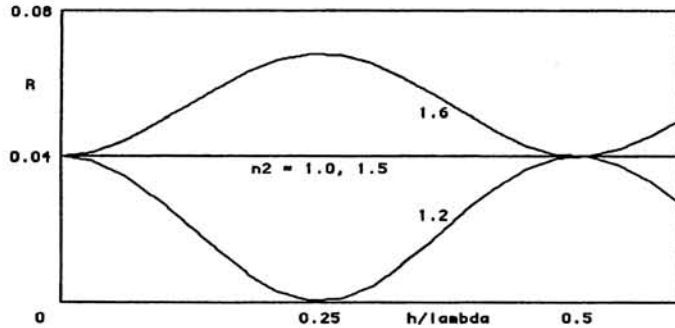
6-4. We write a straightforward program to evaluate Eqs. (9)–(10) in the preceding solution. For example, in TrueBASIC:

```

REM Program to calculate and plot reflection from slab
OPEN #1: screen 0.1, 0.91, 0.1, 0.9
SET WINDOW 0, 0.6, 0, 0.08
BOX LINES 0, 0.6, 0, 0.08
DATA 1.2, 1.5, 1.6
FOR I = 1 TO 3
  READ N2
  LET R12 = (N2 - 1)/(N2 + 1)
  LET R23 = (1.5 - N2)/(1.5 + N2)
  FOR J = 0 TO 20
    LET H = 0.03 * J
    LET CH = COS(2 * PI * H)
    LET R = (R12^2 + R23^2 + 2 * R12 * R23 * CH) / (1 + R12^2 * R23^2 + 2 * R12 * R23 * CH)
    PLOT LINES: H, R;
  NEXT J
  PLOT
NEXT I
CLOSE #1
END

```

The output, with added labeling, is:



6-5. Symmetry considerations suffice to establish that \mathbf{k}_1 and \mathbf{k}_2 are vectors in the plane defined by \mathbf{k}_0 and the normal in Fig. 6-2. For example, if an argument could be presented that \mathbf{k}_1 has a component perpendicular to this plane, then the same argument could be used to show that it has an equal but opposite component. Hence no such component exists.

For an explicit algebraic proof, let the origin lie on the interface and consider points on the interface specified by $\mathbf{r} = (x, y, 0)$. The superposition of the three waves must satisfy the boundary conditions at all points on the interface at all times; consequently the phases of the complex exponentials must be equal, leading to a generalization of Eq. (6.18),

$$\mathbf{k}_0 \cdot \mathbf{r} - \omega t = \mathbf{k}_1 \cdot \mathbf{r} - \omega t = \mathbf{k}_2 \cdot \mathbf{r} - \omega t \quad (1)$$

To show that \mathbf{k}_1 lies in the plane of incidence, which is defined by \mathbf{k}_0 and the interface normal \mathbf{n} , we must show that

$$\mathbf{k}_1 \cdot (\mathbf{k}_0 \times \mathbf{n}) = 0 \quad (2)$$

Use the *BAC-CAB* vector identity [Eq. (A.19)],

$$\mathbf{n} \times (\mathbf{n} \times \mathbf{r}) = (\mathbf{n} \cdot \mathbf{r}) \mathbf{n} - (\mathbf{n} \cdot \mathbf{n}) \mathbf{r} = -\mathbf{r}$$

to write

$$\mathbf{k}_0 \cdot \mathbf{r} = -\mathbf{k}_0 \cdot \mathbf{n} \times (\mathbf{n} \times \mathbf{r}) = -(\mathbf{k}_0 \times \mathbf{n}) \cdot (\mathbf{n} \times \mathbf{r})$$

With a similar relation for $\mathbf{k}_1 \cdot \mathbf{r}$, the first equality in (1) can be written

$$(\mathbf{k}_0 \times \mathbf{n} - \mathbf{k}_1 \times \mathbf{n}) \cdot (\mathbf{n} \times \mathbf{r}) = 0$$

Now in general the factor $(\mathbf{n} \times \mathbf{r})$ is not zero, nor is it perpendicular to the first factor; therefore the first factor must vanish. Taking the scalar product with \mathbf{k}_0 ,

$$\mathbf{k}_0 \cdot (\mathbf{k}_0 \times \mathbf{n} - \mathbf{k}_1 \times \mathbf{n}) = 0$$

and permuting the factors by Eq. (A.18), we obtain (2). The analogous argument holds for \mathbf{k}_2 .

6-6. The ray from Point P at (x_1, y_1, z_1) crosses the interface at $(x, y, 0)$ and proceeds to Point Q at (x_2, y_2, z_2) . The optical length is

$$L = n_1 [(x-x_1)^2 + (y-y_1)^2 + z_1^2]^{1/2} + n_2 [(x-x_2)^2 + (y-y_2)^2 + z_2^2]^{1/2} \quad (1)$$

Fermat's principle states

$$\delta L = \frac{\partial L}{\partial x} \delta x + \frac{\partial L}{\partial y} \delta y = 0$$

Because δx and δy are orthogonal, each of the partial derivatives must vanish separately:

$$\frac{\partial L}{\partial x} = n_1 \left(\frac{x-x_1}{r_1} \right) - n_2 \left(\frac{x-x_2}{r_2} \right) = 0 \quad (2)$$

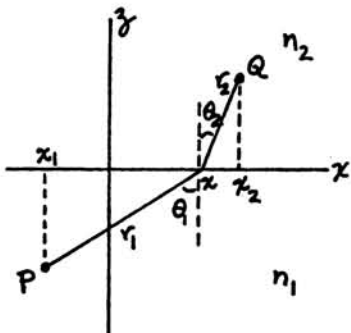
$$\frac{\partial L}{\partial y} = n_1 \left(\frac{y-y_1}{r_1} \right) - n_2 \left(\frac{y-y_2}{r_2} \right) = 0 \quad (3)$$

where r_1 and r_2 are the Pythagorean quantities in (1). There is no loss of generality (and the interpretation is clearer) if we orient the x and y axes, and place the origin, so that both y_1 and y_2 are zero. Then it is easy to see:

(a) Equation (3) requires $y = 0$. That is, the rays must lie in a plane.

(b) The geometrical ratios in (2) can be written as sines (see figure) to yield Snell's law,

$$n_1 \sin \theta_1 = n_2 \sin \theta_2$$



We have shown that if the crossing point $(x, 0, 0)$, determined from Eqs. (2)–(3), is displaced slightly to $(x + \delta x, \delta y, 0)$, then L does not change to first order. The only relevant extremum in this example is of course a *minimum*.

6-7. In matrix form, Eqs. (6.24–25) are

$$\begin{pmatrix} 1 & -1 \\ \cos \theta_0 & \frac{n_2}{n_1} \cos \theta_2 \end{pmatrix} \begin{pmatrix} E_1^0 \\ E_2^0 \end{pmatrix} = E_0^0 \begin{pmatrix} -1 \\ \cos \theta_0 \end{pmatrix}$$

By Cramer's rule and Snell's law [Eq. (6.20)],

$$\begin{aligned} E_1^0 &= \frac{\cos \theta_0 - (n_2/n_1) \cos \theta_2}{\cos \theta_0 + (n_2/n_1) \cos \theta_2} E_0^0 \\ &= \frac{\sin \theta_2 \cos \theta_0 - \sin \theta_0 \cos \theta_2}{\sin \theta_2 \cos \theta_0 + \sin \theta_0 \cos \theta_2} E_0^0 = \frac{\sin(\theta_2 - \theta_0)}{\sin(\theta_2 + \theta_0)} E_0^0 \end{aligned}$$

$$E_2^0 = \frac{2 \cos \theta_0}{\cos \theta_0 + (n_2/n_1) \cos \theta_2} E_0^0 = \frac{2 \sin \theta_2 \cos \theta_0}{\sin(\theta_2 + \theta_0)} E_0^0$$

Similarly, Eqs. (6.30–31) are

$$\begin{pmatrix} \cos \theta_0 & \cos \theta_2 \\ -1 & \frac{n_2}{n_1} \end{pmatrix} \begin{pmatrix} E_1^0 \\ E_2^0 \end{pmatrix} = E_0^0 \begin{pmatrix} \cos \theta_0 \\ 1 \end{pmatrix}$$

from which, using standard trigonometric identities,

$$\begin{aligned} E_1^0 &= \frac{(n_2/n_1) \cos \theta_0 - \cos \theta_2}{(n_2/n_1) \cos \theta_0 + \cos \theta_2} E_0^0 \\ &= \frac{\sin 2\theta_0 - \sin 2\theta_2}{\sin 2\theta_0 + \sin 2\theta_2} E_0^0 = \frac{\tan(\theta_0 - \theta_2)}{\tan(\theta_0 + \theta_2)} E_0^0 \end{aligned}$$

$$E_2^0 = \frac{2 \cos \theta_0}{(n_2/n_1) \cos \theta_0 + \cos \theta_2} E_0^0 = \frac{2 \sin \theta_2 \cos \theta_0}{\sin(\theta_2 + \theta_0) \cos(\theta_2 - \theta_0)} E_0^0$$

6-8. As in Prob. 6-2, we make the substitution $n \rightarrow 1/\eta$ in Eqs. (6.15–16). But Snell's law, Eq. (6.20), is *not* affected. With the notation $\alpha = \eta_2/\eta_1$ and $\beta = \cos \theta_2/\cos \theta_0$, Eqs. (6.26–27) become

$$E_1^0 = \frac{\cos \theta_0 - (\eta_1/\eta_2) \cos \theta_2}{\cos \theta_0 + (\eta_1/\eta_2) \cos \theta_2} E_0^0 = \frac{\alpha - \beta}{\alpha + \beta} E_0^0$$

$$E_2^0 = \frac{2 \cos \theta_0}{\cos \theta_0 + (\eta_1/\eta_2) \cos \theta_2} E_0^0 = \frac{2\alpha}{\alpha + \beta} E_0^0$$

Similarly, Eqs. (6.32–33) become

$$E_1^0 = \frac{(\eta_1/\eta_2) \cos \theta_0 - \cos \theta_2}{(\eta_1/\eta_2) \cos \theta_0 + \cos \theta_2} E_0^0 = \frac{1 - \alpha\beta}{1 + \alpha\beta} E_0^0$$

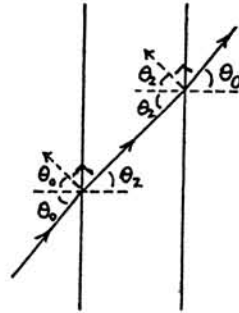
$$E_2^0 = \frac{2 \cos \theta_0}{(\eta_1/\eta_2) \cos \theta_0 + \cos \theta_2} E_0^0 = \frac{2\alpha}{1 + \alpha\beta} E_0^0$$

Note that α is determined by the ratio of the *impedances* ($\sqrt{\mu/\epsilon}$) of the two media, while β involves the ratio of the *refractive indices* ($\sqrt{\mu\epsilon}$), in addition to the angle of incidence. Matching impedances ($\eta_1 = \eta_2$) gives no reflection at normal incidence, but not in general at oblique incidence.

The power transmission coefficient T is computed from $\langle S_2 \rangle \cdot \mathbf{n} / \langle S_0 \rangle \cdot \mathbf{n}$ [see Eq. (6.36)], where the time-average Poynting vector is $\langle S \rangle = (c/8\pi) \mathbf{E} \times \mathbf{H}^* \rightarrow (c/8\pi)(E_0^2/\eta) \mathbf{e}_k$ [Eq. (5.51)], and where the dot product gives $\mathbf{e}_k \cdot \mathbf{n} = \cos \theta$. Thus to write T in terms of the ratio of \mathbf{E} -field amplitudes requires the coefficient

$$\frac{(1/\eta_2) \cos \theta_2}{(1/\eta_1) \cos \theta_0} = \frac{\beta}{\alpha}$$

6-9. From Eq. (6.32), the Brewster condition is $\theta_0 + \theta_2 = \pi/2$. At the first surface, the angles of incidence and (suppressed) reflection are θ_0 , and the angle of refraction is θ_2 . At the second surface of a plane slab, the roles of θ_0 and θ_2 are reversed, but the Brewster condition remains satisfied.



6-10. For a ray passing from a medium with index n_1 into a medium with index n_2 , the condition for total reflection is [Eq. (6.41)]

$$n_1 \sin \theta_1 > n_2 \quad \Rightarrow \quad \frac{n_2}{n_1} < \sin \theta_1$$

The Brewster condition for total transmission is [Eq. (6.34)]

$$n_1 \sin \theta_1 = n_2 \sin\left(\frac{\pi}{2} - \theta_1\right) = n_2 \cos \theta_1 \quad \Rightarrow \quad \frac{n_2}{n_1} = \tan \theta_1$$

If these conditions were to occur at the same time, we would need

$$\tan \theta_1 < \sin \theta_1$$

But, since θ_1 is a first-quadrant angle, this inequality (which amounts to $\cos \theta_1 > 1$) is never true.

6-11. Because the reflection coefficients are reversible, the required diagram is merely a distortion of the abscissa scale of Fig. 6-5, using Snell's law to transform θ_0 to θ_2 . The diagram in the next column is reproduced from (El85, p.276). For an index ratio of 1.5 (~glass/air), the critical angle is 42° (on the glass side), and Brewster's angle is 34° on the glass side or 56° on the air side.

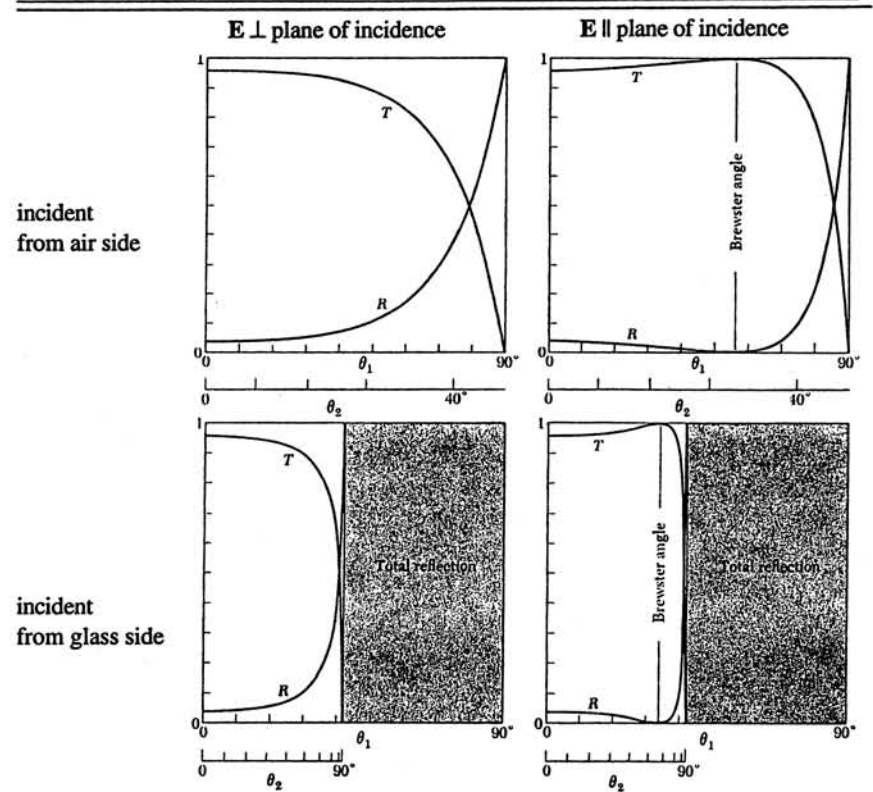
6-12. The k_2 in Eq. (6.54) should be starred; Eq. (6.55) is missing a factor of Q . Implicit in Eq. (6.46) is the *complex conjugate* of the vector propagation constant,

$$k_2^* = k_2 [-\sin \theta_2, 0, (\cos \theta_2)^*] = k_2 (-W, 0, -iQ)$$

where W and Q are defined in Eqs. (6.43) and (6.47); W and Q are real (and positive) under the conditions of total reflection, and $W^2 - Q^2 = 1$. Similarly,

$$E_2 = (iQ E_{1\parallel}, E_{1\perp} e^{i\delta}, W E_{1\parallel})$$

where δ is the phase of the perpendicular component relative to the parallel component of E_2 . Now (tediously!) expand $\langle S_2 \rangle$ as given in Eq. (6.54), to obtain



6-12, cont.

$$\begin{aligned} \text{Re} \langle S_2 \rangle_x &\sim -W (E_{1\parallel}^2 + E_{1\perp}^2) \\ \text{Re} \langle S_2 \rangle_y &\sim 2QW E_{1\parallel} E_{1\perp} \sin \delta \end{aligned}$$

This energy flow parallel to the interface is of significance for finite geometry, as mentioned at the end of Sec. 6.3.

6-13. The sign convention of the formulas in the text is defined in Fig. 6-1: an amplitude reflection coefficient of +1 actually signifies a phase reversal of π in the reflected electric wave. For a conducting medium, the notation is [Eq. (6.68)]

$$\frac{c}{\omega} \hat{k} = \hat{n} = n (1 + i\kappa)$$

Thus the amplitude reflection coefficient, Eq. (6.56), is

$$\begin{aligned}\frac{E_1^0}{E_0^0} &= \frac{\hat{n} - 1}{\hat{n} + 1} = \frac{(n-1) + in\kappa}{(n+1) + in\kappa} \\ &= \frac{(n^2 - 1 + n^2\kappa^2) + i(2n\kappa)}{(n+1)^2 - (n\kappa)^2}\end{aligned}$$

The phase angle ϕ is given by

$$\tan\phi = \frac{2n\kappa}{n^2 - 1 + n^2\kappa^2}$$

Now, for a good conductor [Eq. (6.57)], $\kappa \rightarrow 1$ and $n \rightarrow c/\omega\delta \gg 1$. Consequently,

$$\tan\phi = \frac{2n\kappa}{2n^2} = \frac{\kappa}{n} \rightarrow (+)0$$

For the sign convention of Fig. 6-1, $\phi \rightarrow 0$ —that is, the incident and reflected E-fields are equal and opposite to produce a standing-wave node at the surface of the conductor.

6-14. For the cases of Table 5.1, $\delta \ll \lambda \equiv c/2\pi\nu$, and the approximation of Eqs. (6.62–63) is good. With $n_1 = 1$ and $\sigma(\text{Cu}) = 5.2 \times 10^{17} \text{ s}^{-1}$, we calculate $T = 2\sqrt{\nu/\sigma}$:

Case	ν (Hz)	λ (m)	δ (mm)	$T = 1 - R$
1	10^3	48000	2.1	$8.8 \cdot 10^{-8}$
2	10^4	4800	0.66	$2.8 \cdot 10^{-7}$
3	10^5	480	0.21	$8.8 \cdot 10^{-7}$
4	10^6	48	0.066	$2.8 \cdot 10^{-6}$

6-15. From Eqs. (5.82–84), (5.101), (6.68), and (6.73a), for a good conductor, $\kappa \rightarrow 1$, $n \rightarrow \lambda/\delta \gg 1$, and $\gamma \rightarrow 1/2n$. Therefore, from Eq. (6.72),

$$\begin{aligned}\cos^2\theta_2' &= 1 - \gamma^2(1 - \kappa^2)\sin^2\theta_0 + i2\kappa\gamma^2\sin^2\theta_0 \\ &\rightarrow 1 + i\frac{1}{2}\left(\frac{\delta}{\lambda}\right)^2\sin^2\theta_0 \approx 1\end{aligned}$$

Accordingly, the parameters defined in Eq. (6.73b) are $\alpha \rightarrow 1$, $\phi \rightarrow 0$, and Eq. (6.78) has the limiting value

$$N(\theta_0) \rightarrow \left[\sin^2\theta_0 + \left(\frac{\lambda}{\delta}\right)^2\right]^{1/2} \approx \frac{\lambda}{\delta} \gg 1$$

From Eq. (6.80),

$$\sin\theta_2 \rightarrow \frac{\sin\theta_0}{\lambda/\delta} \ll 1$$

which implies that the planes of constant phase are nearly parallel to the interface even when θ_0 approaches $\pi/2$.

Under the same conditions, the coefficient in Eq. (6.75) is

$$\frac{\omega}{c}n\alpha(\kappa\cos\phi + \sin\phi) \rightarrow \frac{\omega}{c}\frac{\lambda}{\delta} = \frac{1}{\delta}$$

That is, the attenuation distance is that for normal incidence, essentially independent of the actual angle of incidence.

Chapter 7

7-1. (a) The electric field of a long straight wire, carrying (free) charge per-unit-length ρ_ℓ and immersed in a medium of dielectric constant ϵ , can be found easily from Gauss' law for \mathbf{D} , Eq. (1.82), as $\mathbf{E}(r) = \mathbf{D}(r)/\epsilon = 2\rho_\ell/\epsilon r \mathbf{e}_r$ (cylindrical coordinates—see Prob. 1-5). To find the difference of potential between parallel wires with equal and opposite charge, it suffices to integrate Eq. (1.13) along a radial line common to the two wires. Let this be the x axis, with the origin at the center of the negative wire and the center of the positive wire at $x = +d$. The potential difference is then

$$\begin{aligned}\Delta\Phi &= \Phi(d) - \Phi(0) = - \int_a^{d-a} \left(\frac{2(-\rho_\ell)}{\epsilon x} - \frac{2(+\rho_\ell)}{\epsilon x} \right) dx \\ &= \frac{4\rho_\ell}{\epsilon} \ln\left(\frac{d-a}{a}\right) \xrightarrow{d \gg a} \frac{4\rho_\ell}{\epsilon} \ln\left(\frac{d}{a}\right)\end{aligned}$$

[Long straight wires do not allow the convention of taking the zero of potential at "infinity" because of the conflict between axial and radial infinities. Thus, Eq. (1.21) is not helpful. Note also that the influence of one wire's charge on the other spoils the azimuthal symmetry assumed in deriving the field of one wire; but the limit $d \gg a$ allows us to neglect this correction (otherwise, see Prob. 2-7).] The capacitance per-unit-length is defined as the ratio of the charge per-unit-length to the potential difference,

$$C_\ell = \frac{\rho_\ell}{\Delta\Phi} = \frac{\epsilon}{4 \ln(d/a)}$$

The inductance per-unit-length, with $\mu = 1$, was found in the Solution for Prob. 4-1(b), using a simple application of Ampere's law, Eq. (1.37). In the presence of a magnetic material, the appropriate form of Ampere's law is Eq. (1.93) in terms of the \mathbf{H} -field produced by free currents. But the Faraday induction, Eq. (4.9), depends upon the \mathbf{B} -flux, where $\mathbf{B} = \mu\mathbf{H}$. Thus the inductance is multiplied by μ ,

$$L_\ell = \frac{4\mu}{c^2} \ln\left(\frac{d}{a}\right)$$

Therefore we have:

$$V = \frac{1}{\sqrt{L_\ell C_\ell}} = \frac{c}{\sqrt{\epsilon\mu}} = \frac{c}{n}$$

$$(Z_0)_{\text{par.wire}} = \sqrt{\frac{L_\ell}{C_\ell}} = \frac{4}{c} \sqrt{\frac{\mu}{\epsilon}} \ln\left(\frac{d}{a}\right) = \frac{4}{c} \eta \ln\left(\frac{d}{a}\right)$$

where n is the refractive index of the medium, and η is its wave impedance. The speed $V = c/n$ is of course the speed of plane waves in an unbounded medium with these properties.

(b) For the coaxial geometry, the capacitance per-unit-length for $\epsilon = 1$ was found in the Solution for Prob. 1-7. Now we have

$$C_\ell = \frac{\epsilon}{2 \ln(b/a)}$$

and Prob. 4-1(a), modified for $\mu \neq 1$, gives

$$L_\ell = \frac{2\mu}{c^2} \ln\left(\frac{b}{a}\right)$$

Thus,

$$V = \frac{1}{\sqrt{L_\ell C_\ell}} = \frac{c}{\sqrt{\epsilon\mu}} = \frac{c}{n}$$

$$(Z_0)_{\text{coax}} = \sqrt{\frac{L_\ell}{C_\ell}} = \frac{2}{c} \sqrt{\frac{\mu}{\epsilon}} \ln\left(\frac{b}{a}\right) = \frac{2}{c} \eta \ln\left(\frac{b}{a}\right)$$

7-2. (a) Dimensionally, capacitance is $[C] = [Q]/([E] \cdot [\text{length}])$, where the electric field E derives from Coulomb's law. In SI units, Coulomb's law contains the coefficient $1/4\pi\epsilon_0$ ($\approx 9 \times 10^9$ m/F), in place of the unity coefficient of Gaussian units. Thus,

$$C_\ell = \frac{2\pi\epsilon}{\ln(b/a)} \quad (\text{SI})$$

where the permittivity ϵ is now understood to include the constant ϵ_0 . Similarly, inductance is $[L] = [\text{emf}]/[\text{current}]$. In Faraday's law, $[\text{emf}] = [\Phi_m]/[\text{time}]$, the coefficient $1/c$ in Gaussian units is replaced by unity in SI. The magnetic flux, $[\Phi_m] = [B] \cdot [\text{area}]$ derives from the Biot-Savart law, in which the Gaussian coefficient $1/c$ is replaced by the SI coefficient $\mu_0/4\pi$ ($\approx 10^{-7}$ H/m). Thus we multiply by $(c^2\mu_0/4\pi)$ to obtain

$$L_\ell = \frac{\mu}{2\pi} \ln\left(\frac{b}{a}\right) \quad (\text{SI})$$

where μ is now understood to include the μ_0 factor. Thus $1/\sqrt{L_\ell C_\ell} = 1/\sqrt{\epsilon\mu} = c/n$ as before (with $n = \sqrt{\epsilon\mu/\epsilon_0\mu_0}$ in SI notation). And the characteristic impedance becomes

$$(Z_0)_{\text{coax}} = \sqrt{\frac{L_\ell}{C_\ell}} = \frac{1}{2\pi} \sqrt{\frac{\mu}{\epsilon}} \ln\left(\frac{b}{a}\right) = \frac{1}{2\pi} \eta \ln\left(\frac{b}{a}\right) \quad (\text{SI})$$

In free space, the SI wave impedance is $\eta \rightarrow \eta_0 = \sqrt{\mu_0/\epsilon_0} \approx 377$ ohms.

(b) We can now solve for the braid diameter of RG-58 coax,

$$2b = 2a \exp\left(\frac{2\pi Z_0}{\eta_0} \sqrt{\frac{\epsilon_r}{\mu_r}}\right) = (0.085\text{cm}) \exp\left[\frac{2\pi(50\Omega)}{377\Omega} \sqrt{2.3}\right] = 0.30\text{cm}$$

(c) The wave speed relative to free space is $V/c = 1/n = 1/\sqrt{\epsilon_r \mu_r}$. For the polyethylene dielectric, we have $V/c = 1/\sqrt{2.3} = 66\%$.

7-3. (a) The notation of the outbound and reflected waves, of voltage and current, is defined in Eqs. (7.12–13). Equations (7.15) allow the voltage amplitudes, V_+, V_- , to be expressed in terms of the current amplitudes, I_+, I_- . Therefore Eq. (7.14) can be written as

$$Z_0 (I_+ e^{+ik\ell} - I_- e^{-ik\ell}) = Z_l (I_+ e^{+ik\ell} + I_- e^{-ik\ell})$$

Similarly for Eq. (7.16),

$$Z_0 (I_+ - I_-) = Z_g (I_+ + I_-)$$

Both equations can now be solved for the ratio of current amplitudes,

$$\frac{I_-}{I_+} = \frac{Z_0 e^{+ik\ell} - Z_l e^{-ik\ell}}{Z_0 e^{-ik\ell} + Z_l e^{-ik\ell}} = \frac{Z_0 - Z_g}{Z_0 + Z_g} \quad (1)$$

Cross-multiplying and rearranging,

$$\begin{aligned} Z_0 (Z_0 e^{+ik\ell} - Z_0 e^{-ik\ell} - Z_l e^{+ik\ell} - Z_l e^{-ik\ell}) \\ = Z_g (-Z_0 e^{+ik\ell} - Z_0 e^{-ik\ell} + Z_l e^{+ik\ell} - Z_l e^{-ik\ell}) \end{aligned}$$

$$Z_0 (i Z_0 \sin k\ell - Z_l \cos k\ell) = Z_g (-Z_0 \cos k\ell + i Z_l \sin k\ell)$$

which rearranges once again to Eq. (7.17). For Eq. (7.18), using the first form of (1),

$$r \equiv \frac{V_- e^{-ik\ell}}{V_+ e^{+ik\ell}} = -\frac{I_- e^{-ik\ell}}{I_+ e^{+ik\ell}} = -\left(\frac{Z_0 e^{+ik\ell} - Z_l e^{-ik\ell}}{Z_0 e^{-ik\ell} + Z_l e^{-ik\ell}}\right) \frac{e^{-ik\ell}}{e^{+ik\ell}} = \frac{Z_l - Z_0}{Z_l + Z_0}$$

(b) For $Z_l \rightarrow 0$, Eq. (7.17) reduces to $Z_g = -i Z_0 \tan k\ell$. For $Z_l \rightarrow \infty$, it becomes $Z_g = +i Z_0 / \tan k\ell$. Since Z_0 is pure-real (for lossless lines), these input impedances are pure-imaginary, meaning that the current and voltage are 90° out-of-phase. Our sign convention in the complex exponential for time, $e^{-i\omega t}$, is the reverse of the electrical engineers' usual convention, $e^{+j\omega t}$. Therefore, our positive-imaginary impedance is a *capacitive* reactance, and negative-imaginary is *inductive*.

(c) For lines whose length is much less than a wavelength, we have $k\ell \ll 1$, and the tangent can be replaced by its argument. Thus, for the short-circuited line,

$$Z_g \rightarrow -ik\ell Z_0 = -i (\omega \sqrt{L_\ell C_\ell}) \ell \sqrt{\frac{L_\ell}{C_\ell}} = -i \omega L_\ell \ell$$

where we have used $k = \omega/c = \omega \sqrt{L_\ell C_\ell}$. This is just the reactance (more familiarly, $+j\omega L$) of a length ℓ of a "lumped" inductor the inductance of which is L_ℓ per unit length.

Similarly, for the open-circuited line,

$$Z_g \rightarrow +i \frac{Z_0}{k\ell} = +i \frac{\sqrt{L_\ell C_\ell}}{(\omega \sqrt{L_\ell C_\ell}) \ell} = +i \frac{1}{\omega C_\ell \ell}$$

This is the reactance (more familiarly, $-j/\omega C$) of a length ℓ of a "lumped" capacitor the capacitance of which is C_ℓ per unit length. The results agree with the elementary notion that a loop of wire is inductive, while a pair of insulated conductors is capacitive.

7-4. The problem is to use Eq. (7.17) to find a length ℓ and a characteristic impedance Z_0 such that the physical load resistor, $Z_l \rightarrow R_l$, appears to the generator as the desired matched load, $Z_g \rightarrow R_{\text{int}}$. All quantities are now real except for the explicit i in the formula. To provide a real Z_g , the numerator and denominator of the fraction must have the same phase. In general (independent of $k\ell$), this would require $Z_0/Z_l = Z_l/Z_0$, which gives $Z_g = Z_l$ and does not solve the problem. The same unacceptable result occurs for special values of ℓ such that $\tan k\ell = 0$. However, for values of ℓ such that $\tan k\ell \rightarrow (\pm)\infty$, then $Z_g = Z_0^2/Z_l$. Accordingly, we choose:

$$k\ell = \frac{\pi}{2} \implies \ell = \frac{\lambda}{4} \quad \text{and} \quad Z_0 = \sqrt{R_{\text{int}} R_l}$$

Higher odd multiples of $\lambda/4$ would work also, but would be more frequency-sensitive. Note that this is the transmission-line analog of the suppression of optical reflection discussed in Prob. 6-3.

7-5. (a) If we assume that the inner conductor carries a charge per-unit-length ρ_ℓ , an elementary Gauss'-law argument (see Prob. 1-5), gives the electric field, from which we can compute the difference of potential $\Delta\Phi$ between the coaxial conductors:

$$\mathbf{E}(r) = \frac{2\rho_\ell}{\epsilon r} \mathbf{e}_r \quad \Rightarrow \quad V_0 = |\Delta\Phi| = \left| \int_a^b \frac{2\rho_\ell}{\epsilon r} dr \right| = \frac{2\rho_\ell}{\epsilon} \ln\left(\frac{b}{a}\right)$$

Therefore, we can write the field as

$$\mathbf{E}(r) = \frac{V_0}{\ln(b/a)} \frac{1}{r} \mathbf{e}_r$$

(b) Ampere's law gives the magnetic field as (see Prob. 1-19)

$$\mathbf{B}(r) = \frac{2\mu I_0}{c} \frac{1}{r} \mathbf{e}_\theta$$

(c) The spatial dependence of both fields is the function $\psi(r,z) = e^{ikz}/r$, in cylindrical coordinates. It is difficult to compute the Laplacian directly because the non-Cartesian unit vectors \mathbf{e}_r and \mathbf{e}_θ do not commute through ∇^2 . Instead we use Eq. (A.40),

$$\nabla^2 \equiv \text{grad div} - \text{curl curl}$$

with the operators expressed in the cylindrical-coordinate basis, Eqs. (A.44)–(A.46). The divergence of \mathbf{B} is trivially zero since the only vector component is \mathbf{e}_θ but there is no functional dependence on θ . The divergence of \mathbf{E} also vanishes because the $1/r$ dependence cancels out before taking the r derivative. The curls are:

$$\text{curl} \left(\mathbf{e}_r \frac{e^{ikz}}{r} \right) = \begin{vmatrix} \frac{\mathbf{e}_r}{r} & \mathbf{e}_\theta & \frac{\mathbf{e}_z}{r} \\ \frac{\partial}{\partial r} & 0 & \frac{\partial}{\partial z} \\ \frac{e^{ikz}}{r} & 0 & 0 \end{vmatrix} = \mathbf{e}_\theta ik \frac{e^{ikz}}{r}$$

$$\text{curl} \left(\mathbf{e}_\theta \frac{e^{ikz}}{r} \right) = \begin{vmatrix} \frac{\mathbf{e}_r}{r} & \mathbf{e}_\theta & \frac{\mathbf{e}_z}{r} \\ \frac{\partial}{\partial r} & 0 & \frac{\partial}{\partial z} \\ 0 & r \left(\frac{e^{ikz}}{r} \right) & 0 \end{vmatrix} = -\mathbf{e}_r ik \frac{e^{ikz}}{r}$$

The second curl simply interchanges the vector components once again:

$$\text{curl curl} \left(\mathbf{e}_r \frac{e^{ikz}}{r} \right) = -(ik)^2 \left(\mathbf{e}_r \frac{e^{ikz}}{r} \right)$$

$$\text{curl curl} \left(\mathbf{e}_\theta \frac{e^{ikz}}{r} \right) = -(ik)^2 \left(\mathbf{e}_\theta \frac{e^{ikz}}{r} \right)$$

Therefore,

$$\nabla^2 \mathbf{E} = -\text{curl curl} \mathbf{E} = -k^2 \mathbf{E}$$

$$\nabla^2 \mathbf{B} = -\text{curl curl} \mathbf{B} = -k^2 \mathbf{B}$$

Meanwhile, the second time derivative $\partial^2/\partial t^2$ of both fields is elementary, amounting to multiplication by $(-i\omega)^2 = -\omega^2$. Thus the wave equations, Eqs. (5.5–6), are satisfied by these wavefunctions with k and ω linked by the standard dispersion relation, Eq. (5.12),

$$k^2 = \frac{\epsilon\mu}{c^2} \omega^2$$

(d) The time-average Poynting vector for these fields is

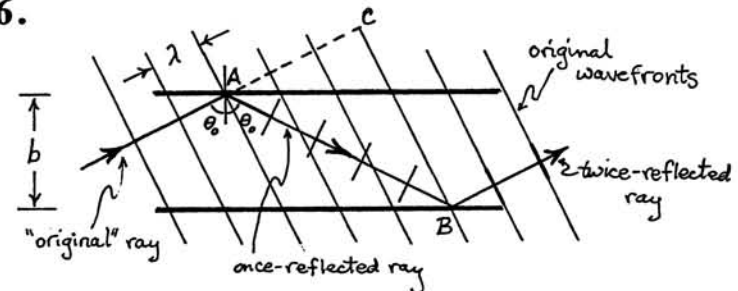
$$\begin{aligned} \langle \mathbf{S}(r) \rangle &= \frac{c}{8\pi} \mathbf{E} \times \left(\frac{\mathbf{B}^*}{\mu} \right) \\ &= \frac{c}{8\pi} \left(\frac{V_0}{\ln(b/a)} \right) \left(\frac{2I_0}{c} \right) \frac{1}{r^2} (\mathbf{e}_r \times \mathbf{e}_\theta) = \frac{V_0 I_0}{4\pi \ln(b/a)} \frac{1}{r^2} \mathbf{e}_z \end{aligned}$$

The total power transmitted in the space between the two conductors is

$$P = \int_a^b \langle \mathbf{S}(r) \rangle 2\pi r dr = \frac{1}{2} V_0 I_0 = V_{\text{rms}} I_{\text{rms}}$$

which of course is the result expected from elementary circuit theory.

7-6.



As in Fig. 7-4, it is useful to represent a wave train by a ray (sometimes called "wave-normal" because the ray is perpendicular to the wavefronts). Let the "original" ray strike the upper wall at Point A, at the angle θ_0 with respect to the wall's normal. The

ray is reflected at the same angle and strikes the lower wall at Point B , where it is again reflected (parallel to the original ray). We want the *phase* of the twice-reflected ray to match that of the original ray carried forward to Point C . If the separation between the walls is b , we have:

$$\frac{b}{(AB)} = \cos\theta_0$$

$$\frac{(AC)}{(AB)} = \cos[2(\frac{\pi}{2} - \theta_0)] = -\cos 2\theta_0 = \sin^2\theta_0 - \cos^2\theta_0$$

To match the phases, the *excess* distance must be an integral multiple of the wavelength,

$$n\lambda = (AB) - (AC) = \frac{b}{\cos\theta_0} [1 - (\sin^2\theta_0 - \cos^2\theta_0)] = 2b \cos\theta_0$$

which reduces to Eq. (7.25) with $k = 2\pi/\lambda$. Depending on the polarization, the wave undergoes a phase shift of either 0 or π at each reflection, or 0 or 2π after the double reflection. This amounts to an offset of n by unity. In either case, $n = 1$ is the smallest integer (largest θ_0) to give constructive double (hence, multiple) reflections.

7-7. The decomposition of total fields into longitudinal and transverse components is stated in Eq. (7.41). Because these components are orthogonal,

$$\mathbf{E} \cdot \mathbf{B} = E_z B_z + \mathbf{E}_t \cdot \mathbf{B}_t$$

For either TE or TM modes, $E_z B_z = 0$. For TE modes, from Eqs. (7.60) and (A.18),

$$\mathbf{E}_{t0} \cdot \mathbf{B}_{t0} = \frac{k_g}{k_0} \mathbf{E}_{t0} \cdot (\mathbf{e}_z \times \mathbf{E}_{t0}) = \frac{k_g}{k_0} \mathbf{e}_z \cdot (\mathbf{E}_{t0} \times \mathbf{E}_{t0}) = 0$$

A similar result follows from Eq. (7.61) for TM modes. Thus, $\mathbf{E} \cdot \mathbf{B}$ vanishes in general.

7-8. (a) The wavefunction has the form given in Eq. (7.35), $e^{i(k_g z - \omega t)}$. Therefore, the phase velocity is $u_{ph} = \omega/k_g$, $v_{lg} = c\lambda_g/\lambda_0 = ck_0/k_g$. By Eq. (7.30) or (7.38), $k_g^2 = k_0^2 - k_c^2$. And for the rectangular TE₁₀ mode, from Eqs. (7.73–74), $k_c = \pi/a$. Therefore,

$$u_{ph} = \frac{ck_0}{\sqrt{k_0^2 - (\pi/a)^2}} = \frac{c}{\sqrt{1 - (\lambda_0/2a)^2}}$$

(b) Substituting the fields of Eqs. (7.75) and using the time-average product theorem of Eq. (5.46), the energy density is [Eq. (4.70)]:

$$\begin{aligned} \langle \mathcal{E} \rangle &= \frac{1}{16\pi} (\mathbf{E} \cdot \mathbf{E}^* + \mathbf{B} \cdot \mathbf{B}^*) \\ &\rightarrow \frac{1}{16\pi} (B^0)^2 \left\{ \left[\left(\frac{k_0 a}{\pi} \right)^2 + \left(\frac{k_g a}{\pi} \right)^2 \right] \sin^2 \left(\frac{\pi x}{a} \right) + \cos^2 \left(\frac{\pi x}{a} \right) \right\} \end{aligned}$$

Integrating over the cross section,

$$\begin{aligned} \left(\frac{\text{energy per}}{\text{unit length}} \right) &= \int_{x=0}^a \int_{y=0}^b \langle \mathcal{E} \rangle_{10} dx dy \\ &= \frac{ab}{32\pi} (B^0)^2 \left[\left(\frac{k_0 a}{\pi} \right)^2 + \left(\frac{k_g a}{\pi} \right)^2 + 1 \right] \end{aligned}$$

(Time-averaging automatically averages the waves spatially in the z direction, so this is equivalently the *space-average* energy per-unit-length.) Using Eqs. (7.31) and (7.74) to evaluate $k_g = 2\pi/\lambda_g$, we find

$$\left(\frac{k_g a}{\pi} \right)^2 + 1 = \left(\frac{a}{\pi} \right)^2 \left[k_0^2 - \left(\frac{\pi}{a} \right)^2 \right] + 1 = \left(\frac{k_0 a}{\pi} \right)^2$$

—that is, the electric and magnetic contributions are equal. Rewriting in terms of $E^0 = (k_0 a/\pi)B^0$,

$$\left(\frac{\text{energy per}}{\text{unit length}} \right) = \frac{1}{16\pi} ab (E^0)^2$$

Dividing this into the power from Eq. (7.79), we have

$$\left(\frac{\text{power}}{\text{energy/length}} \right) = c \sqrt{1 - \left(\frac{\lambda_0}{2a} \right)^2} = c \frac{\lambda_0}{\lambda_g}$$

which is the group velocity, $u_{gr} = c \sin\theta_0$. Thus, in agreement with Eq. (7.33),

$$u_{ph} u_{gr} = \left(c \frac{\lambda_g}{\lambda_0} \right) \left(c \frac{\lambda_0}{\lambda_g} \right) = c^2$$

7-9. (a) From Eq. (7.73), the cutoff frequencies for the mn modes in rectangular waveguide are

$$\frac{\omega_{mn}}{2\pi} = v_{mn} = \frac{c}{2} \sqrt{\frac{m^2}{a^2} + \frac{n^2}{b^2}}$$

where, in the present example, $a = 2.286$ cm and $b = 1.016$ cm. For TE modes, at least one of the mode integers must be greater than zero (for TM modes, both mode integers must be greater than zero). Thus the lowest mode has $m = 1$, $n = 0$, and can only be TE. That is, the so-called *dominant mode* is TE₁₀, and it propagates at frequencies above

$$\nu_{10} = \frac{(2.998 \times 10^{10} \text{ cm/s})}{2 (2.286 \text{ cm})} = 6.56 \text{ GHz}$$

Since a is more than twice b in this case, the second-lowest mode is TE₂₀, which propagates above

$$\nu_{20} = 2\nu_{10} = 13.12 \text{ GHz}$$

[For the TE₀₁ mode, $\nu_{01} = c/2(1.016) = 14.75$ GHz. For both TE₁₁ and TM₁₁, $\nu_{11} = (c/2)[1/(2.286)^2 + 1/(1.016)^2]^{1/2} = 16.15$ GHz, etc., etc.] Thus, nominally, the single-mode bandwidth is the factor-of-two ("octave") from 6.56 to 13.12 GHz. Practical application, however, is usually limited to the band 8.2 to 12.4 GHz because the imperfect conductivity of the copper walls causes significant loss at the low end [and limited power-handling ability—see Part (b)], and excitation of the almost-propagating higher modes is troublesome at the high end. Note that the single-mode bandwidth is reduced when $a < 2b$; thus most commercial waveguides are rectangular rather than square.

(b) Equation (7.79) relates the transmitted power P to the peak electric field E_0 . In SI units,

$$P_{10} = \sqrt{1 - \left(\frac{\lambda_0}{2a}\right)^2} \frac{E_0^2}{4\eta_0} ab$$

where $\eta_0 \approx 377\Omega$ is the SI impedance of free space. At the low end of the single-mode band, where $\lambda_0 \rightarrow 2a$, the square-rooted quantity, and hence the power-transmitting capacity, go to zero. At the nominal high end of the single-mode band, we have

$$P_{\max}(\lambda_0=a) \approx \frac{\sqrt{3}}{2} \frac{(30,000 \text{ V/cm})^2}{4 (377\Omega)} (2.286\text{cm})(1.016\text{cm}) = 1.2 \text{ megawatts}$$

Not only does the power rating change significantly with frequency within the single-mode band, but also it is reduced by the likelihood that reflections will set up a standing wave. If the constructive interference (antinode) is limited to the maximum electric field, then the one-way power is reduced by up to a factor of four.

7-10. (a) In Eqs. (7.75), first make the substitution $i(k_0 a/\pi)B^0 \rightarrow E_0$. That is, the coefficient of E_y is defined to be E_0 . The coefficient of B_z then becomes $-i\pi E_0/k_0 a = -i(\lambda_0/\lambda_c)E_0$, using $\lambda_c = 2a$ from Eq. (7.74). And the coefficient of B_x becomes $(-ik_g a/\pi)(-i\pi E_0/k_0 a) = -(\lambda_0/\lambda_g)E_0$. Finally, taking the real part of $\exp[i(k_g z - \omega t)]$ gives $\cos(k_g z - \omega t)$, while the real part of $-i \exp[i(k_g z - \omega t)]$ gives $+\sin(k_g z - \omega t)$. The results are then as stated.

(b) The wall currents are related to the tangential magnetic field at the wall by Eq. (1.95), with $B \rightarrow 0$ inside the "perfectly conducting" walls. Thus, at the broad "top" and "bottom" walls (parallel to the x - z plane), the components of surface current are:

$$K_x = \pm \frac{c}{4\pi} B_z(y=0, b) = \pm \frac{c}{4\pi} \frac{\lambda_0}{\lambda_c} E^0 \cos\left(\frac{\pi x}{a}\right) \sin(k_g z - \omega t)$$

$$K_z = \mp \frac{c}{4\pi} B_x(y=0, b) = \pm \frac{c}{4\pi} \frac{\lambda_0}{\lambda_g} E^0 \sin\left(\frac{\pi x}{a}\right) \cos(k_g z - \omega t)$$

In the middle of a broad wall ($x = a/2$), K_x goes to zero, while K_z is a maximum. Since the wall current is purely longitudinal here, a narrow slot will cause neither reflection within the guide nor radiation outside. [The \pm comes from the reversal of the normal \mathbf{n} in Eq. (1.95) for the opposite walls at $y = 0$ and b —a detail that doesn't concern us here.]

At the "side" walls (parallel to the y - z plane),

$$K_y = \pm \frac{c}{4\pi} B_z(x=0, a) = \frac{c}{4\pi} \frac{\lambda_0}{\lambda_c} E^0 \sin(k_g z - \omega t)$$

$$K_z = (\mp) \frac{c}{4\pi} B_y(x=0, a) = 0$$

The current in the side walls is purely transverse. Accordingly, one can cut a thin transverse slot (i.e., in the y dimension) at any point along the waveguide without perturbing the wave inside the guide, or allowing radiation outside. [For the side walls at $x = 0$ and a , the reversal of \mathbf{n} and the value of $\cos(\pi x/a) \rightarrow \pm 1$ cancel, so the currents are in the same sense in both walls.]

7-11. The force-per-area is given by an element of the stress tensor, Eq. (4.110) or (4.111), evaluated by the field formulas of Prob. 7-10. The directional sense of the force is given most easily by the "furry rubber band" analogy.

(a) For the "top" and "bottom" walls at $y = 0$ and b , the electric time-averaged force-per-area is

$$\frac{dF_e}{dA} = \frac{1}{8\pi} \langle [E_y(x,y,z,t)]^2 \rangle_{y=0,b} = \frac{1}{16\pi} E_0^2 \sin^2\left(\frac{\pi x}{a}\right)$$

The electric force-per-length of waveguide is then

$$\frac{dF_e}{d\ell} = \int_0^a \frac{dF_e}{dA} dx = \frac{1}{32\pi} E_0^2 a$$

where we have used the shortcut that the average value over an integral number of half-wavelengths is $\langle \sin^2 u \rangle = \langle \cos^2 u \rangle = \frac{1}{2}$. Since the **E**-field is *normal* at these walls, the rubber-band analogy says that the walls are pulled *inward* by the field.

(b) Similarly, the magnetic force-per-area is

$$\begin{aligned} \frac{dF_m}{dA} &= \frac{1}{8\pi} \langle [B_x(x,y,z,t)]^2 + [B_z(x,y,z,t)]^2 \rangle_{y=0,b} \\ &= \frac{1}{16\pi} E_0^2 \left[\left(\frac{\lambda_0}{\lambda_g}\right)^2 \sin^2\left(\frac{\pi x}{a}\right) + \left(\frac{\lambda_0}{\lambda_c}\right)^2 \cos^2\left(\frac{\pi x}{a}\right) \right] \end{aligned}$$

And the force-per-length is

$$\begin{aligned} \frac{dF_m}{d\ell} &= \int_0^a \frac{dF_m}{dA} dx \\ &= \frac{1}{32\pi} E_0^2 \left[\left(\frac{\lambda_0}{\lambda_g}\right)^2 + \left(\frac{\lambda_0}{\lambda_c}\right)^2 \right] a = \frac{1}{32\pi} E_0^2 a \end{aligned}$$

with the final simplification coming from Eq. (7.29). Since the **B**-field at the walls is *tangential*, the force is *outward*.

(c) The aggregate electric and magnetic forces on the broad walls are *equal and opposite*, so the net force is *zero*. Note, however, that the attractive electric and repulsive magnetic forces-per-area do not cancel point-by-point.

(d) For the side walls at $x=0$ and a , the **E**-field goes to zero, and there is only an outward magnetic force:

$$\frac{dF_m}{dA} = \frac{1}{8\pi} \langle [B_z(x,y,z,t)]^2 \rangle_{x=0,a} = \frac{1}{16\pi} \left(\frac{\lambda_0}{\lambda_c}\right)^2 E_0^2 \quad (1)$$

$$\frac{dF_m}{d\ell} = \int_0^b \frac{dF_m}{dA} dy = \frac{1}{16\pi} \left(\frac{\lambda_0}{\lambda_c}\right)^2 E_0^2 b$$

(e) Section 7.2 showed that the boundary conditions at confining conducting planes are met by the superposition of a pair of plane waves, each of which is traveling diagonally and reflecting back-and-forth between the two walls. In fact, the example treated in that section is precisely the TE₁₀ mode in rectangular waveguide, with the plane waves bouncing off what we are calling the "side" walls of the waveguide. (Because the dimension b does not enter the field formulas nor the cutoff-wavelength formula, this mode is compatible with $b \rightarrow \infty$.) For the TE₁₀ mode, the waves do not reflect off the "top" and "bottom" walls. Thus it is physically reasonable that there should be an outward force on the side walls, but no net force on the top and bottom.

This argument can be quantified by application of Prob. 5-9(a), which showed that the radiation pressure normal to a reflecting surface from a plane wave incident at angle θ is given by $p = (2\langle S \rangle / c) \cos^2 \theta$, with the factor of 2 coming from the superposition of the incident and reflected waves at each point of the surface. If we regard the TE₁₀ waveguide case as the superposition of two plane waves, each with amplitude $E_0/2$ and incident at the angle θ_0 (Fig. 7-4), the radiation pressure on a reflecting wall is then

$$p = \frac{2}{c} \frac{c(E_0/2)^2}{8\pi} \cos^2 \theta_0 = \frac{1}{16\pi} \left[1 - \left(\frac{\lambda_0}{\lambda_g}\right)^2 \right] E_0^2 = \frac{1}{16\pi} \left(\frac{\lambda_0}{\lambda_c}\right)^2 E_0^2 \quad (2)$$

where we have used Eqs. (7.28–29). The radiation pressure (2) agrees with the Maxwell stress (1).

7-12. As shown in Eqs. (7.52–55) and Sec. 7.4, TM waves are determined by the function $E_z^0(x,y)$. The solution that satisfies the boundary condition, Eq. (7.68), is

$$E_z^0(x,y) = E^0 \sin\left(\frac{m\pi x}{a}\right) \sin\left(\frac{n\pi y}{b}\right)$$

Equations (7.52–55) then give:

$$E_x^0 = \frac{i}{k_c^2} k_g \frac{\partial E_z^0}{\partial x} = i \frac{k_g}{k_c^2} \frac{m\pi}{a} E^0 \cos\left(\frac{m\pi x}{a}\right) \sin\left(\frac{n\pi y}{b}\right)$$

$$E_y^0 = \frac{i}{k_c^2} k_g \frac{\partial E_z^0}{\partial y} = i \frac{k_g}{k_c^2} \frac{n\pi}{b} E^0 \sin\left(\frac{m\pi x}{a}\right) \cos\left(\frac{n\pi y}{b}\right)$$

$$B_x^0 = -\frac{i}{k_c^2} k_0 \frac{\partial E_z^0}{\partial y} = -\frac{k_0}{k_g} E_y^0$$

$$B_y^0 = \frac{i}{k_c^2} k_0 \frac{\partial E_z^0}{\partial x} = \frac{k_0}{k_g} E_x^0$$

The cutoff frequency follows from Eq. (7.64) by the same argument leading to Eq. (7.73), with the same result,

$$\omega_{mn} = ck_c = \pi c \sqrt{\frac{m^2}{a^2} + \frac{n^2}{b^2}}$$

The integral indices m, n must both be greater than zero, or E_z^0 vanishes; thus the lowest mode is TM_{11} . The ratio of cutoff frequencies is

$$\frac{\omega_c(TM_{11})}{\omega_c(TE_{10})} = \frac{\left(\frac{1}{a^2} + \frac{1}{b^2}\right)^{1/2}}{\frac{1}{a}} = \sqrt{1 + \left(\frac{a}{b}\right)^2}$$

The lowest TE mode assumed $a > b$; thus the lowest TM-mode cutoff is at least a factor of $\sqrt{2}$ higher. More typically, $a/b \approx 2$, and the ratio is about $\sqrt{5}$.

7-13. For cylindrical coordinates appropriate for a circular cross section, using Eq. (A.47), Eq. (7.63) becomes

$$\left(\frac{\partial^2}{\partial r^2} + \frac{1}{r} \frac{\partial}{\partial r} + \frac{1}{r^2} \frac{\partial^2}{\partial \theta^2} + k_c^2\right) B_z^0(r, \theta) = 0$$

This Helmholtz equation is similar to Laplace's equation in cylindrical coordinates. From Sec. 3.5 we have the solutions, regular at the origin and periodic in θ ,

$$B_z^0(r, \theta) = B_m^0 J_m(k_c r) \cos m\theta \quad (1)$$

The boundary condition, Eq. (7.67), is

$$\left. \frac{\partial B_z^0}{\partial n} \right|_S = \left. \frac{\partial B_z^0}{\partial r} \right|_S = 0$$

which becomes, for a waveguide of radius a ,

$$\left[\frac{d}{dr} J_m(k_c r) \right]_{r=a} = 0$$

The n th nonzero root of $dJ_m(u)/du$ can be designated u_{mn} ; that is, $k_c a = u_{mn}$. Consequently the cutoff parameters are [compare Eq. (7.74)]:

$$k_c = \frac{u_{mn}}{a} \quad \lambda_c = \frac{2\pi a}{u_{mn}} \quad \omega_c = 2\pi\nu_c = \frac{c}{a} u_{mn}$$

[The boundary condition for TM modes in circular waveguide requires $k_c a = v_{mn}$ where v_{mn} is the n th root of $J_m(v) = 0$.] From tables such as (Ab65, pp. 409, 411), we find that the lowest root is

$$u_{11} = 1.841 \quad \Rightarrow \quad \omega_{11} = 1.841 \frac{c}{a}$$

To find the other field components, we must rewrite Eqs. (7.46–51) in cylindrical geometry, using Eq. (A.46):

$$\frac{1}{r} \frac{\partial E_z^0}{\partial \theta} - i k_g E_\theta^0 = i k_0 B_r^0 \quad (2)$$

$$i k_g E_r^0 - \frac{\partial E_z^0}{\partial r} = i k_0 B_\theta^0 \quad (3)$$

$$\frac{1}{r} \frac{\partial}{\partial r}(r E_\theta^0) - \frac{1}{r} \frac{\partial E_r^0}{\partial \theta} = i k_0 B_z^0 \quad (4)$$

$$\frac{1}{r} \frac{\partial B_z^0}{\partial \theta} - i k_g B_\theta^0 = -i k_0 E_r^0 \quad (5)$$

$$i k_g B_r^0 - \frac{\partial B_z^0}{\partial r} = -i k_0 E_\theta^0 \quad (6)$$

$$\frac{1}{r} \frac{\partial}{\partial r}(r B_\theta^0) - \frac{1}{r} \frac{\partial B_r^0}{\partial \theta} = -i k_0 E_z^0 \quad (7)$$

From (3) and (5), using $k_c^2 = k_0^2 - k_g^2$ from Eq. (7.38), we obtain:

$$E_r^0 = \frac{i}{k_c^2} \left(k_g \frac{\partial E_z^0}{\partial r} + k_0 \frac{1}{r} \frac{\partial B_z^0}{\partial \theta} \right)$$

$$B_\theta^0 = \frac{i}{k_c^2} \left(k_0 \frac{\partial E_z^0}{\partial r} + k_g \frac{1}{r} \frac{\partial B_z^0}{\partial \theta} \right)$$

And from (2) and (6),

$$E_\theta^0 = \frac{i}{k_c^2} \left(k_g \frac{1}{r} \frac{\partial E_z^0}{\partial \theta} - k_0 \frac{\partial B_z^0}{\partial r} \right)$$

$$B_r^0 = \frac{i}{k_c^2} \left(-k_0 \frac{1}{r} \frac{\partial E_z^0}{\partial \theta} + k_g \frac{\partial B_z^0}{\partial r} \right)$$

Now, for the TE₁₁ mode, $E_z^0 = 0$, and B_z^0 is given by (1). Thus:

$$E_r^0 = -\frac{ik_0}{k_c^2 r} B_z^0 J_1(k_c r) \sin\theta$$

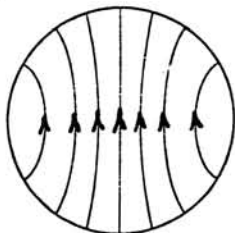
$$E_\theta^0 = -\frac{ik_0}{k_c} B_z^0 J_1'(k_c r) \cos\theta$$

$$B_r^0 = \frac{ik_c}{k_c} B_z^0 J_1'(k_c r) \cos\theta$$

$$B_\theta^0 = -\frac{ik_0}{k_c^2 r} B_z^0 J_1(k_c r) \sin\theta$$

where $J_1'(u) = dJ_1(u)/du = J_0 - J_1/r$. The J_1 function, up to its first maximum, is qualitatively similar to the sine function between zero and $\pi/2$, while J_1' is similar to the cosine. Since E_r varies as $J_1(k_c r)/r$, it is a (finite) maximum at $r = 0$, and then decreases somewhat as $r \rightarrow a$. Meanwhile, E_θ is also a maximum at $r = 0$, but goes fully to zero as $r \rightarrow a$. Representative E-field lines are shown in the sketch. As in the rectangular TE₁₀ mode (Fig. 7-6), the field magnitude is greatest at the central plane, tapering to zero at the sides. The field-lines are no longer straight, but bend to meet the wall perpendicularly. The magnetic field-lines are in loops similar to those of the rectangular mode (see Fig. 7-6 again).

E-field of TE₁₁



7-14. A resonant cavity requires constructive interference of waves reflected back and forth between the ends. Thus the round-trip $2L$ must be an integral number ℓ of guide wavelengths,

$$2L = \ell \lambda_g = \frac{2\pi\ell}{k_g}$$

From Eq. (7.30) or (7.38), the waveguide dispersion relation is

$$k_0^2 = k_c^2 + k_g^2$$

$$\left(\frac{\omega_{mn}\ell}{c}\right)^2 = (k_c)_{mn}^2 + \left(\frac{\pi\ell}{L}\right)^2 \quad (1)$$

In rectangular waveguide, the cutoff wavenumber for the m th mode (either TE or TM) is given by Eq. (7.72),

$$(k_c)_{mn}^2 = \pi^2 \left(\frac{m^2}{a^2} + \frac{n^2}{b^2} \right) \quad (2)$$

In circular waveguide, from the Solution for Prob. 7-13, the cutoff wavenumber is

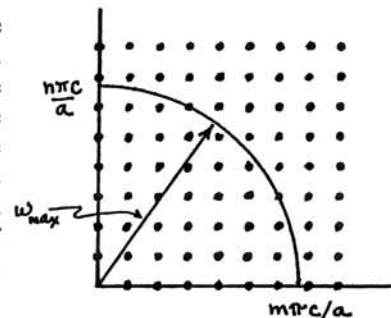
$$(k_c)_{mn}^2 = \left(\frac{u_{mn}}{a} \right)^2 \quad (3)$$

where u_{mn} is the n th root of $dJ_m(u)/du = 0$ for TE modes, or of $J_m(u) = 0$ for TM modes. For the lowest mode (TE₁₁), $u_{mn} \rightarrow 1.841$. Substitution of (2) or (3) in (1) gives the required formula for the resonant frequencies.

7-15. (a) The cutoff frequencies are given by Eq. (7.73),

$$\omega_{mn}^2 = \pi^2 c^2 \left(\frac{m^2}{a^2} + \frac{n^2}{b^2} \right)$$

Construct a graph plotting $(m\pi c/a)$ on the horizontal axis and $(n\pi c/b)$ on the vertical axis. For each pair of integers m, n , place a dot on the graph representing a possible TE and TM mode (the dots on the axes are only TE modes, since the TM boundary conditions require that both m and n be nonzero). The mode-dots form a rectangular grid on the graph, and the length of the radius vector to a particular dot equals the cutoff frequency ω_{mn} of that pair of modes.



The modes whose cutoff frequencies are less than ω_{\max} lie inside the quarter-circle of area $\pi\omega_{\max}^2/4$. The cell-size of the grid of dots is $(\pi c/a) \times (\pi c/b)$. Therefore, if we neglect the "statistical noise" introduced by the discreteness of the cells, we can estimate the number of modes with $\omega_c < \omega_{\max}$ as

$$N \approx 2 \frac{\pi\omega_{\max}^2/4}{\pi^2 c^2 / ab} = \frac{ab}{2\pi c^2} \omega_{\max}^2$$

(b) For the rectangular cavity, we generalize the argument to three dimensions using the resonant-frequency formula of Prob. 7-14, which says that we plot $(\ell\pi c/L)$ on the third axis. Now the number of modes up to some frequency ω is approximately

$$N \approx 2 \frac{\frac{4}{3}\pi\omega^3}{8 \left(\frac{\pi c}{a}\right)\left(\frac{\pi c}{b}\right)\left(\frac{\pi c}{L}\right)} = \frac{abL}{3\pi^2 c^3} \omega^3$$

and the density of modes (number of modes between ω and $\omega+d\omega$) is

$$\frac{dN}{d\omega} = \frac{abL}{\pi^2 c^3} \omega^2$$

This analysis is often used in statistical mechanics to estimate the number of states available to a system up to some maximum energy, or analogous constraint.

(c) If each mode in the volume $V = abL$ has the energy kT , then the electromagnetic energy per-volume, per-frequency-interval $d\nu = d\omega/2\pi$, in the cavity is

$$\frac{d\mathcal{E}}{d\nu} = \frac{(kT)(2\pi)}{(V)} \frac{dN}{d\omega} = \frac{8\pi k T}{c^3} \nu^2$$

The equivalent energy density, per-wavelength-interval $d\lambda = (c/\nu^2)d\nu$, is

$$\frac{d\mathcal{E}}{d\lambda} = \frac{8\pi k T}{\lambda^4}$$

[Historical note: Sir James Jeans' contribution to the *Rayleigh-Jeans formula* for the classical limit of blackbody radiation was to note that Lord Rayleigh forgot to divide by 8 in computing the volume of the *octant* of a sphere! The Rayleigh-Jeans spectrum shows the famous "ultraviolet catastrophe"; this failure of classical physics led to Planck's introduction of the *quantization* of electromagnetic radiation.]

7-16. When \mathbf{a} is a vector of *fixed* direction and magnitude, it commutes with derivative operators with respect to both space and time. Thus, if the scalar function $\psi(\mathbf{r}, t)$ is a solution of the wave equation,

$$\nabla^2 \psi - \frac{1}{c^2} \frac{\partial^2 \psi}{\partial t^2} = 0$$

then so is the vector function $(\mathbf{a}\psi)$. The divergence of $(\mathbf{a}\psi)$ will not be zero, in general. However, the curl is a linear operator that also commutes with ∇^2 and $\partial^2/\partial t^2$. It follows then that the vector function $\mathbf{curl}(\mathbf{a}\psi)$ not only is a solution of the wave equation, but also has vanishing divergence because of the identity (A.42). Such a function is an acceptable electric or magnetic field obeying Eqs. (5.1–6). This argument can be extended to the field $\mathbf{curl} \mathbf{curl}(\mathbf{a}\psi)$, which represents a different divergenceless wave field.

For sinusoidal time dependence given by $e^{-i\omega t}$, the wave equation reduces to the Helmholtz equation,

$$\nabla^2 \psi = -\frac{\omega^2}{c^2} \psi = -k^2 \psi$$

Now consider a possible field $\mathbf{E}_1(\mathbf{r}) \equiv \mathbf{curl}[\mathbf{a}\psi(\mathbf{r})]$ (omitting the time factor $e^{-i\omega t}$ on both sides for convenience). Another possible field is $\mathbf{E}_2(\mathbf{r}) \equiv \mathbf{curl} \mathbf{E}_1 = \mathbf{curl} \mathbf{curl}[\mathbf{a}\psi(\mathbf{r})]$. By the double-curl expansion identity [Eq. (A.40)],

$$\mathbf{E}_2 = \mathbf{grad} \operatorname{div}(\mathbf{a}\psi) - \nabla^2(\mathbf{a}\psi) = \mathbf{grad} \operatorname{div}(\mathbf{a}\psi) + k^2(\mathbf{a}\psi)$$

which in general is an independent function (i.e., not an algebraic multiple of \mathbf{E}_1). However, because the curl of a gradient vanishes [Eq. (A.41)], yet another curl operation gives

$$\mathbf{E}_3 \equiv \mathbf{curl} \mathbf{E}_2 = \mathbf{curl} \mathbf{curl} \mathbf{E}_1 = 0 + k^2 \mathbf{E}_1$$

Similarly, $\mathbf{E}_4 = k^2 \mathbf{E}_2$, etc. Thus, while the single- and double-curl operations on $[\mathbf{a}\psi(\mathbf{r})]$ give the independent fields \mathbf{E}_1 and \mathbf{E}_2 , higher-order multiple curls are redundant in the sense that they simply reproduce \mathbf{E}_1 or \mathbf{E}_2 multiplied by the constant scale-factor k^2 . (In this context, the scalar wavefunction ψ is sometimes called a *Debye potential*.)

7-17. Equation (7.102) defines the parameter V in terms of the refractive properties of the cladded fiber (n_1 and Δ), the fiber radius (a), and the operating wavelength (λ_0). For $V \rightarrow V_{\max} = 2.405$ for single-mode propagation, Eq. (7.105) calculates the maximum fiber diameter as $2a = 4.69 \mu\text{m}$. We now need to solve the dispersion relation, Eq. (7.99), rewritten in the form:

$$\frac{X J_1(X)}{J_0(X)} = \frac{\sqrt{V^2 - X^2} K_1(\sqrt{V^2 - X^2})}{K_0(\sqrt{V^2 - X^2})}$$

That is, we have used Eqs. (7.100–101) to cast each side as a function of X in the spirit of Fig. 7-8. We can now use the approximations (7.103–104) in an iterative program to find the root X that satisfies this equation:

```
REM Iterative program to find root of Eq.(7.99)
DEF J(X)      ! = X*J1/J0
      LET N1 = X + 0.82*(X^2)*SIN(2*X) - 1.83*X^3 + 3.26*X^4
      LET J = X * TAN(N1/(2 + 0.74*X^2 + 3.26*X^3))
END DEF
DEF K(Y)      ! = Y*K1/K0
      LET N2 = 1 - 1.743*Y^2 + 6.56*Y^3 + 13.12*Y^4
      LET K = N2/(LOG(1.135/Y) + 13.12*Y^3)
END DEF
```

```

INPUT PROMPT "For V = ": V
DO
  INPUT PROMPT "Try X = ": X
  LET Y=SQR(V^2-X^2)
  PRINT (J(X) - K(Y)), Y
LOOP
END

```

Visual inspection of Fig. 7-8 suggests that the root is near $X \approx 1.7$. A few iterations finds:

for $V = 2.405$: $X \approx 1.653$ $Y \approx 1.747$ $[J(X)-K(Y) \approx -0.0004]$

These approximation formulas typically leave an error of ~ 0.01 in the X root. For higher precision, one can use sophisticated software, such as Mathematica:

```

In:=
y[x_] := Sqrt[2.405^2 - x^2]
FindRoot[ x*BesselJ[1,x]/BesselJ[0,x] ==
  y[x]*BesselK[1,y[x]]/BesselK[0,y[x]],
  {x, {1.6, 1.8}} ]
Out=
{x -> 1.64657}

```

For the weakly guided LP_{01} mode, the electric field in the cladding is mainly that of Eq. (7.88) with $J_0 \rightarrow K_0$ and $k_c \rightarrow \gamma = Y/a$. The K_0 function is roughly the decaying exponential $e^{-\gamma r}$ [see (Ab65), Fig. 9.7 and §9.7.2]. Thus a rough estimate of the penetration of the guided wave into the cladding is given by $1/\gamma = a/Y$. In this case, $(4.69/2)/1.747 = 1.342 \mu\text{m}$.

With the arbitrarily chosen lower-frequency-limit corresponding to twice the wavelength at which the LP_{11} mode cuts in, $\lambda_0 \rightarrow 2\lambda_0$, and $V \rightarrow V_{\text{max}}/2 = 1.2024$. The approximation formulas give:

for $V = 1.2024$: $X \approx 1.134$ $Y \approx 0.400$ $[J(X)-K(Y) = 0.0006]$

(Mathematica gives $X = 1.13581$.) Now, $1/\gamma = a/Y = (4.69/2)/0.400 = 5.86 \mu\text{m}$.

From Fig. 7-4 and Eq. (7.26), the angle made by the multiply reflected "ray" with respect to the waveguide-fiber axis is the complement of θ_0 . That is, it is given by the inverse-sine of $k_c/k_0 = (X/a)/(2\pi/\lambda_0) = \lambda_0 X/2\pi a$. Numerically,

$$\text{at } \lambda_0 = 2.6 \mu\text{m}: \quad \sin^{-1} \left[\frac{(2.6)(1.134)}{2\pi(4.69/2)} \right] = 11.5^\circ$$

$$\text{at } \lambda_0 = 1.3 \mu\text{m}: \quad \sin^{-1} \left[\frac{(1.3)(1.65)}{2\pi(4.69/2)} \right] = 8.4^\circ$$

The curves in Fig. 7-9 were generated from Eq. (7.88), the corresponding K_0 version, and the linkage provided by Eq. (7.98), using numerical approximations for the J_0 and K_0 functions:

```

DEF J0(X)          ! maximum error ±0.00005
  IF X<=3.47 THEN
    LET J0=(1-0.208827*X^2+0.00621*X^4)
      / (1+0.04103*X^2+0.000967*X^4)
  ELSE
    LET A=X-PI/4-1/(8*X)+0.06/X^3
    LET J0=SQR(2/(PI*X))*(1-1/(16*X^2)+0.08/X^4)*COS(A)
  END IF
END DEF

DEF K0(X)          ! maximum error ±0.00012
  IF X<=0.605 THEN
    LET K0=LOG(1.123/X)*(1+0.2367*X^2)+0.27*X^2
  ELSE
    LET K0=SQR(PI/(2*X))*EXP(-X)
      * (1+0.21432/X)/(1+0.32987/X)
  END IF
END DEF

```

Chapter 8

8-1. The electric flux through a stationary spherical surface of radius R , centered on the instantaneous present position of a fast charge, is

$$\begin{aligned}\Phi_e &= \oint \mathbf{E} \cdot \mathbf{n} \, da = \int_0^\pi \frac{e(1-\beta^2)}{R^2(1-\beta^2\sin^2\theta)^{3/2}} 2\pi R^2 \sin\theta \, d\theta \\ &= \frac{2\pi e(1-\beta^2)}{\beta} \int_{-\beta}^{+\beta} \frac{d\mu}{[(1-\beta^2)+\mu^2]^{3/2}} \\ &= \frac{2\pi e(1-\beta^2)}{\beta} \left\{ \left(\frac{1}{1-\beta^2} \right) \frac{\mu}{[(1-\beta^2)+\mu^2]^{1/2}} \right\}_{-\beta}^{+\beta} = 4\pi e\end{aligned}$$

We have used integral tables (such as Dwight §200.03) or the substitution $\mu^2/(a^2+\mu^2) \rightarrow v^2$. The dependence on β cancels out identically. Note that the field is evaluated at the flux surface at *one* instant of time, i.e., simultaneously in the frame of the stationary flux surface.

8-2. For $\beta = u/c \ll 1$, Eq. (8.64) reduces to

$$\mathbf{B} = e \left[\frac{\boldsymbol{\beta} \times \mathbf{R}}{R^3} + \frac{(\mathbf{a} \cdot \mathbf{R})(\boldsymbol{\beta} \times \mathbf{R})}{c^2 R^3} + \frac{\mathbf{a} \times \mathbf{R}}{c^2 R^2} \right]$$

where $KR = R - \boldsymbol{\beta} \cdot \mathbf{R} \rightarrow R$. The first term is simply

$$\mathbf{B}_1 = \frac{e \mathbf{u} \times \mathbf{R}}{cR^3} \quad (1)$$

Now compare the magnitudes of the second and third terms,

$$\frac{B_2}{B_3} \sim \frac{(a\beta/c^2R)}{(a/c^2R)} = \beta$$

Thus, when $u \ll c$, the third term dominates the second. Similarly, compare the magnitude of the third term to the first,

$$\frac{B_3}{B_1} \sim \frac{(a/c^2R)}{(\beta/R^2)} \sim \frac{aR}{\beta c^2}$$

Therefore, the first term (1) dominates the third (and *a fortiori* the second) for small accelerations such that $a \ll uc/R$. [In ignoring the trig functions hidden in the dot and cross products, we have lost the exceptional case of locations where \mathbf{R} happens to lie along the line parallel to $\boldsymbol{\beta}$: then \mathbf{B}_1 and \mathbf{B}_2 vanish and only \mathbf{B}_3 remains. But even then, for small a , \mathbf{B}_3 (anywhere) can be neglected compared to \mathbf{B}_1 at locations that are not close to this line.]

Now, the specifications of the moving charge are equivalent to [see Eq. (1.49)]

$$e \mathbf{u} \rightarrow e \frac{d\ell}{dt} \rightarrow \frac{dq}{dt} d\ell \rightarrow I d\ell \quad (2)$$

Making the substitution of (2) into (1) gives the integrand of the basic Biot-Savart law, Eq. (1.36). The unretarded integration over the elements $d\ell$ in Eq. (1.36) requires that the transit time, L/c , of electromagnetic effects across the linear dimension L of the circuit be small compared to the period, $1/\omega$, of time variations of the current $I(t)$ —that is, $I(t)$ must be slowly varying such that $\omega \ll c/L$. When retardation is significant, Eq. (1.36) fails and Eq. (8.30) is needed. See also Prob. 4-11.

8-3. With the equivalences $e \mathbf{u} \rightarrow (\rho_\ell d\ell) \mathbf{u} \rightarrow I d\ell$ [Eq. (1.49)], Eq. (8.79) becomes

$$\mathbf{B} = \int \frac{I d\ell \times \mathbf{R} (1-\beta^2)}{cR^3(1-\beta^2\sin^2\theta)^{3/2}}$$

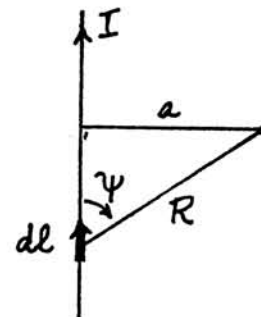
with

$$R = \frac{a}{\sin\psi}, \quad d\ell = \frac{a}{\sin^2\psi} d\psi$$

Thus,

$$\begin{aligned}\mathbf{B} \rightarrow B_\theta &= (1-\beta^2) \frac{I}{c} \int \left(\frac{\sin\psi}{a} \right)^2 \frac{\sin\psi}{(1-\beta^2\sin^2\theta)^{3/2}} \left(\frac{a d\psi}{\sin^2\psi} \right) \\ &= (1-\beta^2) \frac{I}{ca} \int_0^\pi \frac{\sin\psi}{(1-\beta^2\sin^2\theta)^{3/2}} d\psi \\ &= \left(\frac{1-\beta^2}{\beta} \right) \frac{I}{ca} \left[\frac{\mu}{(1-\beta^2)(1-\beta^2+\mu^2)^{1/2}} \right]_{-\beta}^{+\beta} = \frac{2I}{ca}\end{aligned}$$

Here, the substitution $\mu = \beta \sin\psi$ leads to the same integral as in Prob. 8-1. And again the dependence on β cancels out identically.



8-4. The nontrivial time derivatives are tabulated in Eqs. (8.56–61), with $\partial_t/\partial t = 1/K$ from Eq. (8.62). With $\mathbf{n} \equiv \mathbf{R}/R$, Eq. (8.54) expands as follows:

$$\begin{aligned} \frac{\mathbf{E}}{e} &= \left[\frac{\mathbf{n}}{KR^2} \right] + \frac{1}{c} \frac{\partial}{\partial t} \left[\frac{\mathbf{n} - \boldsymbol{\beta}}{KR} \right] \\ &= \frac{\mathbf{n}}{KR^2} + \frac{1}{cKR} \frac{\partial \mathbf{n}}{\partial t} - \frac{1}{cKR} \frac{\partial \boldsymbol{\beta}}{\partial t} - (\mathbf{n} - \boldsymbol{\beta}) \frac{1}{c(KR)^2} \frac{\partial(KR)}{\partial t} \\ &= \frac{1}{K(KR)^2} \left\{ (1 - \boldsymbol{\beta} \cdot \mathbf{n})^2 \mathbf{n} + (1 - \boldsymbol{\beta} \cdot \mathbf{n})(\boldsymbol{\beta} \cdot \mathbf{n} \mathbf{n} - \boldsymbol{\beta}) \right. \\ &\quad \left. - (1 - \boldsymbol{\beta} \cdot \mathbf{n}) \left(\frac{R\mathbf{a}}{c^2} \right) - (\mathbf{n} - \boldsymbol{\beta}) \left(-\boldsymbol{\beta} \cdot \mathbf{n} + \beta^2 - \frac{\mathbf{R} \cdot \mathbf{a}}{c^2} \right) \right\} \\ &= \mathbf{n} \left(1 - 2\boldsymbol{\beta} \cdot \mathbf{n} + (\boldsymbol{\beta} \cdot \mathbf{n})^2 + \boldsymbol{\beta} \cdot \mathbf{n} - (\boldsymbol{\beta} \cdot \mathbf{n})^2 + \boldsymbol{\beta} \cdot \mathbf{n} - \beta^2 + \frac{\mathbf{R} \cdot \mathbf{a}}{c^2} \right) \\ &\quad + \boldsymbol{\beta} \left(-1 + \boldsymbol{\beta} \cdot \mathbf{n} - \boldsymbol{\beta} \cdot \mathbf{n} + \beta^2 - \frac{\mathbf{R} \cdot \mathbf{a}}{c^2} \right) + \mathbf{a} \left(-\frac{R}{c^2} + \frac{(\boldsymbol{\beta} \cdot \mathbf{n})R}{c^2} \right) \\ &= (\mathbf{n} - \boldsymbol{\beta})(1 - \beta^2) + (\mathbf{n} - \boldsymbol{\beta}) \left(\frac{\mathbf{R} \cdot \mathbf{a}}{c^2} \right) - (1 - \boldsymbol{\beta} \cdot \mathbf{n}) \left(\frac{R\mathbf{a}}{c^2} \right) \end{aligned}$$

With a little foresight, the latter two terms can be recognized as the *BAC–CAB* expansion of $\mathbf{R} \times ((\mathbf{n} - \boldsymbol{\beta}) \times \mathbf{a})/c^2$, in agreement with Eq. (8.63). We'll believe that the same kind of tedium would transform Eq. (8.55) to (8.64).

8-5. The Feynman formula contains a second-order time derivative while suppressing the explicit velocity-dependent factors $\boldsymbol{\beta} = \mathbf{u}/c$ and $K = 1 - \boldsymbol{\beta} \cdot \mathbf{n}$. The strategy is to rework Feynman's derivatives into a form with the factor KR in the denominator. Thus we make the formal expansion:

$$\begin{aligned} \frac{R}{c} \frac{\partial}{\partial t} \left(\frac{\mathbf{n}}{R^2} \right) &= \frac{R}{c} \frac{\partial}{\partial t} \left(\frac{\mathbf{n}}{KR} \cdot K \cdot \frac{1}{R} \right) \\ &= \frac{K}{c} \frac{\partial}{\partial t} \left(\frac{\mathbf{n}}{KR} \right) - \frac{\mathbf{n}}{cR^2} \frac{\partial R}{\partial t} + \frac{\mathbf{n}}{cKR} \frac{\partial K}{\partial t} \quad (1) \end{aligned}$$

Using Eq. (8.59),

$$\frac{1}{c^2} \frac{\partial^2 \mathbf{n}}{\partial t^2} = \frac{1}{c^2} \frac{\partial}{\partial t} \left(\frac{\partial \mathbf{n}}{\partial t} \right) = \frac{\partial}{\partial t} \left(\frac{1}{cKR} ((\boldsymbol{\beta} \cdot \mathbf{n})\mathbf{n} - \boldsymbol{\beta}) \right)$$

$$= \frac{\mathbf{n}}{cKR} \frac{\partial}{\partial t} (\boldsymbol{\beta} \cdot \mathbf{n}) + \frac{\boldsymbol{\beta} \cdot \mathbf{n}}{c} \frac{\partial}{\partial t} \left(\frac{\mathbf{n}}{KR} \right) - \frac{1}{c} \frac{\partial}{\partial t} \left(\frac{\boldsymbol{\beta}}{KR} \right) \quad (2)$$

Now, since $K = 1 - \boldsymbol{\beta} \cdot \mathbf{n}$, the third term of (1) cancels the first term of (2), and the second term of (2) cancels part of the first term of (1). The second term of (1) can be evaluated by Eq. (8.57). Thus the full Eq. (8.54a) becomes:

$$\begin{aligned} \frac{\mathbf{E}}{e} &= \frac{\mathbf{n}}{R^2} + \frac{1}{c} \frac{\partial}{\partial t} \left(\frac{\mathbf{n}}{KR} \right) - \frac{\mathbf{n}}{cR^2} c \left(1 - \frac{1}{K} \right) - \frac{1}{c} \frac{\partial}{\partial t} \left(\frac{\boldsymbol{\beta}}{KR} \right) \\ &= \frac{\mathbf{n}}{KR^2} + \frac{1}{c} \frac{\partial}{\partial t} \left(\frac{\mathbf{n}}{KR} \right) - \frac{1}{c} \frac{\partial}{\partial t} \left(\frac{\boldsymbol{\beta}}{KR} \right) \end{aligned}$$

which is Eq. (8.54). Feynman's formula is often written with the notation of a *total* time derivative, d/dt , which presumably is intended as a signal that the derivative is with respect to the time t observed at the (fixed) field point, rather than the retarded time t_r of the (moving) source charge. It is, nevertheless, a partial derivative in the sense that it is independent of the spatial coordinates \mathbf{r} at the field point [see, e.g., Eq. (8.56)].

8-6. For $\beta \ll 1$, the acceleration portion of Eqs. (8.63–64) reduce to:

$$\mathbf{E}_a = \frac{e}{c^2 R} \mathbf{n} \times (\mathbf{n} \times \mathbf{a})$$

$$\mathbf{B}_a = \mathbf{n} \times \mathbf{E}_a = \frac{e}{c^2 R} \mathbf{n} \times (\mathbf{n} \times (\mathbf{n} \times \mathbf{a}))$$

$$= \frac{e}{c^2 R} \left((\mathbf{n} \cdot (\mathbf{n} \times \mathbf{a}))\mathbf{n} - (\mathbf{n} \cdot \mathbf{n})(\mathbf{n} \times \mathbf{a}) \right) = -\frac{1}{c^2 R} (\mathbf{n} \times \mathbf{a})$$

The radiation Poynting vector is then

$$\begin{aligned} \mathbf{S} &= \frac{c}{4\pi} \mathbf{E}_a \times \mathbf{B}_a = -\frac{e^2}{4\pi c^3 R^2} \left((\mathbf{n} \times (\mathbf{n} \times \mathbf{a})) \times (\mathbf{n} \times \mathbf{a}) \right) \\ &= -\frac{e^2}{4\pi c^3 R^2} \left((\mathbf{n} \cdot (\mathbf{n} \times \mathbf{a}))(\mathbf{n} \times \mathbf{a}) - ((\mathbf{n} \times \mathbf{a}) \cdot (\mathbf{n} \times \mathbf{a}))\mathbf{n} \right) \\ &= +\frac{e^2}{4\pi c^3 R^2} |\mathbf{n} \times \mathbf{a}|^2 = \frac{e^2}{4\pi c^3 R^4} |\mathbf{R} \times \mathbf{a}|^2 \end{aligned}$$

That is, only the component of the acceleration that is perpendicular to a particular direction contributes to the radiation in that direction.

8-7. (a) The triangle OQP is geometrically similar to the diagram representing the vector addition $\mathbf{u}_1 + \mathbf{a}\tau = \mathbf{u}_2$. That is, the side QP has the magnitude $(a\tau)\Delta t$. The perpendicular separation of the radius QS from PR is then $a\tau\Delta t \sin\theta$, where θ is the angle between the acceleration \mathbf{a} and the direction of radiation being considered. Therefore the field-line kink between R and S has radial and transverse components in the ratio

$$\frac{E_r}{E_t} = \frac{c\tau}{a\tau\Delta t \sin\theta} = \frac{c}{a\Delta t \sin\theta}$$

(b) We use Coulomb's law to evaluate E_r , and substitute $\Delta t \rightarrow r/c$, to obtain the transverse or radiation electric field as

$$E_t = \frac{ar \sin\theta}{c^2} \frac{q}{r^2} = \frac{qa}{c^2 r} \sin\theta$$

(c) Inferring the associated radiation magnetic field, $\mathbf{B}_t = \mathbf{n} \times \mathbf{E}_t$, we obtain the Poynting vector,

$$\mathbf{S} = \frac{c}{4\pi} \mathbf{E}_t \times \mathbf{B}_t = \frac{c}{4\pi} E_t^2 \mathbf{n} = \frac{q^2 a^2}{4\pi c^3 r^2} \sin^2\theta \mathbf{n}$$

where \mathbf{n} is the outward unit vector parallel to QS . The power through an element of area dA is $P = S dA$, and this area subtends the solid angle $d\Omega = dA/r^2$. Therefore, the power per-solid-angle is

$$\frac{dP}{d\Omega} = r^2 S = \frac{q^2 a^2}{4\pi c^3} \sin^2\theta$$

which is Eq. (8.88). The result holds in general (so long as $u \ll c$) because the field amplitude formula is linear in qa , superposition holds, and an arbitrary acceleration can be modeled simply as a succession of impulses. For further discussion, see the references cited in the footnote following Eq. (8.89).

8-8. The angular dependence in Eq. (8.96) is

$$\frac{dP}{d\Omega} \propto \frac{\sin^2\theta}{(1 - \beta \cos\theta)^5}$$

The derivative with respect to θ goes to zero when

$$(1 - \beta \cos\theta)^5 (2 \sin\theta \cos\theta) = (\sin^2\theta) [5(1 - \beta \cos\theta)^4 (\beta \sin\theta)]$$

$$3\beta \cos^2\theta + 2 \cos\theta - 5\beta = 0$$

$$\cos\theta_{\max} = \frac{-1 + \sqrt{1 + 15\beta^2}}{3\beta}$$

(The other solution of the quadratic is spurious. For *small* β , the limit is $\cos\theta_{\max} \rightarrow \frac{\pi}{2} - \theta_{\max} \approx \frac{5}{2}\beta$.) Now for large β , approaching unity, let $\beta = 1 - \alpha$, where α is a small quantity. Then,

$$\cos\theta_{\max} = \frac{-1 + (16 - 30\alpha + 15\alpha^2)^{1/2}}{3(1 - \alpha)}$$

$$= \frac{-1 + 4 \left[1 - \frac{1}{2} \left(\frac{30\alpha - 15\alpha^2}{16} \right) - \dots \right]}{3(1 - \alpha)}$$

$$= \left(1 - \frac{5}{4}\alpha + \dots \right) (1 + \alpha + \dots) = 1 - \frac{1}{4}\alpha + \dots$$

The cosine expansion for small angles is $\cos\theta \rightarrow 1 - \frac{1}{2}\theta^2 + \dots$. Thus,

$$\theta_{\max}^2 \approx \frac{1}{2}\alpha \quad \Rightarrow \quad \theta_{\max} \approx \sqrt{\frac{1 - \beta}{2}}$$

A similar first-order expansion in terms of $\alpha' = 1 - \beta^2$ gives $\theta_{\max}^2 \approx \frac{1}{4}\alpha'^2$, and hence $\theta_{\max} \approx \frac{1}{2}\sqrt{1 - \beta^2}$. Since $(1 - \beta^2)$ is larger than $(1 - \beta)$, this latter is a poorer approximation. Jackson (Ja75, Eq. 14.40) quotes the inferior form, probably because it is more neatly expressed in terms of the relativistic parameter γ .

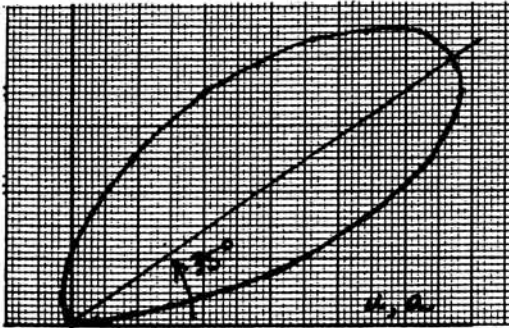
8-9. The angular distribution is given by Eq. (8.96),

$$\frac{dP}{d\Omega} = \frac{e^2 a^2}{4\pi c^3} \left[\frac{\sin^2\theta}{(1 - \beta \cos\theta)^5} \right] \quad (1)$$

From Eq. (14.42), the relation between velocity and kinetic energy is

$$\beta^2 = 1 - \frac{1}{(1 + T/m_e c^2)^2}$$

For $T = 100$ keV and $m_e c^2 = 511$ keV, we have $\beta = 0.548$. The function in square brackets in (1) is plotted below for this velocity (the plot is a figure of revolution about $\theta = 0$). From Prob. 8-8, the radiation is a maximum at $\theta = \cos^{-1} 0.819 = 35.0^\circ$. Note that the angular dependence involves the velocity but not the acceleration, while both parameters determine the magnitude of radiated power.



8-10. The total power is

$$P = \int \left(\frac{dP}{d\Omega} \right) d\Omega = \frac{e^2 a^2}{4\pi c^3} \int_0^\pi \frac{\sin^2 \theta}{(1 - \beta \cos \theta)^5} 2\pi \sin \theta d\theta$$

$$\stackrel{\mu = \cos \theta}{=} \frac{e^2 a^2}{2c^3} \int_{-1}^{+1} \frac{1 - \mu^2}{(1 - \beta \mu)^5} d\mu$$

From integral tables [e.g., Dwight, §90.5 and 92.5],

$$= \frac{e^2 a^2}{2c^3} \left\{ \frac{1}{4\beta(1-\beta\mu)^4} + \frac{1}{\beta^3} \left[-\frac{1}{2(1-\beta\mu)^2} + \frac{2}{3(1-\beta\mu)^3} - \frac{1}{4(1-\beta\mu)^4} \right] \right\}_{-1}^{+1}$$

$$= \frac{2e^2 a^2}{3c^3} \frac{1}{(1-\beta^2)^3}$$

This result for collinear acceleration can be compared with Eq. (8.107) for acceleration transverse to the velocity.

8-11. (a) For constant deceleration in a time τ , $u/c = \beta = \beta_0(1 - t/\tau)$, and the acceleration is $|a| \rightarrow a_0 = c\beta_0/\tau$. Using Eq. (8.97), the total energy radiated (per electron) is then

$$W = \int P(\beta) dt = \frac{2e^2 a_0^2}{3c^3} \int_0^{\beta_0} \frac{1}{(1-\beta^2)^3} \frac{\tau}{\beta_0} d\beta$$

$$= \frac{2e^2 \beta_0}{3c\tau} \left[\frac{\beta}{4(1-\beta^2)^2} + \frac{3\beta}{8(1-\beta^2)} + \frac{3}{16} \ln \left(\frac{1+\beta}{1-\beta} \right) \right]_0^{\beta_0}$$

$$= \frac{e^2 \beta_0}{12c\tau} \left[\frac{\beta_0(5-3\beta_0^2)}{(1-\beta_0^2)^2} + \frac{3}{2} \ln \left(\frac{1+\beta_0}{1-\beta_0} \right) \right] \quad (1)$$

(We have used integral tables, such as Dwight §140.3.)

(b) By integrating Eq. (8.96) over time, we get the average angular distribution (i.e., the distribution pattern produced by the beam):

$$\frac{dW}{d\Omega} = \int \left(\frac{dP}{d\Omega} \right) dt = \frac{e^2 \beta_0}{4\pi c\tau} \sin^2 \theta \int_0^{\beta_0} \frac{1}{(1 - \beta \cos \theta)^5} d\beta$$

$$= \frac{e^2 \beta_0}{4\pi c\tau} \sin^2 \theta \left[\frac{1}{4 \cos \theta (1 - \beta \cos \theta)^4} \right]_0^{\beta_0}$$

$$= \frac{e^2 \beta_0}{16\pi c\tau} \left\{ \frac{\sin^2 \theta}{\cos \theta} \left[\frac{1}{(1 - \beta_0 \cos \theta)^4} - 1 \right] \right\} \quad (2)$$

(c) For $T = 100$ keV, we have $\beta_0 = 0.548$ (Prob. 8-9). Thus,

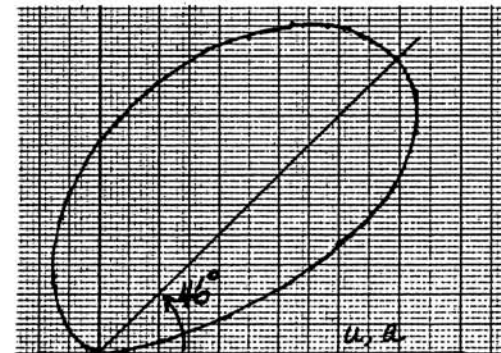
$$\frac{a_0}{g} = \frac{c\beta_0}{\tau g} = \frac{(3 \cdot 10^{10} \text{ cm/s})(0.548)}{(10^{-12} \text{ s})(980 \text{ cm/s}^2)} = 1.7 \times 10^{19}$$

The quantity in the square brackets of (1) has the value 6.43. Using $e^2[\text{Gaussian}] = 1.44 \times 10^{-7} \text{ eV}\cdot\text{cm}$ (Appendix C), the coefficient of (1) is

$$\frac{e^2 \beta_0}{12c\tau} = \frac{(1.44 \cdot 10^{-7} \text{ eV}\cdot\text{cm})(0.548)}{12(3 \cdot 10^{10} \text{ cm/s})(10^{-12} \text{ s})} = 2.2 \times 10^{-7} \text{ eV}$$

Thus the total energy per electron is about $1.4 \times 10^{-6} \text{ eV}$, an insignificant fraction of the incident energy (most of the electron's energy goes into ionizing the target atoms).

The angular function in the curly brackets of (2) is plotted below for $\beta_0 = 0.548$. The maximum is at $\theta \approx 46^\circ$. The contribution of lower-velocity radiation causes the angular distribution to be less sharply forward-peaked than that of Prob. 8-9.



8-12. If we neglect the radiation energy loss, then u is related to r along the trajectory by

$$\frac{1}{2}m u_0^2 = \frac{1}{2}m u^2 + \frac{Z e^2}{r}$$

As a perturbation, the energy lost to radiation is given by the nonrelativistic Larmor formula, Eq. (8.89), as

$$\Delta W = \int_0^\infty P(t) dt = \frac{2e^2}{3c^3} \int \frac{a^2}{u} dr$$

But,

$$a = -\frac{1}{m} \frac{dU}{dr} = \frac{Z e^2}{m r^2}$$

$$u = \mp \sqrt{u_0^2 - \frac{2Z e^2}{m r}}$$

Because of the reentrant path, we calculate the integral during the outbound segment from $r_{\min} = 2Ze^2/mu_0^2$ to $r \rightarrow \infty$, and double the result:

$$\Delta W = \frac{2e^2}{3c^3} \left(\frac{Ze^2}{m} \right)^2 \frac{2}{u_0} \int_{r_{\min}}^\infty \frac{dr}{r^4 \left(1 - \frac{r_{\min}}{r} \right)^{1/2}}$$

Let $x = 1/r$, and $dr = -dx/x^2$, to obtain the integral

$$\begin{aligned} \int_{r_{\min}}^\infty \frac{dr}{\dots} &= \int_0^{x_{\max}} \frac{x^2 dx}{\left(1 - \frac{x}{x_{\max}} \right)^{1/2}} = \left[-2x_{\max}^3 \left(\frac{X^{5/2}}{5} - \frac{2X^{3/2}}{3} + X^{1/2} \right) \right]_0^{x_{\max}} \\ &= \frac{16}{15} x_{\max}^3 = \frac{16}{15} \left(\frac{mu_0^2}{2Ze^2} \right)^3 \end{aligned}$$

(where $X = 1 - x/x_{\max}$, as in Dwight §191.21). Thus,

$$\Delta W = \frac{2e^2}{3c^3} \left(\frac{Ze^2}{m} \right)^2 \frac{2}{u_0} \frac{16}{15} \left(\frac{mu_0^2}{2Ze^2} \right)^3 = \frac{8mu_0^5}{45Zc^3} = \frac{16}{45} \frac{\beta_0^3}{Z} \left(\frac{1}{2}mu_0^2 \right)$$

Since by hypothesis $\beta_0 = u_0/c \ll 1$, the perturbation approach is justified.

8-13. The geometry is defined in Fig. 8-7, and the radiation pattern is given by Eq. (8.106). (a) For the orbital plane, the azimuthal angle φ is 0 or π , and θ measures the polar angle from \mathbf{u} . Inspection of Eq. (8.106) shows that the dependence on φ and θ is such that we can suppress the double-valued φ and interpret θ as an azimuthal angle in this plane (i.e., $0 \leq \theta \leq 2\pi$). Figure 8-9 plots the magnitude of $dP/d\Omega$ as a function of θ with \mathbf{u} (to the right) and \mathbf{a} (up or down). The pattern is symmetrical about the \mathbf{u} axis, and the numerator simplifies to

$$\begin{aligned} (1 - \beta \cos \theta)^2 - (1 - \beta^2) \sin^2 \theta \\ &= (1 - 2\beta \cos \theta + \beta^2 \cos^2 \theta) - (1 - \beta^2)(1 - \cos^2 \theta) \\ &= -2\beta \cos \theta + \beta^2 + \cos^2 \theta \\ &= (\cos \theta - \beta)^2 \end{aligned}$$

Thus in the orbital plane the angular dependence reduces to

$$\left(\frac{dP}{d\Omega} \right)_{u-a \text{ plane}} \propto \frac{(\cos \theta - \beta)^2}{(1 - \beta \cos \theta)^5} \quad (1)$$

The nulls occur when $\cos \theta = \beta$, and for the examples of Fig. 8-9:

$$\begin{aligned} \cos^{-1}(0.1) &= 84.26^\circ & \cos^{-1}(0.7) &= 45.57^\circ \\ \cos^{-1}(0.3) &= 72.54^\circ & \cos^{-1}(0.9) &= 25.84^\circ \\ \cos^{-1}(0.5) &= 60^\circ \end{aligned}$$

(b) The maximum value of (1) [and of the full Eq. (8.106)] occurs for $\theta = 0$, for which $(dP/d\Omega)_{\max} = 1/(1-\beta)^3$. Let α be the value of θ at which the intensity falls to one-half of maximum, so that the beamwidth as defined is $\Delta\theta \equiv 2\alpha$. Expand the cosine for small angles ($\cos \alpha \rightarrow 1 - \frac{1}{2}\alpha^2$) to write the half-power condition as:

$$\frac{(1 - \frac{1}{2}\alpha^2 - \beta)^2}{(1 - \beta + \frac{1}{2}\beta\alpha^2)^5} = \frac{1}{2(1 - \beta)^3}$$

Cross-multiplying and discarding terms beyond α^2 , we have

$$2(1 - \beta)^3 \left[(1 - \beta)^2 - 2(1 - \beta)(\frac{1}{2}\alpha^2) \right] \approx (1 - \beta)^5 + 5(1 - \beta)^4 (\frac{1}{2}\beta\alpha^2)$$

$$(1 - \beta)^5 \approx (1 - \beta)^4 (2\alpha^2 + \frac{5}{2}\beta\alpha^2)$$

$$(\Delta\theta)_{u-a \text{ plane}} = 2\alpha \approx 2 \sqrt{\frac{1 - \beta}{2 + \frac{5}{2}\beta}}$$

$$\rightarrow \frac{2\sqrt{2}}{3} \sqrt{1 - \beta} = 0.943 \sqrt{1 - \beta}$$

In the plane containing \mathbf{u} and the normal to the orbit, we have $\varphi = \frac{\pi}{2}$ or $\frac{3\pi}{2}$. Again we can suppress the double-value of φ and treat θ as an azimuthal angle. Equation (8.106) reduces to

$$\left(\frac{dP}{d\Omega}\right)_{\text{normal}} \propto \frac{1}{(1 - \beta \cos \theta)^3} \quad (2)$$

In this case it is easy to write the half-power condition without approximation,

$$\frac{1}{(1 - \beta \cos \alpha)^3} = \frac{1}{2(1 - \beta)^3}$$

$$\cos \alpha = \frac{1 - 2^{1/3}(1 - \beta)}{\beta} = 1 - \frac{(2^{1/3} - 1)(1 - \beta)}{\beta}$$

For small angles (such that $\cos \alpha \rightarrow 1 - \frac{1}{2}\alpha^2$), we have for the beamwidth normal to the orbital plane

$$(\Delta \theta)_{\text{normal}} = 2\alpha \approx 2 \sqrt{\frac{2(2^{1/3} - 1)(1 - \beta)}{\beta}}$$

$$\rightarrow \sqrt{8(2^{1/3} - 1)} \sqrt{1 - \beta} = 1.442 \sqrt{1 - \beta}$$

For instance, for $\beta = 0.9$ (for which the small-angle limits are not very precise), we have

$$(\Delta \theta)_{u-a \text{ plane}} \approx 17^\circ \quad (\Delta \theta)_{\text{normal}} \approx 28^\circ$$

Thus as $\beta \rightarrow 1$ the radiation pattern forms a "headlight beam" in the direction of \mathbf{u} , but the beam is somewhat narrower in the orbital plane than normal to it. The effect is sketched in Fig. 8-8 (which is drawn for $\beta = 0.9$).

8-14. From Eq. (8.106),

$$P = \int \left(\frac{dP}{d\Omega}\right) d\Omega$$

$$= \frac{e^2 a^2}{4\pi c^3} \int_{\theta=0}^{\pi} \int_{\varphi=0}^{2\pi} \left[\frac{1}{(1 - \beta \cos \theta)^3} - \frac{(1 - \beta^2) \sin^2 \theta \cos^2 \varphi}{(1 - \beta \cos \theta)^5} \right] \sin \theta d\theta d\varphi$$

Carrying out the straightforward φ integration, and substituting $x = \cos \theta$, we have

$$P = \frac{e^2 a^2}{2c^3} \int_{-1}^{+1} \left[\frac{1}{(1 - \beta x)^3} - \left(\frac{1 - \beta^2}{2}\right) \frac{1 - x^2}{(1 - \beta x)^5} \right] dx$$

$$= \frac{e^2 a^2}{2c^3} \left\{ \frac{1}{2\beta X^2} - \left(\frac{1 - \beta^2}{2}\right) \left[\frac{1}{4\beta X^4} + \frac{1}{\beta^3} \left(-\frac{1}{2X^2} + \frac{2}{3X^3} - \frac{1}{4X^4}\right) \right] \right\}_{-1}^{+1}$$

where $X = 1 - \beta x$, and we have used tables such as Dwight §90.3/5 and 92.5. Now note that

$$\left[\frac{1}{X^n}\right]_{-1}^{+1} = \frac{(1 + \beta)^n - (1 - \beta)^n}{(1 - \beta^2)^n}$$

After laborious but straightforward manipulation, the quantity in curly brackets simplifies to:

$$\{ \dots \} = \frac{4}{3(1 - \beta^2)^2}$$

and the result agrees with Eq. (8.107).

8-15. With $a = \omega^2 \rho$, the energy radiated per revolution is

$$\Delta W = P \frac{2\pi}{\omega} = \frac{4\pi e^2 \omega^3 \rho^2}{3c^3} \frac{1}{(1 - \beta^2)^2}$$

Now $\omega = \beta c / \rho$, and the relativistic kinetic energy is $T = mc^2[(1 - \beta^2)^{-1/2} - 1]$ (as in Prob. 8-9). Thus,

$$\Delta W = \frac{4\pi e^2}{3} \frac{\beta^3}{\rho} \left(1 + \frac{T}{mc^2}\right)^4$$

In the highly relativistic domain, $\beta \rightarrow 1$ and $T \gg mc^2$, so that

$$\Delta W \rightarrow \frac{4\pi e^2}{3} \frac{1}{\rho} \left(\frac{T}{mc^2}\right)^4$$

From Appendix C, $e^2[\text{Gaussian}] = 1.44 \times 10^{-7}$ eV-cm, and the coefficient is

$$\alpha = \frac{4\pi(1.44 \cdot 10^{-13} \text{ MeV-cm})}{3(0.511 \text{ MeV})^4} = 8.85 \times 10^{-12} \frac{\text{cm}}{\text{MeV}^3}$$

Examples:

$$(a) \quad T = 20 \text{ MeV}, \quad \rho = 50 \text{ cm} \quad \Rightarrow \quad \Delta W = 0.028 \text{ eV}$$

$$(b) \quad 1000 \quad 500 \quad 17.7 \text{ keV}$$

8-16. (a) We have $a = \omega^2 \rho$ and nonrelativistic kinetic energy $T = \frac{1}{2} m \omega^2 \rho^2 = 13.6 \text{ eV}$. We can write the nonrelativistic Larmor formula, Eq. (8.89), as

$$\begin{aligned} P &= \frac{8e^2 c}{3\rho^2} \left(\frac{T}{mc^2} \right)^2 \\ &= \frac{8(1.44 \cdot 10^{-7} \text{ eV-cm})(3 \cdot 10^{10} \text{ cm/s})}{3(0.53 \cdot 10^{-8} \text{ cm})^2} \left(\frac{13.6}{511000} \right)^2 \\ &= 2.9 \times 10^{11} \text{ eV/s} = 0.46 \text{ erg/s} \end{aligned}$$

(b) For a classical electron in a circular orbit, the potential energy is the negative of twice the kinetic energy, so that the total energy is

$$W = T - \frac{e^2}{\rho} = -T = -\frac{e^2}{2\rho}$$

Thus,

$$\frac{dW}{dt} = -P = -\frac{8e^2 c}{3} \left(-\frac{2W}{e^2} \right)^2 \left(-\frac{W}{mc^2} \right)^2 = -\frac{32cW^4}{3e^2(mc^2)^2}$$

and the time of decay is

$$\begin{aligned} \Delta t &= \int dt = - \int \frac{dW}{P} = - \frac{3e^2(mc^2)^2}{32c} \int_{W_0}^{-\infty} \frac{dW}{W^4} \\ &= + \frac{e^2(mc^2)^2}{32cT_0^3} \\ &= \frac{(1.44 \cdot 10^{-7} \text{ eV-cm})(0.511 \cdot 10^6 \text{ eV})^2}{32(3 \cdot 10^{10} \text{ cm/s})(13.6 \text{ eV})^3} = 1.6 \times 10^{-11} \text{ s} \end{aligned}$$

This calculation, of course, assumes a strictly classical (nonrelativistic, nonquantum) model.

Chapter 9

9-1. From Eq. (9.16), the power radiated by a time-varying dipole is

$$P = \frac{2[\ddot{\mathbf{p}}]^2}{3c^3}$$

From Eq. (2.22), the dipole moment of a system of particles of equal charge-to-mass ratio q/m is

$$\mathbf{p} = \sum_{\alpha} q_{\alpha} \mathbf{r}'_{\alpha} \rightarrow \frac{q}{m} \sum_{\alpha} m_{\alpha} \mathbf{r}'_{\alpha} = \frac{q}{m} M \mathbf{r}'_{\text{cm}}$$

where M is the total mass and \mathbf{r}'_{cm} is the position of the center of mass. Thus,

$$\ddot{\mathbf{p}} = \frac{d^2 \mathbf{p}}{dt'^2} = \frac{q}{m} M \frac{d^2 \mathbf{r}'_{\text{cm}}}{dt'^2}$$

If the center-of-mass is unaccelerated, there is no radiation.

9-2. Let the origin of coordinates \mathbf{r} and \mathbf{r}' be at the center of the sphere. In the retarded-vector-potential integral, Eq. (9.1),

$$\mathbf{A}(\mathbf{r}, t) = \frac{1}{c} \int \frac{\mathbf{J}(\mathbf{r}', t - |\mathbf{r} - \mathbf{r}'|/c)}{|\mathbf{r} - \mathbf{r}'|} dv'$$

the radially oscillating charge constitutes a spherically symmetric current density,

$$\mathbf{J} = J_0(r', t - |\mathbf{r} - \mathbf{r}'|/c) \mathbf{e}_{r'}$$

By symmetry, when we integrate over the sphere for a particular field point \mathbf{r} , the only nonvanishing component of \mathbf{A} must be in the \mathbf{r} direction. That is,

$$\mathbf{A}(\mathbf{r}, t) = A(r, \theta, \varphi, t) \rightarrow A_0(r, t) \mathbf{e}_r$$

Indeed, topologically, it is impossible to have field-lines of any *spherically symmetric* vector field that are anything but *radial* ("you cannot comb the fur on a sphere without a cowlick"). From Eq. (A.51), it follows that $\text{curl } \mathbf{A}$ vanishes identically. That is, there is no magnetic field or any sort, radiation or otherwise. Without a magnetic field, there can be no Poynting vector, and hence no radiation. The topological argument can be applied directly to the magnetic field—and since there is no magnetic monopole within the sphere, there cannot be even a radial \mathbf{B} -field. Note that the *electric* properties

of the system are described by a purely monopole moment, which remains constant in time. By symmetry, all higher-order electric multipole moments are zero.

9-3. At small distances r from the dipole (but still large compared to the dipole's structure size—to avoid significant contributions from higher-order moments), the inverse-square term of Eq. (9.27) will dominate over the inverse-first-power (radiation) term. We also assume that the time-variation is slow enough that we can ignore the retardation between the dipole and the field point. (Both assumptions are equivalent to $r \ll c/\omega$, where ω is a frequency characteristic of the time-variation of p .) Then,

$$\mathbf{B} \rightarrow \frac{\dot{p}}{cr^2} \sin\theta \mathbf{e}_\phi$$

The argument leading to Eq. (9.23) expresses the equivalence between a time-varying dipole and a current element,

$$\dot{p} = I d\ell$$

where $d\ell$ is the (infinitesimal) length of the dipole and current element, and the vector notation has been added. If $d\ell$ defines the polar axis of a spherical coordinate system, then $d\ell \times \mathbf{e}_r = \sin\theta \mathbf{e}_\phi$, where θ is the polar angle. We can now substitute to obtain Eq. (1.36),

$$\mathbf{B} \rightarrow \frac{1}{c} I \frac{d\ell \times \mathbf{e}_r}{r^2}$$

9-4. (a) As shown in Eq. (9.2), the radiation portion of the magnetic field can be obtained from the vector potential by

$$\mathbf{B}_{\text{rad}} = -\frac{1}{c} \mathbf{n} \times \frac{\partial \mathbf{A}}{\partial t}$$

If the currents that contribute to \mathbf{A} depend on time as $e^{-i\omega t}$, then the time derivative reduces to algebraic multiplication, $\partial/\partial t \rightarrow -i\omega$, and $\omega/c = k$ is the wavenumber of the wave of this frequency. In this case, we have

$$\mathbf{B}_{\text{rad}} = -\frac{1}{c} \mathbf{n} \times (-i\omega \mathbf{A}) = ik \mathbf{n} \times \mathbf{A} \quad (1)$$

Similarly, the Poynting vector of Eq. (9.4) becomes

$$\mathbf{S}_{\text{rad}} = \frac{c}{4\pi} (B_{\text{rad}})^2 \mathbf{n} = \frac{\omega k}{4\pi} |\mathbf{n} \times \mathbf{A}|^2 \mathbf{n}$$

(b) The sinusoidal current given by Eq. (9.52),

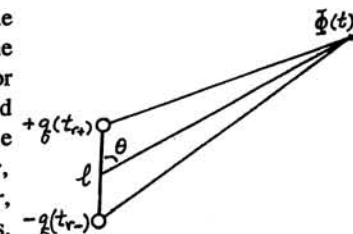
$$\mathbf{J} dv' \rightarrow \mathbf{e}_3 I(x'_3) e^{-i\omega t'} dx'_3$$

is one-dimensional in space, eliminating vector complications in the integration of \mathbf{A} . The retarded time is $t_r \rightarrow t - |\mathbf{r} - \mathbf{r}'|/c$. Thus, we have

$$\mathbf{A} = \int \frac{[\mathbf{J}]}{cR} dv' \rightarrow \mathbf{e}_3 \int \frac{I(x'_3) e^{-i\omega t'} e^{+i\omega |\mathbf{r} - \mathbf{r}'|/c}}{cR} dx'_3$$

The time factor $e^{-i\omega t'}$ comes outside the integral, as does $R \rightarrow r$ in the paraxial limit [Eq. (9.55)]. The cross product in (1) gives $\mathbf{n} \times \mathbf{e}_3 = -\sin\theta \mathbf{e}_\phi$, where \mathbf{e}_3 defines the polar axis of a spherical coordinate system, and $\mathbf{n} = \mathbf{e}_r$. The resulting evaluation of (1) is identical to Eq. (9.58).

9-5. (a) Let $t' = t - r/c$ —that is, t' is the time at which signals would have to leave the center of the dipole to reach the field point at the time t . Now, for a compact dipole ($\ell \ll r$), the upper charge (labeled $+q$) is closer to the field point by the distance $\Delta r = (\ell/2)\cos\theta$, and its retarded time is later, $t_r = t' + \Delta r/c$. The lower charge ($-q$) is farther, and its retarded time earlier, by the same increments. The retarded scalar potential is therefore



$$\begin{aligned} \Phi(r, \theta, t) &= \sum \frac{[q]}{R} = \frac{+q(t' + \Delta r/c)}{r - \Delta r} + \frac{-q(t' - \Delta r/c)}{r + \Delta r} \\ &\rightarrow + \frac{\left(q(t') + \frac{\Delta r}{c} \dot{q}(t') \right) \left(1 + \frac{\Delta r}{r} \right)}{r} - \frac{\left(q(t') - \frac{\Delta r}{c} \dot{q}(t') \right) \left(1 - \frac{\Delta r}{r} \right)}{r} \end{aligned}$$

where we have used a first-order Taylor expansion to represent the time-offsets in the numerators, and likewise to move the spatial-offsets from the denominator to a factor in the numerator. Multiplying out, the zero-order terms in Δr cancel, the first-order terms double, and we discard second and higher orders in the limit as $\Delta r = (\ell/2)\cos\theta \rightarrow 0$. The result is:

$$\Phi \rightarrow \frac{2 \Delta r}{r} \left[\frac{q(t')}{r} + \frac{\dot{q}(t')}{c} \right] = \frac{\ell}{r} \cos\theta \left[\frac{q(t')}{r} + \frac{\dot{q}(t')}{c} \right]$$

If desired, we can substitute $q(t')\ell \rightarrow p(t')$, and $\dot{q}(t')\ell \rightarrow \dot{p}(t')$.

(b) The Lorentz condition is

$$\operatorname{div} \mathbf{A} = -\frac{1}{c} \frac{\partial \Phi}{\partial t}$$

In this case, with the dipole oriented along the z axis,

$$\operatorname{div} \mathbf{A} = \frac{\partial}{\partial z} \left(\frac{\dot{p}(t')}{cr} \right) = \frac{\dot{p}(t')}{c} \left(-\frac{1}{r^2} \frac{\partial r}{\partial z} \right) + \frac{1}{cr} \left(\ddot{p}(t') \frac{\partial t'}{\partial z} \right)$$

But $\partial r / \partial z = z/r = \cos \theta$, and $\partial t' / \partial z = \partial / \partial z (t - r/c) = -(1/c) \cos \theta$. So,

$$\operatorname{div} \mathbf{A} = - \left(\frac{\dot{p}(t')}{cr^2} + \frac{\ddot{p}(t')}{c^2 r} \right) \cos \theta$$

Since $\partial t' / \partial t = 1$, this is transparently equal to $-(1/c)(\partial / \partial t)$ of the scalar potential calculated in Part (a).

9-6. We wish to expand Eq. (9.59) for $r' \ll r$,

$$|\mathbf{r} - \mathbf{r}'| = (r^2 - 2\mathbf{r} \cdot \mathbf{r}' + r'^2)^{1/2} = r \left(1 - 2 \frac{\mathbf{r} \cdot \mathbf{r}'}{r^2} + \frac{r'^2}{r^2} \right)^{1/2}$$

There are two small quantities in the square-root, one of order r'/r and the other $(r'/r)^2$. The m th term in the binomial expansion will contain "small" terms ranging in order from $(r'/r)^m$ to $(r'/r)^{2m}$. In the present case, we seek a result that includes all terms up to order $(r'/r)^2$. The ordering is more visible if we introduce the unit vector $\mathbf{n} = \mathbf{r}/r$. Then,

$$\begin{aligned} & \left(1 - 2 \frac{\mathbf{n} \cdot \mathbf{r}'}{r} + \frac{r'^2}{r^2} \right)^{1/2} \\ &= 1 + \frac{1}{2} \left(-2 \frac{\mathbf{n} \cdot \mathbf{r}'}{r} + \frac{r'^2}{r^2} \right) + \frac{\frac{1}{2}(-\frac{1}{2})}{2!} \left(-2 \frac{\mathbf{n} \cdot \mathbf{r}'}{r} + \frac{r'^2}{r^2} \right)^2 + \dots \\ &= 1 - \frac{\mathbf{n} \cdot \mathbf{r}'}{r} + \frac{1}{2} \frac{r'^2}{r^2} - \frac{1}{8} \left(-2 \frac{\mathbf{n} \cdot \mathbf{r}'}{r} + \dots \right)^2 + \dots \\ &= 1 - \frac{r'}{r} \cos \theta + \frac{1}{2} \frac{r'^2}{r^2} (1 - \cos^2 \theta) + O\left(\frac{r'^3}{r^3}\right) \end{aligned}$$

where θ is the angle between \mathbf{r}' and \mathbf{r} or \mathbf{n} (see Fig. 9-8). Multiplying through by r (and substituting $\sin^2 \theta = 1 - \cos^2 \theta$), we have Eq. (9.60).

9-7. The integral in Eq. (9.64) is, with $x'_3 \rightarrow x$,

$$\int_{-d/2}^0 \sin\left(\frac{1}{2}kd + kx\right) e^{-ikx \cos \theta} dx + \int_0^{+d/2} \sin\left(\frac{1}{2}kd - kx\right) e^{-ikx \cos \theta} dx$$

If we substitute $x \rightarrow -x$ in the first integral, we see that its value is identical to the complex conjugate of the second. Using $2i \sin u = e^{+iu} - e^{-iu}$, the second integral can be evaluated as

$$\begin{aligned} & \frac{1}{2i} \int_0^{+d/2} \left[e^{+i(\frac{1}{2}kd - kx)} - e^{-i(\frac{1}{2}kd - kx)} \right] e^{-ikx \cos \theta} dx \\ &= \frac{e^{+i\frac{1}{2}kd}}{2k} \left[\frac{e^{-i\frac{1}{2}kd(1+\cos \theta)} - 1}{1 + \cos \theta} \right] + \frac{e^{-i\frac{1}{2}kd}}{2k} \left[\frac{e^{+i\frac{1}{2}kd(1-\cos \theta)} - 1}{1 - \cos \theta} \right] \end{aligned}$$

The sum of the two integrals is then twice the real part of this second integral,

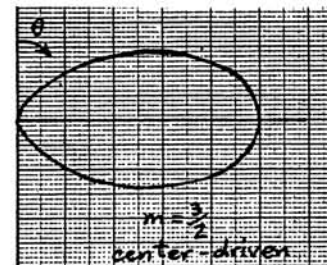
$$\begin{aligned} & \frac{\cos(\frac{1}{2}kdc \cos \theta) - \cos(\frac{1}{2}kd)}{k(1 + \cos \theta)} + \frac{\cos(\frac{1}{2}kdc \cos \theta) - \cos(\frac{1}{2}kd)}{k(1 - \cos \theta)} \\ &= \frac{2 [\cos(\frac{1}{2}kdc \cos \theta) - \cos(\frac{1}{2}kd)]}{k(1 - \cos^2 \theta)} \end{aligned}$$

Substituting $1 - \cos^2 \theta \rightarrow \sin^2 \theta$ in the denominator and inserting the coefficient from Eq. (9.64), we obtain Eq. (9.65).

9-8. From Eq. (9.66), with $\frac{1}{2}kd = 3\pi/4$,

$$\frac{dP}{d\Omega} \propto \left[\frac{\cos\left(\frac{3\pi}{4} \cos \theta\right) + \frac{1}{\sqrt{2}}}{\sin \theta} \right]^2$$

The angular distribution is similar to, and midway between, those for $m = 1$ and 2 (see Fig. 9-9).



9-9. Equation (9.46) for the Hertzian dipole of infinitesimal length ℓ , with $I_0 \rightarrow I_1$ to flag this case, is

$$\frac{dP}{d\Omega} = \frac{\pi I_1^2}{2c} \left(\frac{\ell}{\lambda}\right)^2 \sin^2\theta \quad (1)$$

while Eq. (9.66) for the linear antenna of length d , with $I_0 \rightarrow I_2$, is

$$\frac{dP}{d\Omega} = \frac{I_2^2}{2\pi c} \left(\frac{\cos\left(\frac{1}{2}kd\cos\theta\right) - \cos\left(\frac{1}{2}kd\right)}{\sin\theta} \right)^2 \quad (2)$$

Now the quantity in large parentheses approximates for small kd as:

$$\begin{aligned} & \left(\frac{\left[1 - \frac{1}{2}\left(\frac{1}{2}kd\cos\theta\right)^2\right] - \left[1 - \frac{1}{2}\left(\frac{1}{2}kd\right)^2\right]}{\sin\theta} \right)^2 \\ \rightarrow & \frac{1}{64}(kd)^4 \left(\frac{-\cos^2\theta + 1}{\sin\theta} \right)^2 = \frac{\pi^4}{4} \left(\frac{\ell}{\lambda}\right)^4 \sin^2\theta \end{aligned}$$

That is, the limiting value of (2) for small $kd \rightarrow 2\pi\ell/\lambda$ is

$$\frac{dP}{d\Omega} \rightarrow \frac{\pi^3 I_2^2}{8c} \left(\frac{\ell}{\lambda}\right)^4 \sin^2\theta \quad (2')$$

Both formulas have the "sine-squared" radiation pattern characteristic of dipoles. The difference in the coefficients arises from the labeling of the assumed currents. The Hertzian dipole assumed a current of *spatially constant* amplitude I_1 along the length ℓ . The linear antenna assumes a *sinusoidal* distribution of current—zero at the ends, and rising to the antinode-amplitude I_2 of the standing wave (which is physically present only when $\ell \geq \lambda/2$). For $\ell \ll \lambda$, the actual current varies linearly from zero with the spatial slope $dI/dx = kI_2$, and the *average* current is $\frac{1}{2}(kI_2)(\ell/2) = (\pi/2)(\ell/\lambda)I_2$. Substituting this equivalent-spatial-average current for I_1 in formula (1) reproduces formula (2'), and the two models are consistent.

9-10. The total power is found by integrating Eq. (9.69) over solid angle,

$$P = \frac{I_0^2}{2\pi c} \int_0^\pi \frac{\cos^2\left(\frac{1}{2}\pi\cos\theta\right)}{\sin^2\theta} 2\pi \sin\theta d\theta$$

[substitute $u = \cos\theta$, and use the half-angle identity, $2\cos^2\left(\frac{1}{2}\pi u\right) = 1 + \cos(\pi u)$]

$$= \frac{I_0^2}{2c} \int_{-1}^{+1} \frac{1 + \cos\pi u}{1 - u^2} du$$

[expand denominator in partial fractions]

$$= \frac{I_0^2}{4c} \left[\int_{-1}^{+1} \frac{1 + \cos\pi u}{1 + u} du + \int_{-1}^{+1} \frac{1 + \cos\pi u}{1 - u} du \right]$$

[with the exchange $u \leftrightarrow -u$, the partial integrals (limits -1 to 0 and 0 to $+1$) interchange values, so the full integrals are invariant to this exchange, and hence equal]

$$= \frac{I_0^2}{2c} \int_{-1}^{+1} \frac{1 + \cos\pi u}{1 + u} du$$

[substitute $z = \pi(1 + u)$]

$$= \frac{I_0^2}{2c} \int_0^{2\pi} \frac{1 - \cos z}{z} dz$$

$$= \frac{I_0^2}{2c} [0.577\dots + \ln(2\pi) - Ci(2\pi)]$$

$$= \frac{I_0^2}{2c} (2.438\dots)$$

where $0.577\dots$ is Euler's constant and $Ci(x)$ is the so-called cosine integral, for which numerical tables exist. See (Ab65, §5.2 and Tables 5.1 and 5.3). Alternatively, the integral could be evaluated by numerical methods.

Since I_0 is the peak current at the feed point at the center of the antenna, the radiation resistance is, converting to SI,

$$\frac{2P}{I_0^2} = \left(\frac{2.438 \text{ erg/s}}{3 \cdot 10^{10} \text{ statamp}^2} \right) \left(\frac{1 \text{ watt}}{10^7 \text{ erg/s}} \right) \left(\frac{3 \cdot 10^9 \text{ statamp}}{1 \text{ amp}} \right)^2 = 73.1 \text{ ohms}$$

9-11. For the same current amplitude at the drive point and the same effective current distribution (including the image current), the radiation pattern is identical to that of the half-wave antenna, Eq. (9.69). However the radiation occurs only in the half-space above the conducting plane. The integration over solid angle spans $0 < \theta < \pi/2$, and the total power radiated is one-half that of the isolated half-wave antenna, Eq. (9.72). Consequently, the radiation resistance is $\frac{1}{2}(73.1) = 36.5$ ohms.

9-12. The feed point is an antinode of the current standing-wave; the ends are nulls. Beyond the ends, the sense of the current reverses with respect to the wire but, because the wire is folded back, the current sense in space is the same as on the driven side. Thus the current distribution in the added wire is identical to that in the driven portion (again with an antinode in the center). Since the currents are a negligible distance apart, the system is equivalent to a single half-wave antenna with *twice* the current and hence *four* times the radiated power. Consequently, the radiation resistance is four times that of the single antenna: $4(73) = 292$ ohms.

9-13. Because of the phase change, we no longer want the absolute value in Eq. (9.64). The revised integral is (with $x'_3 \rightarrow x$):

$$\int_{-d/2}^{+d/2} \sin\left(\frac{1}{2}kd - kx\right) e^{-ikx\cos\theta} dx$$

We restrict discussion to the case where $d = m\lambda/2 = m\pi/k$ (with $m = 2, 4, 6, \dots$), for which the integral becomes

$$-\cos\left(\frac{1}{2}m\pi\right) \int_{-m\pi/2k}^{+m\pi/2k} \sin(kx) e^{-ikx\cos\theta} dx$$

(using $2i \sin u = e^{+iu} - e^{-iu}$, and integrating,

$$= i \cos\left(\frac{1}{2}m\pi\right) \left\{ \frac{\sin\left[\frac{1}{2}m\pi(1-\cos\theta)\right]}{k(1-\cos\theta)} - \frac{\sin\left[\frac{1}{2}m\pi(1+\cos\theta)\right]}{k(1+\cos\theta)} \right\}$$

$$= -i \frac{\cos\left(\frac{1}{2}m\pi\right)}{k} \left[\frac{2 \cos\left(\frac{1}{2}m\pi\right) \sin\left(\frac{1}{2}m\pi\cos\theta\right)}{\sin^2\theta} \right]$$

Note that $\cos^2(\frac{1}{2}m\pi) = 1$. Inserting the coefficients from Eqs. (9.64) and (9.66), we obtain Eq. (9.76).

9-14. From Eq. (9.46), the maximum radiation of the infinitesimal Hertzian dipole occurs at $\theta = \pi/2$. Comparing with Eq. (9.47), the directivity is

$$G_{\text{Hertzian}} = \frac{(dP/d\Omega)_{\text{max}}}{P/4\pi} = 4\pi \left(\frac{\pi I_0^2 \ell^2}{2c\lambda^2} \right) \left(\frac{3c\lambda^2}{4\pi^2 I_0^2 \ell^2} \right) = \frac{3}{2}$$

The same result could be obtained from Eqs. (9.35)–(9.36). For the center-fed half-wave antenna, from Eqs. (9.69) and (9.72),

$$G_{\lambda/2} = 4\pi \left(\frac{I_0^2}{2\pi c} \right) \left(\frac{2c}{2.44 I_0^2} \right) = \frac{4}{2.44} = 1.64$$

9-15. The total power radiated by the point quadrupole is, from Eq. (9.123),

$$P = \int \frac{dP}{d\Omega} d\Omega = \frac{\omega^6 Q^2}{128\pi c^5} \int_0^\pi (\sin^2\theta \cos^2\theta) 2\pi \sin\theta d\theta$$

$$= \frac{\omega^6 Q^2}{64c^5} \int_{-1}^{+1} (1-u^2)u^2 du = \frac{\omega^6 Q^2}{240c^5}$$

The maximum radiation is at $\theta = 45^\circ$, for which $\sin^2\theta \cos^2\theta \rightarrow \frac{1}{4}$. The directivity is then (Prob. 9-14):

$$G_{\text{quadrupole}} = 4\pi \left(\frac{\omega^6 Q^2}{512\pi c^5} \right) \left(\frac{240c^5}{\omega^6 Q^2} \right) = \frac{15}{8} = 1.88$$

9-16. The current in the circuit is

$$I(t) = I_0 e^{-i\omega t} = \frac{\mathcal{E}_0 e^{-i\omega t}}{R_{\text{int}} + R_l}$$

The time-average power delivered to the load resistor R_l is

$$P(R_l) = \langle I^2 \rangle R_l = \frac{\mathcal{E}_0^2 R_l}{2(R_{\text{int}} + R_l)^2} \quad (1)$$

Varying R_l with R_{int} fixed, the maximum power occurs when

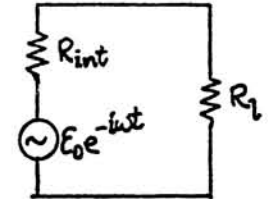
$$\frac{d}{dR_l} \frac{R_l}{(R_{\text{int}} + R_l)^2} = 0$$

$$(R_{\text{int}} + R_l)^2 (1) = (R_l) [2(R_{\text{int}} + R_l)] \Rightarrow R_l = R_{\text{int}}$$

Substituting this optimum in (1), the maximum available power is

$$P_{\text{max}} = \frac{\mathcal{E}_0^2 R_{\text{int}}}{2(R_{\text{int}} + R_{\text{int}})^2} = \frac{\mathcal{E}_0^2}{8R_{\text{int}}}$$

If preferred, one can use the *root-mean-square* emf, $\mathcal{E}_{\text{rms}} = \mathcal{E}_0/\sqrt{2}$.

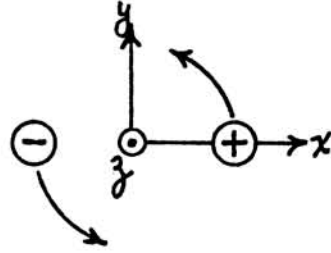


9-17. The system is equivalent to the superposition of two oscillating dipoles, differing in phase by 90° . (a) In the plane of motion, an observer "sees" only the component dipole oscillating perpendicular to the line of sight (the parallel component does not radiate in that direction). The radiation is linearly polarized. (b) The radiation along the axis of rotation has twice the intensity of a single linear dipole since both components contribute. Their fields are orthogonal, and the radiation is circularly polarized.

Quantitatively, we can write Eq. (9.15) as

$$\frac{dP}{d\Omega} = \frac{1}{4\pi c^3} |\dot{\mathbf{p}} \times \mathbf{n}|^2$$

where $\mathbf{n} = \mathbf{e}_r$ is the unit vector in the direction of radiation. Using the Cartesian axes shown,



$$\mathbf{p}(t_r) = qd (\cos\omega t_r, \sin\omega t_r, 0)$$

$$\dot{\mathbf{p}}(t_r) = -\omega^2 qd (\cos\omega t_r, \sin\omega t_r, 0)$$

With the polar axis parallel to z , and $\varphi = 0$ along x ,

$$\mathbf{n} = (\sin\theta \cos\varphi, \sin\theta \sin\varphi, \cos\theta)$$

Therefore,

$$\begin{aligned} \dot{\mathbf{p}} \times \mathbf{n} = & -\omega^2 qd \{ \mathbf{e}_x \cos\theta \sin\omega t_r - \mathbf{e}_y \cos\theta \cos\omega t_r \\ & + \mathbf{e}_z \sin\theta (\sin\varphi \cos\omega t_r - \cos\varphi \sin\omega t_r) \} \end{aligned}$$

The time-average of the magnitude squared is

$$\begin{aligned} \langle |\dot{\mathbf{p}} \times \mathbf{n}|^2 \rangle &= \omega^4 q^2 d^2 \left(\frac{1}{2} \cos^2\theta + \frac{1}{2} \cos^2\theta + \frac{1}{2} \sin^2\theta \right) \\ &= \frac{1}{2} \omega^4 q^2 d^2 (1 + \cos^2\theta) \end{aligned}$$

The radiation pattern is then (with θ measured from the normal to the plane of rotation):

$$\frac{dP}{d\Omega} = \frac{\omega^4 q^2 d^2}{8\pi c^3} (1 + \cos^2\theta)$$

The total power radiated is:

$$P = \frac{\omega^4 q^2 d^2}{8\pi c^3} \int_0^\pi (1 + \cos^2\theta) 2\pi \sin\theta d\theta = \frac{2\omega^4 q^2 d^2}{3c^3}$$

Comparison with Eq. (9.20) shows that the total power of the rotating dipole is twice that of the oscillating linear dipole of strength $p_0 = qd$.

9-18. The first form of Eq. (9.105) is altered by removing the phaseshift of $\pm\pi$ in the second term in curly brackets, equivalent to reversing the sign. So the sine changes to the cosine,

$$E_\theta = -2 \frac{\omega^2 p_0}{c^2 r} \sin\theta \cos\left(\frac{\pi}{2} \sin\theta \cos\varphi\right) e^{-i\omega t'}$$

and the angular distribution is

$$\left\langle \frac{dP}{d\Omega} \right\rangle = \frac{c r^2}{8\pi} \langle E_\theta^2 \rangle = \frac{\omega^4 p_0^2}{2\pi c^3} \sin^2\theta \cos^2\left(\frac{\pi}{2} \sin\theta \cos\varphi\right)$$

To examine this three-dimensional pattern, we plot in three orthogonal planes:

x_1 - x_2 plane ($\theta = \pi/2$, φ is angle from x_1 axis; see Fig. 9-17):

$$\left\langle \frac{dP}{d\Omega} \right\rangle_{12} \propto \cos^2\left(\frac{\pi}{2} \cos\varphi\right)$$

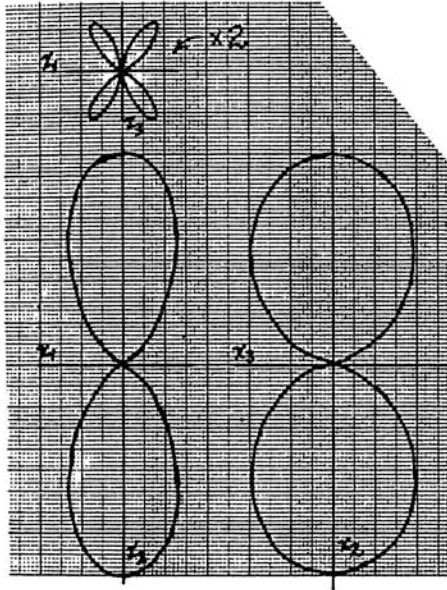
x_1 - x_3 plane ($\varphi = 0$, θ is angle from x_3 axis):

$$\left\langle \frac{dP}{d\Omega} \right\rangle_{13} \propto \sin^2\theta \cos^2\left(\frac{\pi}{2} \sin\theta\right)$$

x_2 - x_3 plane ($\varphi = \pi/2$, θ is angle from x_3 axis):

$$\left\langle \frac{dP}{d\Omega} \right\rangle_{23} \propto \sin^2\theta$$

Most of the radiation is along the x_2 axis. There is no radiation along the x_1 and x_3 axes, and only a very small quadrupole pattern in the x_1 - x_3 plane. This is much like the pattern of Eq. (9.106), shown in Fig. 9-18, except with the x_1 and x_2 axes interchanged. That is, the text case is *end-fire*, while the problem case is *broadside*.



9-19. The geometry is similar to that of Fig. 9-17, but with $\Delta = \lambda/4$ and phases in quadrature ($e^{\pm i\pi/4}$). The geometrical phase offsets are (see Fig. 9-14)

$$\mp \frac{\Delta}{2} \cos \psi = \mp \frac{\lambda}{8} \sin \theta \cos \varphi$$

and the equivalent of Eq. (9.105) is

$$\begin{aligned} E_{\theta} &= -\frac{\omega^2 p_0}{c^2 r} \sin \theta \left\{ \exp \left[i \left(-\frac{k\lambda}{8} \sin \theta \cos \varphi + \frac{\pi}{4} \right) \right] \right. \\ &\quad \left. + \exp \left[i \left(+\frac{k\lambda}{8} \sin \theta \cos \varphi - \frac{\pi}{4} \right) \right] \right\} \exp(-i\omega t) \\ &= -\frac{2\omega^2 p_0}{c^2 r} \sin \theta \cos \left(\frac{\pi}{4} \sin \theta \cos \varphi - \frac{\pi}{4} \right) \exp(-i\omega t) \end{aligned}$$

The angular distribution is then

$$\left\langle \frac{dP}{d\Omega} \right\rangle = \frac{c r^2}{8\pi} \langle E_{\theta}^2 \rangle = \frac{\omega^4 p_0^2}{2\pi c^3} \sin^2 \theta \cos^2 \left(\frac{\pi}{4} \sin \theta \cos \varphi - \frac{\pi}{4} \right)$$

$$= \frac{\omega^4 p_0^2}{4\pi c^3} \sin^2 \theta \left[1 + \sin \left(\frac{\pi}{2} \sin \theta \cos \varphi \right) \right]$$

To examine this three-dimensional pattern, we plot in three orthogonal planes:

x_1 - x_2 plane ($\theta = \pi/2$, φ is angle from x_1 axis; see Fig. 9-17):

$$\left\langle \frac{dP}{d\Omega} \right\rangle_{12} \propto 1 + \sin \left(\frac{\pi}{2} \cos \varphi \right)$$

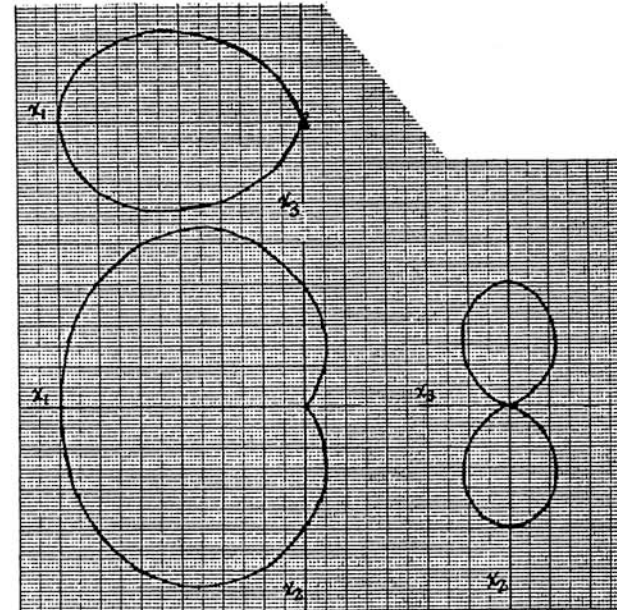
x_1 - x_3 plane ($\varphi = 0$, θ is angle from x_3 axis):

$$\left\langle \frac{dP}{d\Omega} \right\rangle_{13} \propto \sin^2 \theta \left[1 + \sin \left(\frac{\pi}{2} \sin \theta \right) \right]$$

x_2 - x_3 plane ($\varphi = \pi/2$, θ is angle from x_3 axis):

$$\left\langle \frac{dP}{d\Omega} \right\rangle_{23} \propto \sin^2 \theta$$

The main lobe is in the $+x_1$ direction, rather like a tongue in the x_1 - x_2 plane. There is no radiation in the $-x_1$ or $\pm x_3$ directions.



9-20. The subsidiary maxima are extrema of Eq. (9.116). It suffices to find the extrema of the square-root [den num' = num den']:

$$\sin\left(\frac{\alpha}{2}\right) \left[\left(\frac{N}{2}\right) \cos\left(\frac{N\alpha}{2}\right) \right] = \sin\left(\frac{N\alpha}{2}\right) \left[\left(\frac{1}{2}\right) \cos\left(\frac{\alpha}{2}\right) \right]$$

$$\tan\left(\frac{N\alpha}{2}\right) = N \tan\left(\frac{\alpha}{2}\right) \quad (1)$$

An approximate solution of this transcendental equation can be found by linearization. To avoid an infinity in the expansion, rewrite in terms of the cotangent,

$$N \operatorname{ctn}\left(\frac{N\alpha}{2}\right) = \operatorname{ctn}\left(\frac{\alpha}{2}\right)$$

Let $\alpha/2 = u_0 + \varepsilon$ (with $\varepsilon \ll 1$), and Taylor-expand both sides:

$$N \operatorname{ctn}(Nu_0) - \frac{N^2}{\sin^2(Nu_0)} \varepsilon = \operatorname{ctn}(u_0) - \frac{1}{\sin^2(u_0)} \varepsilon$$

$$\varepsilon = - \frac{\operatorname{ctn}(u_0) - N \operatorname{ctn}(Nu_0)}{\frac{N^2}{\sin^2(Nu_0)} - \frac{1}{\sin^2(u_0)}} \quad (2)$$

Now let $u_0 = j\pi/2N$, with $j = 3, 5, 7, \dots$ as suggested in Eq. (9.119). The formula reduces to:

$$\varepsilon_j = - \frac{\operatorname{ctn}(j\pi/2N)}{N^2 - [1/\sin^2(j\pi/2N)]} \quad (3)$$

For instance, for $N = 7$:

j	u_0	ε	$u_0 + \varepsilon$	$N\varepsilon/\pi$
3	0.6732	-0.0270	0.6462	-0.060
5	1.1220	-0.0101	1.1119	-0.023
7	1.5708	0	$\pi/2$	0

If higher accuracy is desired, the improved value $u_0 + \varepsilon$ can be substituted for the original u_0 , and Eq. (2) iterated [e.g., the second-order error for $j = 3$ turns out to be +0.0003]. The significance of the first-order ε 's can be seen by expressing them as fractions of the period between the subsidiary minima, $\Delta(\alpha/2) = \pi/N$, as given in the final column above. For instance, the $j = 3$ maximum is shifted 6% of a period back toward the preceding principal maximum. The maxima at $j = 9$ and 11 are shifted forward toward the next principal maximum, symmetrically with $j = 5$ and 3.

9-21. For the end-fire array, the terms of Eq. (9.111) have alternating signs:

$$1 - e^{i\alpha} + e^{2i\alpha} - \dots \pm e^{(N-1)i\alpha} = \frac{(-e^{i\alpha})^N - 1}{(-e^{i\alpha}) - 1}$$

$$= \frac{e^{iN\alpha/2} (-1)^{N-1} e^{+iN\alpha/2} + e^{-iN\alpha/2}}{e^{i\alpha/2} e^{+i\alpha/2} + e^{-i\alpha/2}}$$

$$= \begin{cases} e^{i(N-1)\alpha/2} \frac{\cos(N\alpha/2)}{\cos(\alpha/2)} & N \text{ odd} \\ -i e^{i(N-1)\alpha/2} \frac{\sin(N\alpha/2)}{\cos(\alpha/2)} & N \text{ even} \end{cases}$$

Picking up the angle-dependent coefficient in Eq. (9.111), the radiation pattern is proportional to

$$\frac{dP}{d\Omega} \propto \left[\frac{\cos\left(\frac{\pi}{2} \cos\theta\right) \left\{ \frac{\cos(N\alpha/2)}{\sin(N\alpha/2)} \right\}}{\sin\theta \cos(\alpha/2)} \right]^2$$

For $\Delta = \pi/2$, and in the midplane $\theta = \pi/2$, $\alpha = k\Delta \sin\theta \cos\varphi \rightarrow \pi \cos\varphi$, and the pattern reduces to the array function

$$\frac{dP}{d\Omega} \propto \left[\frac{\cos\left(\frac{N\pi}{2} \cos\varphi\right)}{\cos\left(\frac{\pi}{2} \cos\varphi\right)} \right]^2$$

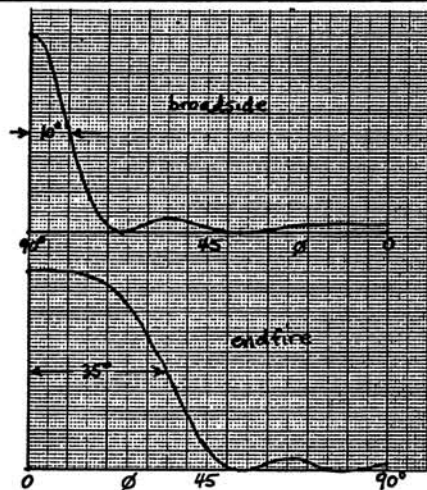
The L'Hôpital limit for both odd and even N gives principal maxima of magnitude N^2 at $\varphi = 0$ and π (the end-fire directions). The pattern is qualitatively similar to the broadside case but considerably broader. This case for $N = 5$, and that of the bottom curve of Fig. 9-21, are compared in Cartesian plots in the adjacent column.

9-22. From Eq. (9.15) or (9.46), the Hertzian dipole pattern is proportional to $\sin^2\theta$. The maximum power occurs for $\theta = \frac{\pi}{2} = 90^\circ$, and half-power at

$$\sin^2\theta_{1/2} = \frac{1}{2} \quad \Rightarrow \quad \theta_{1/2} = 45^\circ$$

So the full beamwidth is $2(90 - \theta_{1/2}) = 90^\circ$. For the half-wave antenna, from Eq. (9.69),

$$\frac{\cos^2\left(\frac{\pi}{2} \cos\theta_{1/2}\right)}{\sin^2\theta_{1/2}} = \frac{1}{2}$$



9-22, cont.

Again the maximum occurs for $\theta = 90^\circ$. With a few strokes on a pocket calculator (remembering that $\pi/2 \rightarrow 90^\circ$ in degree mode!), one finds values of the left-hand side:

$$\begin{array}{rcl} \theta_{1/2} \stackrel{?}{=} 50^\circ & \rightarrow & 0.483 \\ 51 & & 0.501 \\ 52 & & 0.519 \end{array}$$

So the beamwidth is approximately $2(90 - 51) = 78^\circ$. For the $N = 5$ array, from Eq. (9.115) or (9.116),

$$\frac{\sin^2(\frac{5\pi}{2} \cos \phi_{1/2})}{\sin^2(\frac{\pi}{2} \cos \phi_{1/2})} = \frac{1}{2} (5)^2$$

The maximum of 5^2 occurs for $\phi = 90^\circ$. Again we calculate the left-hand side for trial values:

$$\begin{array}{rcl} \phi_{1/2} \stackrel{?}{=} 79^\circ & \rightarrow & 11.4 \\ 79.5 & & 12.3 \\ 80 & & 13.2 \end{array}$$

The beamwidth is approximately $2(90 - 79.5) = 21^\circ$.

9-23. The identity of Eq. (A.61) is obtained by substituting $\mathbf{A} \rightarrow \varphi \mathbf{c}$, where \mathbf{c} is a constant vector (and φ an arbitrary scalar function), in the conventional Stokes' theorem, Eq. (A.54). The vector \mathbf{c} can be taken outside both integrals and, being arbitrary, canceled out. Using this identity, Eq. (9.125) can be transformed to an integral over the area of the current loop:

$$\begin{aligned} \mathbf{E}_{\text{rad}} &= \frac{\omega I_0}{c^2 r} \oint_{\Gamma} \sin \omega(t - R/c) d\ell' \\ &= - \frac{\omega I_0}{c^2 r} \int_S \text{grad}' [\sin \omega(t - R/c)] \times d\mathbf{S}' \end{aligned}$$

where $d\mathbf{S}'$ is a vector element of any surface S bounded by the current loop Γ . The gradient operator (here with respect to the *source* coordinates \mathbf{r}') works only on $R = |\mathbf{r} - \mathbf{r}'|$,

$$\begin{aligned} \text{grad}' [\sin \omega(t - R/c)] &= \cos \omega(t - R/c) \left(- \frac{\omega}{c} \right) \text{grad}'(R) \\ &= \sin \omega(t - R/c) \left(- \frac{\omega}{c} \right) (-\mathbf{e}_R) \end{aligned}$$

(See Prob. 1-22.) Now, if we assume that the current loop is compact so that its dimensions are small compared to the radiated wavelength, we can neglect retardation and put $R \rightarrow r$, the fixed radius from the "center" of the loop to the observation point. Thus,

$$\mathbf{E}_{\text{rad}} \rightarrow \frac{\omega^2 I_0}{c^3 r} \cos \omega t' \mathbf{n} \times \int d\mathbf{S}$$

where $t' = t - r/c$ is the retarded time at the loop, and $\mathbf{n} = \mathbf{e}_r$ is the unit vector in the direction of radiation. The integral is now simply the oriented total area of the current loop; if the loop is not planar, the magnitude is that of the *maximum projection* on a plane, and the direction is normal to that plane (in the right-handed sense). This vector area relates to the vector magnet moment of the loop by Eq. (9.121). With obvious notational adjustments, the general result (1) reduces to Eq. (9.131) for a circular loop of radius a .

In the present case, we can write

$$\mathbf{m}(t') = \frac{I_0 \cos \omega t'}{c} \int d\mathbf{S}$$

and

$$\mathbf{E}_{\text{rad}} \rightarrow \frac{1}{c^2 r} [\ddot{\mathbf{m}}] \times \mathbf{n}$$

which can be compared with the formulas for electric dipoles, Eqs. (9.11-12).

9-24. As in Prob. 5-4, we take the vector function $\mathbf{e}_z(C/r)\exp[i(kr-\omega t)]$ as a solution of the vector wave equation. Again, note the mixed bookkeeping, that the vector component is in Cartesian coordinates, while the functional dependence is in spherical coordinates. To work out the curl, it is easiest to express the unit vector as $\mathbf{e}_z = \cos\theta \mathbf{e}_r - \sin\theta \mathbf{e}_\theta$. Then, the resulting electric field is

$$\begin{aligned} \mathbf{E}_s &= \text{curl}[\mathbf{e}_z \Psi_s(r)] = \begin{vmatrix} \mathbf{e}_r & \mathbf{e}_\theta & \mathbf{e}_\phi \\ r^2 \sin\theta & r \sin\theta & r \\ \frac{\partial}{\partial r} & \frac{\partial}{\partial \theta} & 0 \\ \Psi_s(r) \cos\theta & -r \Psi_s(r) \sin\theta & 0 \end{vmatrix} \\ &= \frac{\mathbf{e}_\phi}{r} \left[\frac{\partial}{\partial r} (-C e^{i(kr-\omega t)} \sin\theta) - \frac{\partial}{\partial \theta} \left(\frac{C}{r} e^{i(kr-\omega t)} \cos\theta \right) \right] \\ &= \frac{\mathbf{e}_\phi}{r} C \left(-ik + \frac{1}{r} \right) \sin\theta e^{i(kr-\omega t)} = -ik^2 C \left[\frac{1}{kr} + \frac{i}{(kr)^2} \right] \sin\theta e^{i(kr-\omega t)} \mathbf{e}_\phi \end{aligned}$$

And then the associated magnetic field is

$$\begin{aligned} \mathbf{B}_s &= -\frac{ic}{\omega} \text{curl} \mathbf{E}_s = -\frac{i}{k} \begin{vmatrix} \mathbf{e}_r & \mathbf{e}_\theta & \mathbf{e}_\phi \\ r^2 \sin\theta & r \sin\theta & r \\ \frac{\partial}{\partial r} & \frac{\partial}{\partial \theta} & 0 \\ 0 & 0 & r \sin\theta E_s(r, \theta) \end{vmatrix} \\ &= -\frac{i}{k} \left[\frac{\mathbf{e}_r}{r^2 \sin\theta} \frac{\partial}{\partial \theta} - \frac{\mathbf{e}_\theta}{r \sin\theta} \frac{\partial}{\partial r} \right] \left[C \left(-ik + \frac{1}{r} \right) \sin^2\theta e^{i(kr-\omega t)} \right] \\ &= \frac{iC \mathbf{e}_r}{kr^2} \left(ik - \frac{1}{r} \right) 2 \cos\theta e^{i(kr-\omega t)} \\ &\quad + \frac{iC \mathbf{e}_\theta}{kr} \left[\left(0 - \frac{1}{r^2} \right) + ik \left(-ik + \frac{1}{r} \right) \right] \sin\theta e^{i(kr-\omega t)} \\ &= iCk^2 \left[\frac{i}{(kr)^2} - \frac{1}{(kr)^3} \right] 2 \cos\theta e^{i(kr-\omega t)} \mathbf{e}_r \\ &\quad + iCk^2 \left[\frac{1}{kr} + \frac{i}{(kr)^2} - \frac{1}{(kr)^3} \right] \sin\theta e^{i(kr-\omega t)} \mathbf{e}_\theta \end{aligned}$$

With $iC \rightarrow [\ddot{m}]/\omega c$, the $1/r$ radiation terms in each field agree with Eq. (9.134). These are the complete fields of an oscillating magnetic dipole. They are the *dual* of the fields of an oscillating electric dipole, with $\mathbf{B}_e \rightarrow \mathbf{E}_m$ and $\mathbf{E}_e \rightarrow -\mathbf{B}_m$.

Chapter 10

10-1. The geometry and notation for a linearly polarized incident wave are shown in Fig. 10-1. The scattered intensity for "unpolarized" incident radiation is calculated leading to Eq. (10.12). To find the state of polarization of the scattered radiation, we compute the components of the scattered electric field parallel and perpendicular to the scattering plane defined by \mathbf{k} and \mathbf{n} . According to Eq. (9.13) the scattered amplitude is proportional to $\sin\theta \mathbf{e}_\theta$, and therefore the components are:

$$E_{\parallel} \propto \sin\theta \mathbf{e}_\theta \cdot \mathbf{e}_\phi$$

$$E_{\perp} \propto \sin\theta \mathbf{e}_\theta \cdot \mathbf{e}_\psi$$

To work out the scalar products of these unit vectors, we must reconcile two sets of angles: φ and ψ are the polar and azimuthal angles, respectively, of the observation direction \mathbf{n} with respect to the incident direction \mathbf{k} as polar axis, while θ is the polar angle of \mathbf{n} with respect to the polarization direction (\mathbf{E}). Let χ be the azimuthal angle (around \mathbf{E}) associated with the polar angle θ , with $\chi = \pi/2$ at the \mathbf{k} axis. Designate the polarization (\mathbf{E}) axis as x_1 , and the $\mathbf{k} \times \mathbf{E}$ axis as x_2 (the \mathbf{k} axis is x_3). Then match the components of the unit vector \mathbf{n} on the three axes, reckoned in the two bookkeepings:

$$\mathbf{e}_1(\mathbf{E}) \quad \cos\theta = \sin\varphi \cos\psi$$

$$\mathbf{e}_2(\mathbf{k} \times \mathbf{E}) \quad \sin\theta \cos\chi = \sin\varphi \sin\psi$$

$$\mathbf{e}_3(\mathbf{k}) \quad \sin\theta \sin\chi = \cos\varphi$$

We can now write out $\sin\theta \mathbf{e}_\theta$, first in θ, χ bookkeeping, and then convert to φ, ψ bookkeeping:

$$\begin{aligned} \sin\theta \mathbf{e}_\theta &= \sin\theta [\mathbf{e}_1(-\sin\theta) + \mathbf{e}_2(\cos\theta \cos\chi) + \mathbf{e}_3(\cos\theta \sin\chi)] \\ &= \mathbf{e}_1(\sin^2\varphi \cos^2\psi - 1) + \mathbf{e}_2(\sin^2\varphi \sin\psi \cos\psi) + \mathbf{e}_3(\sin\varphi \cos\varphi \cos\psi) \end{aligned}$$

More directly,

$$\mathbf{e}_\phi = \mathbf{e}_1(\cos\varphi \cos\psi) + \mathbf{e}_2(\cos\varphi \sin\psi) + \mathbf{e}_3(-\sin\varphi)$$

$$\mathbf{e}_\psi = \mathbf{e}_1(-\sin\psi) + \mathbf{e}_2(\cos\psi) + \mathbf{e}_3(0)$$

Carrying out the scalar products, and simplifying, we find:

$$E_{\parallel} \propto -\cos\varphi \cos\psi \quad E_{\perp} \propto \sin\psi$$

The time-average intensities for random incident polarization (i.e., averaging over ψ) are then:

$$I_{\parallel} \propto \cos^2\varphi \langle \cos^2\psi \rangle = \frac{1}{2} \cos^2\varphi$$

$$I_{\perp} \propto \langle \sin^2\psi \rangle = \frac{1}{2}$$

A measure of the degree of polarization is $I_{\parallel}/I_{\perp} = \cos^2\varphi$. The scattered radiation is most strongly polarized when observed perpendicular to the direction of propagation (i.e., $\varphi = \pi/2$), where it is linearly polarized perpendicular to the plane of \mathbf{k} and \mathbf{n} . The scattered radiation becomes "unpolarized" as $\varphi \rightarrow 0$ or π .

10-2. Using the quantum-mechanical polarizability, $\alpha = \frac{2}{3}a_0^3$, in the classical Lorentz model, we get

$$\omega_0^2 = \frac{e^2}{m\alpha} = \frac{2e^2}{9m} \left(\frac{me^2}{\hbar^2} \right)^3 \Rightarrow \omega_0 = \frac{\sqrt{2}me^4}{3\hbar^3}$$

The actual Lyman-alpha frequency is

$$\omega_{L\alpha} = \frac{3W_R}{4\hbar} = \frac{3}{4\hbar} \left(\frac{me^4}{2\hbar^2} \right) = \frac{3me^4}{8\hbar^3}$$

The scaling with fundamental constants is the same; the numerical coefficient of the classical model is wrong, but not by much:

$$\frac{\omega_0}{\omega_{L\alpha}} = \frac{8\sqrt{2}}{9} = 1.257$$

10-3. We require the extrema of the real and imaginary parts of the refractive index, from Eqs. (10.31–32). The extrema of $(n-1)$ are [using den · num' = num · den', and suppressing the subscript on $\beta\alpha$]:

$$[(\omega_\alpha^2 - \omega^2)^2 + 4\beta^2\omega^2](-1) = (\omega_\alpha^2 - \omega^2)[2(\omega_\alpha^2 - \omega^2)(-1) + 4\beta^2]$$

$$\omega^4 - 2\omega_\alpha^2\omega^2 + (\omega_\alpha^4 - 4\beta^2\omega_\alpha^2) = 0$$

$$\omega_{1,2}^2 = \omega_\alpha^2 \mp 2\beta\omega_\alpha \quad ("n-1" \text{ extrema}) \quad (1)-(2)$$

The extremum of $n\kappa$ is:

$$[(\omega_\alpha^2 - \omega^2)^2 + 4\beta^2\omega^2](1) = (\omega)[2(\omega_\alpha^2 - \omega^2)(-2\omega) + 8\beta^2\omega]$$

$$3\omega^4 - 2(\omega_\alpha^2 - 2\beta^2)\omega^2 - \omega_\alpha^4 = 0$$

$$\begin{aligned} \omega_3^2 &= \frac{(\omega_\alpha^2 - 2\beta^2) + 2(\omega_\alpha^4 - \omega_\alpha^2\beta^2 + \beta^4)^{1/2}}{3} \\ &= \omega_\alpha^2 - \beta^2 + \dots \quad ("n\kappa" \text{ extremum}) \end{aligned} \quad (3)$$

Now substitute (3) in Eq. (10.32) [we omit all coefficients not involving ω],

$$\begin{aligned} (n\kappa)_{\max} &\propto \frac{1 - \beta^2/2\omega_\alpha^2 + \dots}{(\beta^2 + \dots)^2 + 4\beta^2(\omega_\alpha^2 - \beta^2 + \dots)} \\ &= \frac{1}{4\beta^2\omega_\alpha^2} \left(1 + \frac{\beta^2}{4\omega_\alpha^2} + \dots \right) \end{aligned} \quad (4)$$

Similarly, substitute the extrema frequencies (1) and (2),

$$\begin{aligned} (n\kappa)_{1,2} &\propto \frac{\omega_\alpha(1 \mp \beta/\omega_\alpha + \dots)}{(2\beta\omega_\alpha)^2 + 4\beta^2(\omega_\alpha^2 \mp 2\beta\omega_\alpha)} \\ &= \frac{\omega_\alpha(1 \mp \beta/\omega_\alpha + \dots)}{8\beta^2\omega_\alpha^2(1 \mp \beta/\omega_\alpha)} \end{aligned} \quad (5)$$

Thus, for both extrema, formula (5) is one-half of formula (4) at least to order $(\beta/\omega_\alpha)^2$. The full width at half intensity is, from (1)–(2),

$$\omega_2 - \omega_1 = \omega_\alpha \left[\left(1 + \frac{2\beta}{\omega_\alpha} \right)^{1/2} - \left(1 - \frac{2\beta}{\omega_\alpha} \right)^{1/2} \right] \approx 2\beta \left[1 + O(\beta^2/\omega_\alpha^2) \right]$$

10-4. We can choose to express the propagation properties of a dispersive medium in terms of either the phase velocity $V_{ph} = \omega/k$, or the refractive index $n = c/V_{ph}$, as *dependent* variable—and choose either the frequency $\omega = 2\pi\nu$, or the wavelength $\lambda = 2\pi/k = 2\pi V_{ph}/\omega$, as *independent* variable. There is only one degree of freedom in this family of variables: the derivatives are total (not partial), and can be thought of simply as ratios of differentials. Using $V_{ph}(\omega)$, we can express the group velocity as:

$$\begin{aligned} V_{gr} &\equiv \frac{d\omega}{dk} = \frac{d}{dk}(kV_{ph}) = V_{ph} + k \frac{dV_{ph}}{d\omega} \frac{d\omega}{dk} = V_{ph} + \frac{\omega}{V_{ph}} \frac{dV_{ph}}{d\omega} V_{gr} \\ &\Rightarrow V_{gr} = \frac{V_{ph}}{1 - \frac{\omega}{V_{ph}} \frac{dV_{ph}}{d\omega}} \end{aligned} \quad (1)$$

Using $V_{ph}(\lambda)$:

$$\begin{aligned} V_{gr} &= \frac{d}{dk}(kV_{ph}) = V_{ph} + k \frac{dV_{ph}}{d\lambda} \frac{d\lambda}{dk} = V_{ph} + \frac{2\pi}{\lambda} \frac{dV_{ph}}{d\lambda} \left(-\frac{\lambda^2}{2\pi}\right) \\ &= V_{ph} - \lambda \frac{dV_{ph}}{d\lambda} \end{aligned} \quad (2)$$

Using $n(\omega)$:

$$\begin{aligned} \frac{1}{V_{gr}} &= \frac{dk}{d\omega} = \frac{d}{d\omega} \left(\frac{n\omega}{c} \right) = \frac{n}{c} + \frac{\omega}{c} \frac{dn}{d\omega} = \frac{1}{V_{ph}} + \frac{\omega}{nV_{ph}} \frac{dn}{d\omega} \\ \Rightarrow V_{gr} &= \frac{V_{ph}}{1 + \frac{\omega}{n} \frac{dn}{d\omega}} \end{aligned} \quad (3)$$

And using $n(\lambda)$:

$$\begin{aligned} V_{gr} &= \frac{d}{dk} \left(\frac{kc}{n} \right) = \frac{c}{n} + kc \left(-\frac{1}{n^2} \right) \frac{dn}{d\lambda} \frac{d\lambda}{dk} = V_{ph} + \frac{2\pi n V_{ph}}{\lambda} \left(-\frac{1}{n^2} \right) \frac{dn}{d\lambda} \left(-\frac{\lambda^2}{2\pi} \right) \\ &= V_{ph} \left(1 + \frac{\lambda}{n} \frac{dn}{d\lambda} \right) \end{aligned} \quad (4)$$

For "normal" dispersion, $dn/d\omega$ and $dV_{ph}/d\lambda$ are positive, and $dV_{ph}/d\omega$ and $dn/d\lambda$ are negative (or zero). Thus, "normally" we have $V_{gr} \leq V_{ph}$.

10-5. We have (always) $V_{ph} = c/n$, and (in this case) $V_{gr} = c^2/V_{ph} = nc$. Substituting in Eq. (3) from Prob. 10-4,

$$\begin{aligned} nc &= \frac{\frac{c}{n}}{1 + \frac{\omega}{n} \frac{dn}{d\omega}} \Rightarrow \frac{dn}{d\omega} = \frac{n}{\omega} \left(\frac{1}{n^2} - 1 \right) \\ \Rightarrow \frac{d(n^2)}{1 - n^2} &= \frac{2 d\omega}{\omega} \Rightarrow \ln \left(\frac{1}{1 - n^2} \right) = \ln(\omega^2) + \ln(a) \\ \Rightarrow n^2 &= 1 - \frac{1}{a\omega^2} \end{aligned}$$

where $\ln(a)$ is the constant of integration. This special case occurs for propagation in hollow-conductor waveguides [Eq. (7.29)] and in ionized gases [Eq. (10.71)].

10-6. It is easier to work from Eq. (10.36) than from (10.37). Divide the summation into two series (for which $\lambda_\alpha < \lambda$ and $\lambda_\beta > \lambda$, respectively), and expand binomially:

$$\begin{aligned} n &= 1 + \sum_{\alpha} \lambda_{\alpha}^2 \rho_{\alpha} \left(1 - \frac{\lambda_{\alpha}^2}{\lambda^2} \right)^{-1} - \lambda^2 \sum_{\beta} \rho_{\beta} \left(1 - \frac{\lambda^2}{\lambda_{\beta}^2} \right)^{-1} \\ &= 1 + \sum_{\alpha} \lambda_{\alpha}^2 \rho_{\alpha} + \frac{1}{\lambda^2} \sum_{\alpha} \lambda_{\alpha}^4 \rho_{\alpha} + \frac{1}{\lambda^4} \sum_{\alpha} \lambda_{\alpha}^6 \rho_{\alpha} + \dots \\ &\quad - \lambda^2 \sum_{\beta} \rho_{\beta} - \lambda^4 \sum_{\beta} \frac{\rho_{\beta}}{\lambda_{\beta}^2} - \lambda^6 \sum_{\beta} \frac{\rho_{\beta}}{\lambda_{\beta}^4} - \dots \end{aligned}$$

The summations are the coefficients in Eq. (10.39).

10-7. The linear regression (least-squares) routine on a scientific calculator for $(n-1)$ against (λ^{-2}) gives the coefficients:

$$A = 2.87902 \times 10^{-4}$$

$$AB = 1.6184 \times 10^{-4} \\ \text{whence } B = 0.5621$$

The root-mean-square and maximum deviations of the ordinate data points $(n-1)$ from the fitted line are 5 and 8 units, respectively, in the decimal place beyond that given in the data. Thus the formula is as accurate as the precision of the given data warrants.

10-8. From the results of Prob. 10-6, the coefficients in Eqs. (10.39-40) are related, for a single resonance at λ_0 , by:

$$\left. \begin{aligned} A &= \lambda_0^2 \rho \\ AB &= \lambda_0^4 \rho \end{aligned} \right\} \Rightarrow \left\{ \begin{aligned} B &= \lambda_0^2 \\ A/B &= \rho = \frac{Nf_0 e^2}{2\pi m c^2} \end{aligned} \right.$$

where ρ [Eq. (10.35)] is the effective electron density (Nf_0), multiplied by universal constants. Thus,

$$\lambda_0 = \left(\frac{1.05 \times 10^{-14}}{1.360 \times 10^{-4}} \right)^{1/2} = 87.9 \text{ nm} = 879 \text{ \AA}$$

This is in the ultraviolet, far beyond the short-wavelength end of the visible region at 400 nm. Similarly,

$$\rho = \frac{Ne^2}{2\pi mc^2} = \frac{(1.360 \times 10^{-4})^2}{1.05 \times 10^{-14}} = 1.762 \times 10^6 \text{ cm}^{-2}$$

and thus, with $f_\alpha = 1$,

$$\begin{aligned} \frac{e}{m} &= \frac{2\pi(2.998 \cdot 10^{10} \text{ cm/s})^2 (1.762 \cdot 10^6 \text{ cm}^{-2}) (22.4 \cdot 10^3 \text{ cm}^3/\text{mole})}{(2.893 \cdot 10^{14} \text{ esu/mole})(1 \text{ g-cm}^3/\text{esu}^2\text{-s}^2)} \\ &= 7.70 \times 10^{17} \text{ esu/g} \end{aligned}$$

(The final factor in the denominator reconciles the Gaussian unit of charge, the esu, with its cm-g-s equivalent—see Prob. 1-1.) The modern value of the electron's e/m is 5.27×10^{17} esu/g. The Faraday constant, $\mathcal{F} = N_A e$, is a macroscopic quantity, which can be measured to high precision in electrochemical experiments. One might argue that the hydrogen molecule should be counted as having two electrons. That model would reduce the calculated e/m by a factor of 2, which then becomes too low.

10-9. From Eq. (10.23), where $\omega_0 = \sqrt{K/m}$ is the resonant frequency,

$$\mathbf{p} = \frac{(e^2/m)\mathbf{E}}{(\omega_0^2 - \omega^2) - i 2\beta\omega}$$

From Eqs. (9.15) and (10.8),

$$\left\langle \frac{d\sigma}{d\Omega} \right\rangle = \frac{2}{c^4 E_0^2} \langle |\mathbf{p}|^2 \rangle \sin^2\theta = \frac{\omega^4 (e^2/mc^2)^2}{(\omega_0^2 - \omega^2)^2 + (2\beta\omega)^2} \sin^2\theta$$

This cross section exceeds the linearly polarized Thomson cross section of Eq. (10.10) by the factor

$$F = \frac{\omega^4}{(\omega_0^2 - \omega^2)^2 + (2\beta\omega)^2}$$

Since the "atom" is assumed to be isotropic, the same factor multiplies the unpolarized cross section, Eq. (10.11). The angular distributions are unchanged. As a function of ω , the factor F has a maximum at

$$\omega^2 = \frac{\omega_0^4}{\omega_0^2 + 2\beta^2} \approx \omega_0^2$$

where it becomes

$$F_{\max} \approx \frac{\omega_0^2}{4\beta^2}$$

which is very much larger than unity in the typical case of weak damping. On the other hand, far enough below resonance that $\omega^2 \ll \omega_0^2$,

$$F \rightarrow \frac{\omega^4}{\omega_0^4} = \left(\frac{2\pi c}{\omega_0} \right)^4 \frac{1}{\lambda^4}$$

Air molecules have effective resonant frequencies in the ultraviolet, and this limit applies. The λ^{-4} dependence of scattering of "white" light from the Sun produces the blue color of the sky, as discussed in Sec. 10.2.

10-10. (a) According to Eq. (10.9), each molecule scatters the power σS , where σ is the cross section and S is the incident power per-unit-area (Poynting vector). If there are N molecules per-unit-volume, then the volume consisting of a unit-area times the propagation distance $d\zeta$ scatters the total power $(\sigma S)(N d\zeta)$. This represents a loss of directed power-per-area, and therefore the Poynting vector of the beam decreases according to

$$\frac{dS}{d\zeta} = -\sigma N S \quad \Rightarrow \quad h = \sigma N$$

(b) From Eq. (10.41) [and Prob. 10-9], in the limit $\omega_\alpha \rightarrow \omega_0 \gg \omega$,

$$\sigma_{\text{Rayleigh}} = \frac{8\pi}{3} \left(\frac{4\pi^2 e^2}{m\omega_0^2} \right)^2 \frac{1}{\lambda^4}$$

To calibrate the molecular resonance ω_0 , we use Eq. (10.31), which reduces in this limit to

$$n - 1 = \frac{2\pi N e^2}{m\omega_0^2}$$

Thus,

$$h = \frac{8\pi}{3} \left(\frac{4\pi^2 e^2}{m} \right)^2 \left(\frac{m(n-1)^2}{2\pi N e^2} \right)^2 \frac{N}{\lambda^4} = \frac{32\pi^3 (n-1)^2}{3N\lambda^4}$$

(c) Experimental measurements of h and $n-1$ (for a given λ) determine the particle density N . The experimental pressure p and temperature T can also be measured. The ideal gas law is usually written as $p\nu = RT$, where ν is the volume per-mole, and R is the gas constant per-mole. But R is the product of Boltzmann's constant k and Avogadro's number N_A , and our particle density N is N_A/ν . That is, we can write a "particle" form of the ideal gas law as $p = NkT$. Thus $k = p/NT$, and Loschmidt's number is given by

$$N_L = N \left(\frac{\rho_0}{p} \right) \left(\frac{T}{T_0} \right) [\approx 2.7 \times 10^{19} \text{ cm}^{-3}]$$

where $p_0 = 760 \text{ torr} = 1.013 \times 10^6 \text{ dyne/cm}^2$, and $T_0 = 273 \text{ K}$. If we measured the mass density ρ , and knew the molecular weight W , then we could determine Avogadro's number $N_A = WN/\rho$.

10-11. Equation (16) of Example 3.3(a) gives the magnitude of the induced dipole moment as $p = E_0 a^3$, where we now identify the applied field E_0 as that of the incident wave. From Eq. (9.13), the electric-field amplitude is

$$E_{\text{scat}} = \frac{|p|}{c^2 r} \sin \theta = \frac{\omega^2 a^3}{c^2 r} E_0 \sin \theta$$

which is proportional to the volume, $\frac{4\pi}{3} a^3$. From Eqs. (9.20) and (10.8-9), the total cross section is

$$\sigma = \frac{8\pi P}{c E_0^2} = \frac{8\pi \omega^4 a^6}{c^3} = \frac{8}{3} \left(\frac{2\pi a}{\lambda} \right)^4 (\pi a^2)$$

10-12. We evaluate \mathbf{E}_{self} of Eq. (10.43) as the average of the molecular dipole's field over a spherical volume equal to one molecule's share of space:

$$\mathbf{E}_{\text{self}} = \frac{\int_V \mathbf{E}_{\text{dipole}} dV}{V_{\text{molecule}}} = -\frac{4\pi \mathbf{p}/3}{1/N} = +\frac{4\pi}{3} \mathbf{P}$$

The final step follows from Eq. (1.22). Thus, in Eq. (10.47), $\eta = 4\pi/3$. An elaboration of this argument is given in Sec. 9.13 of the *first edition* (1965) of Purcell [Pu85], where space is divided into cubes rather than impossibly packed spheres.

10-13. Equations (10.44-45) and (10.47-48) relate \mathbf{P} and \mathbf{E} in terms of the polarizability α as:

$$\frac{\mathbf{P}}{N} = \mathbf{p} = \alpha \mathbf{E}_{\text{mol}} = \alpha \left(\mathbf{E} + \frac{4\pi}{3} \mathbf{P} \right)$$

$$\Rightarrow \mathbf{P} = \frac{N\alpha}{1 - \frac{4\pi}{3} N\alpha} \mathbf{E}$$

Equation (10.46) relates \mathbf{P} and \mathbf{E} in terms of the dielectric constant ϵ as:

$$\mathbf{P} = \frac{\epsilon - 1}{4\pi} \mathbf{E}$$

Therefore, the relations between the "macroscopic" ϵ and the "microscopic" $N\alpha$ are:

$$\frac{N\alpha}{1 - \frac{4\pi}{3} N\alpha} = \frac{\epsilon - 1}{4\pi}$$

$$\epsilon = 1 + \frac{4\pi N\alpha}{1 - \frac{4\pi}{3} N\alpha} = \frac{1 + \frac{8\pi}{3} N\alpha}{1 - \frac{4\pi}{3} N\alpha} \quad (10.52)$$

$$\epsilon - \epsilon \left(\frac{4\pi}{3} N\alpha \right) = 1 + 2 \left(\frac{4\pi}{3} N\alpha \right) \Rightarrow \frac{4\pi}{3} N\alpha = \frac{\epsilon - 1}{\epsilon + 2} \quad (10.49)$$

10-14. (a) Substituting in $\mathbf{p} = \alpha(\mathbf{E}_{\text{cav-p}} + \mathbf{E}_{\text{cav-E}_0})$, we have

$$\frac{(\epsilon - 1)\mathbf{E}}{4\pi N} = \alpha \left[\frac{2(\epsilon - 1)}{(2\epsilon + 1)a^3} \frac{(\epsilon - 1)\mathbf{E}}{4\pi N} + \frac{3\epsilon}{2\epsilon + 1} \mathbf{E} \right]$$

$$(\epsilon - 1)(2\epsilon + 1) = 4\pi N\alpha \left[\frac{2(\epsilon - 1)^2}{4\pi N a^3} + 3\epsilon \right]$$

which rearranges into the desired formula.

(b) If the Böttcher formula is to reduce to Clausius-Mossotti, Eq. (10.49), then

$$\frac{(\epsilon - 1)(2\epsilon + 1)}{9\epsilon + \frac{3(\epsilon - 1)^2}{2\pi N a^3}} = \frac{\epsilon - 1}{\epsilon + 2}$$

$$2\epsilon^2 + 5\epsilon + 2 = 9\epsilon + \frac{3(\epsilon - 1)^2}{2\pi N a^3} \Rightarrow \frac{4\pi}{3} a^3 = \frac{1}{N}$$

That is, the formulas coincide when the volume of the "Böttcher sphere" equals the volume per molecule. Clausius-Mossotti determines a from the inter-molecular spacing (independent of molecular size), while Böttcher determines a from the molecular diameter (independent of the inter-molecular spacing).

10-15. We calculate the molar refractivity from Eq. (10.54),

$$A_m = \frac{n^2 - 1}{n^2 + 2} \frac{W}{\delta}$$

Using data from the liquid phases, together with the handbook molecular weights:

	$W(\text{g/mole})$	$A_m(\text{cm}^3/\text{mole})$
acetone	58.08	16.177
ethyl ether	74.12	22.524

In the ideal-gas approximation,

$$\frac{W}{\delta} = \left(\frac{22.4 \cdot 10^3 \text{cm}^3}{\text{mole}} \right) \left(\frac{T}{273.2\text{K}} \right) \left(\frac{760 \text{ torr}}{P} \right)$$

Furthermore, the vapor phase is dilute enough that we can use the approximation

$$n - 1 = \frac{n^2 + 2}{n + 1} \frac{A_m}{W/\delta} \approx \frac{3}{2} \left(\frac{A_m}{22.4 \cdot 10^3} \right) \left(\frac{273.2}{T} \right) \left(\frac{p}{760} \right)$$

which is known as the Biot-Arago formula. The results for our example are:

	$T(\text{K})$	$p(\text{torr})$	n
acetone	273.2	67	1.000095
ethyl ether	273.2	180	1.000357

The agreement to 1 or 2% in $(n-1)$ is impressive since we are comparing the properties of liquids and dilute gases, which differ in density by three orders of magnitude.

10-16. By dimensional analysis,

$$\left(\frac{N \text{ electrons}}{\text{cm}^3} \right) = \left(\frac{1 \text{ electron}}{\text{molecule}} \right) \left(\frac{N_A \text{ molecules}}{\text{mole}} \right) \left(\frac{\delta \text{ g}}{\text{cm}^3} \right) \left(\frac{\text{mole}}{W \text{ g}} \right)$$

$$\Rightarrow N = \frac{N_A \delta}{W}$$

It follows from Eqs. (10.51) and (10.53) that contributions to $(n^2-1)/(n^2+2)$ are additive, and therefore

$$\frac{n^2 - 1}{n^2 + 2} = \sum_{\alpha} \frac{\delta_{\alpha}}{W_{\alpha}} A_{\alpha} = \sum_{\alpha} \frac{N_{\alpha}}{N_A} A_{\alpha}$$

where N_{α} is the number of molecules (atoms) per unit volume of the species with refractivity A_{α} , and N_A is Avogadro's number. For a mixture, we define the bulk refractivity A_{mix} by:

$$\left(\frac{\sum N_{\alpha}}{N_A} \right) A_{\text{mix}} = \sum_{\alpha} \frac{N_{\alpha}}{N_A} A_{\alpha}$$

where $\sum N_{\alpha}$ is simply the total number of molecules per volume. For two constituents, for instance, the effective refractivity is

$$A_{\text{mix}} = \frac{N_1}{N_1+N_2} A_1 + \frac{N_2}{N_1+N_2} A_2$$

For further discussion, see Born and Wolf (Bo80, Sec. 2.3.3).

10-17. Table 10.1 gives refractivity data for H_2O and O_2 . We can infer the refractivity of H_2 by considering it to be a mixture of H_2O and "negative" O_2 . From the results of Prob. 10-16,

$$A(\text{H}_2) = A(\text{H}_2\text{O}) - \frac{1}{2} A(\text{O}_2)$$

$$= 3.72 - \frac{1}{2} (4.05) = 1.70$$

The formula in Prob. 10-8 gives $n_{\text{H}} - 1 = 1.390 \times 10^{-4}$ for $\lambda = 589\text{nm}$. Thus, from Eq. (10.54),

$$A(\text{H}_2) = \frac{N_A}{N(\text{STP})} \frac{n^2-1}{n^2+2} = \left(\frac{22.4 \cdot 10^3 \text{cm}^3}{\text{mole}} \right) \left[\frac{2}{3} (1.390 \cdot 10^{-4}) \right] = 2.08$$

The agreement is only fair in this case, but note that we are treating components of a highly stable molecule as a "mixture". It is not surprising that these components no longer act independently.

10-18. From Eq. (16) of Example 3.3(a), we find that a conducting sphere, when placed in a remotely imposed uniform field \mathbf{E}_0 , acquires the dipole moment $\mathbf{p} = a^3 \mathbf{E}_0$. If we take this "remote" \mathbf{E}_0 to be the "local" molecular field \mathbf{E}_{mol} of Eq. (10.43), then the polarizability [Eq. (10.44)] is $\alpha = a^3$. And the molecular density is $N = 1/d^3$. Thus $N\alpha = (a/d)^3$, which substitutes in Clausius-Mossotti in the form Eq. (10.52) to give the desired result. The quantity $f = \frac{4\pi}{3} (a/d)^3$ is the fraction of total volume occupied by the spheres; in terms of this the formula is

$$\epsilon = \frac{1 + 2f}{1 - f}$$

The identification of the " \mathbf{E}_0 " of Example 3.3(a) with the " \mathbf{E}_{mol} " of Eq. (10.43) is legitimate only in the limit where the lattice spacing is much greater than the size of the spheres—so the formula can be expected to become increasingly inaccurate as f

approaches unity. However, note that $\varepsilon \rightarrow \infty$ as $f \rightarrow 1$, which is the appropriate limit for a homogeneous conductor in spite of the nonsensical model of filling all space with spheres. A more sophisticated analysis, and applications to microwave lenses, are given by Collin (Co91, Chap. 12).

10-19. (a) Let $y = p_0 E_{\text{mol}} / kT$, and $u = y \cos\theta$. Then we can write the denominator integral as:

$$\text{den} = \frac{2\pi}{y} \int_{-y}^{+y} e^u du = \frac{2\pi}{y} (e^{+y} - e^{-y}) = \frac{4\pi}{y} \sinh(y)$$

The numerator integral is:

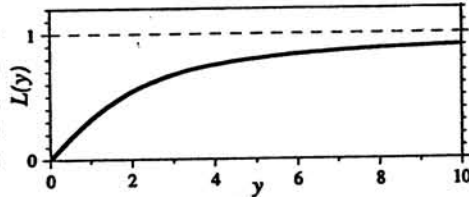
$$\begin{aligned} \text{num} &= \frac{2\pi}{y^2} \int_{-y}^{+y} u e^u du = \frac{2\pi}{y^2} [u e^u - e^u]_{-y}^{+y} \\ &= \frac{4\pi}{y^2} [y \cosh(y) - \sinh(y)] \end{aligned}$$

Thus the effective polarization is

$$\mathbf{P}(y) = \mathbf{P}_{\text{sat}} \left[\coth(y) - \frac{1}{y} \right] = \mathbf{P}_{\text{sat}} L(y)$$

where $\mathbf{P}_{\text{sat}} = Np_0 e_{\mathbf{E}}$ is the saturation polarization when all dipoles are aligned with the applied field.

(b) The Langevin function is similar to the familiar function $(1 - e^{-y})$, in that it starts from zero (for $y = 0$), increases linearly at first, and then approaches unity asymptotically as $y \rightarrow \infty$:



The power series for the hyperbolic cotangent is:

$$\coth(y) = \frac{1}{y} + \frac{y}{3} - \frac{y^3}{45} + \frac{2y^5}{945} - \dots$$

Thus the $1/y$ term cancels, and the first term of the Langevin power series is $y/3$.

(c) In the linear regime (weak field and/or high temperature), the permanent dipoles have an effective polarizability $P/NE_{\text{mol}} = p_0 y / 3E_{\text{mol}} = p_0^2 / 3kT$. Therefore, for a medium whose molecules are both deformable (induced polarization with polarizability

α_0) and alignable (with permanent moments p_0), we substitute $\alpha \rightarrow \alpha_0 + p_0^2 / 3kT$ in the Clausius-Mossotti formula, Eq. (10.49). By measuring the dielectric constant as a function of temperature and plotting $(\varepsilon - 1)/(\varepsilon + 1)$ against T , the two phenomena can be distinguished. In the dielectric case, both contributions are positive; in the magnetic analog, the two effects (dia- and paramagnetism, respectively) have opposite signs.

10-20. In the low-frequency, high-electron-density limit $\omega \ll \nu_c \ll \omega_p$, Eq. (10.68) becomes:

$$\begin{aligned} \hat{n} &= \sqrt{1 - \frac{\omega_p^2}{\omega(\omega + i\nu_c)}} \\ &= \sqrt{i} \sqrt{\frac{\omega_p^2}{\omega\nu_c} \left(\frac{1 - i \frac{\omega\nu_c}{\omega_p^2} - \frac{\omega^2}{\omega_p^2}}{1 - i \frac{\omega}{\nu_c}} \right)^{1/2}} \approx \frac{1+i}{\sqrt{2}} \sqrt{\frac{\omega_p^2}{\omega\nu_c}} \left(1 + i \frac{\omega}{2\nu_c} + \dots \right) \end{aligned} \quad (1)$$

The wavelength in the medium is given by

$$\frac{2\pi}{\lambda} = \frac{\omega}{c} \text{Re}[\hat{n}] \approx \frac{2\pi}{\lambda_0} \sqrt{\frac{\omega_p^2}{2\omega\nu_c}} \left(1 - \frac{\omega}{2\nu_c} + \dots \right) \quad (2)$$

where $\lambda_0 = 2\pi c / \omega$ is the free-space wavelength. The amplitude e -folding distance (attenuation length or skindepth) is given by

$$\begin{aligned} \frac{1}{\delta} &= \frac{\omega}{c} \text{Im}[\hat{n}] \approx \frac{2\pi}{\lambda_0} \sqrt{\frac{\omega_p^2}{2\omega\nu_c}} \left(1 + \frac{\omega}{2\nu_c} + \dots \right) \\ \delta &\approx \sqrt{\frac{2c^2\nu_c}{\omega\omega_p^2}} \left(1 - \frac{\omega}{2\nu_c} + \dots \right) \end{aligned} \quad (3)$$

Now from Eqs. (5.77–79), for highly conductive media, the complex index is related to the real dielectric constant ε and conductivity σ by

$$\hat{n} = \sqrt{\varepsilon} = \sqrt{\varepsilon + i \frac{4\pi\sigma}{\omega}} \quad (4)$$

So in this case, comparing (4) with the limiting value of (1), the conductivity is given by:

$$\frac{4\pi\sigma}{\omega} = \text{Im}[\hat{n}^2] \rightarrow \frac{\omega_p^2}{\omega\nu_c} \Rightarrow \sigma \approx \frac{\omega_p^2}{4\pi\nu_c} = \frac{Ne^2}{m\nu_c}$$

which agrees with Eq. (10.62) with the equivalence $\tau = 1/\nu_c$ [Eqs. (10.64) and (10.69)]. In terms of this conductivity, the leading term of (3) is

$$\delta \approx \sqrt{\left(\frac{2c^2\nu_c}{\omega\omega_p^2}\right)\left(\frac{\omega_p^2}{4\pi\nu_c\sigma}\right)} = \frac{c}{\sqrt{2\pi\sigma\omega}}$$

which agrees with Eq. (5.93) for nonmagnetic media.

10-21. The electron density is

$$N = \left(\frac{1 \text{ electron}}{\text{atom}}\right)\left(\frac{6.02 \cdot 10^{23} \text{ atoms/mole}}{22.4 \cdot 10^3 \text{ cm}^3/\text{mole}}\right)\left(\frac{10^{-3} \text{ torr}}{760 \text{ torr}}\right)\left(\frac{273 \text{ K}}{295 \text{ K}}\right)$$

$$= 3.27 \times 10^{13} \text{ electrons/cm}^3$$

From Eq. (10.69), the electron plasma frequency is

$$\frac{\omega_p}{2\pi} = \frac{1}{2\pi} \left(\frac{4\pi N e^2}{m}\right)^{1/2} = 51.3 \text{ GHz}$$

This is much higher than the wave frequency at 10 GHz. If we assume a negligible collision rate, we are in the evanescent domain. The refractive index of Eq. (10.68) is essentially pure-imaginary,

$$\hat{n} = n(1 + i\kappa) \rightarrow i \sqrt{\frac{\omega_p^2}{\omega^2} - 1} \approx i \frac{\omega_p}{\omega} = i 5.1$$

The wave amplitude decays as $\exp(-n\kappa\omega/c)$, and the penetration depth for 10% power is

$$\Delta z = \frac{\ln(10)}{2n\kappa\omega/c} \approx \frac{\ln(10)}{4\pi} \left(\frac{\omega}{\omega_p}\right) \lambda = 0.11 \text{ cm}$$

where $\lambda = 3.0 \text{ cm}$ is the wavelength of the incident wave in free space. Note that this attenuation occurs without energy dissipation. That is, if an antenna could be immersed in this plasma, it would not radiate; the signal would be totally reflected back along the feed line to the transmitter. If the wave were incident on the plasma from free space outside, it would be totally reflected at the boundary layer where the electron density equals $N_{\text{crit}}(\omega)$.

10-22. From Eq. (5.80), for instance, we have

$$\mathbf{B}_0 = \hat{n} \mathbf{e}_k \times \mathbf{E}_0$$

where \hat{n} is the complex refractive index, and $\mathbf{E}_0, \mathbf{B}_0$ are the vector field amplitudes of a wave propagating in the \mathbf{e}_k direction. Thus using the product theorem of Eq. (5.50), the time-averaged Poynting vector is

$$\langle \mathbf{S} \rangle = \frac{c}{8\pi} [\text{Re}] \mathbf{E} \times \mathbf{B}^*$$

$$= \frac{c}{8\pi} [\text{Re}] \hat{n} |E_0|^2$$

From Eq. (10.68), \hat{n} is purely imaginary for the evanescent domain such that $\nu_c \ll \omega < \omega_p$. Since the real part vanishes, the Poynting vector is zero.

10-23. Numerically, the electron plasma frequency is

$$\frac{\omega_p}{2\pi} = \frac{1}{2\pi} \left(\frac{4\pi N e^2}{m}\right)^{1/2} = 8979 \text{ Hz} \sqrt{N[\text{cm}^{-3}]}$$

For $N \sim 1 \text{ electron/cm}^3$, $\omega_p/2\pi \sim 9 \text{ kHz}$. Below this frequency, the electrons are able to move to shield the interior of a plasma-filled region from impinging electromagnetic waves. Above, the inertia of the electrons prevents this shielding.

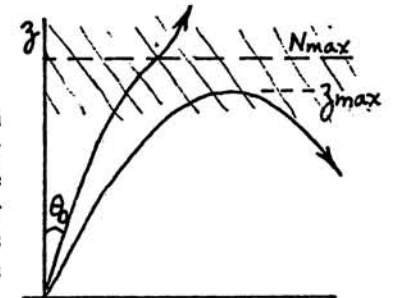
10-24. Converting the variables in Eq. (10.72),

$$N_{\text{crit}} = \left(\frac{m\omega^2}{4\pi e^2}\right)\left(\frac{e^2}{r_0 m c^2}\right)\left(\frac{2\pi c}{\omega\lambda_0}\right)^2 = \frac{\pi}{r_0 \lambda_0^2}$$

10-25. From Eq. (10.71), the refractive index for the ionosphere (neglecting collisions and the Earth's magnetic field!), is

$$n(z) = \sqrt{1 - \frac{N(z)}{N_{\text{crit}}}}$$

where $N(z)$ is the electron density as a function of altitude z , and N_{crit} is the electron density for which the plasma frequency equals the frequency of the radio wave, Eq. (10.72). For a beam (ray) launched at angle θ_0 at the Earth's surface, where the electron density is negligible, Snell's law [Eq. (6.20)] gives



$$\sin\theta_0 = \left[1 - \frac{N(z)}{N_{\text{crit}}}\right]^{1/2} \sin\theta(z)$$

As the electron density $N(z)$ becomes substantial, $\theta(z)$ increases; that is, the wave is refracted toward lower density. When $\theta(z) \rightarrow \pi/2$, the beam becomes horizontal and then continues back to the surface of the Earth. For this reflection from the ionosphere to occur, $N(z_{\text{max}})$ must be less than N_{max} ; thus,

$$\sin\theta_0 = \left[1 - \frac{N(z_{\text{max}})}{N_{\text{crit}}}\right]^{1/2} \sin\left(\frac{\pi}{2}\right)$$

$$N(z_{\text{max}}) = N_{\text{crit}} \cos^2\theta_0 < N_{\text{max}}$$

For given ionospheric conditions (N_{max}), we get reflection of the highest frequencies (largest N_{crit}) for large launch angles θ_0 , with the maximum effective $\theta_0 \approx 75^\circ$ at the lower boundary of the ionosphere. Thus reflection occurs for

$$N_{\text{crit}} \lesssim \frac{N_{\text{max}}}{\cos^2\theta_{0\text{max}}}$$

$$\Rightarrow \omega \lesssim \frac{\omega_p(N_{\text{max}})}{\cos\theta_{0\text{max}}} \approx 4\omega_p(N_{\text{max}})$$

For a typical value of $N_{\text{max}} \sim 10^6$ electrons/cm³, we have $\omega_p/2\pi \sim 9$ MHz, and wave frequencies below $\omega/2\pi \sim 36$ MHz are reflected. For vertical incidence, only frequencies below ~ 9 MHz are reflected.

Because the direct "ground wave" dies out rapidly, ionospheric reflection ("sky wave") is essential to long-distance radio communication. Radio waves launched at large θ_0 's are returned to Earth at a considerable distance from the transmitter, leaving a ring that receives negligible signal. To reach medium distances requires smaller θ_0 's, for which frequencies ~ 30 MHz will pass through the ionosphere and be lost.

10-26. From Prob. 10-16, the atomic density is

$$N = \frac{N_A \delta}{W}$$

where N_A is Avogadro's number, δ is the mass density (from *Handbook of Chemistry and Physics*), and W is the atomic weight. The critical wavelength λ_c corresponds to the electron plasma frequency ω_p of Eq. (10.69). If there were one electron per atom, then

$$\lambda_c = \frac{2\pi c}{\omega_p} = \left(\frac{\pi m c^2}{N e^2}\right) = \frac{3.34 \cdot 10^6 \text{ cm}^{-1/2}}{\sqrt{N}}$$

Since $\lambda_c \propto 1/\sqrt{N}$, the effective number of free electrons per atom is

$$\mathcal{N}_{\text{eff}} = \left[\frac{\lambda_c(\text{calc})}{\lambda_c(\text{obs})}\right]^2$$

	W	δ	$N(\text{calc})$	$\lambda_c(\text{calc})$	\mathcal{N}_{eff}
Li	6.94	0.534g/cm ³	4.63·10 ²² cm ⁻³	1.56·10 ⁻⁵ cm	0.58
Na	22.99	0.971	2.54	2.11	1.01
K	39.10	0.862	1.33	2.92	0.86
Rb	85.47	1.532	1.08	3.23	0.81
Cs	132.90	1.873	0.85	3.65	0.69

10-27. Equations (5.20–21) show how the operations of divergence and curl act on wavefunctions of the form of $\exp(i\mathbf{k}\cdot\mathbf{r})$ —namely, $\text{div} \rightarrow i\mathbf{k}\cdot$ and $\text{curl} \rightarrow i\mathbf{k}\times$. Therefore, we can write Maxwell's equations [Eqs. (4.21–24)] as:

$$\hat{\mathbf{k}} \cdot (\hat{\boldsymbol{\epsilon}} \cdot \mathbf{E}) = 0 \quad (1)$$

$$\hat{\mathbf{k}} \cdot \mathbf{B} = 0 \quad (2)$$

$$\hat{\mathbf{k}} \times \mathbf{E} = \frac{\omega}{c} \mathbf{B} \quad (3)$$

$$\hat{\mathbf{k}} \times \mathbf{B} = -\frac{\omega}{c} \hat{\boldsymbol{\epsilon}} \cdot \mathbf{E} \quad (4)$$

[The free current $\mathbf{J}_f = \sigma\mathbf{E}$, driven by the electric field, and the associated free charge ρ_f determined by the equation of continuity, $i\omega\rho_f = \text{div}\mathbf{J}_f = \sigma \text{div}\mathbf{E}$, are hidden inside the imaginary (conductive) part of $\hat{\boldsymbol{\epsilon}}$. We assume that no other free sources are present.] Now cross $\hat{\mathbf{k}}$ into (3), and then substitute (4):

$$\hat{\mathbf{k}} \times (\hat{\mathbf{k}} \times \mathbf{E}) = \frac{\omega}{c} \hat{\mathbf{k}} \times \mathbf{B} = -\frac{\omega^2}{c^2} \hat{\boldsymbol{\epsilon}} \cdot \mathbf{E}$$

Writing the propagation constant $\hat{\mathbf{k}}$ in terms of the refractive index $\hat{\mathbf{n}} = (c/\omega)\hat{\mathbf{k}}$, we have

$$\hat{\mathbf{n}} \times (\hat{\mathbf{n}} \times \mathbf{E}) = -\hat{\boldsymbol{\epsilon}} \cdot \mathbf{E}$$

The left-hand side expands to $(\hat{\mathbf{n}}\cdot\mathbf{E})\hat{\mathbf{n}} - (\hat{n})^2\mathbf{E}$. Because of the anisotropy, we no longer have $\hat{\mathbf{n}}\cdot\mathbf{E} = 0$, in general; nor can we cancel out the \mathbf{E} . As noted, when \mathbf{E} is written out in terms of its Cartesian components, we have three coupled, linear,

homogeneous, algebraic equations for those components. The determinant of the coefficients must vanish, giving the dispersion relation which relates the three components of $\hat{\mathbf{n}}$ to the nine elements of $\hat{\boldsymbol{\epsilon}}$. To solve the determinantal equation, let $\hat{\mathbf{n}} = \hat{n} \mathbf{e}_n$, where $\mathbf{e}_n = (\alpha, \beta, \gamma)$ is the unit vector in the direction of propagation (thus $\alpha^2 + \beta^2 + \gamma^2 = 1$). For a given \mathbf{e}_n , the dispersion relation is then a biquadratic, i.e., a quadratic in \hat{n}^2 .

10-28. The refractive indices for the two circular polarizations, neglecting collisions, are given by Eq. (10.78),

$$\hat{n}_{\pm}^2 = 1 - \frac{\omega_p^2}{\omega^2 \pm \omega \omega_c}$$

(The case of no magnetic field follows with $\omega_c \rightarrow 0$.) Since \hat{n}_{\pm}^2 is either positive- or negative-real (neglecting collisions), propagation is either unattenuated or evanescent. Conditions when the refractive index goes to zero are conventionally called *cutoffs*; conditions when its magnitude goes to positive infinity are called *resonances*. In this case the cutoffs occur for

$$\left. \begin{matrix} \omega_1 \\ \omega_2 \end{matrix} \right\} = \frac{\mp \omega_c + \sqrt{\omega_c^2 + 4\omega_p^2}}{2}$$

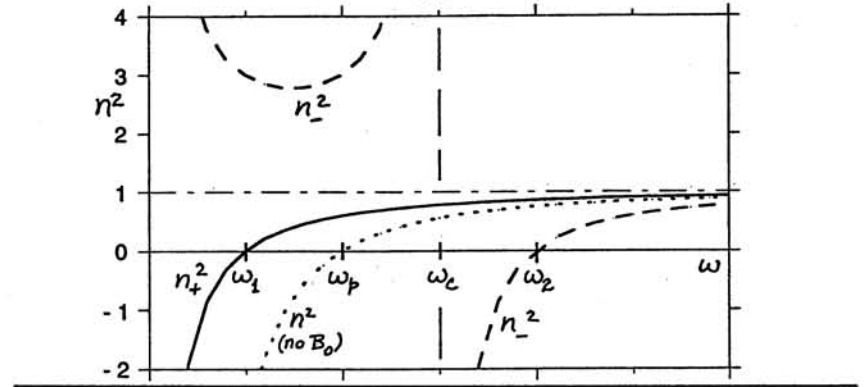
with the subscripts 1 and 2 standing for the smaller and larger cutoff roots (corresponding to the upper and lower sign, respectively). We have the following table of cutoffs and resonances:

	cutoff	resonance
upper sign	$\omega = \omega_1$	(none*)
lower sign	$\omega = \omega_2$	$\omega = \omega_c$ ($\omega \rightarrow 0$)
no B_0	$\omega = \omega_p$	(none)

The resonance for $\omega \rightarrow 0$ is nonphysical because our model has neglected collisions and the motion of the positive ions (*when ion motions are included, there is an upper-sign resonance at the *ion* cyclotron frequency). Propagation can be described in terms of frequency bands as follows:

ω	upper sign	lower sign
$< \omega_1$	evanescent	propagating
$\omega_1 \leftrightarrow \omega_c$	propagating	propagating
$\omega_c \leftrightarrow \omega_2$	propagating	evanescent
$> \omega_2$	propagating	propagating

When there is no magnetic field, we have $\omega_1, \omega_2 \rightarrow \omega_p$. The wave is then evanescent for $\omega < \omega_p$, and propagating for $\omega > \omega_p$. The graph following illustrates n^2 numerically for the special case of $\omega_c = \frac{3}{2}\omega_p$.



10-29. (a) As in Eq. (10.20), the binding of the electrons to the atoms adds the Hooke's-law term $K\mathbf{r}$ to the equation of motion (10.73),

$$m\ddot{\mathbf{r}} + K\mathbf{r} = -e\mathbf{E} - \frac{e}{c}\dot{\mathbf{r}} \times \mathbf{B}_0$$

But with $\ddot{\mathbf{r}} = -\omega^2\mathbf{r}$ and $\omega_0^2 = K/m$, we can write this equation as

$$m\left(1 - \frac{\omega_0^2}{\omega^2}\right)\ddot{\mathbf{r}} = -e\mathbf{E} - \frac{e}{c}\dot{\mathbf{r}} \times \mathbf{B}_0$$

That is, all of the analysis of Sec. 10.5 can be retained if we simply substitute $m \rightarrow m(1 - \omega_0^2/\omega^2)$, from which [Eqs. (10.69) and (10.77)]:

$$\omega_p^2 \rightarrow \omega_p^2 \left(\frac{\omega^2}{\omega^2 - \omega_0^2} \right) \quad \omega_c \rightarrow \omega_c \left(\frac{\omega^2}{\omega^2 - \omega_0^2} \right)$$

Therefore, Eq. (10.78) becomes [with the original definitions of ω_p and ω_c]

$$\hat{n}_{\pm}^2 = 1 - \frac{\omega_p^2}{\omega^2 - \omega_0^2 \pm \omega \omega_c}$$

(b) As discussed near the end of Sec. 10.5, a linearly polarized wave can be represented as a superposition of two counter-rotating circularly polarized waves, which in this case travel at different speeds. Consequently, their relative phase changes as they propagate through the plasma, and the superposition constitutes a linear polarization whose plane gradually rotates.

(c) Introducing the mean index \bar{n} and the difference $\Delta n = n_+ - n_-$, the two indices can then be approximated by

$$\begin{aligned} n_{\pm}^2 &\approx \bar{n}^2 \pm 2\bar{n}\Delta n \\ &= 1 - \frac{\omega_p^2}{\omega^2 - \omega_0^2} \left(1 \pm \frac{\omega\omega_c}{\omega^2 - \omega_0^2} \right)^{-1} \approx 1 + \frac{\omega_p^2}{\omega_0^2 - \omega^2} \pm \frac{\omega_p^2\omega\omega_c}{(\omega_0^2 - \omega^2)^2} \end{aligned}$$

where the final approximation follows so long as $\omega\omega_c \ll |\omega^2 - \omega_0^2|$, which is consistent with the hierarchy for optical frequencies in typical materials in laboratory magnetic fields. Thus for the propagation constants,

$$k_{\pm} = \bar{k} \pm \Delta k = \frac{\omega}{c} (\bar{n} \pm \Delta n)$$

we have

$$\begin{aligned} \Delta k &= \frac{\Delta n}{\bar{n}} \bar{k} \approx \frac{1}{2} \left(\frac{\omega_0^2 - \omega^2}{\omega_0^2 - \omega^2 + \omega_p^2} \right) \left(\frac{\omega_p^2\omega\omega_c}{(\omega_0^2 - \omega^2)^2} \right) \bar{k} \\ &= \frac{\omega_p^2\omega\omega_c}{2(\omega_0^2 - \omega^2 + \omega_p^2)(\omega_0^2 - \omega^2)} \bar{k} \end{aligned}$$

Now consider a wave that is linearly polarized along \mathbf{e}_x at $z=0$. From Eqs. (5.36), we can write this wave as a superposition of two circular polarizations as

$$\begin{aligned} E_x &= \frac{1}{2} E_0 [e^{i(k_+z - \omega t)} + e^{i(k_-z - \omega t)}] \\ &= E_0 e^{i(\bar{k}z - \omega t)} \cos(\Delta k z) \\ E_y &= i \frac{1}{2} E_0 [-e^{i(k_+z - \omega t)} + e^{i(k_-z - \omega t)}] \\ &= E_0 e^{i(\bar{k}z - \omega t)} \sin(\Delta k z) \end{aligned}$$

Thus, in a propagation distance L , the plane of polarization rotates (in the same sense as electron gyration) by the angle

$$\Delta\theta = \Delta k L \approx \frac{\omega_p^2\omega\omega_c}{2(\omega_0^2 - \omega^2 + \omega_p^2)(\omega_0^2 - \omega^2)} \bar{k}L$$

Since $\omega_c = eB_0/mc$, the Verdet constant for this model is

$$V = \frac{\omega_p^2\omega^2(e/mc^2)\bar{n}}{2(\omega_0^2 - \omega^2 + \omega_p^2)(\omega_0^2 - \omega^2)}$$

The corresponding result for a plasma is obtained by letting $\omega_0 \rightarrow 0$, with the frequencies now ordered as $\omega^2 > \omega_p^2 \gg \omega_c^2$.

10-30. (a) Before the displacement, the uniform electron density corresponds to a negative charge density of $-N_0e$, which is neutralized by a background of fixed positive charges (atomic ions) with the charge density $+N_0e$. In a slab of thickness dx , the perturbation $\xi(x)$ produces an incremental electron charge density of $\delta N = -N_0d\xi/dx$. Since the net charge density was originally zero, the perturbed charge density is $\rho = -e\delta N$, and we can write Gauss' law as:

$$\text{div } \mathbf{E} = 4\pi\rho \implies \frac{dE_x}{dx} = 4\pi N_0 \frac{d\xi}{dx}$$

which integrates immediately to $E_x = 4\pi N_0e \xi$ (the constant goes to zero because we assume there is no field in the absence of a perturbation). The electric force on each electron is then

$$F_x = -eE_x = -4\pi N_0e^2 \xi$$

which indeed has the form of a Hooke's-law restoring force.

(b) Neglecting any damping forces, $F = ma$ can be written for the typical electron as

$$m\ddot{\xi} + 4\pi N_0e^2 \xi = F_{\text{ext}} \quad (1)$$

where F_{ext} is the external force producing the initial perturbation. When F_{ext} is suddenly removed, the reduced form of (1) is the standard differential equation for simple-harmonic motion, $\ddot{\xi} + \omega_p^2 \xi = 0$. Physically, each layer of displaced electrons is attracted back toward its equilibrium position; then, because of the electrons' inertia, each layer overshoots the equilibrium and oscillates at the plasma frequency ω_p .

10-31. (a) Far from the perturbing charge Q , the electrons have density N_0 , and we take the scalar potential to be $\Phi = 0$. Therefore the density of electrons near Q is $N(r) = N_0 \exp(e\Phi/kT) \approx N_0(1 + e\Phi/kT + \dots)$, where Φ is the locally perturbed potential. If we assume that the neutralizing positive charge is effectively immobile,

equivalent to the constant density N_0 , then the net charge density in the vicinity of Q becomes $\rho = -e(N - N_0) \approx -N_0 e^2 \Phi / kT$. Poisson's equation for spherical symmetry reduces to:

$$\nabla^2 \Phi = -4\pi\rho \quad \Rightarrow \quad \frac{1}{r^2} \frac{d}{dr} \left(r^2 \frac{d\Phi}{dr} \right) = \frac{4\pi N_0 e^2}{kT} \Phi$$

For the suggested form of solution,

$$\begin{aligned} \frac{1}{r^2} \frac{d}{dr} \left(r^2 \frac{d}{dr} \frac{Q e^{-r/\lambda_D}}{r} \right) &= \frac{1}{r^2} \frac{d}{dr} \left[r^2 Q e^{-r/\lambda_D} \left(-\frac{1}{r^2} - \frac{1}{r\lambda_D} \right) \right] \\ &= \frac{Q e^{-r/\lambda_D}}{r^2} \left(\frac{1}{\lambda_D} - \frac{1}{\lambda_D} + \frac{r}{\lambda_D^2} \right) = \frac{Q e^{-r/\lambda_D}}{r\lambda_D^2} \end{aligned}$$

Therefore, the suggested solution works if we define the parameter λ_D such that

$$\lambda_D^2 = \frac{kT}{4\pi N_0 e^2}$$

The result is the ordinary potential of Q , Q/r , shielded by the exponential factor $\exp(-r/\lambda_D)$. At distances beyond a few Debye lengths λ_D , the plasma electrons hide the presence of the excess charge Q . For further discussion, see Meyer-Vernet, *Am.J.Phys.* **61**, 249 (1993).

(b) We have

$$\lambda_D \omega_p = \sqrt{\left(\frac{kT}{4\pi N_0 e^2} \right) \left(\frac{4\pi N_0 e^2}{m} \right)} = \sqrt{\frac{kT}{m}}$$

There are several "thermal velocities" for a Maxwellian distribution—the average, the root-mean-square, and the most probable—all of which have the form $\sqrt{kT/m}$ but with slightly different numerical coefficients depending upon the criterion used to quantify the distribution. Thus, aside from the precise criterion chosen, this is indeed the "thermal velocity" for the electron gas (note that m is the electron mass, not that of a neutral gas molecule). Since the velocity of sound in a neutral gas is also of order $\sqrt{kT/m}$, we can surmise that plasma oscillations at the cyclic frequency $\omega_p/2\pi$ can propagate as traveling waves with a wavelength of the order of $2\pi\lambda_D$.

10-32. (a) A damped harmonic oscillator, driven at frequency ω , obeys the equation

$$\ddot{r} + 2\beta\dot{r} + \omega_0^2 r = A e^{-i\omega t}$$

where, in this case, we evaluate the damping coefficient as $2\beta = \mathcal{U}m = 2e^2\omega_0^2/3mc^3$. The steady-state solution is:

$$r = \frac{A}{(\omega_0^2 - \omega^2) - i 2\beta\omega} e^{-i\omega t}$$

the amplitude of which is

$$\frac{A}{[(\omega_0^2 - \omega^2)^2 - (2\beta\omega)^2]^{1/2}} \xrightarrow{\beta \ll \omega^2} \frac{A/2\omega_0}{[(\omega_0 - \omega)^2 + \beta^2]^{1/2}}$$

The half-power frequencies are then given by $\omega_0 - \omega = \pm\beta$, and the width of the resonance is

$$\Delta\omega = 2\beta = \frac{2e^2\omega_0^2}{3mc^3}$$

(b) In terms of wavelength, $\lambda = 2\pi c/\omega$,

$$\Delta\lambda = (-) \frac{2\pi c}{\omega^2} \Delta\omega = \frac{4\pi e^2}{3mc^2} = \frac{4\pi}{3} r_0$$

$$= 1.18 \times 10^{-12} \text{ cm} = 1.18 \times 10^{-4} \text{ \AA}$$

Note that ω_0 has canceled out, so that this "natural linewidth" is independent of the x-ray wavelength λ_0 .

Chapter 11

11-1. In the coordinate system of Fig. 6-2, the incident and reflected wave vectors are

$$\mathbf{k}_0 = [\mathbf{e}_x (-\sin\alpha) + \mathbf{e}_z (\cos\alpha)] k$$

$$\mathbf{k}_1 = [\mathbf{e}_x (-\sin\alpha) + \mathbf{e}_z (-\cos\alpha)] k$$

With \mathbf{E} perpendicular to the plane of incidence (Fig. 6-3) and for reflection from a perfect conductor ($n_2 \rightarrow \infty$), Eq. (6.26) gives $E_1^0 = -E_0^0$. Thus,

$$\mathbf{E}_{0\perp} = -\mathbf{e}_y E_0^0 \exp[i(-kx \sin\alpha + kz \cos\alpha - \omega t)]$$

$$\mathbf{E}_{1\perp} = +\mathbf{e}_y E_0^0 \exp[i(-kx \sin\alpha - kz \cos\alpha - \omega t)]$$

The photographic emulsion is sensitive to

$$\begin{aligned} \langle |\mathbf{E}_{0\perp} + \mathbf{E}_{1\perp}|^2 \rangle &= \langle |\mathbf{e}_y E_0^0 [-2i \sin(kz \cos\alpha)] \exp[i(-kx \sin\alpha - \omega t)]|^2 \rangle \\ &= 2 (E_0^0)^2 \sin^2(kz \cos\alpha) \end{aligned}$$

Because of the square, the periodicity Δz of the distance of the blackened strips from the reflecting plane is given by

$$k \Delta z \cos\alpha = \pi \quad \Rightarrow \quad \Delta z = \frac{\lambda}{2 \cos\alpha} \quad (1)$$

Thus, for $\alpha = 45^\circ$, the blackened strips are farther apart by the factor $1/\cos(45^\circ) = \sqrt{2}$, compared with normal incidence [$1/\cos(0) = 1$, Eq. (11.4)].

For \mathbf{E} parallel to the plane of incidence (Fig. 6-4), we have from Eq. (6.32) for reflection from a perfect conductor

$$\mathbf{E}_{0\parallel} = (\mathbf{e}_x \cos\alpha + \mathbf{e}_z \sin\alpha) E_0^0 \exp[i(-kx \sin\alpha + kz \cos\alpha - \omega t)]$$

$$\mathbf{E}_{1\parallel} = (-\mathbf{e}_x \cos\alpha + \mathbf{e}_z \sin\alpha) E_0^0 \exp[i(-kx \sin\alpha - kz \cos\alpha - \omega t)]$$

$$\begin{aligned} \langle |\mathbf{E}_{0\parallel} + \mathbf{E}_{1\parallel}|^2 \rangle &= 2 (E_0^0)^2 [\cos^2\alpha \sin^2(kz \cos\alpha) + \sin^2\alpha \cos^2(kz \cos\alpha)] \\ &= 2 (E_0^0)^2 [\cos 2\alpha \sin^2(kz \cos\alpha) + \sin^2\alpha] \quad \alpha \rightarrow 45^\circ \quad (E_0^0)^2 \end{aligned}$$

Here the \mathbf{E}_x and \mathbf{E}_z components produce respective interference patterns that interlace. In general the components are of unequal amplitude, but for $\alpha = 45^\circ$ the components are equal and the total $\langle |\mathbf{E}_{\parallel}|^2 \rangle$ is spatially uniform. This result may be understood geometrically by noting that, for this particular angle of incidence, the incident and reflected \mathbf{E}_{\parallel} fields are orthogonal and thus have the resultant (peak) amplitude of $\sqrt{2}E_0^0$ at all locations (time-averaging the square of the field then removes the factor of 2).

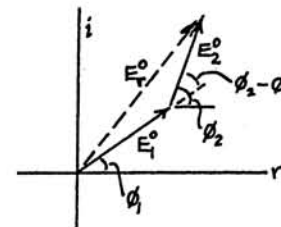
The effects are reversed for the magnetic fields. An additional experiment by Wiener used this fact as further proof that photochemical processes depend upon the *electric* field. See Born and Wolf (Bo80, Sec. 7.4).

11-2. The oscillating function

$$[\text{Re}] \bar{A} e^{-i\omega t} = [\text{Re}] A^0 e^{i\phi} e^{-i\omega t} = A^0 \cos(\omega t - \phi)$$

where $\bar{A} = A^0 e^{i\phi}$ is a complex amplitude (carrying phase information), can be visualized as a radius vector of length A^0 rotating clockwise in time in the complex plane. The orientation at $t = 0$ is determined by the phase ϕ . The projection on the real axis is the physical meaning. The operation of adding two-dimensional vectors commutes with the operation of projecting them onto the real axis. Therefore, if we wish to add two or more oscillatory quantities, of different amplitudes and phases but of the same frequency, we can first add them as vectors in the complex plane (at a particular instant of time and, in the case of waves, at a particular position in space). Then the projection of this resultant rotating vector on the real axis is the desired sum of real parts.

For example, the adjacent diagram represents the sum of the two fields of Eqs. (11.5). By the law of cosines, the square of the resultant amplitude is

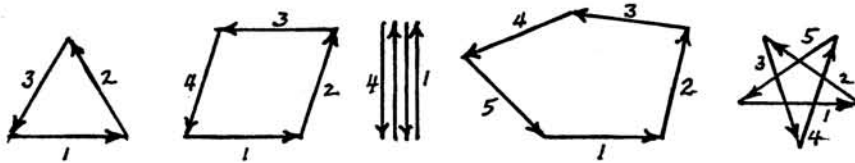


$$(E_r^0)^2 = (E_1^0)^2 + (E_2^0)^2 - 2 E_1^0 E_2^0 \cos[\pi - (\phi_2 - \phi_1)]$$

With $\cos[\pi - (\phi_2 - \phi_1)] = -\cos(\phi_2 - \phi_1) = -\cos(\Delta\phi)$, and the intensity definitions of Eqs. (11.9–10), we obtain Eq. (11.13).

11-3. Let's agree that $\phi_1 \equiv 0$, that the phases are numbered in order of increasing magnitude, and that the increment from one phase to the next is no more than 180° —thus restricting the phasor diagram to a "convex" polygon. We will not count as

distinct a rearrangement of the order, nor the possibility of adding an arbitrary multiple of 360° to any of the phases. Equal amplitudes obviously require phasor arrows of the same length. (a) A null resultant requires that the three arrows, placed head-to-tail, close to form a triangle. There is only one way to do this under our rules: an equilateral triangle. The phases of the waves are uniquely $0, 120^\circ, 240^\circ$. (b) For a null with four phasor arrows of equal length, we have an equal-sided parallelogram, with the phases $0, \phi_2$ (arbitrary but less than 180°), 180° , and $\phi_2 + 180^\circ$ (the special case of $0, 180^\circ, 360^\circ, 540^\circ$ is a reordering of $\phi_2 = 180^\circ$). With five arrows, there are two classes of configurations, each with two degrees of freedom, in general: the possible deformations of a convex pentagon, or of a "star" configuration. Etc., ...



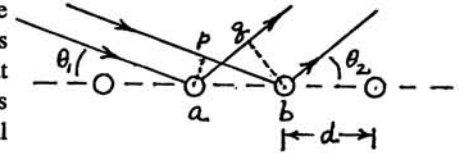
11-4. Consider the displacements of the virtual sources in Figs. 11-9(a-c) as the real source S is displaced toward the top of the diagram. In frames (a) and (b), the virtual sources, S_1 and S_2 , are displaced by nearly equal amounts—both downward in frame (a), both upward in (b) [the figures exaggerate the angles involved]. Thus the interference pattern at Q keeps the same fringe spacing, but the entire pattern is displaced. For a primary source whose width is comparable with the fringe spacing, the pattern at Q is smeared out.

In the case of Lloyd's mirror, frame (c), upward displacement of the real source S displaces the virtual source (below the mirror, not shown) downward. Accordingly, the spacing of the fringes at the observation plane changes (decreases) somewhat, but the center of the pattern at Q_1 is not displaced. The fringe visibility degrades as the observation point moves toward Q_2 , but the fringes remain distinct near Q_1 .

An alternative way to state the same argument is to note that, in the case of frames (a) and (b), the path lengths from the virtual sources to Q change in opposite ways (one increases, the other decreases), and thus the differential path changes significantly. In frame (c), both paths change in the same way, and the differential path remains constant to first order. This topic is discussed by Born and Wolf (Bo80, Secs. 7.3.2 and 7.3.4).

11-5. (a) We draw rays representing a plane wave incident at the glancing angle θ_1 , and reflected as a plane wave at the angle θ_2 . Let the distance between adjacent atoms be d . The incoming wavefront coinciding with atom a intersects the other ray at

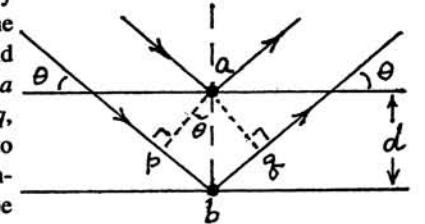
the point p , and the outgoing wavefront coinciding with atom b intersects the other ray at the point q . If the scatterings are to interfere constructively in that direction, then the respective path-lengths \overline{pb} and \overline{aq} must differ by an integral number of wavelengths,



$$\overline{pb} - \overline{pb} = d (\cos\theta_1 - \cos\theta_2) = \pm m\lambda$$

where m is an integer or zero. If d is much larger than λ , there can be several values of θ_2 for a particular choice of θ_1 . But when $d \approx \lambda$, typically, the only condition for constructive reflection is with $m = 0$ —that is, $\theta_2 = \theta_1$, the usual equal-angle condition for specular reflection. With the whole plane of atoms spaced uniformly, all scatterings are in-phase and add coherently, giving a substantial reflected amplitude even when the scattering by a single atom is tiny. Note that the equal-angle condition is independent of the atom-spacing d . Furthermore, it holds for constructive interference from a two-dimensional array of atoms in the reflecting plane even when a principal axis of the array is oblique to the plane of incidence.

(b) Now we have two planes, separated by the distance d [which may or may not be the same as in Part (a)]. The incoming and outgoing wavefronts coinciding with atom a intersect the other rays at the points p and q , respectively. Now, if the scatterings are to interfere constructively, then the excess path-length by way of atom b (that is, \overline{pbq}) must be an integral number, m , of wavelengths,



$$\overline{pbq} = 2\overline{pb} = 2d \sin\theta = m\lambda$$

If many planes are equally spaced, the reflections from all planes will add constructively. Combining Parts (a) and (b), we have the conditions for the constructive interference of scatterings from every atom of the three-dimensional array. The convention of measuring angles from the crystal planes rather than their normal (thus giving a sine rather than a cosine in the Bragg formula) is in fact consistent with the convention of measuring from the normal to a one-dimensional diffraction grating, as in Sec. 11.8 [compare Eq. (11.62), and Prob. 11-14]: the normal of the crystal's "grating" is tangential to the crystal planes. The conditions for constructive reflection from a three-dimensional grating are more restrictive than for a one- or two-dimensional grating in the sense that only a discrete set of incident angles work. See further discussion in, for instance, (El85, Sec. 10.10).

11-6. From Eq. (11.42), the transverse coherence length of visible light from the Sun is

$$L_{tc} = \frac{\lambda}{\Delta\Theta_s} \sim \frac{500 \text{ nm}}{0.009 \text{ rad}} = 0.06 \text{ mm}$$

Thus the pinholes would need to be closer together than this small distance. Alternatively, the Sun's light could be "spatially filtered" by a single pinhole used as a secondary source to provide a much smaller $\Delta\Theta_s$ (see Fig. 11-14). The Sun's light is of course broadband: for visible light, the longitudinal coherence length [Eq. (11.40)] is of the order of one wavelength. Thus the "white-light" interference fringes wash out quickly beyond first order, unless a wavelength-selective filter is used.

11-7. As discussed following Eq. (11.37), the interferometer can be adjusted to give either circular fringes ("bull's-eye" pattern) or parallel-linear fringes. Moving the mirror moves the fringes; a particular pattern is essentially duplicated by a mirror displacement of $\lambda/2 = 295 \text{ nm}$ —the periodicity of the primary intensity variations of Fig. 11-15. With the Na doublet, for certain path differences Δ the bright fringes of one component coincide with those of the other component (left and right margins of Fig. 11-15), while for other Δ 's the bright fringes interlace and the "visibility" of the interference disappears (center of Fig. 11-15). The analysis leading to Eq. (11.47) applies, with $\varepsilon = \frac{1}{2}(k_2 - k_1) \approx \pi(\Delta\lambda)/\lambda^2$. But note that the periodicity of the envelope occurs for an increment in $\varepsilon\Delta$ of π (not 2π). Thus a full cycle from full visibility back to full (or from non-visibility back to non-visibility) requires a mirror displacement ($= \Delta/2$) of $\pi/2\varepsilon = \lambda^2/2(\Delta\lambda) = (589)^2/2(0.597) = 0.291 \text{ mm}$. The numerics plotted in Fig. 11-15 are for $k_0/\varepsilon = 16.3$; for the Na doublet, $k_0/\varepsilon = 2\lambda/\Delta\lambda = 1974$ —that is, the Na case has vastly more fringes between visibility nulls.

11-8. From Eq. (11.56),

$$V(\Delta) = \frac{\sqrt{C^2 + S^2}}{P}$$

Therefore, Eq. (11.52) can be written

$$\begin{aligned} J(\Delta) &= P \left\{ 1 + V(\Delta) \left[\frac{C}{\sqrt{C^2 + S^2}} \cos k_0 \Delta - \frac{S}{\sqrt{C^2 + S^2}} \sin k_0 \Delta \right] \right\} \\ &= P [1 + V(\Delta) \cos(\theta + k_0 \Delta)] \end{aligned}$$

where $\tan\theta = S/C$. The envelope is obtained by putting $\cos(\theta + k_0 \Delta) \rightarrow 1$, so that

$$\frac{J(\Delta)}{P} = 1 + V(\Delta)$$

Thus $V(\Delta)$ is the envelope of the normalized intensity curve $J(\Delta)/P$, measured against its average value of unity.

11-9. Using Eq. (11.49),

$$\begin{aligned} J(\Delta) - \frac{1}{2}J(0) &= 2 \int_0^\infty I_0(k) [1 + \cos k \Delta] dk - \int_0^\infty I_0(k) (2) dk \\ &= 2 \int_0^\infty I_0(k) \cos k \Delta dk \end{aligned}$$

The Fourier transform, Eq. (B.12a), is then

$$A(k) = 2 \int_{-\infty}^{+\infty} \left[\int_0^\infty I_0(k') \cos k' \Delta dk' \right] e^{ik\Delta} d\Delta$$

We can interchange the order of integration if we distinguish the dummy variable $k \rightarrow k'$ in the k -integration from the coefficient k of Δ in the complex exponential of the transform integration (this latter k remains as the argument of the final result). Consider the integral,

$$\int_{-\infty}^{+\infty} \cos k' \Delta e^{ik\Delta} d\Delta = \frac{1}{2} \int_{-\infty}^{+\infty} [e^{i(k+k')\Delta} + e^{i(k-k')\Delta}] d\Delta$$

In turn, consider

$$\int_{-\infty}^{+\infty} e^{im\Delta} d\Delta = \lim_{D \rightarrow \infty} \frac{1}{im} (e^{imD} - e^{-imD}) = 2 \lim_{D \rightarrow \infty} \frac{\sin mD}{m}$$

This limit is zero unless $m = 0$, in which case it blows up. That is, it has the properties of the Dirac delta function $\delta(m)$ discussed in Sec. 1.9. To normalize the delta function in accordance with Eq. (1.97), we find from tables [e.g., Dwight §858.601] that $\int_0^\infty (\sin mD/m) dm = \frac{\pi}{2}$, 0, or $-\frac{\pi}{2}$, as D is positive, zero, or negative. Since the integrand is an even function, it follows that (for $D > 0$)

$$\int_{-\infty}^{+\infty} \frac{\sin mD}{m} dm = \pi \quad \text{whence} \quad \lim_{D \rightarrow \infty} \frac{\sin mD}{m} \leftrightarrow \pi \delta(m)$$

Finally we put the pieces together to establish that

$$\int_{-\infty}^{+\infty} \cos k' \Delta e^{ik\Delta} d\Delta = \pi [\delta(k+k') + \delta(k-k')]$$

Consequently, the Fourier transform becomes, using Eq. (1.98),

$$A(k) = 2\pi \int_0^{\infty} I_0(k') \delta(k-k') dk' = 2\pi I_0(k)$$

Thus a numerical calculation of the Fourier transform of an experimental measurement of $J(\Delta) - \frac{1}{2}J(0)$ yields the spectral intensity function I_0 to within a scale factor.

11-10. The situation is shown in Fig. 11-16(d). We have

$$I_0(\xi) = I_0 \left\{ \exp\left[-\left(\xi + \frac{3\delta k}{2}\right)^2/\alpha^2\right] + \exp\left[-\left(\xi - \frac{3\delta k}{2}\right)^2/\alpha^2\right] \right\}$$

where $\alpha^2 = (\delta k)^2/4 \ln 2$ as in Case II of the Example. Let $u = \xi \pm 3\delta k/2$. Then for the respective Gaussian curves, from Eq. (11.53a),

$$\begin{aligned} P &= P_+ + P_- = 4 I_0 \int_{-\infty}^{+\infty} \exp\left(-\frac{u^2}{\alpha^2}\right) du \\ &= 4 \sqrt{\pi} \alpha I_0 \end{aligned}$$

(using tables, such as Dwight §860.11). Similarly,

$$C_{\pm}(\Delta) = 2 I_0 \int_{-\infty}^{+\infty} \exp\left(-\frac{u^2}{\alpha^2}\right) \cos(u\Delta \mp 3\delta k \Delta/2) du$$

Expand the cosine by the formula for sums of angles (e.g., Dwight §401.03-04) and use the fact that the cosine and sine are even and odd functions, respectively, to reduce the integral to

$$\begin{aligned} &= 4 I_0 \cos\left(\frac{3\delta k \Delta}{2}\right) \int_0^{\infty} \exp\left(-\frac{u^2}{\alpha^2}\right) \cos(u\Delta) du \\ &= 2 \sqrt{\pi} \alpha I_0 \exp\left(-\frac{\alpha^2 \Delta^2}{4}\right) \cos\left(\frac{3\delta k \Delta}{2}\right) \end{aligned}$$

(Dwight §861.20). A similar argument gives

$$S_{\pm} = \mp 2 \sqrt{\pi} \alpha I_0 \exp\left(-\frac{\alpha^2 \Delta^2}{4}\right) \sin\left(\frac{3\delta k \Delta}{2}\right)$$

Thus $C = C_+ + C_- = 2C_{\pm}$, and $S = S_+ + S_- = 0$. Finally,

$$V(\Delta) = \frac{\sqrt{C^2 + S^2}}{P} = \exp\left(-\frac{\alpha^2 \Delta^2}{4}\right) \left| \cos\left(\frac{3\delta k \Delta}{2}\right) \right|$$

which is the visibility curve plotted in Fig. 11-16(d).

11-11. The intensity distribution function is

$$I_0(\xi) = I_0 \left\{ \exp\left(-\frac{\xi^2}{\alpha^2}\right) + \frac{1}{2} \exp\left[-\frac{(\xi - 2\delta k)^2}{\alpha^2}\right] \right\}$$

where $\alpha = (\delta k)^2/4 \ln 2$. We use the subscripts 1 and 2 to distinguish the two components. The integrations are similar to those for Prob. 11-10. We get:

$$P = P_1 + P_2 = \left(1 + \frac{1}{2}\right) 2 I_0 \int_{-\infty}^{+\infty} \exp\left(-\frac{u^2}{\alpha^2}\right) du = 3 \sqrt{\pi} \alpha I_0$$

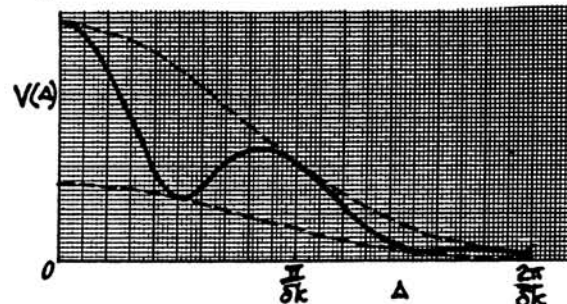
$$C = C_1 + C_2 = \left[1 + \frac{1}{2} \cos(2\delta k \Delta)\right] 2 \sqrt{\pi} \alpha I_0 \exp\left(-\frac{\alpha^2 \Delta^2}{4}\right)$$

$$S = S_1 + S_2 = \left[0 + \frac{1}{2} \sin(2\delta k \Delta)\right] 2 \sqrt{\pi} \alpha I_0 \exp\left(-\frac{\alpha^2 \Delta^2}{4}\right)$$

Finally,

$$V(\Delta) = \frac{\sqrt{C^2 + S^2}}{P} = \left[\frac{5}{4} + \cos(2\delta k \Delta)\right]^{1/2} \frac{2}{3} \exp\left(-\frac{\alpha^2 \Delta^2}{4}\right)$$

The function oscillates between the envelope curves $\exp(-\alpha^2 \Delta^2/4)$ and $\frac{1}{3} \exp(-\alpha^2 \Delta^2/4)$.



11-12. The sum of a finite geometric series can be proved by induction to be

$$a + au + au^2 + \dots + au^{n-1} = \frac{a(1-u^n)}{1-u}$$

In this case, $a \rightarrow 1$ and $u \rightarrow e^{i\Delta\phi}$. The rest of the manipulation is written out in Eq. (11.58). When the argument of a sine is close to an integral multiple of π ,

$$\sin(m\pi + \varepsilon) = \sin(m\pi) \cos(\varepsilon) - \cos(m\pi) \sin(\varepsilon) \rightarrow (-1)^m \varepsilon \quad (\varepsilon \ll 1)$$

Thus, since Nv approaches a multiple of π whenever v does, the limit is

$$\frac{\sin(Nv)}{\sin(v)} \xrightarrow{v \rightarrow m\pi} \frac{Nv}{v} = N$$

If we define the intensity at the principal maxima as I_0 , then Eq. (11.60) follows.

11-13. (a) The condition for the maxima of Eq. (11.61) repeats Prob. 8-20, with $\alpha/2 \rightarrow v$. (b) For large N , the numerator $\sin(Nv)$ oscillates much faster than the denominator $\sin(v)$. Thus the maxima are largely determined by the numerator alone (i.e., when Nv is close to an odd multiple of $\pi/2$), except close to a principal maximum (where $v = m\pi$, as in Prob. 11-12) where the maxima that might be expected at $Nv \approx Nm\pi \pm \frac{1}{2}\pi$ are suppressed by the principal maximum. Thus, in the domain $0 \leq v \leq \pi$, the subsidiary maxima occur for $Nv \approx \frac{3}{2}\pi, \frac{5}{2}\pi, \dots, (N - \frac{5}{2})\pi, (N - \frac{3}{2})\pi$. There are $(N - \frac{3}{2}) - \frac{1}{2} = N - 2$ terms in this sequence. The subsidiary maxima closest to a principal maximum have $Nv \approx \frac{3}{2}\pi$, whence $\sin v \approx 3\pi/2N$, and $I/I_0 \approx (2/3\pi)^2 \approx 1/22$. The subsidiary maximum closest to halfway between principal maxima has $v \approx \pi/2$ and $|\sin Nv| \approx 1$, whence $I/I_0 \approx 1/N^2$.

11-14. (a) In Eq. (11.57), the incremental phaseshift $\Delta\phi$ from one slit to the next now consists of two portions, $kd \sin\theta_1$ on the input side and $kd \sin\theta_2$ on the output side. That is, $\Delta\phi \rightarrow kd(\sin\theta_1 + \sin\theta_2)$, and Eqs. (11.59) and (11.62) are modified by the substitution $\sin\theta \rightarrow \sin\theta_1 + \sin\theta_2$.

(b) The generalized grating equation can be written

$$d [\sin(\delta - \theta_2) + \sin(\theta_2)] = m\lambda$$

Differentiate with respect to θ_2 , setting $d\delta/d\theta_2 = 0$ (with fixed d, m , and λ),

$$\cos(\delta - \theta_2) (0 - 1) + \cos(\theta_2) (+1) = 0 \Rightarrow \cos(\theta_2) = \cos(\delta - \theta_2)$$

Since θ_1 and θ_2 are first-quadrant angles, the extremum is the symmetric condition $\theta_2 = \delta - \theta_2 = \theta_1$, and it is easy to see that this is a *minimum* of δ . Accordingly, in this case, $2d \sin(\delta/2) = m\lambda$. The advantage of this arrangement is that only one angle (δ) need be measured with high precision (since δ is independent of the grating's orientation to first order). Otherwise, one must measure *two* angles with high precision, even when θ_1 is nominally zero. Note that Bragg interference, Prob. 11-5, occurs with the minimum-deviation symmetry.

11-15. From the grating equation (11.62), the third-order yellow components are centered on an angle such that

$$d \sin\theta = m\lambda \rightarrow 3\lambda_y = 1731 \text{ and } 1737 \text{ nm}$$

Meanwhile, the fourth-order blue line is centered on $4\lambda_b = 1743$ in these units. From Eq. (11.66), the finite number of slits broadens the principal maxima so that the resolvable $\Delta\lambda$ is given by

$$m \Delta\lambda_{\text{res}} = \frac{\lambda}{N} \rightarrow \frac{578}{40} \approx 14.5 \text{ nm (yellow), or } \frac{436}{40} \approx 11 \text{ nm (blue)}$$

Thus not only do the two yellow components merge to form a single unresolved line, but also the comparably blurry blue line falls essentially on top of the yellow "singlet" (the superposition appears as a strange-looking pink to the human eye).

In the seventh order, $7\lambda_y = 4039$ and 4054 nm, a difference of 15 nm. So this is the lowest order in which it should be marginally possible to see that the yellow line is in fact a doublet. (There is no confusion from visible lines in another order.)

In the 17th order, $17\lambda_y = 9809$ and 9845 , while $18\lambda_g = 9830$. Now the two yellow components are well resolved (but with indistinguishable color to the human eye), and the bright green line appears neatly halfway between them!

11-16. The factor T in Eqs. (11.76–81) is replaced by $(1 - R - A)$. Consequently, Eq. (11.85) is multiplied by the correction factor

$$\left(\frac{1 - R - A}{1 - R} \right)^2 = \left(1 - \frac{A}{1 - R} \right)^2 = \left(\frac{T}{T + A} \right)^2$$

It should be noted that, when significant absorption is present, there are usually phaseshifts other than 0 or π in the reflections. Accordingly, the incremental phase difference of successive reflections, given by Eq. (11.72), includes an additive constant. See Born and Wolf (Bo80, Sec. 7.6.1).

11-17. The condition for a bright transmission fringe in a Fabry-Perot interferometer is given by Eq. (11.86),

$$2nd \cos\theta_2 = m\lambda$$

where n is the refractive index, and θ_2 is the angle with respect to the normal, in the space between the reflecting surfaces (see Fig. 11-20). Differentiating and eliminating the order m ,

$$\mathcal{D}_{\text{F-P}} = \left| \frac{d\theta_2}{d\lambda} \right| = \frac{m}{2nd \sin\theta_2} \left(\frac{2nd \cos\theta_2}{m\lambda} \right) = \frac{\text{ctn}\theta_2}{\lambda}$$

In most practical embodiments, the medium between the reflecting surfaces is air, and θ_2 is essentially the same as the external (observed) angle θ_0 . Similarly, combining Eqs. (11.62–63),

$$\mathcal{D}_{\text{grating}} = \frac{m}{d \cos\theta} \left(\frac{d \sin\theta}{m\lambda} \right) = \frac{\tan\theta}{\lambda}$$

Fabry-Perots have their maximum dispersion for *small* angles (i.e., close to the axis of the system), while gratings have their maximum at *large* angles ($\theta \rightarrow \pi/2$). But gratings diffract only a small amount of light into high order, while Fabry-Perots are best used close to the axis. Thus, in practice, Fabry-Perots yield much higher dispersion (e.g., for looking at the "fine-structure" of a spectral line, or at Zeeman splitting). On the other hand, Fabry-Perots operate in high order ($d \gg \lambda$), where the presence of many wavelengths at the same time can be confusing. One could use a grating in low-order to pre-select a particular spectral line for analysis by a subsequent Fabry-Perot. See also the following problem.

11-18. (a) The cited equations are

$$\frac{(\Delta\lambda)_{\text{fsr}}}{\lambda} = \frac{1}{m} = \frac{\lambda}{2nd \cos\theta_2}, \quad \frac{\lambda}{(\Delta\lambda)_{\text{res}}} = \frac{2\pi nd \cos\theta_2 \sqrt{R}}{\lambda(1-R)}$$

and so

$$\mathcal{F} \equiv \frac{(\Delta\lambda)_{\text{fsr}}}{(\Delta\lambda)_{\text{res}}} = \frac{\pi\sqrt{R}}{1-R}$$

(In practice, the achievable finesse of a Fabry-Perot is limited by the flatness of the plates.)

(b) The corresponding relations for a grating, using $(m+1)\lambda = m(\lambda + \Delta\lambda_{\text{fsr}})$ and Eq. (11.66), are

$$\frac{(\Delta\lambda)_{\text{fsr}}}{\lambda} = \frac{1}{m}, \quad \frac{\lambda}{(\Delta\lambda)_{\text{res}}} = mN$$

from which

$$\frac{(\Delta\lambda)_{\text{fsr}}}{(\Delta\lambda)_{\text{res}}} = N$$

Typically, a grating's N is substantially greater than a Fabry-Perot's \mathcal{F} .

11-19. The full width at half maximum is the $\delta\phi$ of Fig. 11-24, which is given by Eq. (11.90) as

$$\Gamma = \delta\phi = \frac{4}{\sqrt{\alpha}} = \frac{2(1-R)}{\sqrt{R}} \approx 2(1-R)$$

where the approximation assumes that the reflection coefficient R is close to unity.

The instrument's resolvable wavelength increment can be expressed in terms of the resolving power \mathcal{R} defined in Eq. (11.92) as $(\Delta\lambda)_{\text{instrument}} = \lambda/\mathcal{R}$. When a spectral "line" has fine structure that spreads it over the wavelength range $(\Delta\lambda)_{\text{line}}$, its longitudinal coherence length is given by Eq. (11.40) as $L_{lc} = \lambda_0^2/(\Delta\lambda)_{\text{line}}$. If the Fabry-Perot is to resolve the fine structure, we require

$$(\Delta\lambda)_{\text{instrument}} \ll (\Delta\lambda)_{\text{line}}$$

$$\frac{\lambda}{\mathcal{R}} \ll \frac{\lambda^2}{L_{lc}} \Rightarrow L_{lc} \ll \lambda\mathcal{R} \approx \frac{2\pi d}{1-R}$$

where again we have assumed that both $n\cos\theta_2$ and R are close to unity. The quantity $2\pi d/(1-R)$ can be thought of as the effective distance that a monochromatic wave bounces back and forth between the mirrors before escaping from the Fabry-Perot. When the coherence length of a wave train is longer than this parameter, the F-P presents it as an unstructured "monochromatic" line whose breadth is determined by the instrument. If fine structure is to be resolved, the parameter must be larger than the coherence length of the composite "line", the degree of inequality being determined by the amount of fine structure to be resolved.

Chapter 12

12-1. A straightforward binomial expansion gives

$$\begin{aligned}\delta(\rho) &= (Z^2 + \rho^2)^{1/2} + (Z_0^2 + \rho^2)^{1/2} - (Z + Z_0) \\ &= Z \left(1 + \frac{1}{2} \frac{\rho^2}{Z^2} - \frac{1}{8} \frac{\rho^4}{Z^4} + \dots \right) + Z_0 \left(1 + \frac{1}{2} \frac{\rho^2}{Z_0^2} - \frac{1}{8} \frac{\rho^4}{Z_0^4} + \dots \right) - (Z + Z_0) \\ &\rightarrow \frac{1}{2} \left(\frac{1}{Z} + \frac{1}{Z_0} \right) \rho^2 - O(\rho^4)\end{aligned}$$

From Eq. (12.21),

$$\frac{d}{dn} \left(\frac{\rho^2}{2} \right) = \rho \frac{d\rho}{dn} = \left(\frac{1}{Z} + \frac{1}{Z_0} \right)^{-1} \frac{\lambda}{2}$$

from which Eq. (12.22) follows. The integral in Eq. (12.23) is

$$\int_{n-1}^n e^{i\pi n} dn = \frac{1}{i\pi} [e^{i\pi n}]_{n-1}^n = \frac{1}{i\pi} (e^{i\pi n} - e^{i\pi(n-1)}) = \frac{2}{i\pi} (-1)^n$$

since $e^{\pm i\pi} = -1$. The integral in Eq. (12.25) is

$$\begin{aligned}\int_0^N e^{i\pi n} dn &= \frac{1}{i\pi} [e^{i\pi n}]_0^N = \frac{1}{i\pi} (e^{i\pi N} - 1) = \frac{2}{\pi} e^{i\pi N/2} \left(\frac{e^{i\pi N/2} - e^{-i\pi N/2}}{2i} \right) \\ &= \frac{2}{\pi} (i)^N \sin\left(\frac{\pi N}{2}\right)\end{aligned}$$

since $e^{i\pi/2} = i$. In the results of both integrations, when n or N is non-integral, the complex terms $(-1)^n = e^{i\pi n}$ and $(i)^N = e^{i\pi N/2}$ are simply phase factors of magnitude unity, which wash out in the intensity (proportional to the absolute square).

12-2. Equation (12.14) reduces to Eq. (12.15) for the case of an incident plane wave. The term $1/Z_0$ disappears in Eqs. (12.19), (12.21), and (12.24). Equation (12.22) becomes $da = \pi\lambda Z dn$. In Eqs. (12.23) and (12.25), we make the substitution

$$A \frac{e^{ik(Z+Z_0)}}{Z + Z_0} \rightarrow \psi_0 e^{ikZ}$$

Because the denominator factor $(Z + Z_0)$ has gone away, the intensity I_0 in Eq. (12.26) is no longer dependent on either the ("infinite") input distance Z_0 or the (finite) output distance Z .

12-3. (a) Generalizing Eq. (12.21) for large angles, but putting $Z_0 = Z$,

$$\begin{aligned}n \frac{\lambda}{2} &= \sqrt{Z_0^2 + \rho_n^2} + \sqrt{Z^2 + \rho_n^2} - (Z_0 + Z) \rightarrow 2\sqrt{Z^2 + \rho_n^2} - 2Z \\ \Rightarrow Z^2 + \rho_n^2 &= \left(Z + \frac{n\lambda}{4} \right)^2\end{aligned}$$

from which the area of the n th zone is

$$\begin{aligned}\Delta a_n &= \pi(\rho_n^2 - \rho_{n-1}^2) = n \frac{\pi\lambda Z}{2} + n^2 \frac{\pi\lambda^2}{16} - (n-1) \frac{\pi\lambda Z}{2} - (n-1)^2 \frac{\pi\lambda^2}{16} \\ &= \frac{\pi\lambda Z}{2} + (2n-1) \frac{\pi\lambda^2}{16}\end{aligned}$$

(b) For the n th zone, the radii $r = r_0$ in Fig. 12-7 can be closely approximated by $Z + (n - \frac{1}{2})\lambda/4$. Similarly, $(\mathbf{e}_r - \mathbf{e}_0) \cdot \mathbf{n} = \cos\theta + \cos\theta_0 \approx 2Z/[Z + (n - \frac{1}{2})\lambda/4]$. Thus the relative amplitude contributed by the n th zone is very nearly

$$A_n \propto \left[\frac{2Z}{Z + (n - \frac{1}{2})\lambda/4} \right] \frac{(\pi\lambda/2)[Z + (n - \frac{1}{2})\lambda/4]}{[Z + (n - \frac{1}{2})\lambda/4]^2} \approx \frac{\pi\lambda Z}{(Z + n\lambda/4)^2}$$

The final approximation follows because we assume $Z \gg \lambda$ (but not $Z \gg n\lambda$!).

12-4. (a) The assumptions are equivalent to $|dA_n/dn| \ll A_n$, and $d^2A_n/dn^2 > 0$, where A_n is the amplitude contributed by the n th zone. From the result of the preceding problem:

$$\frac{1}{A_n} \left| \frac{dA_n}{dn} \right| \approx \frac{(Z + n\lambda/4)^2}{\pi\lambda Z} \frac{1 - 2\pi\lambda Z}{(Z + n\lambda/4)^3} \left(\frac{\lambda}{4} \right) = \frac{\lambda}{2(Z + n\lambda/4)}$$

This is at least as small as λ/Z , and goes to zero as $1/n$ when $n \gg Z/\lambda$. Similarly,

$$\frac{d^2A_n}{dn^2} \approx (-2)(-3) \frac{\pi\lambda Z}{(Z + n\lambda/4)^4} \left(\frac{\lambda}{4} \right)^2 = \frac{3\pi\lambda^3 Z}{8(Z + n\lambda/4)^4}$$

This is indeed positive, and at least as small as $(\lambda/Z)^3$.

(b) An estimate of the magnitude of the sum of the terms grouped in parentheses is given by

$$\int_0^\infty \left(\frac{1}{2} \frac{d^2 A_n}{dn^2} \right) \frac{dn}{2} = \frac{3\pi\lambda^2 Z}{8} \int_0^\infty \frac{1}{(Z+u)^4} du = \frac{\pi\lambda^2}{8Z^2}$$

So even this sum remains very small. Therefore the two groupings bracket the magnitude of the total signal A as

$$\frac{A_1 + A_N}{2} < A < \left\{ \frac{2A_1 - A_2 - A_{N-1} + 2A_N}{2} \approx \frac{A_1 + A_N}{2} \right\}$$

(c) When N is even, we can again group the series in two ways:

$$\begin{aligned} A &= \frac{A_1}{2} + \left(\frac{A_1}{2} - A_2 + \frac{A_3}{2} \right) + \left(\frac{A_3}{2} - A_4 + \frac{A_5}{2} \right) + \dots + \frac{A_{N-1}}{2} + A_N \\ &= A_1 - \frac{A_2}{2} - \left(\frac{A_2}{2} - A_3 + \frac{A_4}{2} \right) - \left(\frac{A_4}{2} - A_5 + \frac{A_6}{2} \right) - \dots - \frac{A_N}{2} \end{aligned}$$

which brackets the amplitude as

$$\left\{ \frac{A_1 + A_{N-1} - 2A_N}{2} \approx \frac{A_1 - A_N}{2} \right\} < A < \left\{ \frac{2A_1 - A_2 - A_N}{2} \approx \frac{A_1 - A_N}{2} \right\}$$

When $N \rightarrow \infty$, then $A_N \rightarrow 0$, and $A \rightarrow A_1/2$. Since the paraxial approximation holds for the first zone, Eq. (12.23) shows that one-half the contribution of the first zone is precisely the unobstructed wave.

12-5. (a) Assuming the paraxial approximation, Eqs. (12.19) and (12.21) continue to hold with the understanding that we are now talking about linear strips whose boundaries are measured by the one-dimensional Cartesian variable ρ . Since the strips are of indefinite length perpendicular to the diagram, we normalize the amplitude per-unit-length in that direction. That is, the element of area da reduces to the element of width $d\rho$, doubled because we count the pair of strips on both sides of the symmetry plane as part of the same zone-element. Thus, rearranging and then differentiating Eq. (12.21),

$$\rho(n) = \sqrt{\frac{\lambda Z Z_0}{Z + Z_0}} n^{1/2} \Rightarrow da \rightarrow 2d\rho = 2 \frac{d\rho}{dn} dn = 2 \sqrt{\frac{\lambda Z Z_0}{Z + Z_0}} \frac{1/2}{n^{1/2}} dn$$

In contrast to Eq. (12.22) for circular (annular) zones, the "area" of the linear zones depends upon n even in the paraxial approximation.

(b) The diffraction integral corresponding to Eq. (12.20) is now proportional to

$$\int e^{ik\delta} 2d\rho \propto \int e^{i\pi n} \frac{1}{\sqrt{n}} dn$$

We use a proportionality because it is tricky to write out the full expression for the diffracted amplitude in this case. [The appropriate wavefunctions, replacing Eqs. (12.6) and (12.13), are now *cylindrical* waves varying as $1/\sqrt{r}$, rather than the spherical waves varying as $1/r$. The coefficient of Eq. (12.20) would have to be modified accordingly.] Now, make the substitution $n \rightarrow v^2/2$, so that for the n th zone [analogous to Eq. (12.23)]

$$\int_{n-1}^n e^{i\pi n} \frac{1}{\sqrt{n}} dn = \int_{[2(n-1)]^{1/2}}^{(2n)^{1/2}} e^{i(\pi/2)v^2} \sqrt{\frac{2}{v^2}} \frac{2v}{2} dv$$

Except for the factor of $\sqrt{2}$, this has the desired form, which anticipates the conventional notation of the Fresnel integrals discussed in Sec. 13.1.

12-6. (a) Let the amplitude of the incident plane wave be ψ_0 , from which its intensity is $I_0 \propto \psi_0^2$. This is of course the intensity at the point P for a very large aperture. For an aperture exposing one Fresnel zone, from Eq. (12.23), the intensity is $4I_0$ [$\propto (2\psi_0)^2$]. If the exposed zones of a zone plate are for $n = 1, 3, 5, \dots, N$ (and paraxial conditions prevail), the contributions all add constructively and the intensity at P is

$$\propto \left(\frac{N+1}{2} 2\psi_0 \right)^2 \rightarrow (N+1)^2 I_0$$

When N is large, this intensity is very great, but it falls rapidly away from P (both axially and radially) because the hardware boundaries of the zone plate no longer match the geometric zones for the displaced point (see Fig. 12-12).

(b) From Eq. (12.21), the given radii $\rho_n = \sqrt{n\lambda Z}$ are the zone boundaries for an incident plane wave ($Z_0 \rightarrow \infty$) and a "focal point" P at the observation distance Z . But now consider a second observation point, P' , at the distance $Z/3$. Then the open aperture between the axis and $\rho_1 = \sqrt{\lambda Z}$ exposes *three* zones at P' , which deliver the amplitude $(+2-2+2)\psi_0 = 2\psi_0$. More generally, with respect to P' the zone plate exposes zones 1-3, 7-9, 13-15, ..., and masks zones 4-6, 10-12, The intensity at P' is now approximately $(N/3)^2 I_0$. (Note that at the observation distance $Z/2$, the zones are *paired*, and there is zero intensity on axis. At distances of Z divided by a non-integer, the phases from exposed sets of zones are scrambled and the intensity is typically of order I_0 .) Generalizing this argument, we see that there are subsidiary "focal points" at Z/k , for odd k , with intensities of about $(N/k)^2 I_0$.

(c) Returning to Eq. (12.21) and assuming that a spherical wave is incident from a source point at the distance Z_0 ,

$$\frac{\lambda}{2} = \left(\frac{1}{Z} + \frac{1}{Z_0} \right) \frac{\rho_1^2}{2} \Rightarrow \frac{1}{Z_0} + \frac{1}{Z} = \frac{\lambda}{\rho_1^2}$$

For an extended source (subject to the paraxial limit), each pixel in the source plane at distance Z_0 maps to a corresponding pixel in the image plane at distance Z . Thus the principal "focal image" of the zone plate obeys the standard equation for thin lenses of focal length $f = \rho_1^2/\lambda$.

12-7. The function of the lens is to convert plane wavefronts into spherical wavefronts converging on the observation point P . The aperture plane coincides with a wavefront of the incident wave. The variation in r that must be included in the phase factor e^{ikr} can be identified with the incremental path δ between the aperture plane and the diffracted plane reference wavefront. Since the ray passing through the center of the lens is undeviated, the angle between these two reference planes is $\tan^{-1}(x/f) = x/f$. More generally, the direction cosines of the parallel diffracted rays, which are gathered by the lens and focused on P , are [compare Eqs. (12.32)]:

$$\alpha \approx \frac{x}{f}, \quad \beta \approx \frac{y}{f}$$

The incremental path δ is a linear function of the aperture coordinates ξ, η . Thus, the expression for r , replacing Eq. (12.33), is

$$r = f + \alpha\xi + \beta\eta$$

The diffraction integral is now of the Fraunhofer form, Eq. (12.37), with $Z \rightarrow f$ in the coefficient. Note that the use of lenses implies the paraxial approximation in order to avoid the lens aberrations of geometrical optics. However, so long as the aperture width is small compared to f , one can tilt the lens to observe diffraction at a large angle; the obliquity factor $\frac{1}{2}(1 + \cos\theta)$ then would appear in the coefficient.

12-8. The wavelength of visible light is about 550 nm. Let's use the engineers' criterion cited in the footnote to Eq. (12.34), $R \geq 2D^2/\lambda$. For a narrow slit of width $D = 0.1$ mm, we have $2D^2/\lambda \approx 3.6$ cm. So source and observation distances of a few centimeters are sufficient. With $D = 2$ cm, we have $2D^2/\lambda \approx 1.5$ kilometers; a lens is almost surely required (or one can rule the grating on a concave mirror). If $D = \lambda/2$, then $2D^2/\lambda = \lambda/2$, and Fraunhofer conditions pertain beyond distances of

the order of the size of the antenna itself. For the FM radio band, $\nu \approx 100$ MHz, and $\lambda/2 \approx 1.5$ m. (Note: In diffraction theory, the Kirchhoff boundary conditions, discussed in Sec. 12.2, are valid only for apertures of width $D \gg \lambda$. But radio antennas can have well-defined current distributions with $D \leq \lambda$.)

12-9. Using $(\text{den})(\text{num})' = (\text{num})(\text{den})'$, the extrema of $\sin u/u$ occur when

$$(u)(\cos u) = (\sin u)(1) \Rightarrow \tan u = u$$

This transcendental equation has no root in the first quadrant (other than $u = 0$), but beyond that there is a root as u approaches $3\pi/2, 5\pi/2$, etc. To evaluate the shortfall, rewrite the equation as

$$\cot u = \frac{1}{u}$$

and let the roots be at $u_m = \frac{1}{2}m\pi - \epsilon_m$ ($m = 3, 5, 7, \dots$). Now Taylor-expand each side to first order:

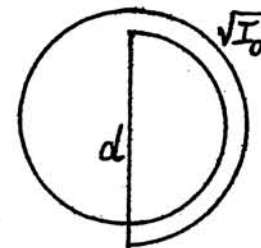
$$\cot\left(\frac{m\pi}{2}\right) - \frac{1}{\sin^2(m\pi/2)}(-\epsilon_m) \approx \frac{2}{m\pi} - \left(\frac{2}{m\pi}\right)^2(-\epsilon_m)$$

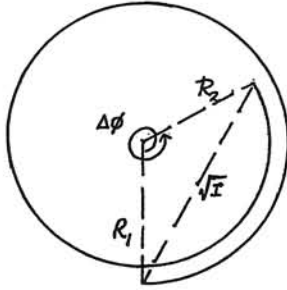
$$\Rightarrow \epsilon_m \approx \frac{2/m\pi}{1 - (2/m\pi)^2}$$

As fractions of the period (π) between subsidiary maxima, the results are:

m	ϵ_m/π
3	0.071
5	.041
7	.029
9	.023

12-10. (a) The diameter of a circle such that $3/2$ times the circumference is $\sqrt{I_0}$ is given by $\frac{3}{2}\pi d = \sqrt{I_0}$. The resultant chord of this phasor is the diameter, corresponding to the intensity $d^2 = (2/3\pi)^2 I_0 \approx I_0/22$. The actual maximum resultant occurs with the spiral slightly unwound: the resultant is then less than the diameter, but the diameter is bigger (this is the $m = 3$ case of the previous problem).





(b) By the law of cosines,

$$(\sqrt{I})^2 = R_1^2 + R_2^2 - 2R_1R_2\cos\Delta\phi$$

and this holds for angles $\Delta\phi$ that are greater than 2π (the sketch illustrates $\Delta\phi \approx \frac{8}{3}\pi$). But under paraxial conditions, the radius of curvature is constant: that is, $R_1 = R_2 = \sqrt{I_0}/\Delta\phi = \sqrt{I_0}/2u$. Thus,

$$I = 2R^2 [1 - \cos(2u)] = 2 \left(\frac{I_0}{4u^2} \right) (2 \sin^2 u) = I_0 \left(\frac{\sin u}{u} \right)^2$$

12-11. The nulls occur at $u = m\pi$ ($m = 1, 2, 3, \dots$), so only the Si function contributes. The desired evaluation is

$$\frac{2}{\pi} \int_0^{m\pi} \left(\frac{\sin u}{u} \right)^2 du = \frac{2}{\pi} \text{Si}(2m\pi)$$

Table 5.3 (p. 244) of Abramowitz and Stegun (Ab65) gives $\text{Si}(\pi x)$:

m	$\text{Si}(2m\pi)$	$(2/\pi)\text{Si}$
1	1.418	0.903
2	1.492	.950
3	1.518	.966
4	1.531	.975
5	1.539	.980

Series expansions suitable for computer evaluation are given in A&S's §§ 5.2.8, 5.2.14, and 5.2.34–39.

12-12. (a) The angular size of the diffraction pattern, measured from center to first null in each dimension, is $\Delta\alpha = \pi/ka = \lambda/2a$ by $\Delta\beta = \pi/kb = \lambda/2b$. That is, the area on the observation screen illuminated by the aperture is proportional to

$$\Delta\alpha \Delta\beta = \frac{\lambda^2}{4ab}$$

which, in turn, is inversely proportional to the aperture area $S = 4ab$. Given that the intensity of the pattern is proportional to S^2 [Eq. (12.50)], but this intensity (power per area) is spread over an observation area proportional to $1/S$, then the total power observed is directly proportional to S , consistent with conservation of energy.

(b) Using Eqs. (12.48) and the integral relation given in the preceding problem, the integral of Eq. (12.49) over its entire diffraction pattern is

$$\begin{aligned} P_{\text{total}} &= \iint I(\alpha, \beta) dx dy = \left(\frac{\lambda Z}{2\pi} \right)^2 \frac{1}{ab} I_0 \int_{-\infty}^{+\infty} \left(\frac{\sin u_a}{u_a} \right)^2 du_a \int_{-\infty}^{+\infty} \left(\frac{\sin u_b}{u_b} \right)^2 du_b \\ &= \left(\frac{\lambda Z}{2\pi} \right)^2 \frac{1}{ab} \cdot \left(\frac{4ab}{\lambda Z} \right)^2 |\psi_0|^2 \cdot 2\text{Si}(u_a \rightarrow \infty) \cdot 2\text{Si}(u_b \rightarrow \infty) = 4ab |\psi_0|^2 = P_{\text{inc}} \end{aligned}$$

where $P_{\text{inc}} = (\text{incident intensity}) \times (\text{aperture area}) = \text{power entering the aperture}$.

12-13. The mirror reflects back the diffraction pattern that would be produced by an aperture of dimensions $2a \times 2b$. In Eq. (12.50), $I_{\text{inc}} = |\psi_0|^2$ is the incident power-per-area. An area ΔS_{rec} in the observation plane (in this case, at the radar transmitter-receiver) subtends the solid angle $\Delta\Omega = \Delta S_{\text{rec}}/Z^2$, and receives the power $P_{\text{rec}} = I_0 \Delta S_{\text{rec}}$ (assuming $\Delta\Omega \ll 1$). Thus,

$$4\pi \frac{P_{\text{rec}}/\Delta\Omega}{I_{\text{inc}}} = 4\pi \frac{I_0 Z^2}{|\psi_0|^2} = 4\pi \left(\frac{4ab}{\lambda} \right)^2 = \frac{4\pi S^2}{\lambda^2}$$

12-14. The revision of Eq. (12.38) gives the integral

$$\int_{\sigma} A(\xi) e^{-i(k\sin\theta)\xi} d\xi$$

(a) For cosine illumination, we have:

$$\int_{-a}^{+a} \cos\left(\frac{\pi\xi}{2a}\right) e^{-i(k\sin\theta)\xi} d\xi = \frac{2a}{\pi} \int_{-\pi/2}^{+\pi/2} \cos(y) e^{-i(2u/\pi)y} dy$$

where $y = \pi\xi/2a$, and with $u = ka\alpha = k\text{asin}\theta$ as before. From integral tables [e.g., Dwight §576.1], this equals:

$$\begin{aligned} &= \frac{2a}{\pi} \left[\frac{e^{-i(2u/\pi)y}}{1 - (2u/\pi)^2} \left(i \frac{2u}{\pi} \cos y + \sin y \right) \right]_{-\pi/2}^{+\pi/2} = \frac{2a}{\pi} \left[\frac{e^{+iu} + e^{-iu}}{1 - (2u/\pi)^2} \right] \\ &= \frac{4a}{\pi} \frac{\cos u}{1 - (2u/\pi)^2} \\ \Rightarrow I &= I_0 \left[\frac{\cos u}{1 - (2u/\pi)^2} \right]^2 \end{aligned}$$

where I_0 is the maximum intensity at $u = 0$. Compared with the uniformly illuminated slit [Eq. (12.41)], this has a broader central maximum and reduced sidelobes.

(b) With infinite limits, the integral is the Fourier transform of a Gaussian function:

$$\int_{-\infty}^{+\infty} e^{-\xi^2/2a^2} e^{-i(k\sin\theta)\xi} d\xi = \int_{-\infty}^{+\infty} e^{-\xi^2/2a^2} [\cos(k\sin\theta \xi) - i \sin(k\sin\theta \xi)] d\xi$$

Since the Gaussian is an even function, the integral of the sine term in the Euler expansion of the complex exponential vanishes. From tables [e.g., Dwight §861.20],

$$\int_{-\infty}^{+\infty} e^{-\xi^2/2a^2} \cos(k\sin\theta \xi) d\xi = \sqrt{\frac{\pi}{2}} a e^{-(k\sin\theta)^2/2} = \sqrt{\frac{\pi}{2}} a e^{-u^2/2}$$

$$\Rightarrow I = I_0 e^{-u^2}$$

The amplitude and intensity functions are also Gaussians, the famous case of a function that is its own Fourier transform. The standard deviation of the intensity Gaussian is $\sigma_u = 1/\sqrt{2}$.

(c) The Fourier transform of the sinc function (once again an even function) gives:

$$\int_{-\infty}^{+\infty} \frac{\sin(\pi\xi/a)}{\pi\xi/a} e^{-i(k\sin\theta)\xi} d\xi = 2 \int_0^{+\infty} \frac{\sin(\pi\xi/a)}{\pi\xi/a} \cos(k\sin\theta \xi) d\xi$$

$$\stackrel{\text{Dwight } \S 858.701}{=} \begin{cases} a & (|u| \equiv k a \sin\theta < \pi) \\ a/2 & (|u| = \pi) \\ 0 & (|u| > \pi) \end{cases}$$

$$\Rightarrow I = \begin{cases} I_0 & (|u| < \pi) \\ 0 & (|u| > \pi) \end{cases}$$

The amplitude, and hence the intensity, are *box functions* of width $-\pi < u < +\pi$ [see Boas (Bo83, pp. 651–2)]. This case is just the Fourier-inverse of the uniformly illuminated slit, whose diffraction pattern is the sinc function of Eqs. (12.39) and (12.41).

12-15. We wish to expand the exponential in Eq. (12.59),

$$\psi(\theta) = C \int_0^a \rho d\rho \int_0^{2\pi} e^{-ik\rho\theta\cos\phi} d\phi$$

where the ρ -dependence of the ϕ integral is part of the integrand of the ρ integral. The expansion of e^x is:

$$e^x = 1 + x + \frac{1}{2}x^2 + \frac{1}{6}x^3 + \dots = \sum_m \frac{x^m}{m!}$$

The ρ integration of the m th term is

$$\int_0^a \rho^{m+1} d\rho = \frac{1}{m+2} a^{m+2}$$

From symmetry considerations and tables [Dwight §858.44], the ϕ integration is

$$\int_0^{2\pi} \cos^m \phi d\phi = \begin{cases} 0 & (m \text{ odd}) \\ \frac{(m-1)! \pi}{(\frac{1}{2}m)! (\frac{1}{2}m-1)! 2^{m-2}} & (m \text{ even}) \end{cases}$$

Thus the m th term in the series for ψ is

$$\begin{aligned} C \frac{(-ik\theta)^m}{m!} \left(\frac{a^{m+2}}{m+2} \right) \left[\frac{(m-1)! \pi}{(\frac{1}{2}m)! (\frac{1}{2}m-1)! 2^{m-2}} \right] \\ \stackrel{m \rightarrow 2\lambda}{=} \pi a^2 C (-1)^\lambda \left(\frac{1}{2}ka\theta \right)^{2\lambda} \frac{4(2\lambda-1)!}{(2\lambda)! (2\lambda+2) \lambda! (\lambda-1)!} \\ = \pi a^2 C (-1)^\lambda \frac{(\frac{1}{2}ka\theta)^{2\lambda}}{(\lambda+1)! \lambda!} \end{aligned}$$

From Eq. (3.95b), we find the λ th term of J_n is

$$(-1)^\lambda \frac{(\frac{1}{2}u)^{2\lambda+1}}{(\lambda+n)! \lambda!}$$

The two series match for $n = 1$ and $u = ka\theta$. Thus we confirm Eq. (12.65),

$$\psi(\theta) = \pi a^2 C \frac{2J_1(ka\theta)}{ka\theta}$$

12-16. In Eq. (12.37) or (12.53), the integrations over the two Cartesian coordinates ξ and η are independent except insofar as they may be coupled by the limits on the integrals—that is, by the shape of the aperture. Suppose we stretch or compress the aperture by a factor b in the ξ direction. That is, the limits on the ξ integral are multiplied by the factor b ,

$$\int_{\eta_{\min}}^{\eta_{\max}} d\eta \int_{b\xi_{\min}(\eta)}^{b\xi_{\max}(\eta)} e^{-ik(\alpha\xi+\beta\eta)} d\xi$$

Now, substitute the new variable $\xi' = \xi/b$, and the integral becomes

$$\int_{\eta_{\min}}^{\eta_{\max}} d\eta \int_{\xi_{\min}(\eta)}^{\xi_{\max}(\eta)} e^{-ik(ab\xi'+\beta\eta)} b d\xi'$$

This integral has the same *formal* limits as the unstretched prototype, Eq. (12.53). Therefore, it is identical to the prototype except that it has been multiplied by b , and α has been replaced by $b\alpha$ in the exponent. Accordingly, the diffracted intensity I' for the stretched aperture is

$$I'(\alpha, \beta) = b^2 I(b\alpha, \beta)$$

where $I(\alpha, \beta)$ is the intensity pattern of the original unstretched aperture. Now, α, β are the direction cosines measuring the location of the observation point in the x and y directions, parallel to ξ and η , respectively [see Fig. 12-13 and Eqs. (12.32)]. With the factor b multiplying α , we require a *smaller* excursion in x (for $b > 1$) to reach a given feature of the pattern—that is, the diffraction pattern has shrunk by the factor $1/b$ in that direction.

As a special case, note that a circle stretched uniformly in one direction is an ellipse, and thus that this theorem gives an easy way to find the diffraction pattern of an elliptical aperture.

12-17. The subsidiary maxima of Eq. (12.67) are at the extrema of $J_1(u)/u$,

$$(u)(J_1') = (J_1)(1)$$

where the prime signifies the derivative with respect to the argument u . The recursion relation of Eq. (3.109) gives

$$u J_n' - n J_n = -u J_{n+1} \Rightarrow u J_1' = J_1 - u J_2$$

Thus the extrema of the amplitude function occur at the roots of $J_2(u) = 0$. These are the *maxima* of the intensity function, whose *minima* (nulls) occur at the roots of J_1 .

12-18. In the assumed small-angle limit, the annular element of area in the observation plane is $d\Omega = 2\pi r^2 \sin\theta d\theta \rightarrow 2\pi Z^2 \theta d\theta$. Thus from Eqs. (12.66–68) the power diffracted within the conical angle θ_0 is

$$\begin{aligned} P(\theta_0) &= \left(\frac{\pi a^2}{\lambda Z}\right)^2 |\psi_0|^2 \int_0^{\theta_0} \left[\frac{2J_1(ka\theta)}{ka\theta}\right]^2 2\pi Z^2 \theta d\theta \\ &= \pi a^2 |\psi_0|^2 \int_0^{ka\theta_0} \frac{2J_1^2(u)}{u} du \end{aligned}$$

The coefficient is simply the power incident on the aperture. The integral can be evaluated using recursion relations [see Eq. (3.109), or alternatively Eq. (3.113)]:

$$u J_n' = n J_n + u J_{n+1} \Rightarrow J_1 = -J_0'$$

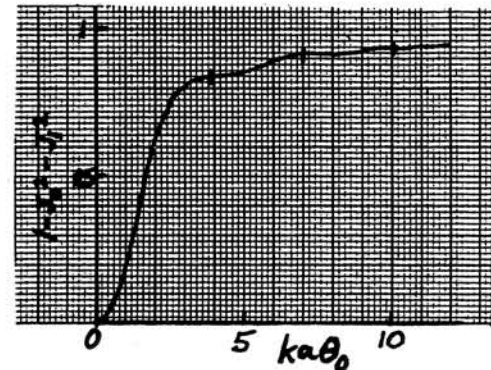
$$u J_n' = -n J_n + u J_{n-1} \Rightarrow \frac{J_1}{u} = J_0 - J_1'$$

Thus,

$$\begin{aligned} 2 \int (J_1) \left(\frac{J_1}{u}\right) du &= -2 \int (J_0 J_0' + J_1 J_1') du \\ &= -[J_0^2 + J_1^2]_0^{ka\theta_0} = 1 - J_0^2(ka\theta_0) - J_1^2(ka\theta_0) \end{aligned}$$

The values of $u_0 = ka\theta_0$ for the nulls of J_1 (i.e., the centers of the dark rings) are given preceding Eq. (12.69). From Abramowitz and Stegun (Ab65, p. 411), we have:

dark ring	$ka\theta_0$	$J_0(ka\theta_0)$	$1 - J_0^2$
1	3.832	-0.4028	0.8378
2	7.016	0.3001	0.9099
3	10.173	-0.2497	0.9376



12-19. The lower limit of the integral in Eq. (12.63) is replaced by the inner radius b of the annulus, with the resulting intensity, in place of Eq. (12.67),

$$I(\theta) = [\psi(a) - \psi(b)]^2 = \left(\frac{\pi}{\lambda Z}\right)^2 \left[a^2 \frac{2J_1(k\theta a)}{k\theta a} - b^2 \frac{2J_1(k\theta b)}{k\theta b} \right]^2$$

If we put $b = ra$ (and $u = k\theta a$ as usual), this becomes

$$I(\theta) = \left(\frac{\pi a^2}{\lambda Z}\right)^2 \left[\frac{2J_1(u)}{u} - r^2 \frac{2J_1(ru)}{ru} \right]^2$$

The nulls occur at

$$J_1(u) = r J_1(ru) \quad (1)$$

The subsidiary maxima are given by

$$(u)[J_1'(u) - r^2 J_1'(ru)] = [J_1(u) - r^2 J_1(ru)]$$

Using Eq. (3.109), this condition can be written

$$J_2(u) = r^2 J_2(ru) \quad (2)$$

The transcendental equations (1) and (2) can be solved graphically or by linearization. For instance, putting $u = u_0 + \varepsilon$, we expand (1) as

$$J_1(u_0) + J_1'(u_0) (\varepsilon) = r J_1(ru_0) + r^2 J_1'(ru_0) (\varepsilon)$$

Thus, again with the help of Eq. (3.109),

$$\varepsilon = - \frac{J_1(u_0) - r J_1(ru_0)}{\left[J_0(u_0) - \frac{J_1(u_0)}{u_0} \right] - r^2 \left[J_0(ru_0) - \frac{J_1(ru_0)}{ru_0} \right]}$$

For $r = 1/2$, for instance, a rough graph from tables (Ab65, p. 390) shows that the first root occurs somewhat below the first null of J_1 at 3.83. For $u_0 = 3.2$, we get $\varepsilon = -0.055$, and hence the first dark ring at $u = 3.145$ or $\theta = (3.145/2\pi)\lambda/a = 0.50 \lambda/a$. Compare with $u = 3.83$, and $\theta = 0.61 \lambda/a$, for the full circular aperture.

By similar linearization, we get $u = 4.82$ for the first root of (2) with $r = 1/2$. The relative height of the first subsidiary maximum is thus

$$\frac{I(u)}{I(0)} = \frac{1}{(1-r^2)^2} \left[\frac{2J_1(u)}{u} - r^2 \frac{2J_1(ru)}{ru} \right]^2 \rightarrow 0.096$$

which compares with the relative height of 0.018 for the full aperture. Thus obstructing the central portion of the aperture has improved the resolution, but reduced the intensity of the central maximum and increased it in the subsidiary maximum—that is, the contrast has been reduced. For further discussion see Born and Wolf (Bo80, Sec. 8.6.2).

12-20. From Eq. (12.70), the Rayleigh criterion for the resolution of a circular aperture is

$$\Delta\theta = 0.61 \frac{\lambda}{a}$$

The dark-adapted human eye has a diameter of about 6 mm. Thus the telescope provides an improvement by a factor of about $60/0.6 = 100$. The resolutions are:

$$\Delta\theta_{\text{eye}} \approx 0.61 \left(\frac{550 \times 10^{-7} \text{ cm}}{0.3 \text{ cm}} \right) = 1.1 \times 10^{-4} \text{ rad} = 20 \text{ sec of arc}$$

$$\Delta\theta_{\text{telescope}} \approx 1.1 \times 10^{-6} \text{ rad} = 0.2 \text{ sec of arc}$$

The Earth–Sun distance (the so-called Astronomical Unit) is 1.5×10^{13} cm. A light-year is $(3.0 \times 10^{10} \text{ cm/s})(3.16 \times 10^7 \text{ s}) = 9.5 \times 10^{17}$ cm. Thus the distances at which the double star system would be resolvable are:

$$\text{eye: } \frac{(1.5 \times 10^{13})}{(1.1 \times 10^{-4})(9.5 \times 10^{17})} = 0.14 \text{ light-yr}$$

$$\text{telescope: } 14 \text{ light-yrs}$$

Alpha Centauri is at 4.3 light-years; Sirius is at 8.6. For further discussion of the resolution of the eye, see Miles, *Am.J.Phys.* 58, 552 (1990).

12-21. Details of the resolution of a microscope are complicated [see Born and Wolf (Bo80, Sec. 8.6.3), and Higbie, *Am.J.Phys.* 49, 40 (1981)]. However, a heuristic argument based on reciprocity suggests that the minimum angular separation of resolvable structure is approximately that of the Rayleigh criterion, $\Delta\theta \approx 0.61 \lambda/a$, where a is the radius of the objective lens. Compound microscopes are usually operated with the object very nearly at the focal distance f from the objective lens. Therefore the linear separation of resolvable points is about

$$\Delta x \approx f \Delta\theta \approx 0.61 \frac{\lambda f}{a}$$

The ratio of focal length to diameter, $f/2a$, of a lens is known as its speed or "f/number" and is limited to values greater than approximately unity for practical lenses because of aberrations (the oil-immersion technique can do somewhat better). Thus we conclude that the microscope can resolve structure in the object plane that is somewhat larger than one wavelength. This is about three orders of magnitude larger than the interatomic spacing of the material of the pin.

A tolerable image of an alphanumeric character can be made with a 5×7 matrix of dots. Therefore we conclude that a legible character requires approximately $35 \times (1.2)^2 = 50$ square-wavelengths, or $50 \times (550 \times 10^{-7})^2 = 1.5 \times 10^{-7} \text{ cm}^2$. If we take the proverbial "head of a pin" to have an area of 1 mm^2 , then we can put about $10^{-2}/10^{-7} = 10^5$ characters, or $\sim 2 \times 10^4$ words on the pin. This is about 30 pages of double-spaced typescript text. An electron microscope (deBroglie wavelength \ll visible wavelength) could do better.

This exercise (traditionally phrased as "how many times can the Lord's Prayer be written on the head of a pin?") is of contemporary relevance in connection with the achievable density of integrated-circuit electronics since the circuit designs are transferred to the silicon chips by optical or electron-beam techniques.

12-22. For the circular aperture, the "saddle" occurs for $u \approx 3.832/2 \approx 1.916$, whence $J_1(1.916) \approx 0.5807$, and from Eq. (12.67),

$$\frac{I_{\text{sad}}}{I_0} = 2 \left(\frac{2 J_1(1.916)}{1.916} \right)^2 = 0.735$$

The analogous situation for linear slits occurs for $u = \pi/2$, whence from Eq. (12.41),

$$\frac{I_{\text{sad}}}{I_0} = 2 \left(\frac{\sin(\pi/2)}{\pi/2} \right)^2 = \frac{8}{\pi^2} = 0.811$$

For the Fabry-Perot, Fig. 11-24, the saddle height is $2(\frac{1}{2}I_0) = I_0$ by definition. In this case the adjacent peaks are greater than I_0 . From Eqs. (11.88) and (11.90), the peak height is

$$\begin{aligned} I_0 + I(\Delta\phi = 2m\pi + \delta\phi) &= I_0 \left[1 + \frac{1}{1 + \alpha \sin^2(m\pi + \delta\phi/2)} \right] \\ &\approx I_0 \left[1 + \frac{1}{1 + \alpha (2/\sqrt{\alpha})^2} \right] = \frac{6}{5} I_0 \end{aligned}$$

So here the valley to peak ratio is $5/6 = 0.833$.

12-23. (a) As discussed at the end of Sec. 12.8, the effective area of a paraboloidal antenna is typically about one-half of its geometric area,

$$A_2 \approx \frac{1}{2} \left(\frac{\pi}{4} d_2^2 \right) = 3.5 \text{ m}^2$$

and the required Poynting intensity is

$$S = \frac{P_2}{A_2} \approx 1.4 \times 10^{-13} \text{ W/m}^2$$

(b) Using the Rayleigh criterion of Eq. (12.70) to determine the illuminated area, and translating into the current notation,

$$\begin{aligned} \frac{D\lambda}{h} &\approx \Delta\theta_{\text{Ray}} = 1.22 \frac{c}{f} \\ \Rightarrow d_1 &\approx \frac{2.44ch}{fD} = \frac{2.44(3.0 \times 10^8 \text{ m/s})(36 \times 10^6 \text{ m})}{(4 \times 10^9 \text{ s}^{-1})(2.5 \times 10^6 \text{ m})} = 2.6 \text{ m} \end{aligned}$$

In practice, because this antenna is nonuniformly illuminated by its feed, the radiation pattern to the first nulls would be somewhat broader than D (see Prob. 12-14a). But we probably want the nulls to come some distance outside the service area anyhow.

(c) From Eq. (12.68), with the total radiated power $P = \pi a^2 |\psi_0|^2$, we have

$$\begin{aligned} S(Z \rightarrow h) &= I_0 = \left(\frac{\pi a^2}{\lambda Z} \right)^2 \frac{P}{\pi a^2} \rightarrow \frac{\pi d_1^2 P_1}{4c^2 h^2} \\ \Rightarrow P_1 &\approx \frac{4}{\pi} \left(\frac{ch}{fd_1} \right)^2 S = \frac{4}{\pi} \left[\frac{(3.0 \times 10^8)(36 \times 10^6)}{(4 \times 10^9)(2.6)} \right]^2 (0.5 \times 10^{-12}) = 0.7 \text{ W} \end{aligned}$$

(d) If we ignore diffraction and assume that the satellite antenna delivers all its power uniformly over the circle of radius D at the distance h , then from Eq. (9.77) its directivity is

$$G_1 = \frac{4\pi}{\Delta\Omega} = 4\pi \left(\frac{h^2}{\pi D^2/4} \right) = \frac{16h^2}{D^2} = 3300$$

From Eq. (9.84) or (12.52), and the rule of thumb that the effective area is one-half the geometric area,

$$\begin{aligned} \frac{1}{2} \left(\frac{\pi}{4} d_1^2 \right) &\approx A_1 = G_1 \frac{\lambda^2}{4\pi} \\ \Rightarrow d_1 &\approx \frac{4\sqrt{2}hc}{\pi fD} = \frac{1.80hc}{fD} = 1.9 \text{ m} \end{aligned}$$

This is about 35% less than the value estimated in Part (b)—good agreement considering the crudity of both calculations. Writing Eq. (9.87) in a mixed form appropriate to our given parameters, we have

$$\frac{P_{\text{rec}}}{P_{\text{trans}}} = \frac{G_1 A_2}{4\pi h^2} \approx \frac{(16h^2/D^2)(\pi d_2^2/8)}{4\pi h^2} = \frac{d_2^2}{2D^2}$$

$$\Rightarrow P_{\text{trans}} \rightarrow P_1 \approx \frac{2P_2 D^2}{d_2^2} = \frac{2(0.5 \times 10^{-12})(2.5 \times 10^6)^2}{(3)^2} = 0.7 \text{ W}$$

which agrees fortuitously well with that calculated in Part (c). The result when cast in this form is intuitively obvious: we are spreading the transmitted power P_1 over the service area of the order of D^2 , and capturing the small portion P_2 in the receiving antenna's area of the order of d_2^2 . Note also that this is a very modest power, so it is not difficult to provide a terrestrial signal P_2 that is a couple of orders of magnitude above the threshold value.

12-24. The deBroglie wavelength is $\lambda_{\text{deB}} = h/p = h/\sqrt{2mE}$, where p is the particle momentum, E its (nonrelativistic) energy, and h is Planck's constant. The energy of a photon is $E = h\nu$, where ν is the (cyclic) frequency. Thus the wavelength of an electromagnetic quantum of energy E is $\lambda_{\text{em}} = c/\nu = hc/E$. For equal energies,

$$E = \frac{h^2}{2m\lambda_{\text{deB}}^2} = \frac{hc}{\lambda_{\text{em}}} \Rightarrow \lambda_{\text{deB}}^2 = \frac{h}{2mc} \lambda_{\text{em}}$$

The coefficient $h/2mc \equiv \lambda_C$ is known as the Compton wavelength. By Newtonian mechanics, a particle whose deBroglie wavelength is equal to this coefficient would have the energy

$$E = \frac{p^2}{2m} = \frac{(h/\lambda_C)^2}{2m} = 2mc^2 ?$$

But this violates the nonrelativistic assumption. Thus, under nonrelativistic conditions, we have $\lambda_C \ll \lambda_{\text{deB}}$, and hence $\lambda_{\text{deB}} \ll \lambda_{\text{em}}$. Since the energy of the incident particle or photon is limited by the possibility of destruction of the target material, an electron microscope will generally operate with a shorter effective wavelength, and hence higher resolution.

13-1. (a) From Eqs. (13.7):

$$\frac{dC}{du} = \cos\left(\frac{\pi}{2}u^2\right), \quad \frac{dS}{du} = \sin\left(\frac{\pi}{2}u^2\right)$$

$$\Rightarrow \text{slope} = \frac{dC}{dS} = \tan\left(\frac{\pi}{2}u^2\right)$$

Since the slope of a curve is the tangent function of the angle θ that the curve makes with the horizontal axis, in this case $\theta = \frac{\pi}{2}u^2$.

(b) A small increment of arc length, Δs , subtends the angle $\Delta\theta = \Delta s/R$ at the center of a circle of radius R . The angle $\Delta\theta$ is also the *change* in the angle of the arc over this increment. That is, $\Delta\theta/\Delta s \rightarrow d\theta/ds = 1/R$. Applying this relation to the Cornu spiral, with u measuring arc length along the spiral [Eq. (13.9)],

$$R = \left(\frac{d\theta}{ds}\right)^{-1} \rightarrow \left[\frac{d\left(\frac{\pi}{2}u^2\right)}{du}\right]^{-1} = \frac{1}{\pi u}$$

Here, R and u are in the normalized units of the Cornu spiral. But because of the linear relation, the equation holds for R and u measured in any length unit.

(c) In an inertial frame, an object moving with speed V on a (locally) circular trajectory of radius R has the centripetal acceleration of V^2/R . Therefore, a person of mass M riding in the reference frame of the train experiences the centrifugal force MV^2/R . For constant $V \rightarrow V_0$, there is no tangential (forward/backward) force. When the track is laid out as a Cornu spiral, with $u = u_0 + V_0 t$, then the sidewise force is

$$\frac{MV^2}{R} \rightarrow \pi M V_0^2 (u_0 + V_0 t)$$

13-2. From Eq. (13.12), the opaque strip has the normalized width $\Delta u = W/\sqrt{\lambda Z/2}$. The amplitude received at the observation point consists of two signals, one from each side of the obstacle. Formally, for a centered observation point, the diffraction integral, Eq. (13.6), breaks into two: one with limits from $u \rightarrow -\infty$ to $u_1 = -\Delta u/2$ and the other with limits from $u_2 = +\Delta u/2$ to $u \rightarrow +\infty$. These signals can be represented by phasors, one drawn from the limit point in the third quadrant of Fig. 13-2 to the point where $u = -\Delta u/2$, and the other is from the point where $u = +\Delta u/2$ to the limit point in the first quadrant. By symmetry, the two phasors are

parallel (i.e., have the same phase), and have the same magnitude. Thus the intensity is four times the square of the length of one of these phasors:

$$I(\Delta u) = \frac{I_0}{2} 4 \left\{ \left[\frac{1}{2} - C\left(\frac{\Delta u}{2}\right) \right]^2 + \left[\frac{1}{2} - S\left(\frac{\Delta u}{2}\right) \right]^2 \right\}$$

The normalization, $I_0 \propto 2$, comes from the square of the phasor between the two limit points, as in Eq. (13.11). Since the length of the chord from the point where $u = \Delta u/2$ to the limit point decreases monotonically, so does the intensity as W increases.

If one wishes to consider non-centered observation points [located by $u_{cen}(x)$ of Eq. (13.13)], then the limits $u_1 = u_{cen} - \Delta u/2$ and $u_2 = u_{cen} + \Delta u/2$ are no longer symmetrical, and the two phasors have neither the same amplitude nor the same phase. The computation is tedious but straightforward:

$$I(\Delta u; u_{cen}) = \frac{I_0}{2} \left\{ \left[\frac{1}{2} - C(u_2) + C(u_1) - \left(-\frac{1}{2}\right) \right]^2 + \left[\frac{1}{2} - S(u_2) + S(u_1) - \left(-\frac{1}{2}\right) \right]^2 \right\}$$

Can you see Babinet's principle lurking in the comparison of this expression with Eq. (13.11)?

13-3. In Fig. 13-1, let the opaque "knife" extend from $\xi = a_2$ to $+\infty$, and hold the observation point at the reference line, $x = 0$ (that is, we'll move the knife-edge, rather than the observation point). Then in Eq. (13.11) $u_1 \rightarrow -\infty$, and $u_2 = a_2/\sqrt{\lambda Z/2}$. Geometrically, in the Cornu plot of Fig. 13-2, the intensity is proportional to the square of the chord that extends from the limit point in the third quadrant to the point defined by u_2 (the observation point is in the geometrical shadow for negative values of u_2). From the graph, we see that the maximum of this chord occurs near $u_2 \approx +1.2$. A reasonable approximation is to find the point where the slope of the spiral is 135° (45° in the second quadrant): from Prob. 13-1(a), $\frac{\pi}{2}u_2^2 \approx \frac{3}{4}\pi$, or $u_2 \approx \sqrt{3/2} = 1.225$. A rigorous solution requires calculating the maximum of

$$I(u_2) = \frac{I_0}{2} \left\{ \left[\frac{1}{2} + C(u_2) \right]^2 + \left[\frac{1}{2} + S(u_2) \right]^2 \right\}$$

From tables (Ab65, p. 321),

u_2	$C(u_2)$	$S(u_2)$	$I(u_2)/I_0$
1.20	0.71544	0.62340	1.36966
1.22	.70212	.63831	1.37042
1.24	.68769	.65216	1.36905

Interpolation gives $u_2 = 1.217$, and a maximum intensity of $1.37044I_0$. From Eq. (12.21) (with $Z_0 \rightarrow \infty$, and $\rho \rightarrow a_2$) and the concept of linear zones developed in Prob. 12-5, the zone parameter at the knife-edge is $n = a_2^2/\lambda Z = u_2^2/2 \rightarrow 0.741$. A value close to $3/4$ is hardly surprising in view of the discussion in the paragraph following Eq. (13.17) (the -45° -slope condition is precisely the $3/4$ -zone condition).

13-4. We can use Eqs. (13.18–21) to approximate the Fresnel integrals in Eq. (13.11). The raw abscissa in the frames of Fig. 13-4 is $X \equiv x/(W/2)$, so that the geometric shadow edges come at the same place ($X = \pm 1$) in each frame. The labeling shown is $u_{cen} = X\sqrt{2N}$, from Eqs. (13.12–13) using $\Delta u = \sqrt{8N}$ from Eq. (13.17). Thus, $u_1 = u_{cen} - \Delta u/2 = (X - 1)\sqrt{2N}$, and $u_2 = (X + 1)\sqrt{2N}$.

Step size: From the figure, we infer that there are N cycles of oscillations within the "geometrically illuminated" range $\Delta X = 2$. That is, the major oscillations have an average "wavelength" of $2/N$, but this wavelength is not at all uniform and there is fine structure upon the major oscillations. Something like 16 points per average-wavelength would capture most of the structure. We'll use 32, that is, a step size $\delta X = 1/(16N)$.

Range of abscissa: For large N , in the wings of the pattern, the upper limit is essentially at the limit point $u_2 \rightarrow +\infty$, and the lower limit u_1 is in the spiral close to that limit. Therefore the magnitude of the phasor is essentially the radius of curvature of the Cornu spiral at u_1 , which was shown in Prob. 13-1 to be $R = 1/\pi u_1$. Therefore,

$$\frac{I}{I_0} \approx \frac{1}{2} \left(\frac{1}{\pi u_1} \right)^2 = \frac{1}{4\pi^2 N (X-1)^2}$$

If we arbitrarily choose the criterion that the relative intensity is 1% at $X = \pm X_{max}$, then

$$X_{max} = 1 + \sqrt{\frac{100}{4\pi^2 N}} \approx 1 + \frac{1.6}{\sqrt{N}}$$

Further discussion of practical computations of Fresnel patterns, including for the circular aperture, is given by Heald, *Am.J.Phys.* **54**, 982 (1986).

The numerical case suggested is for a slit of size N zones where, from Eq. (13.17),

$$N = \frac{W^2}{4\lambda Z} \rightarrow \frac{(2 \times 10^{-3} \text{m})^2}{4(500 \times 10^{-9} \text{m})(1.00 \text{m})} = 2$$

The real-space coordinate x in the observation plane is related to the normalized coordinates by:

$$x = \begin{cases} X \left(\frac{W}{2} \right) \rightarrow X \times 1 \text{ mm} \\ u_{\text{cen}} \frac{W/2}{\sqrt{2N}} \rightarrow u_{\text{cen}} \times 0.5 \text{ mm} \end{cases}$$

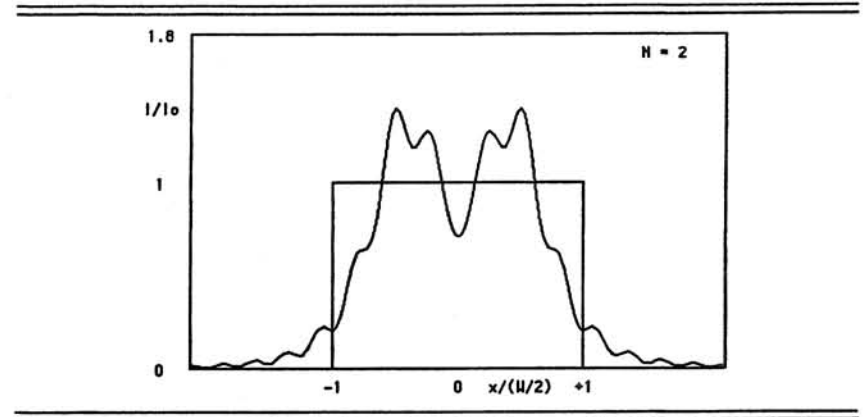
The following program uses the graphing syntax of TrueBASIC. This version chooses an appropriate abscissa scale for each N value; it could be modified slightly to give a family of patterns all with the same X scale, as in Fig. 13-4.

```

REM Fresnel diffraction by slit of N zones
REM   Abscissa X = x/(W/2)
DIM X(500),I(500)           !(increase dimension for N > 10)
OPEN #1: screen 0.1, 0.9, 0.1, 0.9
LET N = 2                   !specify zone size
SUB FRES(U, C, S)           !subroutine for Fresnel integrals
  LET SU = SGN(U)
  LET U = ABS(U)
  LET F = (1+0.882*U)/(2+1.722*U+3.017*U^2)
  LET G = 1/(2+4.167*U+3.274*U^2+6.89*U^3)
  LET UU = PI*U^2/2
  LET C = SU * (0.5 + F * SIN(UU) - G * COS(UU))
  LET S = SU * (0.5 - F * COS(UU) - G * SIN(UU))
END SUB
LET RN = SQR(2 * N)
LET DX = 1/(16*N)           !step size
LET NX = INT((1 + 1.6/SQR(N))/DX) !max number of steps
LET XMAX = NX * DX
SET WINDOW -XMAX, XMAX, 0, 1.8
BOX LINES -XMAX, XMAX, 0, 1.8
PLOT LINES: -1, 0; -1, 1; 1, 1; 1, 0 !"geometrical" limit
FOR J = 0 TO NX
  LET XX = J * DX
  LET X(250-J) = -XX        !*250* is one-half
  LET X(250+J) = XX        ! of "500" dimension
  LET U1 = (XX - 1) * RN
  LET U2 = (XX + 1) * RN
  CALL FRES(U1,C1,S1)
  CALL FRES(U2,C2,S2)
  LET I(250-J),I(250+J) = 0.5 * ((C2-C1)^2 + (S2-S1)^2)
NEXT J
FOR J = -NX TO NX
  PLOT LINES: X(250+J), I(250+J);
NEXT J
CLOSE #1
END

```

The output for $N = 2$ (with labeling added) is shown in the following column.



13-5, cont.

$$V_0 = \begin{pmatrix} r_0 \\ r_0' \end{pmatrix}$$

where $r_0' = dr/dz = \tan \alpha$ is the slope of the ray with respect to the axis. Traversing the axial distance L and passing through the next lens (of focal length f_1), the ray vector is multiplied by the matrix product [Eqs. (13.31) and (13.33)]

$$N_1 M = \begin{pmatrix} 1 & 0 \\ -1/f_1 & 1 \end{pmatrix} \begin{pmatrix} 1 & L \\ 0 & 1 \end{pmatrix} = \begin{pmatrix} 1 & L \\ -1/f_1 & 1 - L/f_1 \end{pmatrix}$$

A similar matrix product $N_2 M$ transforms the ray vector to the value as it exits the third lens (focal length f_2 , which is a duplicate of the first lens). That is, one full cycle through the unfolded equivalent of Fig 13-9 is represented by the matrix product

$$N_2 M N_1 M = \begin{pmatrix} 1 & L \\ -1/f_2 & 1 - L/f_2 \end{pmatrix} \begin{pmatrix} 1 & L \\ -1/f_1 & 1 - L/f_1 \end{pmatrix} = \begin{pmatrix} A & B \\ C & D \end{pmatrix}$$

where:

$$A = 1 - \frac{L}{f_1} \qquad B = L + L \left(1 - \frac{L}{f_1} \right)$$

$$C = -\frac{1}{f_2} - \frac{1}{f_1} \left(1 - \frac{L}{f_2} \right) \qquad D = -\frac{L}{f_2} + \left(1 - \frac{L}{f_2} \right) \left(1 - \frac{L}{f_1} \right)$$

If we label the entrance plane by the index s , and the exit plane by $s+1$, then the matrix operation $V_{s+1} = N_2 M N_1 M V_s$ is equivalent to the pair of equations

$$r_{s+1} = Ar_s + Br_s' \quad (1)$$

$$r_{s+1}' = Cr_s + Dr_s' \quad (2)$$

Now we seek a recursion relation between r_s , r_{s+1} , and r_{s+2} . The key is to note that we can express r_{s+1}' in terms of unprimed r quantities in two different ways. We can solve (1)–(2) for

$$r_{s+1}' = Cr_s + \frac{D}{B}(r_{s+1} - Ar_s) \quad (3)$$

And we can rearrange (1) and increment the index to obtain

$$r_{s+1}' = \frac{1}{B}(r_{s+2} - Ar_{s+1}) \quad (4)$$

Equating and rearranging,

$$r_{s+2} - (A+D)r_{s+1} + (AD-BC)r_s = 0$$

One coefficient is

$$A+D = 2 - \frac{2L}{f_1} - \frac{2L}{f_2} + \frac{L^2}{f_1 f_2}$$

which is symmetrical in the two lenses, f_1 and f_2 , as it should be for a full cycle. The other is

$$\begin{aligned} AD-BC &= \left[1 - \frac{L}{f_1}\right] \left[-\frac{L}{f_2} + \left(1 - \frac{L}{f_2}\right) \left(1 - \frac{L}{f_1}\right)\right] \\ &\quad - \left[L + L\left(1 - \frac{L}{f_1}\right)\right] \left[-\frac{1}{f_2} - \frac{1}{f_1} \left(1 - \frac{L}{f_2}\right)\right] \\ &= \left(1 - \frac{L}{f_1}\right) \left(1 - \frac{L}{f_2}\right) \left[\left(1 - \frac{L}{f_1}\right) + \frac{L}{f_1}\right] \\ &\quad + \left(1 - \frac{L}{f_1}\right) \left[-\frac{L}{f_2} + \frac{L}{f_2}\right] - L \left[-\frac{1}{f_2} - \frac{1}{f_1} \left(1 - \frac{L}{f_2}\right)\right] \\ &= 1 \end{aligned}$$

[insert homework above]

Thus we have verified Eqs. (13.36) and (13.40). The condition for an oscillatory solution of the recursion relation is that $\cos\beta$ of Eq. (13.40) is bounded between the limits of ± 1 :

$$-1 \leq 1 - \frac{L}{f_1} - \frac{L}{f_2} + \frac{L^2}{2f_1 f_2} \leq +1$$

Add +1 to each of the three quantities, and divide through by 2, to get

$$0 \leq 1 - \frac{L}{2f_1} - \frac{L}{2f_2} + \frac{L^2}{4f_1 f_2} \equiv \left(1 - \frac{L}{2f_1}\right) \left(1 - \frac{L}{2f_2}\right) \leq 1$$

With the translation back to the equivalent mirrors of Fig. 13-9, $2f \rightarrow R$, we have Eq. (13.41).

13-6. (a) The stability test of Eq. (13.41) gives

$$\left(1 - \frac{L}{R_1}\right) \left(1 - \frac{L}{R_2}\right) = \left(1 - \frac{30}{75}\right)^2 = 0.36$$

Since this lies between 0 and 1, the system is stable.

(b) Equations (13.55) give

$$-z_1 = +z_2 = \frac{L(R-L)}{R+R-2L} = \frac{L}{2} \rightarrow 15 \text{ cm}$$

which is obvious enough from the symmetry.

(c) The simplified form of Eq. (13.56) for symmetric mirrors gives

$$z_0 = \sqrt{\frac{1}{4}L(2R-L)} = \sqrt{\frac{1}{4}(30)(150-30)} = 30 \text{ cm}$$

Therefore from Eq. (13.45),

$$w_0 = \sqrt{\frac{\lambda z_0}{\pi}} = \sqrt{\frac{(632.8 \times 10^{-7})(30)}{\pi}} = 0.246 \text{ mm}$$

(d) Although there are phase corrections near $z=0$ [given by the η term in Eq. (13.46)], the modes are quantized such that the axial mode number is a large integer n that is very close to $L/(\lambda/2)$. [The situation is analogous to the Fabry-Perot interferometer, as in Eq. (11.87).] The resonant frequencies can be written as

$$f_n = \frac{c}{\lambda_n} \approx n \frac{c}{2L}$$

and therefore the spacing between modes is

$$\Delta f = \frac{c}{2L} \rightarrow \frac{3 \times 10^{10} \text{ cm/s}}{2(30 \text{ cm})} = 500 \text{ MHz}$$

with $n \approx 2(30)/(632.8 \times 10^{-7}) = 948,000$.

Chapter 14

14-1. The Galilean transformation considers time to be universal; no distinction is made between the t' and t of Eq. (14.1b), and the invariance expressed by Eq. (14.3) follows essentially trivially: Equation (14.1a) can be written as a vector equation,

$$\mathbf{x}' = \mathbf{x} - \mathbf{v}t$$

The first time derivative gives the velocity transformation,

$$\mathbf{u}' = \mathbf{u} - \mathbf{v}$$

and the second time derivative gives the invariance of acceleration, so long as the relative velocity \mathbf{v} is constant.

Now, when we include time as a fourth dimension and compare the four-dimensional coordinates in two frames, the formal relations between *partial* derivatives are given by Eqs. (14.5a–b). The *total* time derivative, which figures in the velocity and acceleration, is then given by (summation convention with $j = 1, 2, 3$)

$$\frac{d}{dt} = \frac{\partial}{\partial t} + \frac{dx_j}{dt} \frac{\partial}{\partial x_j} = \frac{\partial}{\partial t} + u_j \frac{\partial}{\partial x_j}$$

which leads, for instance, to the identity

$$u_3 = \frac{d}{dt} x_3 = \left(\frac{\partial}{\partial t} + u_j \frac{\partial}{\partial x_j} \right) x_3 = u_3$$

Expanding in terms of primed coordinates, using Eqs. (14.5a–b), we obtain a similar identity,

$$\begin{aligned} u_3 &= \left[\left(\frac{\partial}{\partial t'} - v \frac{\partial}{\partial x'_3} \right) + u_3 \left(\frac{\partial}{\partial x'_3} \right) \right] (x'_3 + vt') \\ &= v - v + u_3 = u_3 \end{aligned}$$

In general, to relate velocities (and accelerations) as perceived in the two frames, one must form a quotient of differentials, as in the Solution for Prob. 14-5.

14-2. From the Lorentz transformation of Eqs. (14.25), we get in place of Eqs. (14.5a–b):

Chapter 14

$$\frac{\partial}{\partial x_1} = \frac{\partial}{\partial x'_1} \qquad \frac{\partial}{\partial x_2} = \frac{\partial}{\partial x'_2}$$

$$\frac{\partial}{\partial x_3} = \frac{\partial x'_3}{\partial x_3} \frac{\partial}{\partial x'_3} + \frac{\partial t'}{\partial x_3} \frac{\partial}{\partial t'} = \gamma \left(\frac{\partial}{\partial x'_3} - \frac{\beta}{c} \frac{\partial}{\partial t'} \right)$$

$$\frac{\partial}{\partial t} = \frac{\partial x'_3}{\partial t} \frac{\partial}{\partial x'_3} + \frac{\partial t'}{\partial t} \frac{\partial}{\partial t'} = \gamma \left(-v \frac{\partial}{\partial x'_3} + \frac{\partial}{\partial t'} \right)$$

Thus,

$$\frac{\partial^2}{\partial t^2} = \gamma^2 \left(\frac{\partial^2}{\partial t'^2} - 2v \frac{\partial^2}{\partial x'_3 \partial t'} + v^2 \frac{\partial^2}{\partial x'^2_3} \right)$$

$$\nabla^2 = \nabla'^2 - \frac{\partial^2}{\partial x'^2_3} + \gamma^2 \left(\frac{\partial^2}{\partial x'^2_3} - \frac{2\beta}{c} \frac{\partial^2}{\partial x'_3 \partial t'} + \frac{\beta^2}{c^2} \frac{\partial^2}{\partial t'^2} \right)$$

and

$$\begin{aligned} \nabla^2 &= \frac{1}{c^2} \frac{\partial^2}{\partial t^2} \\ &= \nabla'^2 + \left(-1 + \gamma^2 - \gamma^2 \frac{v^2}{c^2} \right) \frac{\partial^2}{\partial x'^2_3} \\ &\quad + \left(-\gamma^2 \frac{2\beta}{c} + \gamma^2 \frac{2v}{c^2} \right) \frac{\partial^2}{\partial x'_3 \partial t'} + \left(\gamma^2 \frac{\beta^2}{c^2} - \gamma^2 \frac{1}{c^2} \right) \frac{\partial^2}{\partial t'^2} \\ &= \nabla'^2 - \frac{1}{c^2} \frac{\partial^2}{\partial t'^2} \end{aligned}$$

Thus the d'Alembertian (wave-equation) operator is indeed invariant.

The transformation of the acceleration is calculated in Eqs. (14.100). Since the acceleration is not invariant, neither is $\mathbf{F} = m\mathbf{a}$.

14-3. If $\tanh\alpha = \sinh\alpha/\cosh\alpha = \beta$, and $\cosh^2\alpha - \sinh^2\alpha = 1$, then

$$\sinh\alpha = \frac{\beta}{\sqrt{1-\beta^2}} = \gamma\beta$$

$$\cosh\alpha = \frac{1}{\sqrt{1-\beta^2}} = \gamma$$

With these substitutions, the given equations reduce to Eqs. (14.25). From the definitions of the circular and hyperbolic functions in terms of exponentials, we have:

$$\sinh\alpha = -i \sin(i\alpha)$$

$$\cosh\alpha = \cos(i\alpha)$$

Thus,

$$x'_3 = x_3 \cos(i\alpha) + ict \sin(i\alpha)$$

$$ict' = ict \cos(i\alpha) - x_3 \sin(i\alpha)$$

which represent formally a rotation in the $(x_3)-(ict)$ plane (a subset of four-space) by the angle $i\alpha$.

14-4. At time t by the K clock, the K' clock reads

$$t' = \gamma \left(t - \frac{\beta}{c} vt \right) = t \sqrt{1 - \beta^2}$$

However, as seen by a telescope, the reading of the moving clock is further retarded by the transit time of the light signal. The reading t'_r , emitted at K' 's time t , reaches K at $t + vt/c = t(1 + \beta)$. Thus the K' reading as received at t is

$$t'_r = \frac{t \sqrt{1 - \beta^2}}{1 + \beta} = t \sqrt{\frac{1 - \beta}{1 + \beta}}$$

An alternative approach is to calculate that, in order to reach K at t , the signal must have been emitted by K' at a retarded time reckoned by K as

$$t_r = t - \frac{vt_r}{c} \quad \Rightarrow \quad t_r = \frac{t}{1 + \beta}$$

at which time the K' clock reads

$$t'_r = \left(\frac{t}{1 + \beta} \right) \sqrt{1 - \beta^2} = t \sqrt{\frac{1 - \beta}{1 + \beta}}$$

14-5. The position vector can be resolved into components perpendicular and parallel to \mathbf{v} ,

$$\mathbf{x} = \mathbf{x}_\perp + \mathbf{x}_\parallel$$

where $\mathbf{x}_\parallel = (\mathbf{x} \cdot \mathbf{v})\mathbf{v}/v^2$. From Eqs. (14.25),

$$\mathbf{x}'_\perp = \mathbf{x}_\perp \quad \mathbf{x}'_\parallel = \gamma(\mathbf{x}_\parallel - \mathbf{v}t)$$

so that

$$\mathbf{x}' = \mathbf{x}'_\perp + \mathbf{x}'_\parallel = \mathbf{x} + \left[\frac{\mathbf{x} \cdot \mathbf{v}}{v^2} (\gamma - 1) - \gamma t \right] \mathbf{v}$$

Similarly,

$$t' = \gamma \left(t - \frac{\beta}{c} x_\parallel \right) = \gamma \left(t - \frac{\mathbf{x} \cdot \mathbf{v}}{c^2} \right)$$

The velocity transformation is found by computing differentials,

$$d\mathbf{x}' = d\mathbf{x} + \left[\frac{d\mathbf{x} \cdot \mathbf{v}}{v^2} (\gamma - 1) - \gamma dt \right] \mathbf{v}$$

$$dt' = \gamma \left(dt - \frac{d\mathbf{x} \cdot \mathbf{v}}{c^2} \right)$$

$$\mathbf{u}' = \frac{d\mathbf{x}'}{dt'} = \frac{\mathbf{u} + \left[\frac{\mathbf{u} \cdot \mathbf{v}}{v^2} (\gamma - 1) - \gamma \right] \mathbf{v}}{\gamma \left(1 - \frac{\mathbf{u} \cdot \mathbf{v}}{c^2} \right)}$$

Rearrangement of the factor $\gamma = 1/\sqrt{1 - \beta^2}$ puts the formula in the form given. For \mathbf{u} parallel to \mathbf{v} , the formula reduces to

$$u'_\parallel = \frac{u_\parallel - v}{1 - \frac{u_\parallel v}{c^2}}$$

which is the well-known one-dimensional velocity addition formula. When \mathbf{u} is perpendicular to \mathbf{v} ,

$$u'_\perp = \frac{u_\perp}{\gamma} - \mathbf{v}$$

where the factor of γ is essentially the time dilation between the two frames (there being no length contraction for perpendicular lengths).

14-6. The plane wave remains plane because the transformation is linear. The wavefunctions are:

$$\begin{aligned} \text{in } K \quad \psi &= \psi_0 e^{i(\mathbf{k}\cdot\mathbf{x} - \omega t)} \\ \text{in } K' \quad \psi' &= \psi_0 e^{i(\mathbf{k}'\cdot\mathbf{x}' - \omega' t')} \end{aligned}$$

The functions are the same when \mathbf{x}, t and \mathbf{x}', t' are related by a Lorentz transformation. We can write the phase factors as:

$$\begin{aligned} \mathbf{k}\cdot\mathbf{x} - \omega t &= (\mathbf{k}, i\omega/c) \cdot (\mathbf{x}, ict) \\ \mathbf{k}'\cdot\mathbf{x}' - \omega' t' &= (\mathbf{k}', i\omega'/c) \cdot (\mathbf{x}', ict') \end{aligned}$$

By Eq. (14.28), $\mathbf{X} = (\mathbf{x}, ict)$ is a four-vector. Since the scalar product is invariant, $\mathbf{K} = (\mathbf{k}, i\omega/c)$ is also a four-vector. That is, the components of \mathbf{K} transform in a manner identical to the components of \mathbf{X} . Thus we can paraphrase the t' formula in Prob. 14-5, with $t \rightarrow \omega/c^2$ and $\mathbf{x} \rightarrow \mathbf{k}$, to obtain

$$\frac{\omega'}{c^2} = \gamma \left(\frac{\omega}{c^2} - \frac{\mathbf{k} \cdot \mathbf{v}}{c^2} \right)$$

If θ is the angle between \mathbf{k} and \mathbf{v} , then with $k = \omega/c$ and $\beta = v/c$, we have the relativistic Doppler formula

$$\omega' = \gamma \omega (1 - \beta \cos \theta)$$

14-7. We want to find the sum of the three terms of the form $\partial F_{\mu\nu} / \partial x_\lambda$ when λ, μ, ν are permuted cyclically and $F_{\mu\nu} = \partial A_\nu / \partial x_\mu - \partial A_\mu / \partial x_\nu$. Write the terms out explicitly:

$$\left(\frac{\partial^2 A_\nu}{\partial x_\lambda \partial x_\mu} - \frac{\partial^2 A_\mu}{\partial x_\lambda \partial x_\nu} \right) + \left(\frac{\partial^2 A_\lambda}{\partial x_\mu \partial x_\nu} - \frac{\partial^2 A_\nu}{\partial x_\mu \partial x_\lambda} \right) + \left(\frac{\partial^2 A_\mu}{\partial x_\nu \partial x_\lambda} - \frac{\partial^2 A_\lambda}{\partial x_\nu \partial x_\mu} \right) = 0$$

The derivatives are independent and the order of differentiation can be commuted. For any given component (e.g., A_ν), the second-order mixed derivative (with respect to x_λ and x_μ) appears twice, with opposite sign, and everything cancels. Since λ, μ, ν are three different indices selected from the four values, one value does not appear; thus there are four different identities of this form. As discussed following Eq. (14.63), these represent the homogeneous Maxwell equations, $\text{div} \mathbf{B} = 0$ and $\text{curl} \mathbf{E} + \dot{\mathbf{B}}/c = 0$.

14-8. If the four-dimensional gradient is to be a four-vector, its components must transform in the same way as the components of the position four-vector, Eq. (14.10) (with implied summation),

$$\frac{\partial \psi}{\partial x'_\mu} \stackrel{?}{=} \lambda_{\mu\nu} \frac{\partial \psi}{\partial x_\nu}$$

where ψ is a Lorentz scalar. By the chain rule for the derivative of a function of several variables,

$$\frac{\partial \psi}{\partial x'_\mu} = \frac{\partial \psi}{\partial x_\nu} \frac{\partial x_\nu}{\partial x'_\mu}$$

From Eq. (14.71a), $\partial x_\nu / \partial x'_\mu = \lambda_{\mu\nu}$. Therefore the gradient does indeed transform as a four-vector. [In general, the gradient of a tensor of rank r is a tensor of rank $r+1$, and the divergence of a tensor of rank r is a tensor of rank $r-1$.]

14-9. The tensor F transforms according to Eq. (14.73),

$$F'_{\mu\nu} = \lambda_{\mu\sigma} \lambda_{\nu\rho} F_{\sigma\rho}$$

Similarly, using Eq. (14.71a),

$$\frac{\partial F'_{\mu\nu}}{\partial x'_\lambda} = \lambda_{\lambda\kappa} \lambda_{\mu\sigma} \lambda_{\nu\rho} \frac{\partial F_{\sigma\rho}}{\partial x_\kappa} \quad (1)$$

With the implicit summation, the right-hand side is actually $4^3 = 64$ terms! Now sum three versions of (1) for the three permutations of λ, μ, ν in the primed version of Eq. (14.63). The $3 \times 64 = 192$ terms on the right can be partitioned into 64 clusters, each of which has a particular set of values κ, σ, ρ , with a common factor $\lambda_{\lambda\kappa} \lambda_{\mu\sigma} \lambda_{\nu\rho}$ multiplying a sum of three permuted derivatives that vanish by Eq. (14.63). Therefore, the entire sum vanishes, and Eq. (14.63) holds in the primed frame—i.e., it is covariant.

For Eq. (14.64), the left-hand side is (1) with $\lambda = \nu$, so that [using Eq. (14.11)]

$$\begin{aligned} \frac{\partial F'_{\mu\nu}}{\partial x'_\nu} &= \lambda_{\nu\kappa} \lambda_{\mu\sigma} \lambda_{\nu\rho} \frac{\partial F_{\sigma\rho}}{\partial x_\kappa} \\ &= \delta_{\kappa\rho} \lambda_{\mu\sigma} \frac{\partial F_{\sigma\rho}}{\partial x_\kappa} = \lambda_{\mu\sigma} \frac{\partial F_{\sigma\rho}}{\partial x_\rho} \end{aligned}$$

The right-hand side involves

$$J'_\mu - \lambda_{\mu\sigma} J_\sigma$$

Thus,

$$\left(\frac{\partial F'_{\mu\nu}}{\partial x'_\nu} - \frac{4\pi}{c} J'_\mu \right) = \lambda_{\mu\sigma} \left(\frac{\partial F_{\sigma\rho}}{\partial x_\rho} - \frac{4\pi}{c} J_\sigma \right)$$

If either quantity in parentheses is zero, so is the other, and Eq. (14.64) is shown to be covariant.

14-10. (a) With the implicit summation over both indices, the operations represented by the first two quantities in Eq. (14.67) are simply the sum of the squares of the sixteen elements of Eqs. (14.62) and (14.65), respectively:

$$\begin{aligned} F_{\mu\nu}F_{\mu\nu} &= \sum_\mu \sum_\nu F_{\mu\nu}F_{\mu\nu} = (0)^2 + (B_3)^2 + (-B_2)^2 + (-iE_1)^2 + \dots \\ &= 2(B_1^2 + B_2^2 + B_3^2 - E_1^2 - E_2^2 - E_3^2) = 2(B^2 - E^2) \\ G_{\mu\nu}G_{\mu\nu} &= (0)^2 + (-E_3)^2 + (E_2)^2 + (-iB_1)^2 + \dots = 2(E^2 - B^2) \end{aligned}$$

The third operation is

$$\begin{aligned} F_{\mu\nu}G_{\mu\nu} &= (0)^2 + (B_3)(-E_3) + (-B_2)(E_2) + (-iE_1)(-iB_1) + \dots \\ &= -4(E_1B_1 + E_2B_2 + E_3B_3) = -4\mathbf{E} \cdot \mathbf{B} \end{aligned}$$

(b) From the transformation equations, Eqs. (14.76),

$$\begin{aligned} \mathbf{E}' \cdot \mathbf{B}' &= E'_1B'_1 + E'_2B'_2 + E'_3B'_3 \\ &= \gamma^2(E_1 - \beta B_2)(B_1 + \beta E_2) + \gamma^2(E_2 + \beta B_1)(B_2 - \beta E_1) + E_3B_3 \\ &= \gamma^2(E_1B_1 + \beta E_1E_2 - \beta B_1B_2 - \beta^2 E_2B_2 + E_2B_2 - \beta E_1E_2 + \beta B_1B_2 - \beta^2 E_1B_1) + E_3B_3 \\ &= E_1B_1 + E_2B_2 + E_3B_3 = \mathbf{E} \cdot \mathbf{B} \end{aligned}$$

Similarly,

$$\begin{aligned} E'^2 - B'^2 &= \gamma^2(E_1 - \beta B_2)^2 + \gamma^2(E_2 + \beta B_1)^2 + E_3^2 \\ &\quad - \gamma^2(B_1 + \beta E_2)^2 - \gamma^2(B_2 - \beta E_1)^2 - B_3^2 \\ &= \gamma^2(E_1^2 + \beta^2 B_2^2 + E_2^2 + \beta^2 B_1^2 - B_1^2 - \beta^2 E_2^2 - B_2^2 - \beta^2 E_1^2) + E_3^2 - B_3^2 = E^2 - B^2 \end{aligned}$$

(c) From Eqs. (4.66) and (4.70), we have (for free space):

$$S = \frac{c}{8\pi} 2|\mathbf{E} \times \mathbf{B}| \quad c\mathcal{E} = \frac{c}{8\pi} (E^2 + B^2)$$

The absolute-square of the Poynting vector's cross-product is most easily evaluated by noting that, where θ is the angle between \mathbf{E} and \mathbf{B} ,

$$|\mathbf{E} \times \mathbf{B}|^2 = E^2B^2 \sin^2\theta = E^2B^2(1 - \cos^2\theta) = E^2B^2 - (\mathbf{E} \cdot \mathbf{B})^2$$

Therefore,

$$\begin{aligned} 4|\mathbf{E} \times \mathbf{B}|^2 - (E^2 + B^2)^2 &= 4[E^2B^2 - (\mathbf{E} \cdot \mathbf{B})^2] - [(E^2)^2 + 2E^2B^2 + (B^2)^2] \\ &= -(E^2 - B^2)^2 - 4(\mathbf{E} \cdot \mathbf{B})^2 \end{aligned}$$

which is composed of our two invariants. Therefore, $S^2 - c^2\mathcal{E}^2$ is also an invariant quantity. The same result can be obtained by contracting the energy-momentum tensor, Eq. (14.131) or (14.134)—that is, evaluating the invariant scalar resulting from the operation $T_{\mu\nu}T_{\mu\nu}$, in analogy with Part (a).

For further discussion of the invariants of the electromagnetic field, see Salingeros, *Am.J.Phys.* 53, 361 (1985); 55, 352 (1987), and Zaghoul, et al., *Am.J.Phys.* 56, 274 (1988).

14-11. Write $\mathbf{E}' = \mathbf{E}'_{\parallel} + \mathbf{E}'_{\perp}$ and $\mathbf{B}' = \mathbf{B}'_{\parallel} + \mathbf{B}'_{\perp}$, where the subscripts indicate components parallel and perpendicular to the velocity of the frame K' . Equations (14.76) can then be written directly as

$$\begin{aligned} \mathbf{E}'_{\parallel} &= \mathbf{E}_{\parallel} \\ \mathbf{E}'_{\perp} &= \gamma \left(\mathbf{E}_{\perp} + \frac{1}{c} \mathbf{v} \times \mathbf{B}_{\perp} \right) \end{aligned}$$

Therefore, summing, and adding and subtracting $\gamma\mathbf{E}_{\parallel}$, we have:

$$\mathbf{E}' = \gamma \mathbf{E} + (1 - \gamma) \frac{\mathbf{E} \cdot \mathbf{v}}{v^2} \mathbf{v} + \frac{\gamma}{c} \mathbf{v} \times \mathbf{B}$$

The formulas for \mathbf{B}' are identical with the substitutions $\mathbf{E} \rightarrow \mathbf{B}$ and $\mathbf{B} \rightarrow -\mathbf{E}$.

14-12. From Eqs. (1.53) and (14.39):

$$\frac{d}{dt} \left[\frac{m_0 \mathbf{u}}{(1 - u^2/c^2)^{1/2}} \right] = q \left(\mathbf{E} + \frac{1}{c} \mathbf{u} \times \mathbf{B} \right)$$

$$\frac{m_0 \dot{\mathbf{u}}}{(1 - u^2/c^2)^{1/2}} + \frac{m_0 (\mathbf{u} \cdot \dot{\mathbf{u}}) \mathbf{u}}{c^2 (1 - u^2/c^2)^{3/2}} = q \left(\mathbf{E} + \frac{1}{c} \mathbf{u} \times \mathbf{B} \right)$$

To eliminate the second term, dot \mathbf{u} into the equation, to obtain:

$$\frac{m_0}{(1 - u^2/c^2)^{3/2}} \left[\left(1 - \frac{u^2}{c^2} \right) + \frac{u^2}{c^2} \right] (\mathbf{u} \cdot \dot{\mathbf{u}}) = q (\mathbf{u} \cdot \mathbf{E})$$

$$\frac{m_0}{(1 - u^2/c^2)^{3/2}} (\mathbf{u} \cdot \dot{\mathbf{u}}) = q (\mathbf{u} \cdot \mathbf{E})$$

Accordingly,

$$\mathbf{a} = \dot{\mathbf{u}} = \frac{q}{m_0} \left(1 - \frac{u^2}{c^2} \right)^{1/2} \left[\mathbf{E} + \frac{1}{c} \mathbf{u} \times \mathbf{B} - \frac{(\mathbf{u} \cdot \mathbf{E}) \mathbf{u}}{c^2} \right]$$

14-13. With $\gamma = 1/(1 - u^2/c^2)^{1/2}$, Eq. (14.117a) reduces to:

$$m_0 \frac{d}{dt} (\gamma \mathbf{u}) = \frac{q}{c} \mathbf{u} \times \mathbf{B}$$

$$\Rightarrow \begin{cases} m_0 \frac{d}{dt} (\gamma \dot{x}) = \frac{qB}{c} \dot{y} \\ m_0 \frac{d}{dt} (\gamma \dot{y}) = -\frac{qB}{c} \dot{x} \\ m_0 \frac{d}{dt} (\gamma \dot{z}) = 0 \end{cases}$$

Thus, the parallel momentum, $p_z = \gamma m_0 \dot{z}$, is constant, and the transverse equations integrate to:

$$\left. \begin{aligned} \gamma m_0 \dot{x} &= \frac{qB}{c} (y - y_0) \\ \gamma m_0 \dot{y} &= -\frac{qB}{c} (x - x_0) \end{aligned} \right\} \quad (1)$$

Cross-multiply the two equations to obtain

$$(x - x_0) \dot{x} + (y - y_0) \dot{y} = 0$$

$$\Rightarrow (x - x_0)^2 + (y - y_0)^2 = \text{constant} = R^2$$

From equations (1),

$$R^2 = \left(\frac{\gamma m_0 c}{eB} \right)^2 (\dot{x}^2 + \dot{y}^2) = \left(\frac{\gamma m_0 c}{eB} \right)^2 u_0^2$$

$$R = \left(\frac{\gamma m_0 c}{eB} \right) u_0$$

Define the relativistic cyclotron frequency [compare Eq. (10.77)],

$$\omega_c = \frac{qB}{\gamma m_0 c}$$

Then, $R = u_0/\omega_c$. Finally, from Eq. (14.117b) and the fact that there is no \mathbf{E} -field,

$$\frac{dW}{dt} = \frac{d}{dt} (\gamma m_0 c^2) = 0$$

There is no change in the particle's kinetic energy, and so γ and the speed $u = |\mathbf{u}|$ remain constant in time. These are the same results obtained in Prob. 1-30 for the nonrelativistic case, except for the substitution $m \rightarrow \gamma m_0$.

14-14. Equation (14.104) is

$$P = \frac{2e^2}{3c^3} \frac{1}{(1 - \beta^2)^2} \left[(\dot{\mathbf{u}} \cdot \dot{\mathbf{u}}) + \frac{(\mathbf{u} \cdot \dot{\mathbf{u}})^2}{c^2 (1 - \beta^2)} \right]$$

If the angle between \mathbf{u} and $\dot{\mathbf{u}}$ is θ , then

$$|\mathbf{u} \times \dot{\mathbf{u}}|^2 = u^2 \dot{u}^2 \sin^2 \theta$$

$$(\mathbf{u} \cdot \dot{\mathbf{u}})^2 = u^2 \dot{u}^2 \cos^2 \theta = u^2 \dot{u}^2 (1 - \sin^2 \theta)$$

Thus the equation can be written:

$$\begin{aligned}
 \mathbf{P} &= \frac{2e^2}{3c^3} \frac{1}{(1-\beta^2)^2} \left[(\dot{\mathbf{u}} \cdot \dot{\mathbf{u}}) \left(1 + \frac{\beta^2}{1-\beta^2} \right) - \frac{|\mathbf{u} \times \dot{\mathbf{u}}|^2}{c^2(1-\beta^2)} \right] \\
 &= \frac{2e^2}{3c^3} \frac{1}{(1-\beta^2)^3} \left[(\dot{\mathbf{u}} \cdot \dot{\mathbf{u}}) - \frac{1}{c^2} |\mathbf{u} \times \dot{\mathbf{u}}|^2 \right]
 \end{aligned}$$

For $\mathbf{u} \perp \dot{\mathbf{u}}$, the cross-product term reduces to $\beta^2 \dot{u}^2 / (1-\beta^2)$, while for $\mathbf{u} \parallel \dot{\mathbf{u}}$ the term vanishes. That is, the formula reduces to Eqs. (14.104a-b).

For $T = (\gamma-1)m_0c^2$ from Eq. (14.42a),

$$\frac{dT}{dx} = \frac{dT}{dt} \frac{dt}{dx} = \frac{m_0c^2}{u} \frac{d}{dt} \gamma = \frac{m_0c^2}{u} \frac{(\mathbf{u} \cdot \dot{\mathbf{u}})/c^2}{(1-\beta^2)^{3/2}} \rightarrow \frac{m_0\dot{u}}{(1-\beta^2)^{3/2}}$$

so that the parallel formula can be written

$$P_{\parallel} = \frac{2e^2}{3m_0c^3} \left(\frac{dT}{dx} \right)^2$$

14-15. From Eqs. (14.35) and (14.120a-b) we have

$$\begin{aligned}
 \mathbf{K} \cdot \mathbf{U} &= (\rho\mathbf{E} + \frac{\rho}{c} \mathbf{u} \times \mathbf{B}, \frac{i}{c} \mathbf{E} \cdot \mathbf{J}) \cdot (\gamma\mathbf{u}, i\gamma c) \\
 &= \gamma\mathbf{E} \cdot (\rho\mathbf{u} - \mathbf{J})
 \end{aligned}$$

But $\rho\mathbf{u}$ is simply a microscopic description of the current density \mathbf{J} . Therefore the term in parentheses is zero. The product of the space part of the two four-vectors is the force-density times velocity, which is the rate at which the electromagnetic field does work on the particle. The product of the time parts is the same thing. In the four-scalar the two terms cancel because of the negative sign from i^2 .

14-16. The Hamiltonian is defined by

$$H = \mathbf{u} \cdot \mathbf{P} - L$$

where from Eq. (14.105) the Lagrangian is

$$L = -m_0c^2 \left(1 - \frac{u^2}{c^2} \right)^{1/2} + \frac{e}{c} u_j A_j - e\Phi$$

The generalized or canonical momentum \mathbf{P} is defined by

$$P_j = \frac{\partial L}{\partial u_j} = \frac{m_0 u_j}{(1-u^2/c^2)^{1/2}} + \frac{e}{c} A_j \quad (1)$$

—the first term being the familiar particle momentum, the space portion of Eq. (14.36). The explicit form of the Hamiltonian must contain only the variables (x_j, P_j, t) , and not u_j . Rearranging (1), squaring, and summing over j ,

$$\begin{aligned}
 \frac{m_0^2 u^2}{1-u^2/c^2} &= \left(\mathbf{P} - \frac{e}{c} \mathbf{A} \right)^2 \\
 \Rightarrow u^2 &= \frac{c^2 (\mathbf{P} - \frac{e}{c} \mathbf{A})^2}{(\mathbf{P} - \frac{e}{c} \mathbf{A})^2 + m_0^2 c^2} \\
 \Rightarrow \left(1 - \frac{u^2}{c^2} \right)^{1/2} &= \frac{m_0 c}{[(\mathbf{P} - \frac{e}{c} \mathbf{A})^2 + m_0^2 c^2]^{1/2}}
 \end{aligned}$$

Thus,

$$\begin{aligned}
 H &= u_j P_j + m_0 c^2 \left(1 - \frac{u^2}{c^2} \right)^{1/2} - \frac{e}{c} u_j A_j + e\Phi \\
 &= \frac{c (P_j - \frac{e}{c} A_j)}{[(\mathbf{P} - \frac{e}{c} \mathbf{A})^2 + m_0^2 c^2]^{1/2}} \left(P_j - \frac{e}{c} A_j \right) + m_0 c^2 \frac{m_0 c}{[(\mathbf{P} - \frac{e}{c} \mathbf{A})^2 + m_0^2 c^2]^{1/2}} + e\Phi \\
 &= c \left[(\mathbf{P} - \frac{e}{c} \mathbf{A})^2 + m_0^2 c^2 \right]^{1/2} + e\Phi
 \end{aligned}$$

Now, the three-vector generalized momentum, $P_j = \gamma m_0 u_j + \frac{e}{c} A_j$, is the space part of a four-vector, the "time" part of which can be expressed as

$$\frac{iE}{c} = \frac{iW}{c} + \frac{e}{c} i\Phi \quad \Rightarrow \quad E = W + e\Phi$$

where E is the total energy of the particle in the electromagnetic field, W is the sum of the particle's kinetic and rest energies [see Eqs. (14.43) and (14.46)], and $e\Phi$ is the energy due to the presence of the field [see Eq. (14.56)]. Since the squares of four-vectors are invariant scalars, we can write:

$$\begin{aligned}
 (\gamma m_0 \mathbf{u}, \frac{iW}{c})^2 &= -m_0^2 c^2 \\
 &= [(\mathbf{P}, \frac{iE}{c}) - \frac{e}{c}(\mathbf{A}, i\Phi)]^2 = (\mathbf{P} - \frac{e}{c}\mathbf{A})^2 - \frac{1}{c^2}(E - e\Phi)^2 \\
 \Rightarrow E &= c \left[(\mathbf{P} - \frac{e}{c}\mathbf{A})^2 + m_0^2 c^2 \right]^{1/2} + e\Phi
 \end{aligned}$$

Thus, as usual, we can identify the Hamiltonian with the total energy of the system.

14-17. From Eqs. (14.54) and (14.56), the Lagrangian density of Eq. (14.123) can be written in three-vector notation as

$$\mathcal{L}' = \frac{1}{c} \mathbf{J} \cdot \mathbf{A} - \rho\Phi - \frac{1}{8\pi}(B^2 - E^2)$$

The variations δ are performed with respect to the potentials \mathbf{A}, Φ . Thus,

$$\begin{aligned}
 \delta B^2 &= 2 \mathbf{B} \cdot \delta \mathbf{B} = 2 \mathbf{B} \cdot \mathbf{curl}(\delta \mathbf{A}) \\
 &= 2 B_i \varepsilon_{ijk} \frac{\partial}{\partial x_j} (\delta A_k) \quad [\text{using Eq. (A.15)}]
 \end{aligned}$$

Paraphrasing the argument leading from Eq. (14.126) to (14.127), we integrate by parts to obtain

$$\begin{aligned}
 &= -2 \varepsilon_{ijk} \frac{\partial B_i}{\partial x_j} \delta A_k = +2 \varepsilon_{kji} \frac{\partial B_i}{\partial x_j} \delta A_k \\
 &= 2 (\mathbf{curl} \mathbf{B}) \cdot \delta \mathbf{A}
 \end{aligned}$$

Similarly,

$$\begin{aligned}
 \delta E^2 &= 2 \mathbf{E} \cdot \left(-\mathbf{grad}(\delta \Phi) - \frac{1}{c} \frac{\partial}{\partial t} (\delta \mathbf{A}) \right) \\
 &= 2 E_i \left(-\frac{\partial}{\partial x_i} (\delta \Phi) - \frac{1}{c} \frac{\partial}{\partial t} (\delta A_i) \right)
 \end{aligned}$$

(integrating by parts)

$$\begin{aligned}
 &= 2 \left(\frac{\partial E_i}{\partial x_i} \delta \Phi + \frac{1}{c} \frac{\partial E_i}{\partial t} \delta A_i \right) \\
 &= 2 \left(\mathbf{div} \mathbf{E} \delta \Phi + \frac{1}{c} \frac{\partial \mathbf{E}}{\partial t} \cdot \delta \mathbf{A} \right)
 \end{aligned}$$

Thus we have:

$$\begin{aligned}
 \delta \int \mathcal{L}' dv dt &= \int \left[\left(-\rho + \frac{1}{4\pi} \mathbf{div} \mathbf{E} \right) \delta \Phi \right. \\
 &\quad \left. + \left(\frac{1}{c} \mathbf{J} - \frac{1}{4\pi} \mathbf{curl} \mathbf{B} + \frac{1}{4\pi c} \frac{\partial \mathbf{E}}{\partial t} \right) \cdot \delta \mathbf{A} \right] dv dt = 0
 \end{aligned}$$

Since the variations $\delta \Phi$ and $\delta \mathbf{A}$ are independent, the two quantities in parentheses must each be zero. These are indeed the two inhomogeneous Maxwell equations.

 **BROOKS/COLE**
CENGAGE Learning

Visit Brooks/Cole online at www.brookscole.com

For your learning solutions: www.cengagelearning.com

ISBN 0-03-097278-7

